


**Theoretical and experimental investigation of Polymer  
Dispersed Liquid Crystal glazing for Net-Zero energy buildings  
in Saudi Arabia and UK**

Submitted by **Abdulmohsin Hemaïda** to the University of Exeter  
as a thesis for the degree of  
Doctor of Philosophy in Renewable Energy  
In June 2022

This thesis is available for Library use on the understanding that it is copyright material and that no quotation from the thesis may be published without proper acknowledgement.

I certify that all material in this thesis which is not my own work has been identified and that no material has previously been submitted and approved for the award of a degree by this or any other University.

Signature: .....  .....

## **Abstract**

In the last few years, energy consumption in the building sector has increased significantly because of the economic and population growth in Saudi Arabia and the United Kingdom. Governmental bodies and policymakers have invested greatly to implement measures to reduce the energy demand and carbon emissions for the building sector. Recently, a new technology of smart windows has emerged such as Polymer Dispersed Liquid Crystal Smart Glazing (PDLC). It has the potential to dynamically control the transmittance of solar radiation into a building by altering the optical and thermal properties. To evaluate the PDLC glazing for building applications, certain properties such as spectral transmission, thermal, and daylight performance need to be investigated. Therefore, this research aims to investigate PDLC glazing to characterise the thermal and daylight performance for energy efficiency for buildings in Saudi Arabia and the United Kingdom.

To investigate the thermal and daylight performance of PDLC glazing, theoretical and experimental methodologies were used. In the indoor experiment, the PDLC glazing was investigated to evaluate the spectral transmission and determine the thermal properties. In the outdoor experiment, the PDLC glazing was investigated with and without a solar control film to evaluate the thermal behaviour and daylight performance under various sky conditions. Furthermore, the EnergyPlus simulation tool was used to perform building energy modelling and daylight analysis to evaluate the potential of energy saving of the PDLC glazing for an office building in Saudi Arabia (arid climate) and the United Kingdom (temperate climate).

The result of the indoor investigation showed that the investigated PDLC glazing has  $2.79 \text{ W/m}^2\cdot\text{K}$  and  $2.44 \text{ W/m}^2\cdot\text{K}$  for transparent and opaques states, respectively. In addition, the outdoor evaluation revealed that the PDLC glazing effectively reduced solar heat gain when switched to the opaque state. Visual comfort was also achieved in all sky conditions (sunny, intermittent, cloudy) when a solar control film was attached to the PDLC glazing. In terms of energy savings, the EnergyPlus analysis showed that the PDLC glazing reduced cooling load by 12.7% in Riyadh and heating load by 4.9% in London.

## Table of contents

<b>Abstract</b> .....	<b>2</b>
<b>Table of contents</b> .....	<b>3</b>
<b>Acknowledgment</b> .....	<b>7</b>
<b>List of Figures</b> .....	<b>9</b>
<b>List of Tables</b> .....	<b>16</b>
<b>List of publications</b> .....	<b>19</b>
<b>Nomenclature</b> .....	<b>20</b>
<b>List of abbreviations</b> .....	<b>22</b>
<b>Chapter 1. Introduction and literature review</b> .....	<b>24</b>
<b>1.1 Background</b> .....	<b>24</b>
<b>1.2 Research justification</b> .....	<b>28</b>
<b>1.3 Review of electrically actuated switchable glazing</b> .....	<b>30</b>
1.3.1 Solar heat gain coefficient (SHGC) .....	30
1.3.2 Overall heat loss coefficient ( <i>U</i> -value).....	31
1.3.3 Daylight.....	32
1.3.4 Glare .....	33
1.3.5 Suspended Particle Device (SPD) .....	34
1.3.6 Electrochromic glazing (EC).....	37
1.3.7 Liquid Crystal (LC) glazing .....	41
<b>1.4 Research aims and objectives</b> .....	<b>46</b>
<b>1.5 Research methodology</b> .....	<b>47</b>
<b>1.6 Structure of thesis</b> .....	<b>48</b>
<b>1.7 Contribution to knowledge</b> .....	<b>49</b>
<b>1.8 Conclusion</b> .....	<b>49</b>
<b>Chapter 2. Research methodology and experimental setup</b> .....	<b>51</b>
<b>2.1 Introduction</b> .....	<b>51</b>
<b>2.2 Overall methodology</b> .....	<b>51</b>
<b>2.3 Review of outdoor test cell</b> .....	<b>52</b>
<b>2.4 PDLC glazing performance parameters evaluation</b> .....	<b>55</b>
<b>2.5 Description of PDLC glazing system</b> .....	<b>59</b>
2.5.1 PDLC glazing for indoor experiment .....	60
2.5.2 PDLC glazing for outdoor experiment .....	61
2.5.3 PDLC glazing combined with solar control film .....	62
2.5.4 Spectrophotometer measurement .....	63
<b>2.6 Description of test cell</b> .....	<b>64</b>
<b>2.7 Experimental setup</b> .....	<b>67</b>

2.7.1 Indoor experiment.....	67
2.7.2 Outdoor experiment.....	68
<b>2.8 Simulation modelling.....</b>	<b>71</b>
2.8.1 Building model.....	72
2.8.2 Shading control strategy.....	74
2.8.3 Weather Data and Climate Zone.....	75
2.8.4 Energy simulation parameters.....	81
2.8.5 Daylight simulation parameters.....	81
2.8.6 Artificial lighting system.....	83
<b>2.9 Conclusion.....</b>	<b>83</b>
<b><i>Chapter 3. Indoor investigation of thermal performance for an electrically switchable polymer dispersed liquid crystal (PDLC) glazing.....</i></b>	<b><i>84</i></b>
<b>3.1 Introduction.....</b>	<b>84</b>
<b>3.2 Optical properties of PDLC glazing.....</b>	<b>84</b>
<b>3.3 Evaluation of solar material protection and solar skin protection factor....</b>	<b>86</b>
<b>3.4 Calculation of Solar heat gain coefficient.....</b>	<b>87</b>
<b>3.5 Calculation of Overall heat transfer coefficient.....</b>	<b>88</b>
<b>3.6 Experimental setup.....</b>	<b>89</b>
<b>3.7 Results of the indoor investigation.....</b>	<b>90</b>
3.7.1 PDLC transmission measurements.....	90
3.7.2 Solar material and solar skin protection factors.....	93
3.7.3 PDLC glazing thermal performance.....	94
3.7.4 Solar heat gain coefficient (SHGC).....	101
3.7.5 Overall heat transfer ( <i>U</i> -value).....	102
<b>3.8 Conclusion.....</b>	<b>103</b>
<b><i>Chapter 4. Outdoor investigation of thermal and daylight performance of PDLC glazing and PDLC<sub>F</sub> combined with solar control film.....</i></b>	<b><i>105</i></b>
<b>4.1 Introduction.....</b>	<b>105</b>
<b>4.2 First experiment.....</b>	<b>105</b>
<b>4.3 Second experiment.....</b>	<b>105</b>
<b>4.4 Thermal performance of PDLC glazing and PDLC combined with solar film.....</b>	<b>105</b>
<b>4.5 Daylight glare discomfort.....</b>	<b>108</b>
<b>4.6 Experimental setup.....</b>	<b>108</b>
<b>4.7 Results of the outdoor investigation.....</b>	<b>108</b>
4.7.1 Thermal analysis of the PDLC glazing prototype.....	108
4.7.2 Visual comfort analysis of the PDLC glazing prototype.....	115

4.7.3 Thermal analysis of the PDLC <sub>F</sub> glazing prototype combined with the solar control film .....	118
4.7.4 Visual comfort analysis of the PDLC <sub>F</sub> glazing prototype combined with the solar control film .....	125
<b>4.8 Conclusion .....</b>	<b>129</b>
<b><i>Chapter 5. Simulation energy modelling study for a smart switchable adaptive polymer dispersed liquid crystal for two climate zones.....</i></b>	<b>131</b>
<b>5.1 Introduction .....</b>	<b>131</b>
<b>5.2 Simulation modelling .....</b>	<b>131</b>
<b>5.3 Building energy simulation .....</b>	<b>132</b>
<b>5.4 Daylight simulation .....</b>	<b>133</b>
<b>5.5 Simulation results .....</b>	<b>135</b>
5.5.1 Evaluation of heating, cooling, and lighting energies in relation to solar radiation in Riyadh.....	135
5.5.2 Evaluation of heating, cooling, and lighting energies in relation to solar radiation in London.....	138
5.5.3 Evaluation of heating, cooling, and lighting energies in relation to outdoor temperature in Riyadh .....	141
5.5.4 Evaluation of heating, cooling, and lighting energies in relation to outdoor temperature in London .....	143
5.5.5 Daylight performance of PDLC window in Riyadh in relation to solar radiation .....	146
5.5.6 Daylight performance of PDLC window in London relation to solar radiation .....	149
5.5.7 Daylight performance of PDLC window in Riyadh in relation to outdoor temperature .....	152
5.5.8 Daylight performance of PDLC window in London in relation to outdoor temperature .....	154
<b>5.6 Conclusion .....</b>	<b>157</b>
<b><i>Chapter 6. Evaluation of artificial lighting saving for a smart switchable adaptive polymer dispersed liquid crystal glazing PDLC for two climate zones .....</i></b>	<b>159</b>
<b>6.1 Introduction .....</b>	<b>159</b>
<b>6.2 Artificial lighting energy savings .....</b>	<b>159</b>
<b>6.3 Simulation modelling .....</b>	<b>161</b>
<b>6.4 Simulation results .....</b>	<b>161</b>
6.4.1 Evaluation of artificial lighting load in relation to solar radiation in Riyadh.....	161
6.4.2 Evaluation of artificial lighting load in relation to solar radiation in London .....	167
6.4.3 Evaluation of artificial lighting load in relation to outdoor temperature in Riyadh....	171
6.4.4 Evaluation of artificial lighting load in relation to outdoor temperature in London...	177

6.5 Conclusion .....	182
<b>Chapter 7. Conclusions and recommendations .....</b>	<b>183</b>
7.1 Conclusions .....	183
7.2 Recommendations and future research .....	185
<b>Bibliography .....</b>	<b>186</b>

## **Acknowledgment**

I would like to state my initial thanks and praise to Allah, and peace and blessings go to his prophet (Muhammad, peace be upon him). All praises and gratitude be to Allah, who give me the faith, foresight, strength, and endurance to be able to complete my research. Likewise, it would have been impossible to fulfil all the requirements of this research without the aid of various individuals, who have assisted in many ways.

Firstly, it is imperative that my heartfelt thanks go to my parents may Allah be pleased with them, who have always provided love and continual support have lit in my life. Their dream to see me in this place was a big motive. It is because of them; I did not give up when things became difficult. I can never thank them enough for what they have done for me. In this same vein, very deep and special thanks go to my family, who have continued to assist and motivate me on this journey. To my lovely wife and beautiful daughters, who have provided love, patience, encouragement, and perpetual comprehension of my efforts. To my little son, who has brightened my days during the last few months in my PhD journey. It is my hope that these accomplishments will help to inspire my daughters and son in the future to pursue their own ambitions. Special thanks to my siblings that have always provided support and there is no doubt that their thoughts and prayers have helped enormously in my achievement.

My sincere thanks and appreciation are extended to my Director of Studies, Professor Tapas K. Mallick. I would like to declare my special appreciation and sincere gratitude for his continual motivation, cooperation, a generous of help, and support throughout my research, as well as his professional guidance throughout this journey. This research would certainly not have been possible without his support and knowledge. I also, would like to register my sincere gratitude Dr. Senthilarasu Sundaram for his guidance and support. Similarly, I wish to extend my gratitude and profound appreciation to Dr. Aritra Ghosh, as he has provided invaluable insight and effort during my research; without these supervisors' team, this research would not have been possible. It is from these people that I derive my greatest inspiration. I thank them all for their relentless support and encouragement.

Additionally, my gratitude goes to the entire staff of the renewable energy group for their useful comments and highlights. I gratefully acknowledge the support, guidance, and assistance of James Yule, who dedicated his time and effort to support me in the experimental setup.

Lastly, I acknowledge with grateful the government of Saudi Arabia, the High Ministry of Education, for granting me the scholarship and sponsoring my undertaking of this PhD programme.

I will be eternally grateful to you all.



## List of Figures

Figure 1-1 Shows the energy consumption in Saudi Arabia in 2014 based on sectors. [8].....	25
Figure 1-2. The chart shows the energy demand in 2016 based on sectors in the United Kingdom. a) reports the natural gas consumption: b) reports the petroleum consumption [10]. .....	26
Figure 1-3 a) Shows the SPD glazing in the transparent state when the particles are aligned and allows light to pass through. b) Illustrates the SPD glazing in the opaque state when the particles are randomly aligned reducing the light passing through. c) An actual photograph of the SPD in the transparent state. d) An actual photograph of the SPD in the opaque state. [55].....	35
Figure 1-4 Schematic diagram of EC glazing in transparent and dark states. .	38
Figure 1-5. Illustration of PDLC glazing design where a) shows that the particles are aligned which allows light to pass through in the transparent (ON) state. b) Demonstrates that the particles are randomly aligned resulting in reducing the light passing through in the opaque (OFF) state. ....	42
Figure 2-1. Shows a schematic diagram of the experimental methodology. ....	58
Figure 2-2. Illustrates a schematic diagram of the building energy modelling. .	59
Figure 2-3. Illustration of the light transmission through the PDLC glazing. a) Shows the particles are aligned when power is ON resulting the light to pass through the glazing. b) The particles are randomly aligned causing the light to scatter when the power is OFF. c) Actual photograph of the PDLC glazing in the transparent state. d) Actual photograph of the PDLC glazing in the opaque state. ....	61
Figure 2-4. a) shows an actual photograph of the PDLC glazing in transparent state (On). b) The PDLC glazing in the opaque states (Off). .....	62
Figure 2-5. Schematic diagram of the combined PDLC glazing with solar control film.....	63
Figure 2-6. Schematic diagram of Perkin Elmer® Lambda 1050 UV/VIS/NIR spectrophotometer. M1, M2, and M3 are mirrors reflecting the sample beam and reference beam. ....	64
Figure 2-7. Photograph of the test cell that used to investigate the PDLC in an indoor environment.....	66

Figure 2-8. Schematic diagram of a test cell used for the outdoor investigation. ....	66
Figure 2-9. Photograph of the indoor experimental setup. ....	67
Figure 2-10. Photograph of the outdoor experiment showing the sensors and equipment.....	69
Figure 2-11. Photograph of PDLC <sub>F</sub> glazing combined with the solar film. a) shows applying the solar film on the glazing. b) shows the PDLC <sub>F</sub> glazing with the solar control film. ....	70
Figure 2-12. Schematic diagram illustrates the locations of the sensors. ....	71
Figure 2-13. a) The picture presents a two-story office building model with 60% window to wall ratio. b) shows the perimeter zones. ....	73
Figure 2-14. Workflow chart that illustrates the shading control strategy logic. The system simulates each variable independently for each control strategy. ....	75
Figure 2-15. Comparative analysis of monthly average temperature for Riyadh and London climate zones.....	77
Figure 2-16. a) The graph reports the hourly direct solar radiation in Riyadh and London. b) shows the monthly average of direct solar radiation.....	79
Figure 2-17 a) The graph presents the annual global horizontal illuminance in Riyadh and London. b) presents the monthly average values of global horizontal illuminance. ....	81
Figure 2-18. Illustration of DGI reference points and daylight zones. ....	82
Figure 3-1. Total transmission (regular + diffuse) and reflection of PDLC glazing for the transparent and opaque states.....	91
Figure 3-2. Regular and diffuse transmission of PDLC glazing for the transparent state and opaque state. ....	93
Figure 3-3. Measured temperature of external and internal glazing surface, test cell and ambient temperature in transparent state under 1000 W/m <sup>2</sup> solar radiation.....	95
Figure 3-4. Measured temperature of external and internal glazing surface, test cell and ambient temperature in the opaque state under 1000 W/m <sup>2</sup> .....	96
Figure 3-5. Measured temperature of external and internal glazing surface, test cell and ambient temperature in the transparent state under 800, 600, 400 W/m <sup>2</sup> solar radiation.....	97

Figure 3-6. Measured temperature of external and internal glazing surface, test cell and ambient temperature in the opaque state under 800, 600, 400 W/m <sup>2</sup> solar radiation.....	98
Figure 3-7. The time variation of the temperature difference ( $\Delta T_g$ ) between the internal and external PDLC glazing surfaces for both the transparent (blue line) and opaque (red line) states under various radiation intensities.....	100
Figure 3-8. The time variation of the temperature difference ( $\Delta T_{cell}$ ) between the test cell and the ambient temperature for both the transparent (blue line) and opaque (red line) states under various radiation intensities. ....	101
Figure 3-9. <i>U</i> -value and temperature difference between the ambient and test cell when PDLC glazing was in the transparent state. ....	102
Figure 3-10. <i>U</i> -value and temperature difference between the ambient and test cell when the PDLC glazing was in the opaque state.....	103
Figure 4-1. The solar transmittance of the PDLC glazing prototype and combined PDLC <sub>F</sub> for the transparent and opaque states.....	107
Figure 4-2. Temperature variation as a function of time for the PDLC glazing prototype in the transparent state for different sky conditions. a) Shows sunny sky condition. b) Shows intermittent sky condition. c) Shows cloudy sky condition. ....	110
Figure 4-3. Temperature variation as a function of time for the PDLC glazing prototype in the opaque state for different sky conditions. a) shows sunny sky condition. b) shows intermittent sky condition. c) shows cloudy sky condition. ....	112
Figure 4-4. The time variation of the temperature difference between the internal test cell temperature and the ambient temperature for the PDLC glazing in the transparent and the opaque states for different sky conditions. ....	114
Figure 4-5. The time variation of the temperature difference between the external glass and the internal glass temperature of the PDLC glazing in the transparent and the opaque states for different sky conditions. ....	115
Figure 4-6. The time variation of the discomfort glare (SR) level for the PDLC glazing prototype in the transparent state for different sky conditions. ....	116
Figure 4-7. The time variation of the discomfort glare (SR) level for the PDLC glazing prototype in the opaque state for different sky conditions. ....	117

Figure 4-8. The time variation of the external (red lines), internal illuminance (green lines) and working plane illuminance (purple lines) of the PDLC glazing prototype in the transparent and opaque states for different sky conditions. Graphs from a to c show sunny, intermittent, and cloudy sky conditions when PDLC in transparent state. Graphs from e to f show sky condition when PDLC in opaque state..... 118

Figure 4-9. Temperature variation as a function of time for the PDLC<sub>F</sub> glazing prototype combined with the solar control film in the transparent state for different sky conditions. a) Shows sunny condition. b) Shows intermittent sky condition. c) Shows cloudy condition..... 120

Figure 4-10. Temperature variation as a function of time for the PDLC<sub>F</sub> glazing prototype combined with the solar control film in the opaque state for different sky conditions. a) Shows sunny condition. b) Shows intermittent sky condition. c) Shows cloudy condition..... 122

Figure 4-11. The time variation of the temperature difference between the internal test cell temperature and the ambient temperature for the PDLC<sub>F</sub> (with solar control film) glazing in transparent and opaque states for different sky conditions. .... 124

Figure 4-12. The time variation of the temperature difference between the external glass and the internal glass temperature of the PDLC<sub>F</sub> glazing in transparent and opaque states for different sky conditions. .... 125

Figure 4-13. The time variation of the discomfort glare (SR) level for the PDLC<sub>F</sub> glazing prototype combined with solar control film in the transparent state for sunny, intermittent, and cloudy sky conditions. .... 126

Figure 4-14. The time variation of the discomfort glare (SR) level for the PDLC<sub>F</sub> glazing prototype combined with solar control film in the opaque state for sunny, intermittent, and cloudy sky conditions..... 128

Figure 4-15. The time variation of the external (red lines), internal (green lines) and working plane illuminance (purple lines) of the PDLC<sub>F</sub> glazing with solar control film in the transparent and opaque states for different sky conditions. Graphs from a to c show sunny, intermittent, and cloudy sky conditions when combined PDLC<sub>F</sub> in transparent state. Graphs from e to f show sky condition when combined PDLC<sub>F</sub> in opaque state..... 129

Figure 5-1 Total annual cooling, heating, and lighting energy consumption in relation to solar radiation in Riyadh. The graph illustrates the performance of PDLC glazing at various solar radiation intensities (green bars) compared to the reference window (blue bar). ..... 136

Figure 5-2. Total monthly cooling, heating, and lighting energy consumption in relation to solar radiation in Riyadh. The graph shows the performance of the PDLC window at various solar radiation intensities (light blue, green, grey, dark blue, and yellow bars) compared to the reference window (orange bar). ..... 137

Figure 5-3. Total annual cooling, heating, and lighting energy consumption in relation to solar radiation in London. The graph illustrates the performance of the PDLC glazing at various solar radiation intensities (green bars) compared to the reference window (blue bar). ..... 139

Figure 5-4. Total monthly cooling, heating, and lighting energy consumption in relation to solar radiation in London. The graph shows the performance of the PDLC window at various solar radiation intensities (light blue, green, grey, dark blue, and yellow bars) compared to the reference window (orange bar). ..... 140

Figure 5-5. Total annual cooling, heating, and lighting energy consumption in relation to outdoor temperature in Riyadh. The graph illustrates the performance of the PDLC glazing at various outdoor temperatures (green bars) compared to the reference window (blue bar). ..... 141

Figure 5-6. Total monthly cooling, heating, and lighting energy consumption in relation to outdoor temperature in Riyadh. The graph shows the performance of the PDLC window at various outdoor temperatures (yellow, light blue, and green bars) compared to the reference window (orange bar). ..... 142

Figure 5-7. Total annual cooling, heating, and lighting energy consumption in relation to outdoor temperature in London. The graph illustrates the performance of the PDLC glazing at various outdoor temperatures (green bars) compared to the reference window (blue bar). ..... 144

Figure 5-8. Total monthly cooling, heating, and lighting energy consumption in relation to outdoor temperature in London. The graph shows the performance of the PDLC window at various outdoor temperatures (yellow, light blue, and green bars) compared to the reference window (orange bar). ..... 145

Figure 5-9. Percentage of annual daylight glare index above 22 in relation to solar radiation in Riyadh. .... 147

Figure 5-10. Percentage of annual daylight illuminance comfort in Riyadh in relation to solar radiation. ....	148
Figure 5-11. Percentage of annual daylight glare index in London in relation to solar radiation. ....	150
Figure 5-12. Percentage of annual daylight illuminance comfort in London in relation to solar radiation. ....	151
Figure 5-13. Percentage of annual daylight glare index in Riyadh in relation to outdoor temperature. ....	152
Figure 5-14. Percentage of annual daylight illuminance comfort in Riyadh in relation to outdoor temperature. ....	154
Figure 5-15. Percentage of annual daylight glare index in London in relation to outdoor temperature. ....	155
Figure 5-16. Percentage of annual daylight illuminance comfort in London in relation to outdoor temperature. ....	156
Figure 6-1. Total annual artificial lighting load in relation to solar radiation for the PDLC compared to a reference window for high, intermediate, and low daylighting zones in Riyadh. ....	162
Figure 6-2. Monthly artificial lighting energy consumption in relation to solar radiation for the PDLC glazing compared to a reference window in Riyadh. ...	164
Figure 6-3. The average annual interior illuminance reading in relation to solar radiation for the PDLC glazing compared to a reference window for all daylighting zones in Riyadh. ....	166
Figure 6-4. Total annual artificial lighting energy consumption in relation to solar radiation for the PDLC glazing compared to a reference window in London. .	168
Figure 6-5. Monthly artificial lighting energy consumption in relation to solar radiation for the PDLC glazing compared to a reference window in London. .	169
Figure 6-6. The average annual interior illuminance readings in relation to solar radiation of the PDLC glazing compared to a reference window for all daylighting zones in London. ....	171
Figure 6-7. The total annual artificial lighting energy consumption in relation to outdoor temperature compared to a reference window in Riyadh. ....	172
Figure 6-8. Monthly artificial lighting energy consumption in relation to outdoor temperature for the PDLC glazing compared to a reference window in Riyadh. ....	174

Figure 6-9. The average annual interior illuminance readings in relation to outdoor temperature for the PDLC glazing compared to the reference window for all daylighting zones in Riyadh..... 176

Figure 6-10. Total annual artificial lighting energy consumption in relation to outdoor temperature for the PDLC glazing compared to a reference window in London. .... 178

Figure 6-11. Monthly artificial lighting energy consumption in relation to outdoor temperature for the PDLC and reference window for all daylighting zones in London. .... 179

Figure 6-12. The average annual interior illuminance readings in relation to outdoor temperature for the PDLC glazing compared to the reference window for all daylighting zones in London. .... 181

## List of Tables

Table 1-1. Thermal and transmittance data of SPD glazing.....	37
Table 1-2 performance parameters of electrochromic windows [86]. .....	39
Table 1-3: Thermal and visible transmittance of PDLC glazing.....	44
Table 2-1. Details of PDLC film in transparent (On) and opaque (OFF) state. .	60
Table 2-2. Solar control film specification.....	63
Table 2-3. Details of the glazing used in the experiments. ....	64
Table 2-4. Details of instrument for the indoor experiment.....	65
Table 2-5. Details of the instrument for the outdoor experiment.....	65
Table 2-6. The envelope properties of the building model according to ASHRAE standards 90.1.....	73
Table 2-7. Details of the optical and thermal properties of the PDLC and reference windows.....	73
Table 2-8. Weather data for Riyadh and London climate zones.....	76
Table 3-1. Values of relative spectral distribution $D_{65}V(\lambda)\Delta\lambda$ at different wavelengths, which were used for the calculation of the visible transmittance and visible reflectance [18].....	86
Table 3-2. Parameters required to calculate $U$ -value .....	89
Table 3-3. Measurements of the spectrophotometer for PDLC glazing for the transparent and opaque states.....	92
Table 3-4. List of factor values for PDLC glazing for the transparent and opaque states.....	94
Table 3-5. The maximum temperature ( $^{\circ}\text{C}$ ) of the PDLC glazing system.....	99
Table 4-1. Levels of discomfort glare indexes. ....	108
Table 4-2. The temperature readings for the PDLC glazing prototype in the transparent state. ....	110
Table 4-3. The solar irradiance measurements for different sky conditions when the PDLC glazing prototype was in the transparent state.....	111
Table 4-4. The temperature readings for the PDLC glazing prototype in the opaque state.....	112
Table 4-5. The solar irradiance measurements for different sky conditions when the PDLC glazing was in the opaque state.....	113
Table 4-6. The temperature readings for the PDLC <sub>F</sub> glazing prototype combined with the solar control film in the transparent state. ....	120



Table 4-7. The solar irradiance measurements for different sky conditions when the PDLC <sub>F</sub> glazing was in the transparent state. ....	121
Table 4-8. The temperature readings for the PDLC <sub>F</sub> glazing prototype combined with the solar control film in the opaque state.....	122
Table 4-9. The solar irradiance measurements for different sky conditions when the PDLC <sub>F</sub> glazing was in the opaque state. ....	123
Table 5-1. Levels of discomfort glare indexes. ....	134
Table 5-2. The total annual energy consumption in Riyadh in relation to solar radiation.....	136
Table 5-3. Total monthly cooling, heating, and lighting loads in relation to solar radiation in Riyadh.....	137
Table 5-4. The total annual energy consumption in London in relation to solar radiation.....	139
Table 5-5. Total monthly cooling, heating, and lighting energies in relation to solar radiation in London.....	140
Table 5-6. The total annual energy consumption in Riyadh in relation to outdoor temperature.....	142
Table 5-7. Total monthly cooling, heating, and lighting energy consumption in relation to outdoor temperature in Riyadh .....	143
Table 5-8. The total annual energy consumption in London in relation to outdoor temperature.....	145
Table 5-9. Total monthly cooling, heating, and lighting energies in relation to outdoor temperature in London .....	146
Table 5-10. Percentage of annual daylight glare index (DGI) in Riyadh in relation to solar radiation.....	147
Table 5-11. Interior daylight illuminance in Riyadh in relation to solar radiation. ....	149
Table 5-12. Exceeded hours of DGI above 22 in London in relation to solar radiation.....	150
Table 5-13. Percentage of annual daylight illuminance comfort in London in relation to solar radiation.....	151
Table 5-14. Percentage of annual daylight glare index in Riyadh in relation to outdoor temperature.....	153

Table 5-15. Percentage of annual daylight illuminance comfort in Riyadh in relation to outdoor temperature. ....	154
Table 5-16. Percentage of annual daylight glare index in London in relation to outdoor temperature. ....	155
Table 5-17. Percentage of annual daylight illuminance comfort in London in relation to outdoor temperature. ....	156
Table 6-1. Total annual artificial lighting loads (kW) for the PDLC and reference window in Riyadh. ....	163
Table 6-2. Monthly artificial lighting load (kW) for the PDLC glazing and reference window in Riyadh. ....	164
Table 6-3. Average annual interior illuminance in (lux) for the PDLC and reference window in Riyadh. ....	166
Table 6-4. Total annual artificial lighting loads (kW) for the PDLC and reference window in London. ....	168
Table 6-5. Monthly artificial lighting load (kW) for the PDLC glazing and reference window in London. ....	170
Table 6-6. Average annual interior illuminance in (lux) for the PDLC and reference window in London. ....	171
Table 6-7. Total annual artificial lighting loads (kW) for the PDLC and reference window in Riyadh. ....	173
Table 6-8. Monthly artificial lighting load (kW) for the PDLC glazing and reference window in Riyadh. ....	174
Table 6-9. Average annual interior illuminance in (lux) for the PDLC and reference window in Riyadh. ....	176
Table 6-10. Total annual artificial lighting loads (kW) for the PDLC and reference window in London. ....	178
Table 6-11. Monthly artificial lighting load (kW) for the PDLC glazing and reference window in London. ....	180
Table 6-12. Average annual interior illuminance in (lux) for the PDLC and reference window in London. ....	181

## List of publications

### Journal Articles published

1. Hemaida, A., Ghosh, A., Sundaram, S., Mallick, T.K., 2021. Simulation study for a switchable adaptive polymer dispersed liquid crystal smart window for two climate zones (Riyadh and London). *Energy Build.* 251, 111381. <https://doi.org/10.1016/j.enbuild.2021.111381>.
2. Hemaida, A., Ghosh, A., Sundaram, S., Mallick, T.K., 2020. Evaluation of thermal performance for a smart switchable adaptive polymer dispersed liquid crystal (PDLC) glazing. *Sol. Energy* 195, 185–193. <https://doi.org/10.1016/j.solener.2019.11.024>.

### Journal Articles in Process

3. Hemaida, A., Ghosh, Mallick, T.K., 2022. Thermal and daylight characterisations of PDLC glazing with and without solar control film under real weather conditions.
4. Hemaida, A., Ghosh, Mallick, T.K., 2022. Potential of artificial lighting reduction through a switchable PDLC glazing for an office building in two climate zones.

### Conference Articles

5. Hemaida, A., Ghosh, A., Sundaram, S., Mallick, T.K., 2019. Spectral analysis of a smart switchable polymer dispersed liquid crystal (PDLC) glazing for building application. *Sustainability in Energy and Buildings*, July 2019. Hungary, Budapest.

## Nomenclature

$A_{PDLC}$	Aperture area of PDLC glazing ( $m^2$ )
$A_{wall}$	Interior wall surface area ( $m^2$ )
$C_{air}$	Heat capacity of air ( $kJ/kg \cdot K$ )
$D_{65}$	The relative spectral distribution of illuminant
$h_o$	Heat transfer coefficient from test cell outer surface ( $W/m^2 \cdot K$ )
$h_i$	Heat transfer coefficient from test cell inside surface ( $W/m^2 \cdot K$ )
$I$	Incident radiation ( $W/m^2$ )
$(I_{h,g})$	Horizontal global solar irradiance ( $W/m^2$ )
$(I_{h,d})$	Horizontal diffuse solar irradiance ( $W/m^2$ )
$K_{pl}$	Thermal conductivity of polystyrene ( $W/m \cdot K$ )
$L_{pl}$	Thickness of polystyrene (m)
$L_{ext}$	Exterior illuminance (lux)
$L_i$	Vertical illuminance (lux)
$L_{win}$	PDLC Interior illuminance (lux)
$L_h$	Workplan horizontal illuminance (lux)
$M_{tc}$	Mass of the air inside test cell (kg)
$PDLC_F$	PDLC glazing with solar control film
$Q_{in}$	Total energy incident on the glazing (W)
$Q_{loss}$	Heat loss through the glazing
$Q_{PDLC}$	Heat through the glazing due to incident solar radiation (W)
$Q_{testcell}$	Total energy inside the test cell (W)
$R(\lambda)$	Reflection of glazing
$S_{uv}(\lambda)$	Relative spectral distribution of ultraviolet solar radiation
$S(\lambda)$	Spectral distribution of solar radiation
$T(\lambda)$	Spectral transmission of glazing
$T_{in,tc}$	Interior temperature of test cell ( $^{\circ}C$ )
$T_{out,tc}$	Ambient temperature ( $^{\circ}C$ )
$U_{PDLC}$	Overall heat transfer coefficient of glazing ( $W/m^2 \cdot K$ )
$V(\lambda)$	Spectral efficiency of a standard photopic observer
$\alpha$	Absorptance
$\tau_{dir}$	Direct transmittance
$\tau_{diff}$	Diffuse transmittance

$\tau_{\text{vis}}$	Visible transmittance
$E_V^{\text{out}}$	External illuminance
$E_V^{\text{in}}$	Internal illuminance
$E_H^{\text{in}}$	Internal horizontal illuminance
$E_{V,\text{win}}^{\text{in}}$	PDLC glazing interior illuminance

## List of abbreviations

AC	Alternating current
ASHRAE	American Society of Heating, Refrigerating and Air-conditioning Engineers
BGI	British glare index
BEM	Building Energy Modelling
CGI	CIE glare index
°C	Degree centigrade
DC	Direct current
DGI	Daylight glare index
DGP	Daylight glare probability
EC	Electrochromic
EU	European Union
ESP	Expanded polystyrene
GWh/year	Giga Watt hours per year
HVAC	Heating, Ventilation, and Air Conditioning
ITO	Indium tin oxide (In <sub>2</sub> O <sub>3</sub> :Sn)
kton/year	Kilo ton per year
MWh/year	Mega Watt hours per year
Min	Minimum
Max	Maximum
LC	Liquid crystal
NIR	Near infra radiation
SHGC	Solar heat gain coefficient
SPD	Suspended particle device
SR	Subjective Rating Glare
PASSYS	Passive Solar Systems and Component
PDLC	Polymer Dispersed Liquid Crystal
PIR	Polyisocyanurate insulation board
TRE-L	Test reference environmental of Lleida
<i>U</i> -value	Overall heat transfer coefficient
UGR	Unified glare rating
UV	Ultraviolet

V	Volt (unit of voltage)
VCP	Visual comfort probability
Wp	Watt peak
WWR	Window to Wall Ratio
XPS	Extruded polystyrene

# Chapter 1. Introduction and literature review

## 1.1 Background

Fossil fuels are used worldwide at an alarming rate, which causes environmental issues and strains future resources. Building activities such as cooling, heating, and lighting contribute to a significant concern related to environmental problems and energy demand [1]. The building sector is responsible for one-third of the carbon dioxide emissions and accounts for 32% of the global energy [2]. In developed countries building sector consumes 30- 40% of the total energy consumption, which is higher than the proportion needed for industry and transportation [3,4]. In the European Union (EU), the building sector uses about 40% of the total energy consumption, which is responsible for 36% of CO<sub>2</sub> emissions [5]. The residential building sector is responsible for 25% of the energy consumption, leading to 16% of greenhouse gas emissions [6]. In the US, commercial and residential buildings are responsible for approximately 39% of the total primary energy used in the country [7].

In Saudi Arabia, about 76% of the overall energy is consumed through the building sector, and 49% of that energy demand goes to the residential buildings [8]. Figure 1-1 shows the energy demand in Saudi Arabia by sector. The high energy consumption levels within Saudi Arabia occur mainly in the summer months during all hours (day and night), as the elevated temperatures result in increased cooling loads. Additionally, other contributing factors lead to increased energy demands in the country, such as population growth, economic development, and low prices for energy resources [9].

Petroleum and natural gas are the most common fuel used for energy production in the UK; each account for 38% of the total energy consumption [10]. Notably, the commercial buildings consume 10% of the total natural gas production and 2% of the total petroleum production. Figure 1-2 reports the demand for natural gas and crude oil in the UK by sector.



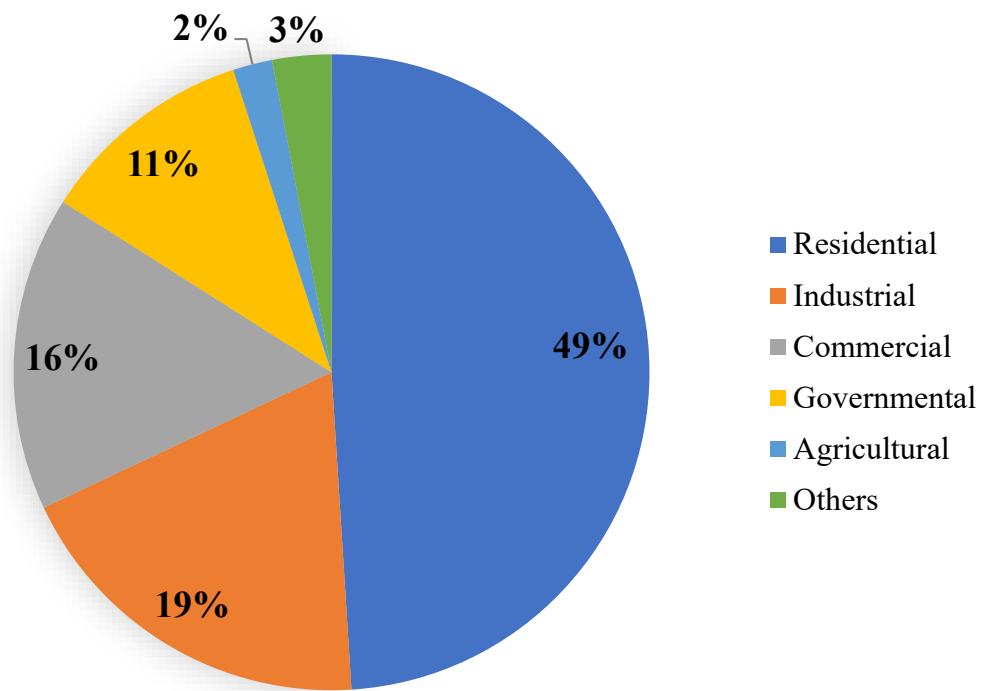
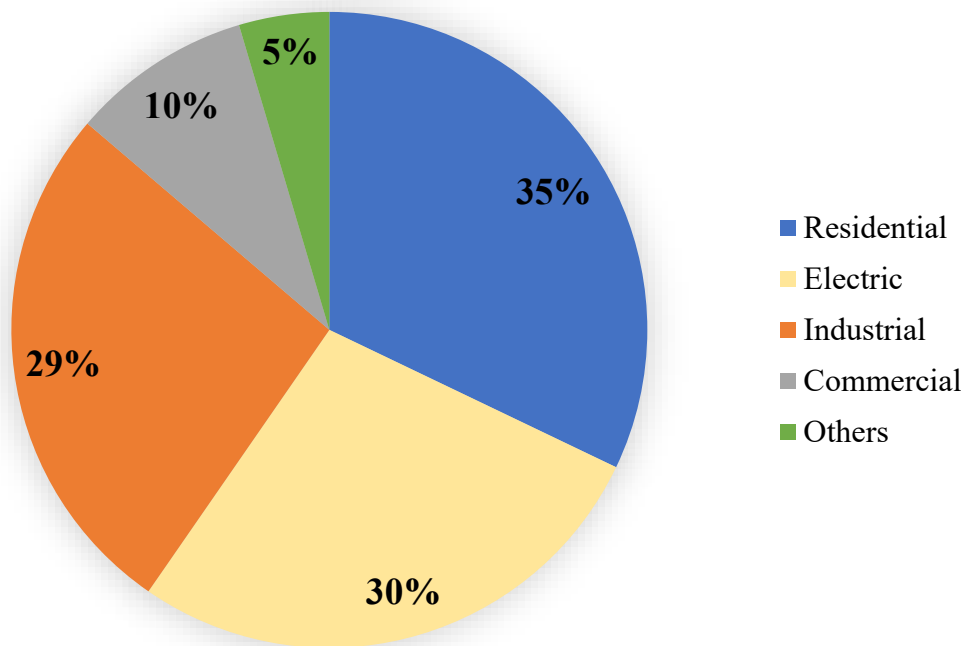


Figure 1-1 Shows the energy consumption in Saudi Arabia in 2014 based on sectors. [8].

a)



b)

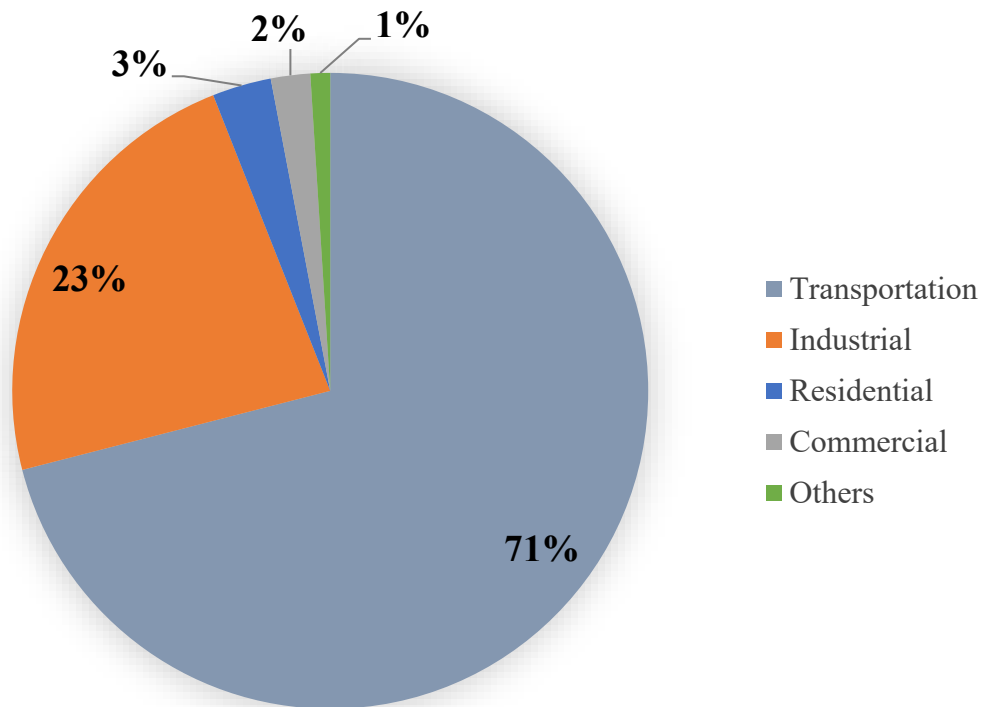


Figure 1-2. The chart shows the energy demand in 2016 based on sectors in the United Kingdom. a) reports the natural gas consumption: b) reports the petroleum consumption [10].

Building activities such as cooling, heating, and artificial lighting contribute to significant environmental issues and energy demand [1]. Different strategies can be utilised to improve building energy efficiency, such as active or passive energy efficiency strategies. Active energy efficiency can be implemented using improved heating, ventilating, air conditioning (HVAC) systems, and electrical lighting. In contrast, improvements to building envelope components can utilise passive energy efficiency. In recent years, considerable interest has been given to passive building energy efficiency. Fenestration plays a crucial role in building design, which adds aesthetic values, provides indoor thermal comfort, and natural daylight. In the last decade, there has been significant development in glazing technologies. Windows play an essential role in the energy and environmental performance of buildings and significantly affect the levels of thermal and visual comfort for occupants in addition to energy demand. In general, occupants in a building receive natural daylight, air ventilation, and

passive solar gain through windows. These vital functions make windows selection very important, especially from energy usage and visual comfort prospective. However, windows are responsible for approximately 60% of the total energy consumption in a building due to the high level of heat loss and heat gain [11]. *U*-value and solar heat gain coefficient (SHGC) are the major factors that determine windows' energy performance. In order to decrease heating and cooling loads, high SHGC and low *U*-value are required for cold climates and hot climates, respectively [12]. Thus, it is vital that windows have appropriate SHGC and *U*-values to bring thermal comfort to occupants and diminish energy demands. In addition, admitted solar radiation could have an adverse impact on the well-being of occupants and the degradation of materials inside a building [13]. In this respect, it is essential to take decisive measures to reduce global energy demand and greenhouse gas emissions.

In recent years, there have been significant developments within the Saudi economy as the 2030 vision has been implemented, where green and renewable energy have received considerable attention. The vision of 2030 in Saudi Arabia aims to mitigate the emissions of CO<sub>2</sub> by 130 million tons and improve the energy efficiency in the building sector. The Saudi government has put a significant effort to promote and explore new technologies and green façades for the building sector to reduce energy consumption. The retrofit programme proposed by King Abdullah Petroleum Studies and Research Centre (KAPSARC) aims to improve the energy efficiency in buildings and lead to electricity generation reduction [14]. The retrofit programme specifically targets new window technologies for existing and new buildings.

In order to meet the Saudi 2030 vision, the retrofit programme has set the following targets:

- 1- Avoid electricity consumption by 62,800 GWh/year for residential buildings and 100,00 GWh/y for total stock buildings.
- 2- Avoid electricity generation capacity by 14,300 MW/year for residential buildings and 22,900 MW/year for total stock buildings.
- 3- Reduce carbon emissions by 47,600 kton/year for residential buildings and 76,000 kton/year for total stock buildings.

In the United Kingdom, the building sector has received significant attention in order to improve energy efficiency and reduce carbon emissions. Heating and cooling are important aspects in the Energy Performance of Buildings Directives (EPBD) and need to move toward a clean and carbon-neutral energy systems. The United Kingdom is committed to improving energy efficiency for homes and reducing CO<sub>2</sub> emissions by 2050 [15]. In the UK, the residential sector is responsible for 22% of greenhouse gas emissions [16]. In addition, the industry sector aims to reduce the emissions by half for new buildings by 2050 by utilising high efficient and low carbon technologies [17]. High energy efficiency systems, including high-performance insulation and highly efficient windows, are required to meet the UK's new targets for low carbon buildings.

## 1.2 Research justification

Building envelopes, particularly windows have become a considerable interest topic for regulatory bodies, researchers, developers and building designers in both new and existing buildings. The main goal is to explore new technologies of windows that can adapt to the environmental conditions and user behaviour in a dynamic way that provides thermal and visual comfort for occupants in addition to energy balance. The evidence provided related to the energy crisis for buildings above strongly suggests that glazing is a key factor that can mitigate the energy demand. Glazings available in the market are classified into; low heat loss control, solar gain heat control, and daylight glare control glazings; however, these technologies do not possess variable  $U$ -value and SHGC. Additionally, electrically actuated glazings are classified into; electrochromic (EC), suspended particles device (SPD), and polymer dispersed liquid crystal (PDLC) glazings.

PDLC glazing has considerable potential for low energy building applications. Studies related to building energy consumption using the PDLC smart glazing are limited in the literature. Therefore, this research aims to investigate electrically switchable PDLC glazing for low energy building applications. The following reasons provide an understanding of the scope of the research.

- Electrically actuated glazings can change the optical and thermal properties according to occupants needs.

- Colour changing in EC glazing is fairly slow as it takes 5 min to 12 min to change to dark state depending on the glass size, making it difficult to adapt to rapid fluctuations of sky conditions.
- EC glazing control solar radiation mainly by absorption, which leads to high surface temperature, which could negatively impact the indoor temperature of a room.
- Both EC and SPD have good solar transmittance modulation; however, they do not offer privacy.
- Privacy is a critical factor in building design in Saudi Arabia. Therefore, there is a necessity to explore a new technology of glazing that provides privacy and has the potential to improve indoor thermal and visual comfort, such as PDLC glazing.
- Saudi Arabia and the United Kingdom aim to improve energy efficiency for buildings and reduce cooling and heating demands; therefore, investigating PDLC glazing for energy savings is required.
- No attempt was carried out to investigate PDLC glazing for building applications in Saudi Arabia and the United Kingdom. Therefore, it is imperative to investigate PDLC glazing under real weather conditions and assess its potential for energy savings.

## **1.3 Review of electrically actuated switchable glazing**

### **1.3.1 Solar heat gain coefficient (SHGC)**

The solar heat gain coefficient (SHGC) is defined as the fraction of external solar radiation that is admitted through a window, both directly transmitted and absorbed and subsequently released inward [18]. The solar heat gain coming through the transparent envelope of buildings plays a significant part in cooling load; some of the solar heat transfers to the inner space. A portion of the solar radiation is reflected, some is absorbed by the fenestration, and some is transferred to the building as infrared radiation. Solar heat gain is measured by the solar heat gain coefficient [19]. Many studies have been done on SHGC as it is a critical thermal property factor of glazing.

The less solar heat passes through a window, the lower the SHGC value it has. SHGC may be expressed for the glass alone and in some cases may refer to the entire window assembly. The concept has been presented in order to calculate the total energy gain of elements of a building as a result of incident solar radiation. In such a situation, it is assumed that direct solar radiation is perpendicular to the surface of the element [20]. Because of the significance of this coefficient and the need for advancement many research labs have invested in studies throughout the year. SHGC can be measured using steady-state laboratory conditions or transient conditions [12].

To calculate solar heat gain coefficient (SHGC) for double glazing windows, supply-air windows and smart facades, Computational Fluid Dynamic (CFD) simulations were employed [21]. SHGC depends on the transmissivity of the glass; thus, single glass panes glazing has higher SHGC than double or triple glazing. A higher airflow rate through the air channel enhances the SHGC value [22]. Studies and experiments to provide information on Energy Ratings for building envelopes were developed by Lawrence Berkeley National Laboratory and the U.S Department of Energy National Laboratory [23]. Many researchers have provided more or less simplified mathematical models and numerical simulations to determine the SHGC value. Bhandari and Bansal have presented a simple method to select, optimise and size an indirect solar heating system. The method presented requires the minimum metrological data and can take into

account the effect of insulation [24]. Gueymard and duPont have investigated the SHGC and visible transmittance that resulted from a deliberate change in the reference spectrum [25]. They found that replacing the direct spectrum would lead to changes of about -2% to +7% in the SHGC of windows and around -3% to +11% in the SHGC of the skylights, which tend to make most glazing systems look less energy-efficient in cooling-dominated buildings. Also, they recommended that the calculation of visible transmittance be with the same spectral weighting function as SHGC [25]. A study has proposed a model for calculating solar heat gain through glazed surfaces to be used in the simplified calculation of thermal energy requirements in air-conditioned buildings [26]. The conclusion obtained from this work can be summarised as follow:

- 1- Solar heat gain through a glazed surface is evaluated by summing three contributions: the direct optical contribution, the secondary direct contribution, and the indirect secondary contribution due to the radiation reflected internally.
- 2- A more accurate monthly evaluation was obtained from the new calculation procedure of the solar heat gains, with less than 2% deviations compared to the TRNSYS code [26].

Many studies have been done on calculating and measuring solar heat gain coefficient by Aritra [27], Shunyao Lu [19], and Aleo, F [28].

### **1.3.2 Overall heat loss coefficient (*U*-value)**

Overall heat transfer coefficient (*U*-value) is defined by the difference in the internal and external heat transfer coefficient and thermal conductance of glazing. Heat loss through a window occurs when the inside temperature of a room is higher than the outside temperature. When glazing is exposed to an outdoor environment, interact with the outside real-time condition. This exposure offers a variation of convective heat loss from the outside surface [29]. This review will discuss several methods to evaluate the solar heat gain coefficient and the overall heat transfer coefficient.

Many studies have been done to predict the  $U$ -value of glazing using different measurement methods. For instance, Wright has investigated the  $U$ -value for glazing systems by an analytical computer program called VISION. His research noted that the introduction of supply airflow consistently decreased the  $U$ -value and increased the shading coefficient of the various glazing system. Also, he proposed that effective  $U$ -value and effective shading coefficient can be replaced with the input of  $U$ -value and shading coefficient in a building energy analysis program [30]. Simulations to evaluate thermal transmittance coefficients for the ventilated double window were conducted. Experimental measurements during the night period were used to validate the calculations. Then, these values were used in a whole building simulation program. It was found in system 1 that the useful  $U$ -value has increased with the increase of airflow. Whereas system 2 has given the opposite. However, the useful  $U$ -value of system 2 was always lower than the one of system 1 which mean that system 1 was able to recover more heat [31].

Thermal performance of the supply-air window was simulated using Computational Fluid Dynamic (CFD). Also, a simplified model based on the analytical solution was proposed to investigate the thermal properties of the same window. Then, the result obtained from the (CFD) and the simplified model were compared. Three different methods were found to consider in thermal building simulation. First, the effective  $U$ -value and solar factor must be pre-calculated and used only for constant airflow. Second, the infrared radiative calculation can be affected by the large pane outside surface temperature. Third, a simplified method can be implemented with fewer equations [21]. Several studies have been conducted to measure the overall heat transfer coefficient for different types of glazing systems, refer to the available work, e.g. Baker, P. H. [32], Hoffmann [33], W. Zhang [34], A. Ghosh [27,35].

### **1.3.3 Daylight**

Daylighting is an excellent and sustainable alternative to artificial lighting that can improve visual comfort, energy efficiency, and green building developments. Windows allow daylighting to enter a room to create a pleasant atmosphere and provide occupants with contact with the outside environment. Daylight is the best



source of light because it has an excellent colour rendering and closely matches the human eyes response.

Electric lighting is one of the main energy consumers, accounting for 20-30% of the total power consumption of office buildings and 10% of residential buildings [36,37]. Natural light is an economical way to provide light for buildings. Natural daylight can improve vision efficiency and reduce electric lighting load using proper lamp fittings with lighting controls [38]. Lately, daylight has been widely recognised to contribute to building energy savings [39]. Appropriate daylighting strategies with lighting controls have shown great potential to reduce artificial lighting load [40]. Studies have shown that daylight with light control strategies can reduce annual artificial lighting consumption by 30% to 60% of the total energy consumption [41,42]. Adapting an appropriate daylighting strategy can potentially lead to energy saving in buildings and lead to reduce greenhouse gas emissions [39,43].

#### **1.3.4 Glare**

Glare is a sensation produced by luminance that results in disturbance or discomfort when the human eyes receive luminance greater than the eyes adaptation [44]. Discomfort glare caused by natural daylight and artificial lighting has been studied, and several metrics methodologies have been proposed to measure glare phenomena. The Visual Comfort Probability (VCP) method [45], the CIE Glare Index (CGI) [46], and the Unified Glare Rating (UGR) system [47] are methods that are applicable for evaluating glare coming from artificial lights or uniform light source. In addition, none of these methods is suitable for predicting discomfort glare coming from sunlight [48]. British Glare Index (BRS or BGI) system [49] is appropriate for small glare sources that have solid angles inferior to 0.027 sr [50], without mentioning the monitoring procedure of the required parameters [51]. Most of these methods are not sufficient for evaluating user comfort as they react only to the horizontal illuminance. Daylight glare probability (DGP) is a method that evaluates glare in a simplified way in terms of the correlation between the vertical illuminance to the levels of glare [52]. Additional elements must be considered to evaluate glare discomfort from windows, such as the magnitude of discomfort glare which substantially depends

on the brightness of the sky portion visible from the window. Glare originated from daylight at mild degrees seems to exhibit greater tolerance effects compared to the glare originated from artificial lighting sources. However, it may not be noticeable at higher glare levels [48]. Glare sensation is affected by non-uniform luminance distribution from windows [53].

### **1.3.5 Suspended Particle Device (SPD)**

Suspended Particle Devices (SPDs) were invented during the 1930s and function through the same principle as light valves. This is where a cell is created using two transparent sheets of insulating material separated by a small space and containing a suspension of mini-particles in a liquid form [54]; particles are either heraphathite or dihydrocinchonidine bisulfite polyiodide. The shape and structure of a particle can be needle-, rod- or lath-shaped in form. The presence of an electrical field enables the liquid suspended particles to move in a random formation, resulting from Brownian movement that absorbs the light directed into the cell. Figure 1-3 presents the design of SPD glazing for the transparent and opaque states. Hence, during the opaque or no power state, the light valve is dark. The overall percentage of light absorption is dependent upon the structure of the cell, the natural environment, and the concentration of particles with light energy content.

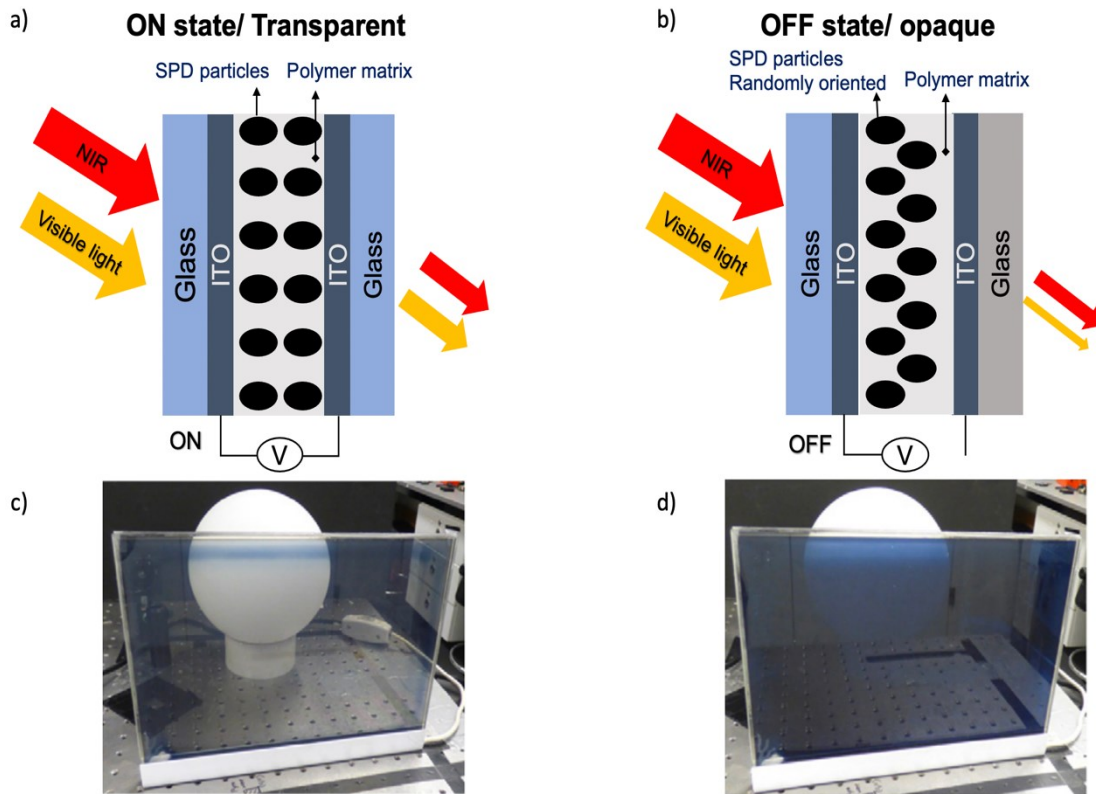


Figure 1-3 a) Shows the SPD glazing in the transparent state when the particles are aligned and allows light to pass through. b) Illustrates the SPD glazing in the opaque state when the particles are randomly aligned reducing the light passing through. c) An actual photograph of the SPD in the transparent state. d) An actual photograph of the SPD in the opaque state. [55].

Ghosh states that particles become aligned and enable the majority of light to pass through a cell when an applied electrical field is present, which is why a light valve becomes transparent [56]. This technology has been applied for approximately seventy years in light modulation in alphanumeric and television display areas of use, which also functions in optical devices as a filter. Additionally, plastic films are the preference for liquid suspension in regard to glazing applications, as a plastic film removes the swelling effects during high column suspension because of the device's hydrostatic pressure and leakage possibilities. With a plastic film, only a small number of particles are present, and these do not agglomerate noticeably during repeated film activation that uses applied electrical fields. The SPD light valve utilises a film of a cross-linked polymer matrix with a refractive index (1.4), together with the suspended-liquid light valve distributed through the matrix [56]. Furthermore, in shatter resistant

laminated SPDs, two sheets of glass were used with a laminated inter-layer in between. Specifically, Research Frontiers Inc (RFI) manufactures commercial SPD devices used for different appliances, such as goggles, eyeglasses, and windows.

Two different groups have investigated SPD glazing properties through thermal, daylighting and optical usage on outdoor and indoor characterisation: the Dublin energy lab, Dublin; and the Grupo de Displays Aplicaciones Fotonicas, Spain. An outdoor test cell characterisation was used to investigate: SPD glazing thermal behaviour [57]; electrical and daylighting behaviour [27,56]. The SPD glazing changes transmission by up to 55% from 5% when 110V, 0.07W AC power is present [55,58]. Moreover, it was determined that SPD glazing possesses an intermediate transmittance state when variable applied power is used during an indoor experiment. Studies have reported that SPD glazing increased the overall heat transfer to 5.9 W/m<sup>2</sup>·K, which is switchable single glazing, although this does have the potential to control solar heat gains that are measured at 0.05 whilst opaque to 0.38 whilst transparent [57,59]. Therefore, it can be stipulated that SPD has the potential to be used in the summer and within hot climates, although SPD double-glazing is able to save 66% in heat loss when compared to SPD single glazing, and thus, is suitable to be used in cold climates [57]. In cold climates, SPD vacuum glazing has been noted to be the best option compared to SPD single glazing; this can save 83% in heat loss [27]. What is more, SPD glazing produces comfortable daylight within the indoor environment, which increases occupant satisfaction [60]. Meanwhile, SPD glazing can offer comfortable daylight, which creates an intermediate state of 30% improvement.

In addition, SPD glazing's durability was researched following four years of exposure, where a single year laboratory environment and the Dublin outdoor environment for three years demonstrated contrasting ratios that changed from 1:11 (opaque) to 1:10 (transparent). Therefore, it can be noted that it is imperative that additional research is conducted to acquire strong statements regarding SPD glazing's stability [54]. Furthermore, it was determined that the requirement for SPD glazing voltage is not dependent on surface temperature. Table 1-1 shows the key parameters of the investigated SPD windows. The SPD single glazing

had identical heat absorbing capacity for the transparent and opaque states. Thus, the rise of temperature of the SPD glazing surfaces for the transparent and opaque state were the same resulting in identical heat transfer values. The electrical and optical behaviour of a 28 cm x 22 cm commercial SPD window was investigated [61]. A Solartron 1260 analyser was utilised to carry out the impedance analysis. The optical response was measured using a lamp with an emission similar to the A illuminant. The transmittance measurements were taken using an optical fibre bundle near the SPD glazing surface. The results showed that the SPD had poor switching times and the device breakdown after 1000 cycles. It was found that the abrupt changes in applied voltages caused the stresses.

Table 1-1. Thermal and transmittance data of SPD glazing.

size (cm)	Type	States	U-value	SHGC	$\tau(\lambda)$	Ref.
21 × 28	SPD single	Transparent	5.9	0.35	55%	[57,59]
		Opaque	5.9	0.05	5%	
21 × 28	SPD double	Transparent	1.9	NA	NA	[57]
		Opaque	1.9	NA	NA	
22 × 28	SPD single	Transparent	NA	NA	40%	[62]
		Opaque	NA	NA	6%	

### 1.3.6 Electrochromic glazing (EC)

Electrochromic glazing changes optical properties from transparent to dark when direct current is applied and usually composed of several layers. Figure 1-4 illustrates a generic design of EC glazing. The first layer is a glass or a plastic attached to, mostly (ITO) transparent conducting film. The following layer is an ion storage film. The last layer is another transparent conducting film. The middle layer of EC glazing is an electrolyte which can be a polymer material or transparent thin film. The ions are transported in an electric field. Therefore, they should be small for easy transportation; protons (H<sup>+</sup>) and lithium ions (Li<sup>+</sup>) are common alternatives. The ion conductor layer is attached to an EC thin film that works as a mixed conductor and conducts ions and electrons when the electrical field is applied [63]. Tungsten-based oxide is a good example and it is commonly used for manufacturing EC glazing [64]. An ion storage film is on the opposite

side of the ion conductor and also works as a mixed conductor. It is recommended that the ion storage film possesses EC properties to enhance the other layers' performance.

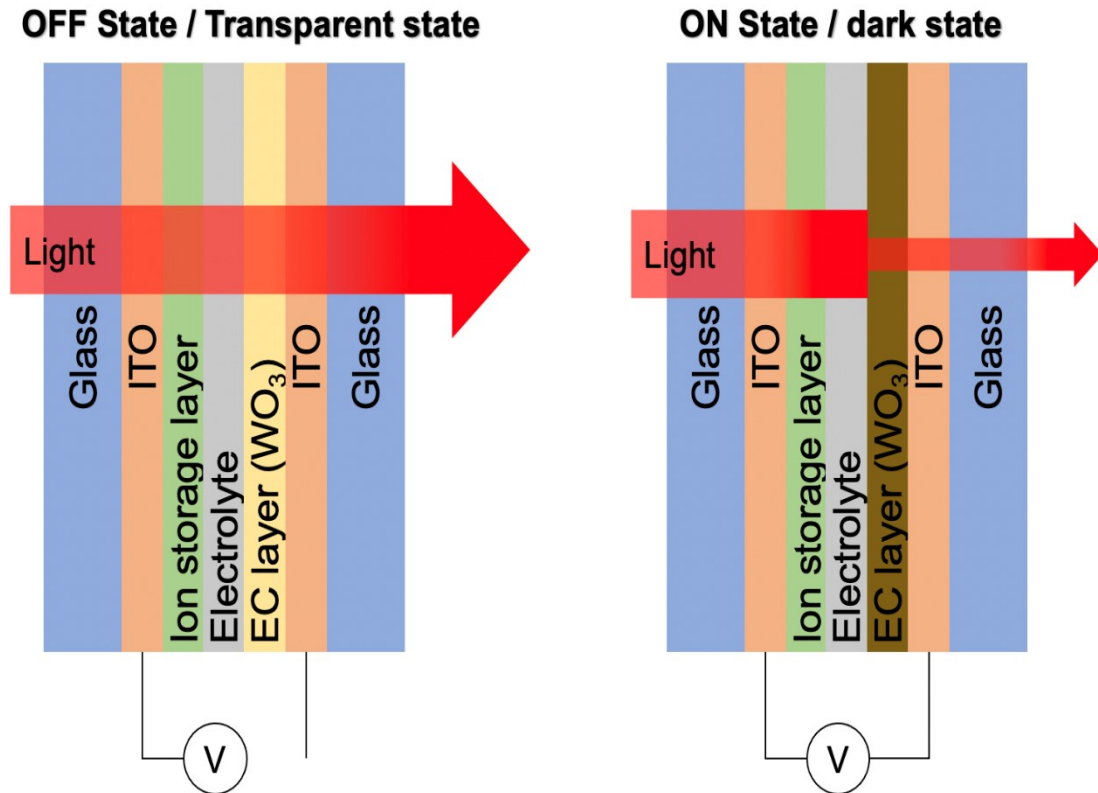


Figure 1-4 Schematic diagram of EC glazing in transparent and dark states.

Electrochromic (EC) materials have been attractive due to their potential usage and applications within energy conservation development [65]. For instance, smart windows, automotive rear-view mirrors, and sunglasses all use electrochromic materials [66]. In particular, the most vital aspect of producing an ideal EC window is to include: high-initial transparency; large optical contrasts between the states that are coloured and bleached; a reduced switch time; and cyclic stability that is long-term [67]. Additionally, EC materials are classified into organic and inorganic materials. Certain inorganic EC materials are traditional metal oxide semiconductors, which include:  $\text{WO}_3$  [68];  $\text{TiO}_2$  [69];  $\text{MoO}_3$  [70];  $\text{Nb}_2\text{O}_5$  [71,72];  $\text{NiO}$  [73]. EC windows based on  $\text{WO}_3$  demonstrate fantastic electrochromic properties, which have now been utilised in many appliances: smart windows [74]; automotive rear-view mirrors [75]; electrochromic displays [76]. Furthermore, nickel oxide ( $\text{NiO}$ ) thin film has been attractive to researchers

for two main reasons: acceptable cost and excellent electrochromic properties [77]. It can also be enhanced by incorporating NiO with a wide range of bandgap oxide materials [78].

Organic conjugated polymers have been extensively researched, which include: polythiophene, polyaniline (PANI), polypyrrole (PPy), and Poly(3,4-ethylene-dioxythiophene) (PEDOT), as well as its derivatives [79]. Many of these show quality and beneficial electrochromic properties. PANI is a common organic electrochromic material. Its derivatives are vital organic conjugated polymers to EC windows, as they function with short colouring and bleaching switching times, alongside high optical contrasts and increased efficiency colouration [80]. Additionally, PEDOT, together with its derivatives, also presents quality EC conjugated polymers, resulting from the elevated colouration efficiency and diverse colours' ability that they produce [81,82]. Contrastingly, the disadvantage of short lifespans is a result of conjugated polymers' low electrochemical and thermal stability, which are detrimental to organic EC application development in the future [83].

EC technology reverses its colour because of oxidation and reduction reaction if an external electrical field is applied. Electrochromic materials, therefore, change their optical properties of transparency and adsorption of solar radiation, which result in reducing both the visible light ( $\tau_{vis}$ ) and near-infrared (NIR) transmitted through the window [84]. Dynamic EC glazing has the potential to control NIR, which can save up to 5 to 15 kWh/m<sup>2</sup> year of the heating and cooling loads of commercial and residential buildings [85]. Table 1-2 presents EC glazing performance parameters [86].

Table 1-2 performance parameters of electrochromic windows [86].

<b>Performance indicator</b>	<b>Value</b>
<b>Switching voltage</b>	≤ 5V
<b>Switching time</b>	≤ 10 s to 5 min
<b>Optical memory</b>	2 – 24 h
$\tau(\lambda)$	60 – 70 % (bleached)
	6 – 7% (coloured) – energy tasks

	< 3% (coloured) – visual comfort tasks
<b>SHGC</b>	≥ 0.6 (bleached)
	≤ 0.2 (coloured)
	$SGHC_{max}/ SGHC_{min} \geq 3$ – energy tasks
<b><math>\rho_{nir}</math></b>	≤ 0.1 (bleached)
	≥ 0.7 (coloured)
<b>U (<math>W m^{-2} K^{-1}</math>)</b>	≤ 1.2
<b>CRI</b>	≥ 80
<b>Lifetime</b>	20 – 30 years
	25,000 – 50,000 cycles
<b>Operating temperatures</b>	-30 to 90 °C

The EC glazing available in the market usually produces blue colour due to using  $WO_3$  as common electrochromic material. The colour changes from clear when the device is off to dark when the device is on [85]. Solar Heat Gain coefficient has been observed in EC devices as 0.49 in the clear state and 0.09 in the full dark state, with light transmission values ( $\tau_{vis}$ ) ranging between 69% to 1%. The power required to change the state of an EC window is very minimal ( $2.5 Wp/m^2$ ) and even less power is required to maintain a dark state (less than  $0.4 Wp/m^2$ ). This is due to the electrochromic materials' stability [84]. The transition time is reasonably slow for an instant; a 10 x 30 cm glass requires about 5 min, while a 1.2 x 0.8 cm glass takes about 12 min for a dark state and clear state [87]. Furthermore, the switching time is dependent on panel size, where the bleaching cycle is typically faster and increases as the glass temperature decreases. Slow transition speed is not considered a disadvantage instead, it allows occupants to cope naturally with daylight [84].

Nevertheless, experimental and numerical evaluations have found remarkable performance in controlling glare where EC windows are oriented to the South and acceptable performance where EC windows are oriented to the East and West [88,89]. Another experiment was conducted using a small-scale EC glazing prototype in real environmental conditions, which showed reasonable glare control for diffuse daylight. The investigation has shown that EC glazing successfully reduces glare and brings comfort even though it cannot transmit to full dark state when direct sunlight passes through [88,90]. The durability of EC



glazing has been proven since the 2000s with installed EC devices still in operation. A warranty of 10 years is offered for EC products with maintenance service from 30 to 50 years [91].

### **1.3.7 Liquid Crystal (LC) glazing**

Liquid crystal (LC) is used as an AC powered electrically activated switchable glazing application, placed between two panes of glass. It was noted that in LC devices, the main liquid crystals used are nematic, ferroelectric, guest host, and polymer dispersed [92]. Smectic is also a liquid crystal (SmA), while PDLC is also a form of LC, where polarisers are not a requirement in operation. For these applications, SmA needs a few ms, while PDLC requires 1-10 ms to switch on. The scattering process of SmA LC devices commences from the devices' edges or conductive electrodes that move centrally. Hence, the device's size defines the scattering and states, whilst higher voltages are needed to obtain uniform performance. The alignment of non-uniform particles can result in localised hot spots that create LC device arcing [93]. In this system, the voltage level strongly changes the response time [94]. Meanwhile, Anjaneyulu and Yoon state that LC material-based glazing had a variance of 30%- 55%, with a dimension of 12.5 cm × 12.5 cm and a thickness of 6 μm [95]. A study has suggested that the organic-based SmA LC panels of 1 × 1 m<sup>2</sup> change from a clear to a fully scattered state through the process of more than three orders to several tens of milliseconds [93].

Different forms of PDLC are the most relevant in usage for glazing, as they do not need a polarizer in their operation; moreover, they do not require high brightness due to high transparency; wide angled views; fast response times, through milliseconds; no surface treatment; or for intermediate electrically controllable transmission levels to possibly be present [96]. Figure 1-5 presents an illustration of the PDLC glazing design in transparent (ON) and opaque (OFF) states. Generally, PDLC films in a solid polymer matrix are composed of lower molecular weight micro-sized liquid crystal droplets. These are situated between two separate transparent conducting electrodes. Lights are scattered when power is absent due to the refractive index mismatch that is present between droplets and the polymer matrix. Moreover, power LC molecules are present as

they pass the light and refractive index between the polymer matrix and droplets. The droplets' sizes define PDLC scattering, while the radius of the droplets is smaller than the incident wavelength, which enables light to pass through without any form of scattering.

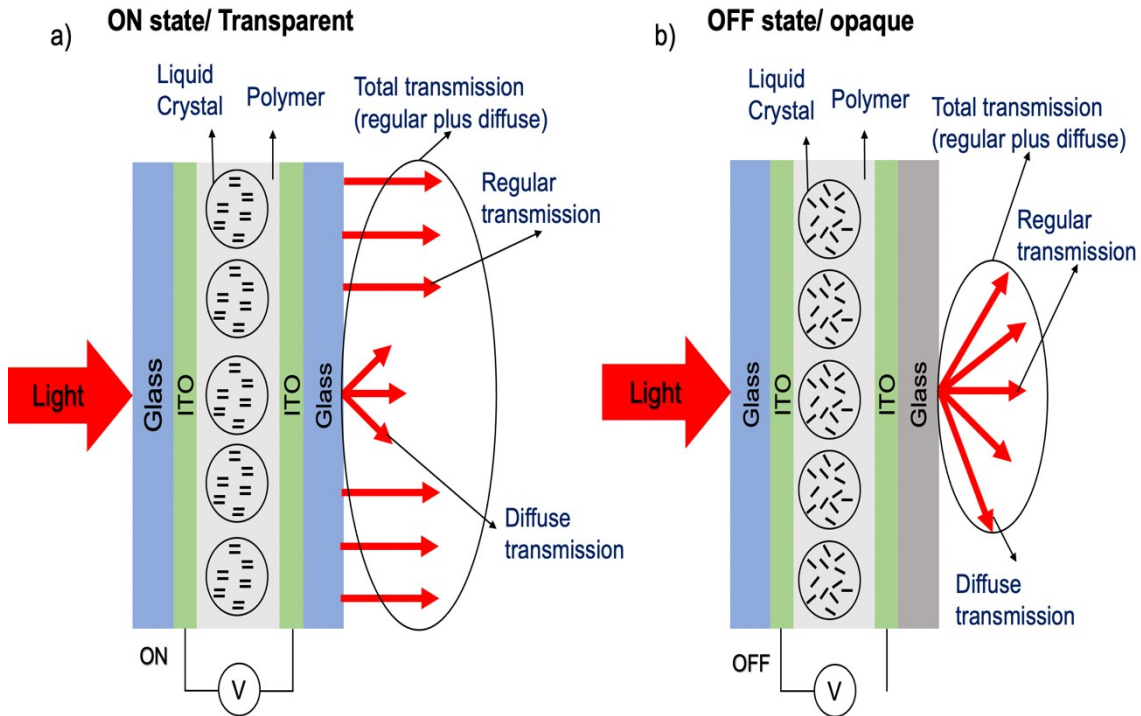


Figure 1-5. Illustration of PDLC glazing design where a) shows that the particles are aligned which allows light to pass through in the transparent (ON) state. b) Demonstrates that the particles are randomly aligned resulting in reducing the light passing through in the opaque (OFF) state.

The thermal conductivity of a PDLC film rises as the applied electric field increases because it improves LC droplets' thermal conductivity. Hadj Sahraoui et al. add that the rate of increment relies upon LC concentration in composites, which is able to be controlled; this is also dependent upon incident light's temperature and angles [97]. Moreover, PDLC films can block 98% of all UV rays and modulate the NIR between 12- 38% [98]. A study has suggested that PDLC films have a stability level of temperature measured between 0-60 °C [99]. Meanwhile, one PDLC film demonstrates durable levels of up to 3 million times the electrical switching at 100 VAC and 60Hz with switching intervals of 1 second [100]; lower thickness levels of LC material do not require as much time to switch.

The electro-optical switching effect from a 50 mm thickness PDLC film produces a 190  $\mu$ s time of rising in order to become transparent. At the same time, 2 ms of daylight are required when an external electric field is utilised.

It is possible for the combination of PDLC and electrochromic guest-host molecules to produce rapid switching from a state of opaque scattering to a transmissive transparent state, which helps to control daylight and the results of glare [101,102]. Moreover, reverse mode PDLC glazing was researched that had a transparent (OFF) state and an opaque (ON) state [103]. It was also possible to switch off this device using a light source. Accordingly, daylight characterisation with the use of PDLC glazing was researched using outdoor test cells in Dublin, which produced 71% transparency from a 20 V AC supply, while there was 27% transparency with a power supply absence [104]; there was also 82.6% haze with this particular form [105,106]. PDLC glazing was not able to control the glare for both states (transparent and translucent) when there were clear sunny days, while PDLC glazing performance was acceptable to control glare when there were intermittent overcast or cloudy day [104].

Certain disadvantages are clear from LC glazing made of PDLC films, as they require a continuous power supply to maintain their transparency and create haze as a result of scattering at wider angles of views in the state of transparency. Scattering occurs in PDLCs as there is a difference between the refractive index and the droplets of LC and the polymer matrix that suspends them. The reduction of diameters with the droplets increases the scattering levels, although a higher driving voltage level is required. Due to droplet sizes being reduced by transmitting red light without noticeable scatter, PDLC films scatter blue and green light efficiently [94]. PDLC requires increased driving voltage and haze that produce considerable scattering levels and unwanted yellow colouring as UV ageing occurs. In addition, the replacement of polymer with glass was researched in order to lower the effects stated previously. In particular, a 5 x 5 cm<sup>2</sup> PDLC device was produced that created a switching time of 10 times less, together with 85% lower voltage levels (15 V), to offer 80% transmission compared to other PDLC devices [107]. Table 1-3 shows the key parameters of the PDLC glazing.

Table 1-3: Thermal and visible transmittance of PDLC glazing.

size (cm)	States	U-value	SHGC	$\tau_{vis}$	Ref.
20 x 15	Transparent	NA	0.53	71%	[77]
	Opaque	NA	0.39	27%	

The PDLC device exhibits several advantages: it can be operated without polarisers, high transparency transmission, large viewing angle, fast switching time, and the potential to control the transmission level [96]. Thus, these features have attracted researchers to investigate PDLC for windows applications. A PDLC window has been investigated by employing a smart room equipped with sensors and a computer system to control the PDLC transparency based on sun exposure and occupant motion inside the smart room [108]. The computer can detect the sunlight and the occupant's motion and adjust the PDLC transparency accordingly. The performance of the PDLC was compared against a typical room with standard system. The investigation results showed that the PDLC window was able to reduce the energy consumption by 38% in comparison to the standard system and provide privacy in the room.

The Nasir et al. (2020) study aims to improve the optical properties by fabricating the PDLC switchable glazing directly onto glass called "vacuum glass coupling" instead of plastic polymers. The study has demonstrated a cost-effective and straightforward method to prepare PDLC switchable glazing directly from a commercially available polymer and liquid crystal with nano-beads on glass substrates via vacuum glass coupling on a large scale. The study has performed an experiment using a commercially prepared liquid crystal, E7 to fabricate the PDLC film. They used a wire-bar coater to coat the PDLC mixture on indium-tin-oxide-coated glass and assembled the PDLC cell by coupling another glass in a vacuum. They characterised the switching behaviour of the cells by ramping the AC voltage and measured a transmittance change of 70%.

The study results indicated that the PDLC switchable glazing exhibited low haziness and wide-angle vision and could be fabricated at a large scale by a vacuum-coupling process, with potential use as glass windows for energy-efficient buildings. The fabricated PDLC device exhibited a high transmittance

change with a low driving voltage of 60 V. Their fabrication method could be used widely for general solid substrates without limitation of size. The glass-based smart window could be used for indoor privacy purposes and also for energy saving purposes under direct sunlight due to the glass durability for UV irradiation. Therefore, switchable glazing has significant potential for numerous commercial and industrial applications.

In 2022, Shaik et al. investigated the efficacy, cost savings, and performance advantages of the PDLCs glazing in a hot-dry climate installed in place of existing tinted bronze glazing of a library building in Vellore, India [109]. The study aimed to explore the Solar-optical properties of different coloured PDLCs glazing systems and compute reductions in the cooling costs during the summer months for the cooling-dominant climate. The study has performed an experiment in the entire solar spectrum in order to measure the solar and visible light properties for four different coloured PDLC film glazing (pink, yellow, blue, and white) in transparent (ON) and translucent states (OFF). Thermal analysis has been conducted to calculate the glazing thermal properties ( $U$ -value,  $g$ -value) and their influence on the heat gain/loss through PDLC glazing in buildings. The thermal analysis has been performed on a real building in order to calculate the energy-saving potential of the building when the existing building glazing was retrofitted with different PDLC glazing. The measured solar optical properties were used to calculate the solar heat gains and cost savings. Also, they performed daylight simulations in order to know daylight accessibility through PDLC glazing inside the building.

This study provides statistics related to a visual acceptability range in the PDLC buildings with respect to colour rendering index and daylight factors. The study suggests information related to net energy savings of PDLC glazing systems by considering PDLCs' operational energy consumption. The results showed that the PDLC glazing had demonstrated substantial reductions in building cooling loads, corresponding to cooling cost savings. The PDLC glazing thermal performance was superior to existing tinted bronze glazing (TBG), concluding cost savings (\$/m<sup>2</sup>) and carbon emission mitigations (tCO<sub>2</sub>/year). The cost-benefit analysis indicated significant cost savings (\$) with retrofitting existing

tinted bronze glazing in the building. In addition, the Daylight analysis had concluded adequate natural daylight accession in the building interiors for various library tasks as per the green building codes to shed artificial daylighting costs. The average daylight factor (DF) metric of PDLC glazing was above the minimum recommended level for building interiors as per Indian codes.

#### **1.4 Research aims and objectives**

This research aims to investigate Polymer Dispersed Liquid Crystal Glazing (PDLC) for commercial building applications in the United Kingdom and Saudi Arabia. Optical characterisation was performed in an indoor environment to determine the solar transmission, visible transmission, reflectance, and absorption. In addition, the thermal properties were also characterised in an indoor condition to find out the thermal transmission ( $U$ -value) and solar heat gain coefficient (SHGC). The optical and thermal properties were used to perform energy modelling and daylight analysis using EnergyPlus for the United Kingdom and Saudi Arabian Climates. A comparison between PDLC glazing and a reference double window system was evaluated. A test cell was fabricated to investigate the thermal and daylight characteristics of the PDLC prototype in an outdoor environment under real weather conditions. The thermal and daylight characteristics were analysed to assess the device performance.

The objectives of the research are to investigate the following:

- 1- Theoretical evaluation using EnergyPlus to evaluate the thermal performance of the PDLC prototype to assess energy savings for cooling, heating, and artificial lighting loads for the United Kingdom (temperate) and Saudi Arabia (arid) climates.
- 2- Theoretical investigation of daylighting analysis to evaluate the daylight performance and Daylight Glare Index (DGI) for the two mentioned climates.
- 3- Experimental evaluation of the thermal and daylight performance under real weather conditions to establish rationale of using such technologies in the UK and Saudi Arabia.

- 4- The use of solar control film to assess its effect on the PDLC prototype behaviour under real weather conditions.

The objective will be achieved through:

- 1- Characterise the optical and thermal properties of the PDLC prototype in an indoor condition.
- 2- Develop an office building model using EnergyPlus to evaluate the energy savings in the UK and Saudi Arabian climatic conditions.
- 3- Develop a shading control strategy to control the PDLC prototype in both transparent and opaque states according to the user's desire to obtain indoor comfort.
- 4- Design and fabrication of a test cell to investigate the PDLC prototype in outdoor condition.
- 5- Analyse the thermal behaviour of the PDLC prototype for the transparent and opaque states using the test cell under real weather conditions.
- 6- Analyse daylight performance and glare levels of the PDLC prototype for both states.
- 7- Integrate a solar control film with the PDLC prototype to evaluate its effect on the PDLC glazing behaviour for transparent and opaque states.

### **1.5 Research methodology**

- 1- A comprehensive review of existing literature focusing on electrically actuated switchable windows was conducted.
- 2- A review of previous studies was conducted to select an experimental setup to achieve the aim and objectives of the research.
- 3- Two experimental setups were utilised:
  - a. Indoor experimental setup was utilised to determine the thermal transmission ( $U$ -value) and solar heat gain coefficient. The data collected were ambient temperature, glazing surfaces temperature, test cell temperature and solar radiation.
  - b. Outdoor experimental setup was used to evaluate the thermal behaviour of the PDLC prototype by using field measurement of ambient temperature, glazing surfaces temperature, test cell

temperature, and solar radiation (global plus diffuse). In addition, glare level was calculated by the data for external and internal illuminance.

- 4- For the theoretical evaluation, an office building model that meets the ASHRAE standards 90.1 was developed using EnergyPlus to assess the energy savings. The evaluation was carried out for two different climates and the weather data was obtained from the EnergyPlus website. A shading control strategy was developed to control the PDLC glazing prototype in relation to solar radiation and outdoor temperature.

## **1.6 Structure of thesis**

This section provides an outline of the content of this research.

Chapter one presents the introduction of the research illustrating the energy problem for the building sector in Saudi Arabia and the United Kingdom. It describes the main aim of the research and defines specific objectives and methodology used to execute the research. In addition, it provides a comprehensive literature review of the state of the art of electrically actuated switchable glazing systems.

Chapter two explains the methodology carried out to achieve the aim and objectives of the research. Furthermore, details of the design, experimental setup and equipment are provided. The theoretical evaluation to assess the energy savings and daylight performance was also discussed.

Chapter three discusses the results of the indoor experiment for the calculated  $U$ -value and SHGC. Thermal behaviour of the PDLC prototype in an indoor environment was also discussed.

Chapter four provides a detailed discussion of the outdoor investigation of the PDLC glazing and PDLC<sub>F</sub> glazing combined with solar control film. Thermal behaviour of the PDLC glazing and PDLC<sub>F</sub> glazing with solar control film were discussed in detail. In addition, the daylight performance and glare level were also provided.



Chapter five presents the results of the energy savings, daylight analysis, and daylight glare index for an office building in Riyadh and London. The results and findings of the energy savings for an office building in Riyadh and London were described in detail. Critical evaluation of daylight performance and daylight glare index in three daylighting zones were also discussed.

Chapter six explores the potential of artificial lighting load reduction by employing PDLC glazing for an office building in Riyadh and London. Analysis of the results of the evaluation of artificial lighting reduction in relation to solar radiation and outdoor temperature were provided.

Chapter seven provides a summary of the research results and recommendations for future research.

### **1.7 Contribution to knowledge**

This research contributes to the knowledge by providing more understating of smart PDLC glazing behaviour as follows:

- Comprehensive analysis of the thermal and daylight characteristics of PDLC glazing under real weather conditions for temperate climate.
- Outdoor evaluation of the effect of solar control film on PDLC switchable glazing thermal and daylight behaviour.
- Indoor investigation to determine the overall heat transfer coefficient ( $U$ -value) and solar heat gain coefficient (SHGC).
- Comprehensive theoretical analysis of energy savings for cooling, heating, and artificial lighting for an office building in arid and temperate climates.
- Provides theoretical evaluation of interior illuminance and daylight glare index for PDLC switchable glazing for transparent and opaque states.

### **1.8 Conclusion**

In this chapter, the main aims and objectives of this research have been introduced. In addition, the extensive literature on electrically actuated switchable windows has been discussed. The following conclusion of this chapter can be summarised as follows:

1. The building sector is a primary energy consumer in Saudi Arabia and the United Kingdom. Both countries have regulations in place to minimise the energy consumption of cooling, heating, and artificial lighting using new advanced technologies of windows.
2. Electrically actuated switchable windows such as EC, SPD, and PDLC are new technology of windows that change optical properties when an electrical field is introduced. They have the potential to modulate solar radiation, which could bring thermal and visual comfort to occupants. EC glazing has been extensively investigated for building applications. However, EC glazing suffers significant drawbacks such as slow switching time, not uniformed switching process, and requires intervals to be connected to a power supply. EC glazing rejects solar heat mainly by absorption, which causes the glazing surface to be very hot and that could lead to indoor thermal discomfort. Furthermore, SPD and EC glazing do not offer privacy when switched to dark state. SPD glazing suffers mechanical stresses after 1000 cycles because of the abrupt changes in the applied voltages [61].
3. PDLC possess advantages that make it an excellent candidate for building application. PDLC can be operated without polarisers, has a high transparency level, fast switching time, and the potential to control the transmission level. So far, no investigation has been done to investigate the potential of PDLC for building applications in Saudi Arabia and the UK.

## Chapter 2. Research methodology and experimental setup

### 2.1 Introduction

This chapter presents in detail the methodology used to investigate a PDLC switchable glazing in transparent and opaque state. Description of the PDLC glazing, experimental setup, and simulation modelling parameters are also discussed.

### 2.2 Overall methodology

In this research, a PDLC switchable glazing was investigated in indoor, outdoor conditions, and by using EnergyPlus simulation software. Thermal and daylight characterisation of the PDLC switchable glazing were performed in two stages.

First, thermal and daylight performance of the PDLC switchable glazing was characterised by employing indoor and outdoor experimental setup. To experimentally investigate thermal and daylight performance of the PDLC switchable glazing two test cells were utilised and several key parameters were measured. In order to characterise the PDLC glazing, the optical properties were determined using indoor spectrophotometer instrument.

Second, EnergyPlus simulation modelling tool was utilised to evaluate the energy performance of the PDLC switchable glazing for an office building. Evaluation of annual energy saving for cooling, heating, and artificial lighting loads was performed for two climate zones. Additionally, daylight glare discomfort analysis was also conducted.

In indoor experiment, solar heat gain (SHGC) and thermal transmittance ( $U$ -value) were calculated for the PDLC glazing. To calculate the SHGC and  $U$ -value, parameters such as incident solar radiation, solar transmittance and absorption, and the area of the PDLC glazing were required. The incident solar radiation was measured using solar simulator AAA type. A Spectrophotometer was utilised to measure the solar transmittance, reflectance, and absorption. Ambient, glazing surfaces, and test cell temperature were measured to evaluate the PDLC glazing

thermal performance for indoor condition. All equations used to calculate the SHGC and  $U$ -value are explained in detail in Chapter 3.

In outdoor experiment, characterisation of thermal performance and daylight glare were carried out for the PDLC switchable glazing and the PDLC combined with solar control film for different sky conditions (sunny, intermittent, and cloudy sky conditions). To evaluate the thermal behaviour and daylight glare discomfort weather data was considered such as ambient temperature, glazing surface temperature, and solar radiation. Same procedures were used to investigate the PDLC glazing and the PDLC combined with solar control film. Description of the experiment in is provided in Chapter 4.

Building energy modelling was performed to evaluate the energy performance of PDLC switchable glazing on cooling, heating, and artificial lighting loads. Daylight glare discomfort and interior illuminance analysis for three daylight zones were also performed. Two different climate zones were utilised to perform the simulation. The weather data was obtained from EnergyPlus database for Riyadh, Saudi Arabia and London, United Kingdom. An office building model was constructed to perform the simulation and the building's envelope properties were characterised as required by ASHRAE standards. The parameters used in the simulation modelling to characterise PDLC glazing were determined by the indoor experiment. The evaluation of energy performance and artificial lighting saving were explained in Chapter 5 and Chapter 6. Description of experimental setup and building energy modelling parameters are explained in the following sections.

### **2.3 Review of outdoor test cell**

The assessment of the effectiveness of Façade elements and its multi-functional, that do one or more of functions is a complex task. Researchers and standardisation bodies attempted to establish the appropriate procedures in order to evaluate the actual behaviour of building components in the simple and cost-effective way.

The assessment procedure usually performed by three main facility group: outdoor real-scale facilities, laboratory indoor facilities and outdoor test cells

[110]. The outdoor real-scale facilities correspond to in-field measurements with boundary conditions specified by weather and occasionally occupants' behaviour. The laboratory indoor facilities and outdoor test cells corresponding to measurements under laboratory-controlled boundary conditions. However, not all the outdoor test cells are under control of the research team.

Indoor testing experiments allow accurately controlling the key parameters such as ambient temperature, relative humidity, and air velocity. Guarded hot box is an example of an indoor testing for building components for measuring thermal transmittance particularly with reference standards IOS. 8990:1994 and ISO 12567- 1:2010. Indoor experiments generally have steady-state boundaries or pre-defined sequence. Weather conditions can be mimicked by different means of dynamic schedules, but they never represent the actual interaction with real climate. However, outdoor condition such as diffused radiation by the sky and ground are difficult to mimic. The following section provides extensive literature about used test cell for building component investigation.

Test cells are facilities which have an internal volume below  $8 \text{ m}^3$ , corresponding to internal dimensions of  $2 \text{ m} \times 2 \text{ m} \times 2 \text{ m}$  (LxWxH). They are utilised to characterise thermal and daylight performance for building components. Many studies used test cell method in their research. For example, study of Lopez et al. used a test cell method in order to investigate the thermal behaviour of a double glazing with a circulating water chamber [111]. In this study, the device contains a cubic box with an interior edge of 0.6 m and one open side. The stratigraphy of the test cell from the inside to the outside is: 12 mm thick plywood with anti-damp treatment, 160mm thick extruded polystyrene and 4 mm thick reflective insulation comprising an  $8 \mu\text{m}$  pure aluminium sheet and a 4 mm layer of polyethylene bubbles. The estimated thermal transmittance was about  $0.18 \text{ W/m}^2\cdot\text{K}$ .

Similarly, Olivieri et al. used the test cell to characterise the thermal, daylighting and electrical performance of semi-transparent photovoltaic modules and then contrast it with a code-compliant conventional glass [112]. The test cell is made of 160mm thick extruded polystyrene (XPS) board with phenolic plywood in both

sides and a protective plastic film as outer layer. The overall estimated thermal transmittance was about  $0.2 \text{ W/m}^2\cdot\text{K}$ . Piccolo study also used a small cubic test cell with the interior edge of 43 cm in order to examine the thermal and optical properties of a small-size double glazing unit where the outer pane has an electrochromic behaviour [90]. The thermal transmittances of the front-wall and the side wall of the test box were estimated to be 2.4 and  $1.2 \text{ W/m}^2\cdot\text{K}$ . Another experiment in Hong Kong Polytechnic University used test box to investigate the fluid flow in the air cavity and thermal performance of a double-sided façade with transparent thin-film or a-Si solar cells [113]. The testing facility is composed of two identical test cells. Each cell with the dimensions of  $1.22 \text{ m} \times 0.82 \text{ m} \times 0.9 \text{ m}$ .

In Lodie et al. study, they stated that the Test Reference Environment of Lleida (TRE-L) is composed by a thermally well insulated wooden box with external dimensions of  $2.06 \text{ m} \times 2.36 \text{ m} \times 0.37 \text{ m}$  and a support structure that let to incline the device [114]. The box walls are sandwich panels formed by 0.02 m thick plywood layers filled with a 0.2 m thick expanded polystyrene (EPS). The walls of box painted with white varnish to reduce the solar absorption. Their prototype had a south facing opening where a glass-Tedlars monocrystalline-Si PV module, dimensions of  $0.98 \text{ m}$  by  $1.51 \text{ m}$  is positioned.

Moreover, Ahmad et al. study examines the thermal performance of building components incorporating a phase change material coupled with a vacuum insulation panel (VIP) [115]. The two-test cell constructed includes one glazed face and five opaque faces insulated with VIPs. These placed on a frame made of white PVC profiles. One of the cells is equipped with five panels containing PCM, while the other is kept as reference.

In 2013, a round robin test box experiment started within IEA ECBCS Annex 58 “Reliable Building Energy Performance Characterisation Based on Full Scale Dynamic Measurements” [116]. The test box sent to various institutes in order to be monitored under different climatic conditions. Also, obtained dynamic data sets sent to different institutes to characterise the test box. The goal of this experiment was to explore the reliability of full-scale testing and dynamic data analysis, understand the effect of climatic conditions on characterisation,

present well-documented data set for validation and conclude the state-of-the-art and the next steps to do towards more complex (real) buildings. Test cells enable researchers to investigate building components in a way that allow to keep indoor conditions under control, while outdoor parameters vary as in real weather conditions.

#### **2.4 PDLC glazing performance parameters evaluation**

The PDLC switchable glazing is characterised by the ability to changing the optical properties under the power of voltage. Thus, it modulates the incoming solar radiation into a building to provide thermal and visual comfort according to users need. When such technology is integrated with building application, potential energy saving and enhanced daylighting are expected. To effectively investigate the switchable PDLC glazing to accomplish the energetic and environmental objectives, certain parameters must be considered. The following parameters are commonly selected to evaluate a switchable glazing [117–119]: a) switching speed; c) optical transmittance; d) solar heat gain coefficient (SHGC); e) thermal transmittance *U*-value.

The switching time is defined as the time required for the PDLC glazing to reach the maximum and minimum level of the transmittance. The switching time required for the PDLC glazing to switch to transparent state is  $\leq 100$  ms and  $\leq 10$  ms to the opaque state. A fast-switching time for smart glazing is desirable for energy efficiency and visual comfort. In contrary, smart glazings such as EC glazing suffer from slow switching speed, which takes up to 12 min depending on the size of the glazing to switch to the dark state [87]. Fast switching time gives the PDLC glazing an advantage over the other smart glazings. When the switching time is slow, the smart glazing takes longer time to optimize the transmittance against the external environmental conditions. This problem occurs with automated venetian blinds as when the activation time is longer the lighting energy consumption increases [120].

The optical properties of a glazing determine the amount of solar radiation that is transmitted, reflected, and absorbed by the glazing. The transmitted solar radiation through a glazing is absorbed by the interior room surroundings. Thus,

it influences the heat balance inside the room. In addition, the absorbed solar radiation by each layer of the glazing contributes to the heat gain inside the room. Therefore, these parameters are important to determine the  $u$ -value and SHGC. It is also noteworthy to mention that low values of solar radiation and visible transmittance in the opaque state are desirable as the PDLC glazing should provide shade and neutralise glare caused by the direct solar radiation. In addition, blocking as much as possible of solar radiation helps to reduce overheating and potentially results in reducing cooling load in summer months.

A small amount of solar radiation is reflected when the PDLC glazing is switched the opaque state. This means that the internal surface of the glazing absorbs a considerable amount of solar radiation, which then released into the indoor environment through convection and radiative heat transfer. Thus, in order to evaluate the energy performance of the PDLC glazing, solar heat gain coefficient should be considered as an important parameter. Building simulation study suggests that  $SHGC_{(bleached)}/SHGC_{(colour)} > 3$  should offer at minimum 10% energy saving compared to low-e glazing [121]. When indoor temperature is higher than the ambient air temperature, heat loss occurs through windows. They accounts for 40% of the total heat loss in buildings [122]. Highly efficient glazings that possess low  $u$ -value are desired to reduce the energy loss. Thus, it essential to determine the  $u$ -value of the PDLC glazing in the transparent and opaque state.

The current research aims to provide comprehensive analysis of the switchable PDLC glazing, which could help in defining the potential of the PDLC for building applications. The research undertakes two approaches to evaluate the PDLC glazing performance. First, experimental setup was used to investigate the thermal and daylight performance of the PDLC glazing in an indoor and outdoor environment. Second, building energy modelling was performed to evaluate the potential of energy saving in two climate zones using EnergyPlus simulation tool.

In order to perform the experimental investigation, test cells were required. Test cells fill the gap between the laboratory evaluation and full-scale buildings by enabling to control the indoor conditions and varying outdoor real weather conditions. Test cell setup is an excellent methodology to characterise a glazing



system under real weather conditions and in an indoor environment [112,123,124]. An insulated test cell is a representative of a small scale room [125] and allows the evaluation of thermal and daylight performance of a glazing [126]. Therefore, two test cells were fabricated to investigate the PDLC glazing. To ensure accurate measurements are obtained, several technical points were taken into account during the fabrication process and installation of the experimental setup as follows:

- Two test cells were designed to accomplish the purpose and the objective of the experiment.
- The test cells were fabricated using insulation board materials to ensure that one dimensional heat transfer was considered for the analysis and calculations.
- The test cells were positioned away from any obstruction or shading to ensure uniformed exposure to solar irradiance.
- The outdoor test cell was oriented to face south in order to perform full analysis and validate the collected data.
- The readings were taken for sufficient period of time to ensure different sky conditions were covered.
- Convenient temperature sensors with good accuracy were selected to ensure reliable data was collected.
- The daylight sensors (lux meters) were selected with spectral sensitivity that is visible to the human eye in wavelength between 350 and 750 nm.
- High industrial quality data logger was utilised for data collection and was compatible with the daylight and temperature sensors.
- All components were selected to withstand temperature of 60 °C.
- All electrical components were housed in a weatherproof enclosure to avoid any interruption for the data collection.

For the indoor experiment, the solar irradiance was replaced with AAA type solar simulator, which has similar spectrum to the solar radiation between 250 nm and 3000 nm. In order to calculate the  $u$ -value and SHGC, the readings were collected when the PDLC glazing surface temperatures achieved a steady state. For the outdoor experiment, the PDLC glazing was investigated with and without solar

control film to characterise the thermal and daylight performance under different sky conditions. The data was collected every five minutes from 9:00 to 17:00. Figure 2-1 presents a schematic diagram of the experimental methodology.

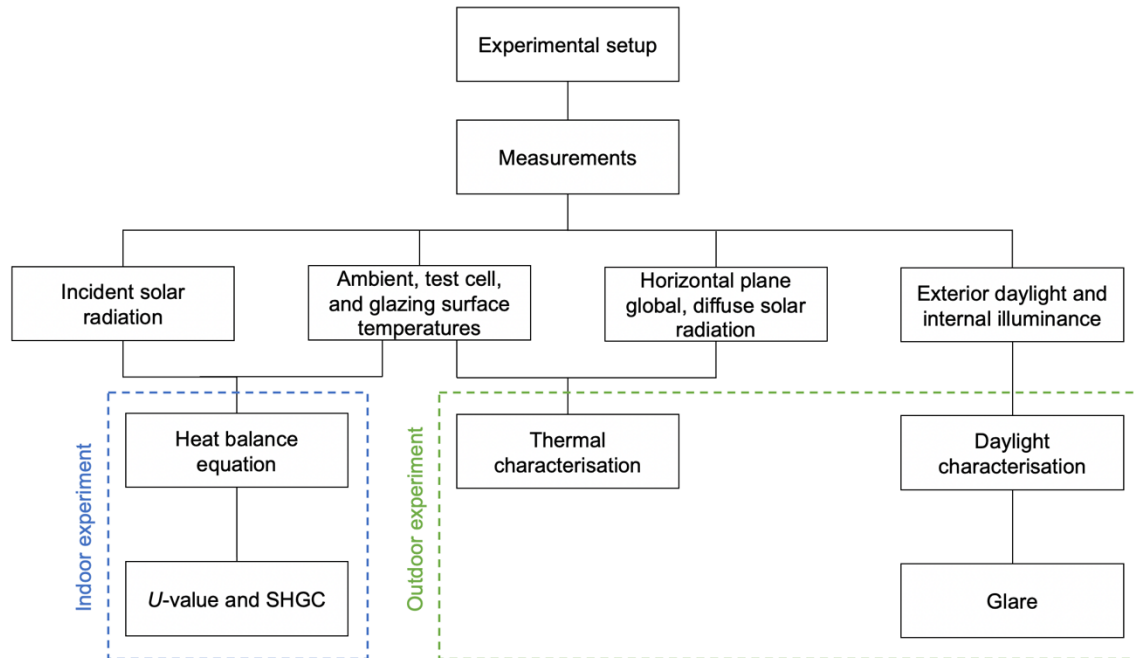


Figure 2-1. Shows a schematic diagram of the experimental methodology.

Building Energy Modelling (BEM) was utilised to perform energy and daylight analysis for the PDLC glazing by employing an office building for two climate zones. The analysis focus was assessing the potential of the PDLC glazing to reduce heating, cooling, and artificial lighting loads using two shading control strategies to control the PDLC glazing transmission. Building energy modelling is the activity of performing computer-based simulation tool to acquire detailed information of a building’s energy use and daylight visual comfort. The simulation tool uses an enhanced mathematical model that provides an approximate representation of the building energy and daylight performance. Thus, it is important to properly model window heat transfer mechanism to assess the effect of enhanced window design on building energy consumption and occupant comfort. The mechanism include conduction through glazing, solar heat gain, daylighting, and natural ventilation. EnergyPlus has a library that contains over 200 glazing systems built up of entries from the glass including single glass, double glass, and triple glass window with different tints, coatings, gas fills and

glass thickness [127]. EnergyPlus uses heat balance and daylight comfort equations to determine the performance of a window.

In this regards, EnergyPlus was utilised to investigate the impact of the PLDC glazing on heating, cooling, and artificial lighting loads and daylight performance, for an office building using solar radiation and outdoor temperature to control the switchable PDLC glazing. The energy modelling simulation was performed for Riyadh, Saudi Arabia (arid climate zone) and London, United Kingdom (temperate climate zones). The results of the energy and daylight performance of the switchable PDLC glazing was compared to a double-glazing reference window. Figure 2-2 illustrates a schematic diagram of the building energy simulation study.

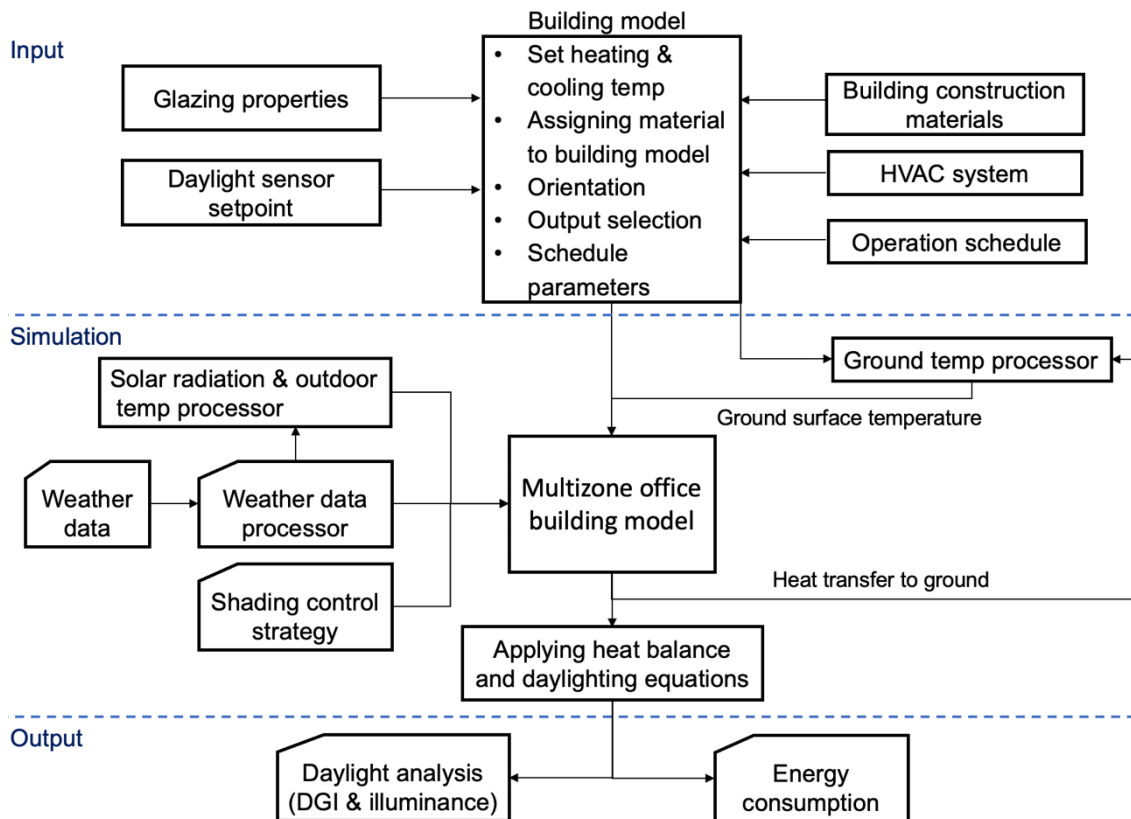


Figure 2-2. Illustrates a schematic diagram of the building energy modelling.

## 2.5 Description of PDLC glazing system

PDLC switchable film is an electrically actuated film that changes transparency from transparent (On state) to opaque (OFF state) when power is applied. PDLC

switchable film was selected to investigate its suitability for building application. The PDLC switchable film used in this research consists of a 20  $\mu\text{m}$  polymer layer sandwiched between two 188  $\mu\text{m}$  ITO layers. The film was sandwiched between two low iron glasses where each glass was 4 mm thick. Different sizes of PDLC glazing were used in this research. Details of the PDLC film is shown in Table 2-1.

Table 2-1. Details of PDLC film in transparent (On) and opaque (OFF) state.

		Mode	Specification
<b>Optical</b>	Visible Light Transmission	On	83
		OFF	55
	Viewing Angle	On	>140
<b>Electrical</b>	Operate Voltage	On	AC/V (50/60 HZ)
	Response time	On $\rightarrow$ Off	ms $\leq$ 100
		Off $\rightarrow$ On	ms $\leq$ 10

### 2.5.1 PDLC glazing for indoor experiment

A small size PDLC switchable glazing was used in the indoor experiment to calculate the SHGC and  $U$ -value. A schematic diagram of PDLC switchable glazing in both transparent and opaque state is shown in Figure 2-3.

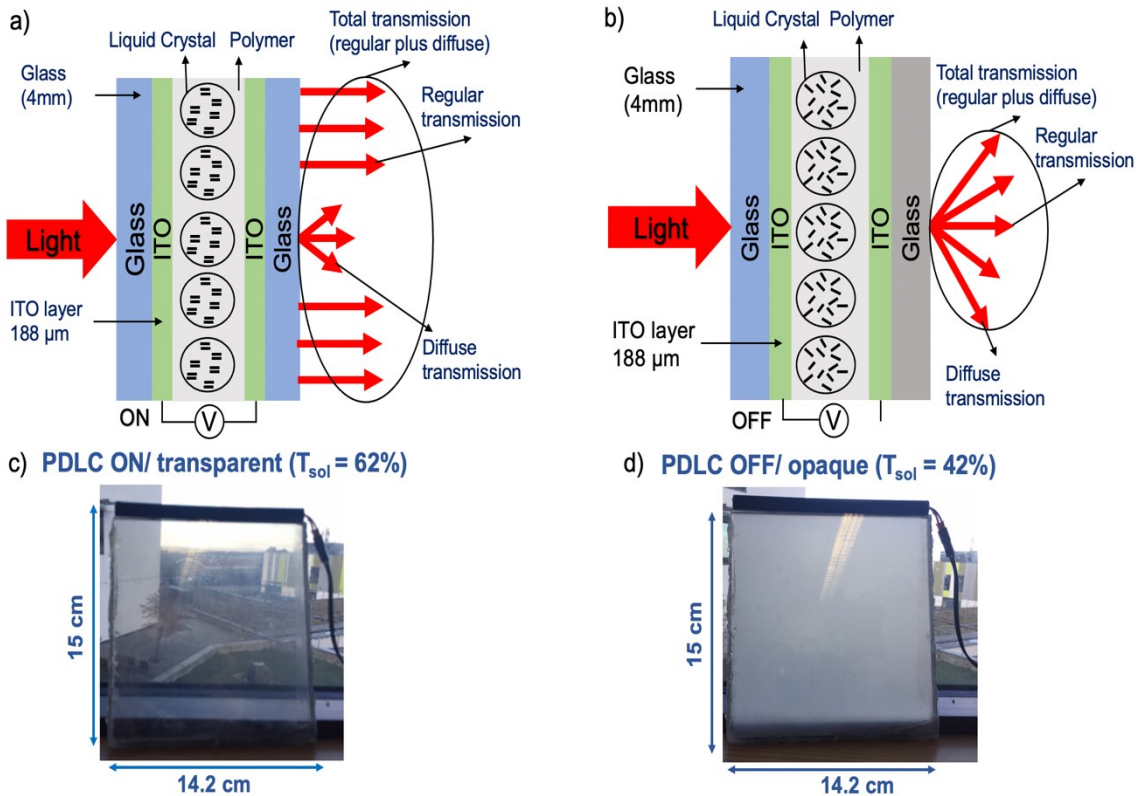


Figure 2-3. Illustration of the light transmission through the PDLC glazing. a) Shows the particles are aligned when power is ON resulting the light to pass through the glazing. b) The particles are randomly aligned causing the light to scatter when the power is OFF. c) Actual photograph of the PDLC glazing in the transparent state. d) Actual photograph of the PDLC glazing in the opaque state.

### 2.5.2 PDLC glazing for outdoor experiment

For outdoor experiment an A4 size PDLC glazing was employed to characterise thermal and daylight performance. Figure 2-4 shows a photograph of the PDLC switchable glazing in transparent (On) and opaque (OFF) state.

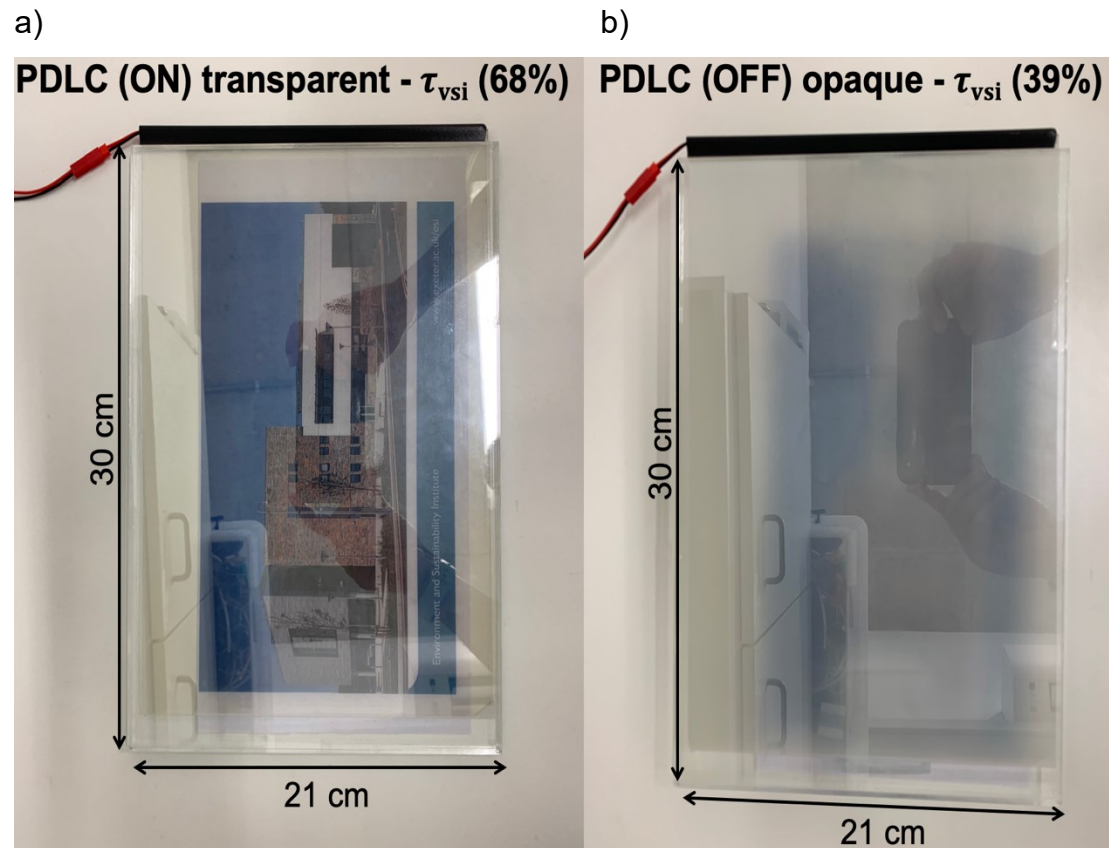


Figure 2-4. a) shows an actual photograph of the PDLC glazing in transparent state (On). b) The PDLC glazing in the opaque states (Off).

### 2.5.3 PDLC glazing combined with solar control film

Solar control film was considered to investigate its effect on solar heat gain and glare discomfort. The solar control film was attached to an A4 size PDLC glazing. The combined glazing then was investigated in outdoor under real weather condition. The thickness of the solar control film was 62  $\mu\text{m}$ . This combined glazing was employed to characterise thermal and daylight performance for different sky condition. Schematic diagram of the combined glazing is shown Figure 2-5. Table 2-2 shows the solar control film details.

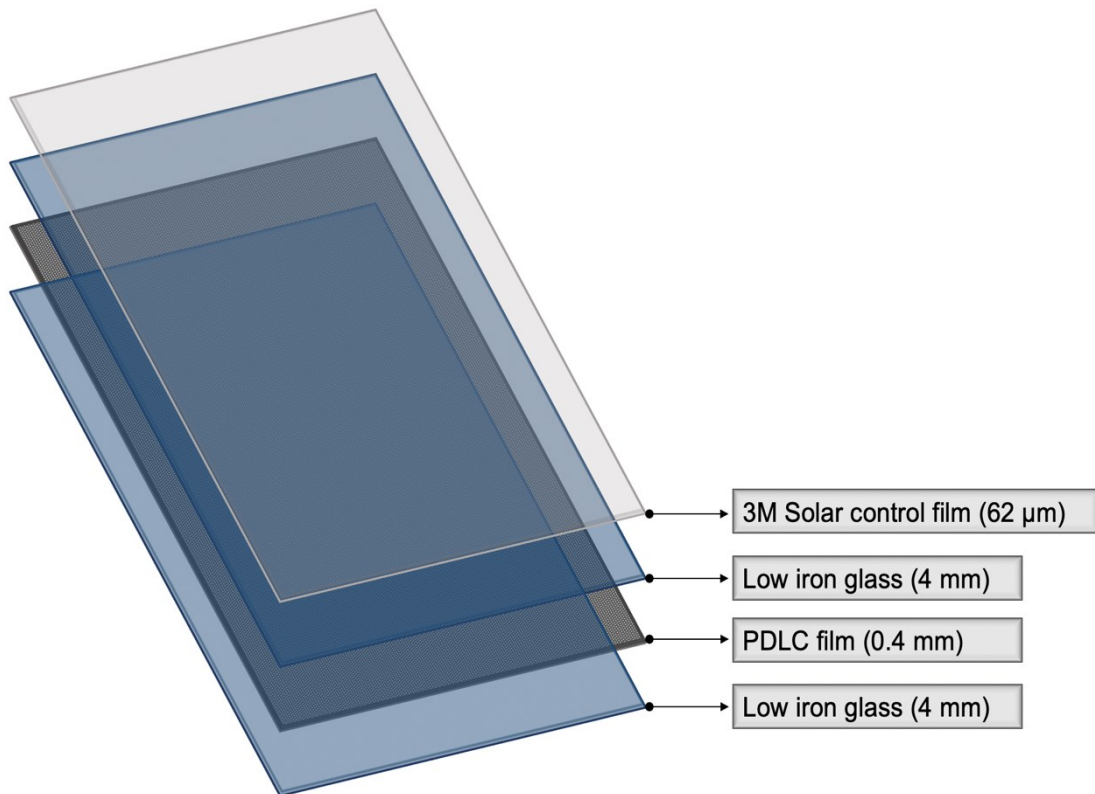


Figure 2-5. Schematic diagram of the combined PDLC glazing with solar control film.

Table 2-2. Solar control film specification.

	Thickness	Visible Transmission	Visible Reflection Exterior	Visible Reflection Interior
<b>3M film</b>	62μm	70%	7%	7%

#### 2.5.4 Spectrophotometer measurement

The measurements were undertaken using a Perkin Elmer® Lambda 1050 UV/VIS/NIR spectrophotometer to measure the solar transmittance, reflectance, and absorptance of the PDLC glazing systems for the transparent and opaque state. The instrument features a double-beam; double-monochromator; ratio recording optical system; and a LabSphere 150mm. The sphere feature enables an effective collection surface for the detectors, equivalent to the sphere input ports area (1 in. /25.4 mm). Figure 2-6 illustrates the schematic diagram of Perkin Elmer® Lambda 1050 UV/VIS/NIR spectrophotometer. The optical measurements of the PDLC glazings and PDLC glazing with solar control film are provided in Table 2-3.

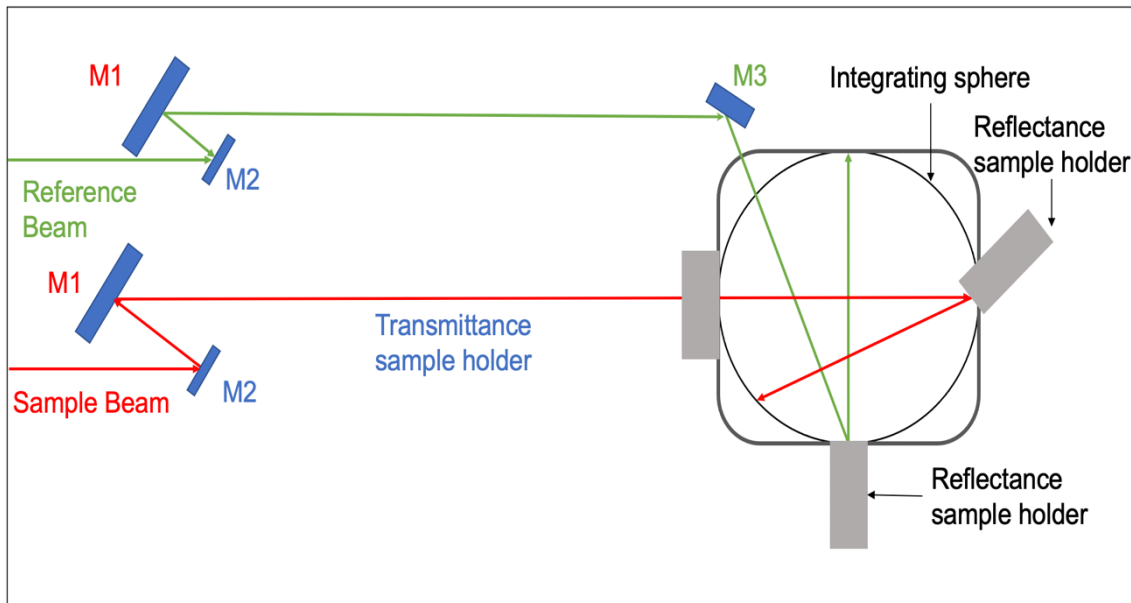


Figure 2-6. Schematic diagram of Perkin Elmer® Lambda 1050 UV/VIS/NIR spectrophotometer. M1, M2, and M3 are mirrors reflecting the sample beam and reference beam.

Table 2-3. Details of the glazing used in the experiments.

	Dimension (m)	Transmission (ON/OFF)	Visible transmittance	Supplier
<b>PDLC (indoor)</b>	0.15 × 0.14	62% / 42%	79% / 44%	HOHO industry
<b>PDLC (outdoor)</b>	0.30 × 0.21	49% / 28%	68% / 39%	HOHO industry
<b>PDLC with 3M film</b>	0.30 × 0.21	17% / 13%	54% / 28%	N/A

## 2.6 Description of test cell

Two test cells were fabricated in the solar lab in University of Exeter using polyisocyanurate (PIR) material. The first test cell was used for the indoor characterisation to determine  $U$ -value and SHGC. The test cell walls thickness were 0.025 m and the dimensions were 0.36 m × 0.19 m × 0.25 m. Figure 2-7 shows a photograph of the test cell. The test cell was equipped with temperature sensors and a data logger to collect the data. Details of the instruments are shown in Table 2-4. The second the test cell was used for the outdoor experiment and its exterior was covered with aluminium sheets to minimise thermal disturbance and protects it from rain, dust, and bad weather. The test cell dimensions were 0.9 m × 0.9 m × 0.9 m. Figure 2-8 shows schematic diagram of



the outdoor test cell. It was placed in University of Exeter, in top of the ESI building in the north roof. It was positioned to face south orientation to unobstructed view to the solar radiation. The test cell represented a small unfurnished room with 1:8 window to wall ratio. The thermal conductivity of the polyisocyanurate and the aluminium were 0.022 W/m·K and 160 W/m·K, respectively. Several sensors and instruments were attached to the test cell. Details of the sensors and equipment are listed in Table 2-5

Table 2-4. Details of instrument for the indoor experiment.

<b>Instrument</b>	<b>Specification</b>	<b>Measurement</b>
<b>Thermocouple</b>	T type	Temperature
<b>Data logger</b>	Picolog: High resolution and accuracy, temperature range (-270 to 1820 °C)	Record data
<b>Solar simulator</b>	AAA Type, class A spectral match	Incident solar radiation

Table 2-5. Details of the instrument for the outdoor experiment.

<b>Instruments</b>	<b>Specification</b>	<b>Sensitivity</b>	<b>measurement</b>
<b>Thermocouple (K Type)</b>	-40 °C < t° < 1000 °C Accuracy = ± 1.5°C	N/A	Temperature
<b>Light sensors (MESA)</b>	Operating temperature (-40 °C to 60 °C)	Spectral response (350 to 750 nm)	Illuminance
<b>Light sensors (CS300)</b>	Operating temperature (-40 °C to 70 °C)	Spectral response (360 to 1120 nm)	Illuminance
<b>Pyranometer (CMP)</b>	Range (0-2000 W/m <sup>2</sup> 40), O.P temperature (-40 °C to 80 °C)	7 to 14 μV/W/m <sup>2</sup> , Spectral response (285 to 2800 nm)	Solar irradiance (global plus diffuse)
<b>Data logger (CR1000X)</b>	Accuracy: ±3 min per year, Resolution: 1 ms	N/A	Data recording

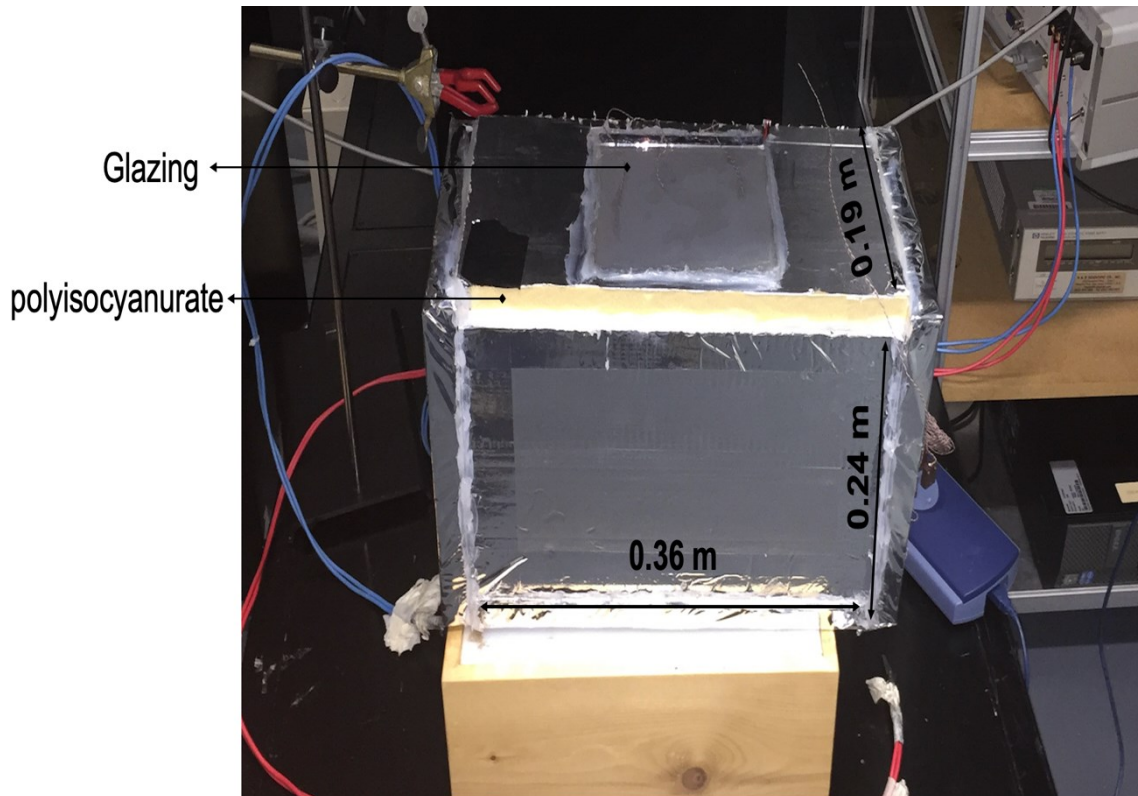


Figure 2-7. Photograph of the test cell that used to investigate the PDLC in an indoor environment.

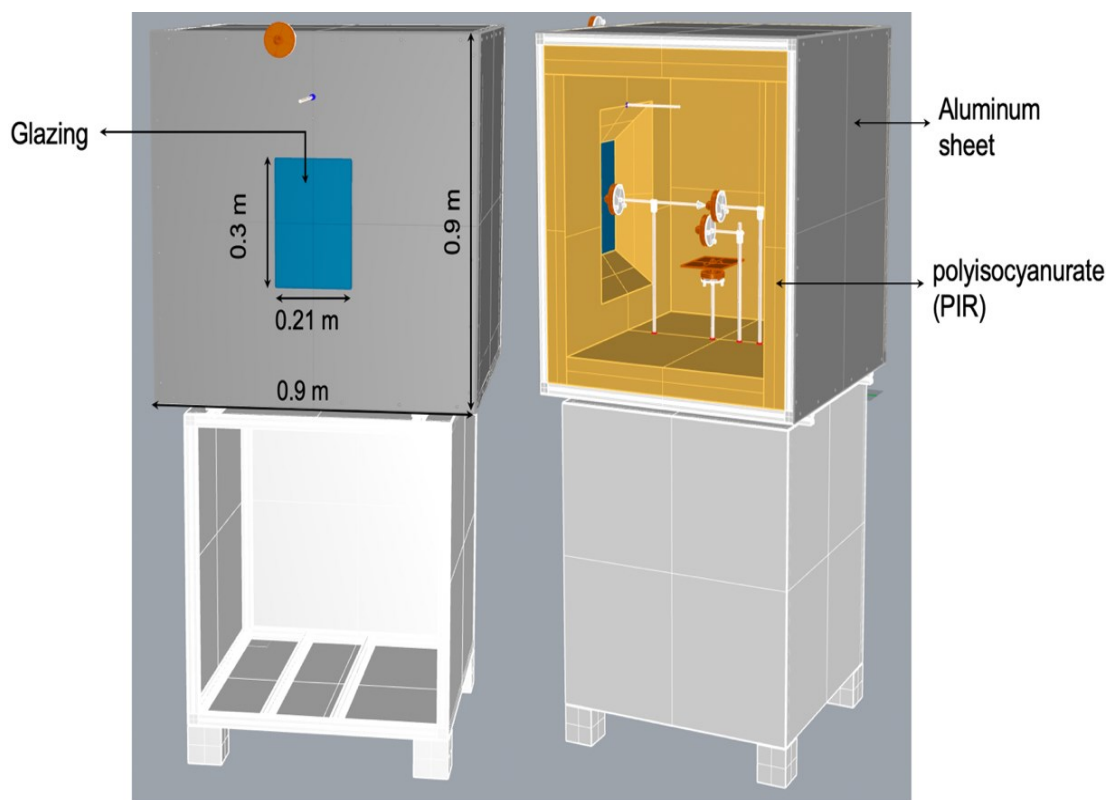


Figure 2-8. Schematic diagram of a test cell used for the outdoor investigation.

## 2.7 Experimental setup

### 2.7.1 Indoor experiment

To calculate the  $U$ -value and SHGC key data were required to be measured such as incident solar radiation, ambient temperature, PDLC glazing surfaces temperature, internal test cell temperature. All temperatures were measured using T type thermocouples. External and internal surface temperature of the glazing were measure using one thermocouple for each surface. To measure the internal and ambient temperature, a thermocouple was placed in the centre of the test cell and another was placed 10 cm away from the test cell, respectively. A solar simulator type AAA was employed to simulate the solar irradiance at various intensities (1000, 800, 600, 400  $W/m^2$ ). All thermocouples were connected to a Pico data logger to record the temperature data every 5 minutes. The data logger was connected to a computer where the data was retrieved from. Figure 2-9 shows a photograph of the indoor experiment. Details of the instruments used are presented in Table 2-4. All mathematical equations used to calculate  $U$ -value and SHGC are provided in Chapter 3.

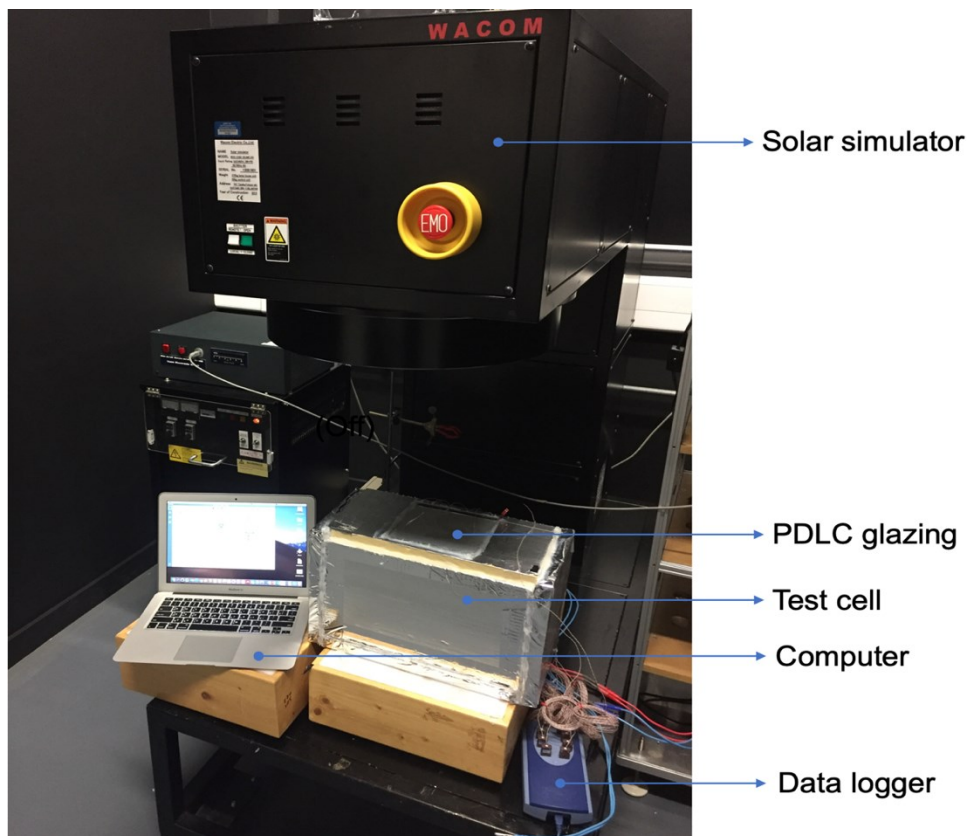


Figure 2-9. Photograph of the indoor experimental setup.

## 2.7.2 Outdoor experiment

The PDLC glazing was investigated under real weather condition to evaluate thermal and daylight glare performance. The PDLC glazing combined with solar control film was also investigated.

### 2.7.2.1 Thermal characterisation

The experiment was performed for 26<sup>th</sup> of March to 24<sup>th</sup> of September of 2021. Thermal characterisation was investigated for the PDLC glazing for different sky conditions from 9:00 to 17:00. The focus of the experiment was to study the thermal behaviour of the PDLC glazing for south orientation. Figure 2-10 show a photograph of the experiment. To perform the experiment real weather data was required to be measured such as horizontal global solar irradiance ( $I_{h,g}$ ), horizontal diffuse solar irradiance ( $I_{h,d}$ ) using two pyranometers. Four K type thermocouples were used to measure the temperature in the test cell. Temperature data for ambient, glazing surfaces, and internal temperature of the test cell were required to evaluate thermal behaviour of the PDLC glazing. The PDLC glazing surfaces temperature were measured using two thermocouples placed in the centre of each surface. The thermocouple that was attached to the external surface of the PDLC glazing was covered with aluminium foil for protection and to avoid solar heat gain from the solar radiation. The internal test cell temperature was measured using one thermocouple placed in the centre of the test cell. To measure the ambient temperature a thermocouple was placed on top of the test cell. Four thermocouples in total were used to collect the required temperature data and they were all connected to CR1000x data logger. The same procedures and instrument were used to characterise the PDLC glazing combined with solar control film. Figure 2-11 shows a photograph of the PDLC glazing combined with the solar film. The interval time for recording the data was every five minutes. The recorded data was retrieved from a computer that was connected to the data logger. Table 2-5 provides detail of the instruments used in the experiment.

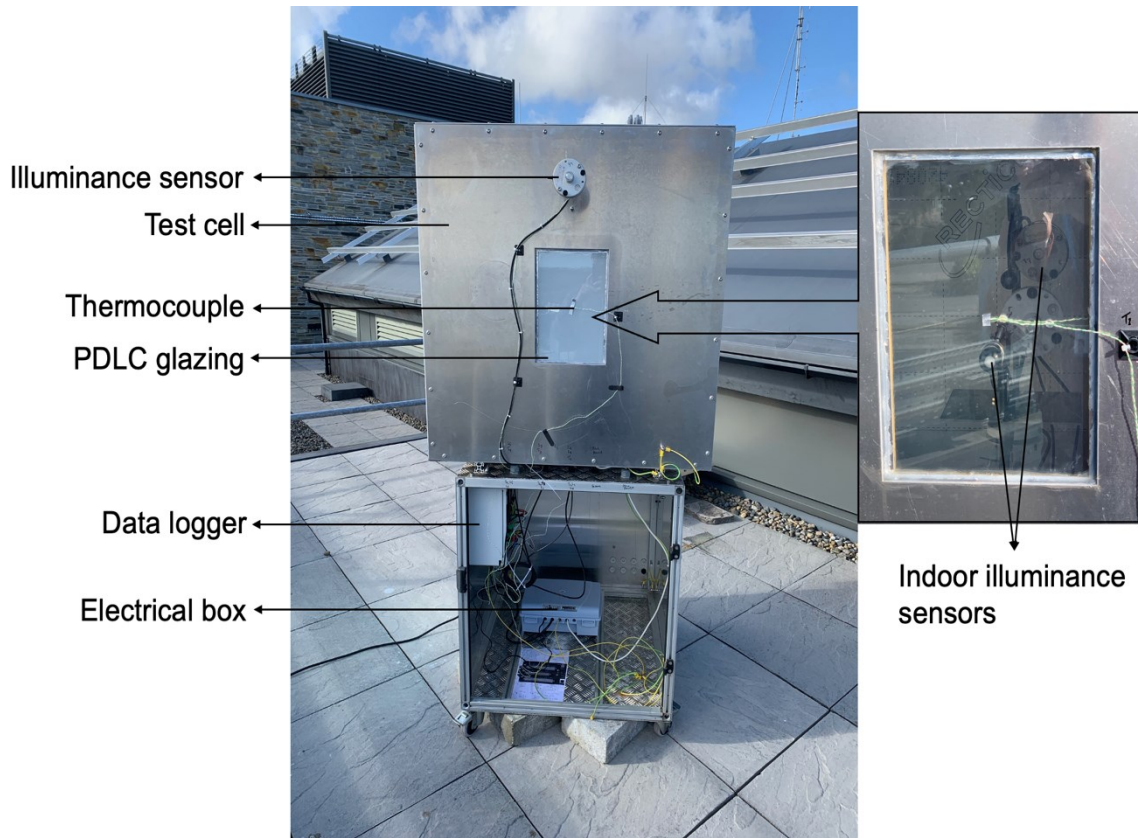
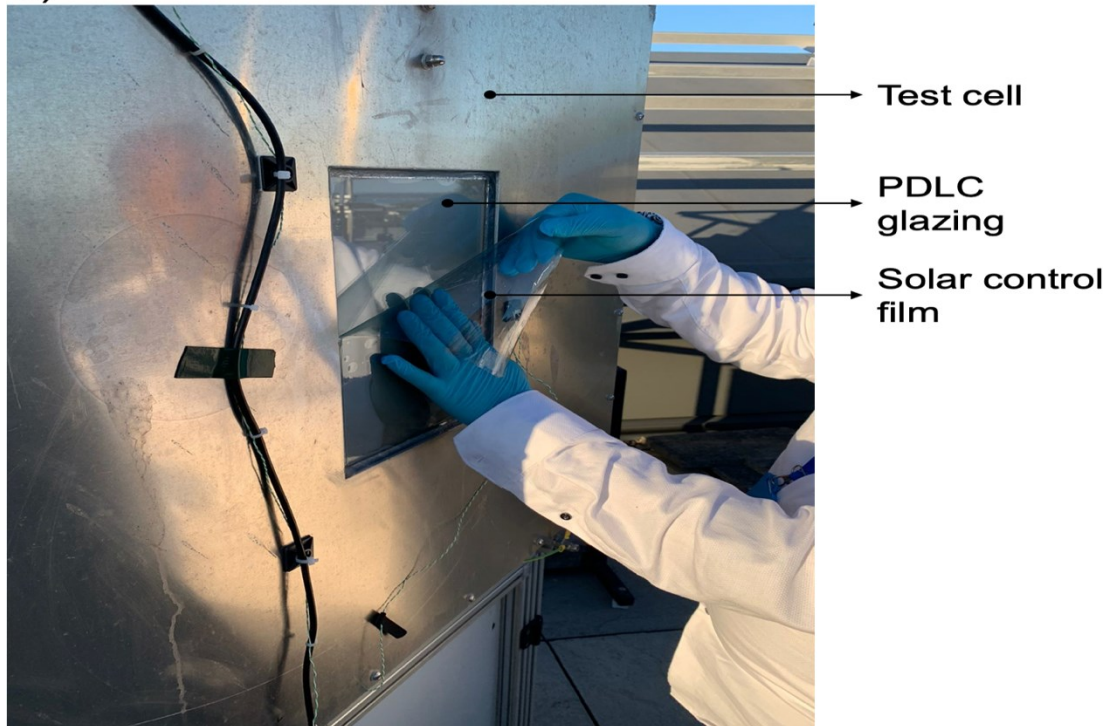


Figure 2-10. Photograph of the outdoor experiment showing the sensors and equipment.

a)



b)

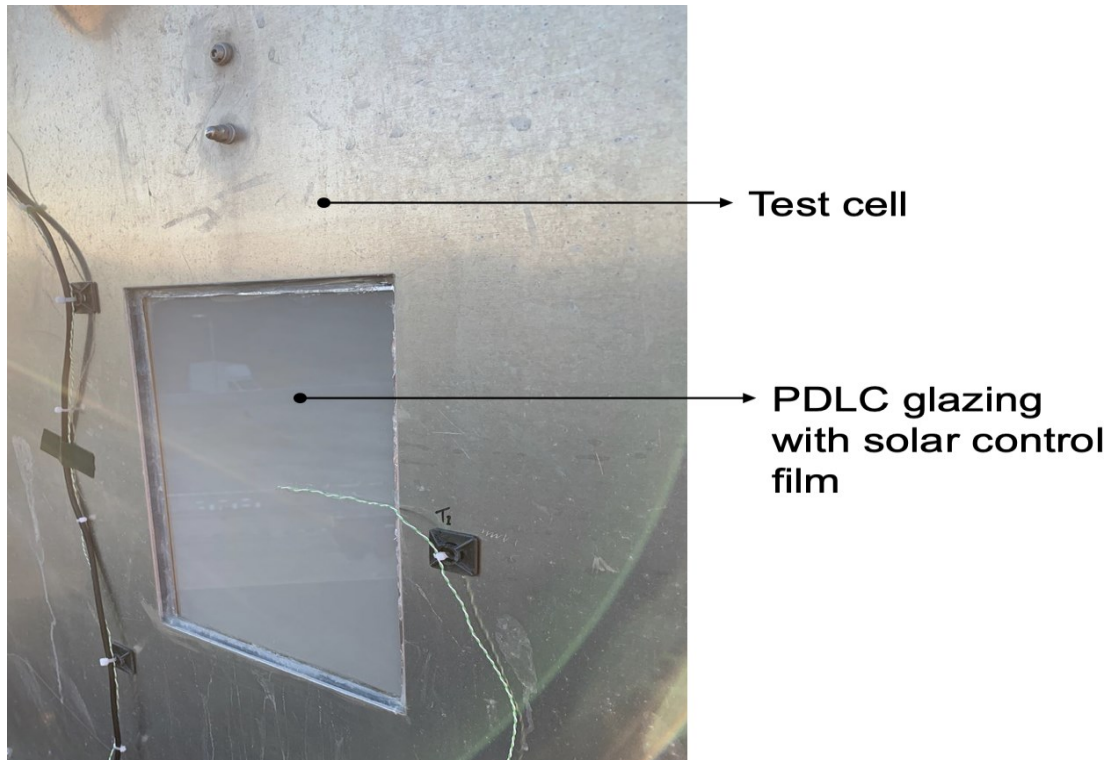


Figure 2-11. Photograph of PDLC<sub>F</sub> glazing combined with the solar film. a) shows applying the solar film on the glazing. b) shows the PDLC<sub>F</sub> glazing with the solar control film.

### 2.7.2.2 Daylight glare characterisation

To perform daylight glare analysis illuminance values were required to be measured. Four illuminance sensors (lux meter) were employed to measure the illuminance outside and inside of the test cell at different locations. The exterior illuminance ( $L_{ext}$ ) was measured using MESA lux meter and was placed on the vertical surface of the front side of the test cell. The sensor was equipped with a transparent filter to measure spectral range visible to the human eye in wave lengths of 350 to 750 nm. The other three sensors were placed inside the test cell at different locations. One sensor was placed 1 cm behind the PLDC glazing ( $L_i$ ) to measure the illuminance transmitted through the glazing. The interior illuminance ( $L_{win}$ ) was measured by a sensor that was placed 45 cm away from the front wall and was facing the centre of the glazing. Another sensor was placed on a work plane 35 cm away from the front wall to measure the horizontal

illuminance ( $L_h$ ). All light sensors were calibrated by the manufacture. Figure 2-12 a schematic diagram illustrates the location of the sensors.

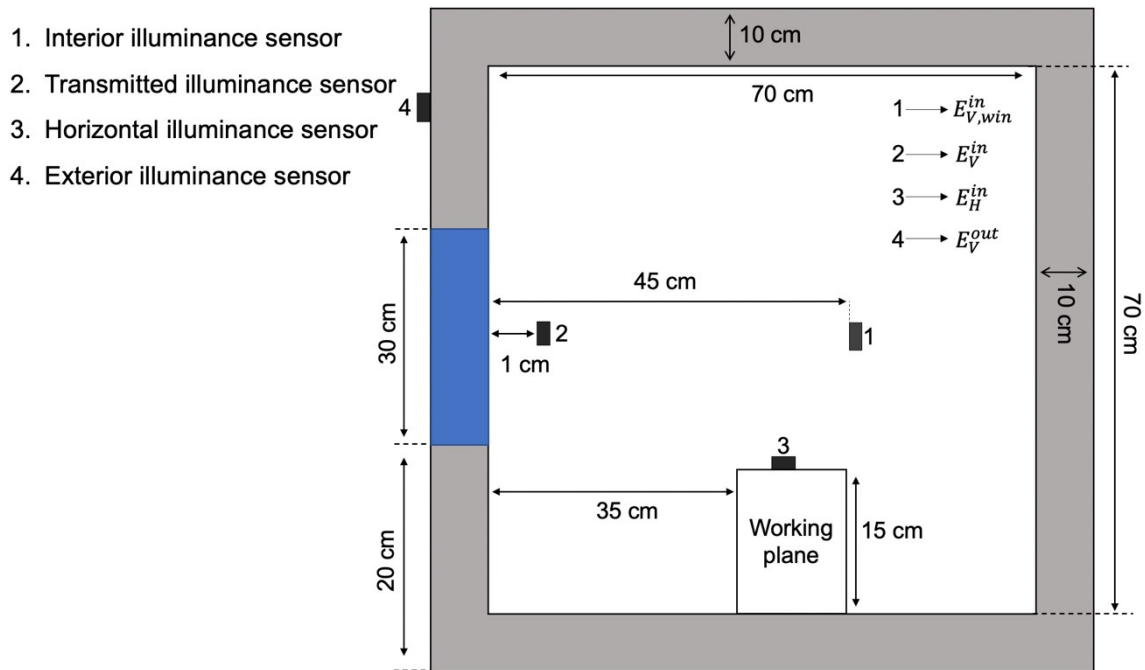


Figure 2-12. Schematic diagram illustrates the locations of the sensors.

## 2.8 Simulation modelling

In this section, the energy building modelling for the PDLC window is discussed. Energy simulation study was performed to evaluate the effect of PDLC Window on cooling, heating, and artificial lighting loads for two contrasting climate zones and the results were compared against a double pane reference window. The building model was developed utilising Rhinoceros© modelling tool, integrated with a graphical algorithm editor Grasshopper© [128]. The software has excellent capabilities that enable modelling for energy and daylight simulation. Several scripts have been developed and integrated with Grasshopper© tool to perform building energy simulation such as Ladybug and Honeybee [129]. Grasshopper© can provide components such as EnergyPlus/ OpenStudio and Radiance/ Daysim to perform thermal and daylight analysis. This software was utilised as the main tool to perform building energy simulation for the PDLC switchable window to evaluate the cooling, heating, and artificial lighting loads, and daylight performance for a two-story office building. Building model, shading control

strategies used, and climate zones in the energy building modelling are discussed in the following sections.

### **2.8.1 Building model**

In order to evaluate the impact of PDLC window in enhancing the energy performance of an office building the heating, cooling, and artificial lighting loads and daylight performance were investigated using EnergyPlus 8.9. The developed prototype building is a model with ideal constructions that meet the minimum requirements of ASHRAE standards 90.1 [130]. Figure 2-13 shows the building model, which comprises four perimeter zones and two core zones. The model envelope properties were constructed as required by the American Society of Heating, Refrigerating and Air-conditioning Engineers ASHRAE standards. EnergyPlus allows users to add building envelop components from its database library, thus the exterior walls and reference window were selected to perform the building energy simulation [131]. Table 2-6 provides the envelope properties of the model building. The selected model is a two-story office building with a total conditioned area of 4391.29 m<sup>2</sup>, a floor height of 3 m, and a 60% window to wall ratio.

Table 2-7 presents the optical and thermal properties of the PDLC and reference window. The reference window was selected from the EnergyPlus database library according to the insulation requirements of ASHRAE standards 90.1 [132]. The PDLC glazing properties were obtained from the indoor experiment results as reported in Table 3-3 and Table 3-4. An ideal air load system was adopted from the EnergyPlus library and used as a HVAC system to eliminate mechanical related problems. The heating and cooling setpoint during occupied hours were set to 20 °C and 26 °C. The internal load contributed by equipment was 7.6 W/m<sup>2</sup>, artificial lighting was 11.8 W/m<sup>2</sup>, and people were 0.0565 person/ m<sup>2</sup> as recommended by ASHRAE standards [132]. The operation schedule was selected adopting a typical office building type starting from 8:00-16:00 hrs from Monday to Friday.



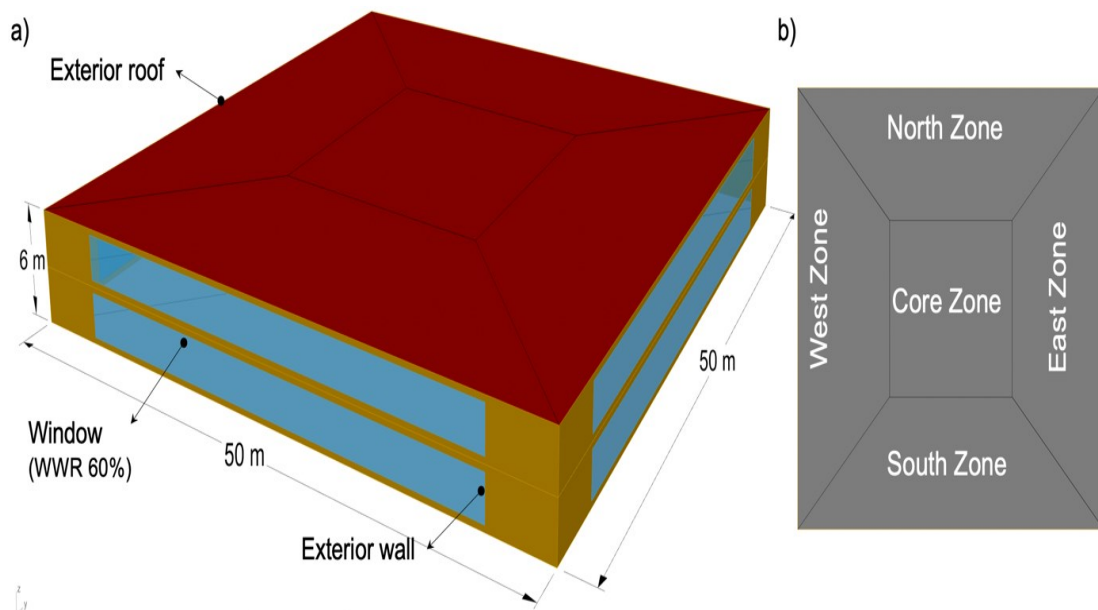


Figure 2-13. a) The picture presents a two-story office building model with 60% window to wall ratio. b) shows the perimeter zones.

Table 2-6. The envelope properties of the building model according to ASHRAE standards 90.1.

Construction	United Kingdom	Saudi Arabia	Reference
	$U$ -Factor [ $W/m^2 \cdot K$ ]	$U$ -Factor [ $W/m^2 \cdot K$ ]	
Exterior Wall	0.591	2.377	[132]
Exterior Roof	0.273	0.358	
Exterior Floor	2.945	2.945	

Table 2-7. Details of the optical and thermal properties of the PDLC and reference windows.

Properties	PDLC OFF (opaque)	PDLC ON (transparent)	Reference window
Visible transmittance	44%	79%	81%
SHGC	0.63	0.68	0.76
$U$ -value	2.44 $W/m^2$	2.79 $W/m^2$	3.1 $W/m^2$
Reference			[132]

## 2.8.2 Shading control strategy

The PDLC switchable window can be operated by electrical power to switch to ON/OFF state; its optical and thermal properties can be controlled by users. The shading control of the PDLC can be categorised by manual control according to user needs and automatic control by the external environmental conditions. The automatic control includes variables such as outdoor temperature, indoor temperature, solar radiation, and external illuminance. From the user perspective, the objective of the PDLC switchable window is to control its properties in order to obtain indoor comfort. The objective of this study is to assess the PDLC performance at the highest and lowest temperatures for the selected climates. The highest and lowest temperature vary significantly and to achieve better evaluation another temperature 20 °C was chosen to evaluate the PDLC performance at the same outdoor temperature in two contrasting climate zones. Therefore, the control strategy is limited to external environmental conditions in relation to outdoor temperature and solar radiation in order to achieve the optimum control variables.

In this study, the PDLC window was controlled by the solar radiation and the outdoor temperature. Each control strategy contained several variables and each variable was simulated independently in both strategies to avoid contradictions in the algorithm logic. Figure 2-14 illustrates the switching logic of the PDLC window where only one variable is selected to perform the simulation. The PDLC window was controlled by various solar radiation levels upon vertical surfaces of the window. In addition, several outdoor temperature variables including the minimum and maximum temperatures were used to control the PDLC window. The PDLC shading control variables utilised in this study were set as follows:

1. The PDLC window was controlled by changing the solar radiation levels on the vertical window surface. When the solar radiation on the window surface exceeded the thresholds of 100 W/m<sup>2</sup>, 250 W/m<sup>2</sup>, 500 W/m<sup>2</sup>, 750 W/m<sup>2</sup>, and 1000 W/m<sup>2</sup>, the PDLC window changed to opaque; otherwise, it became Transparent.

- The PDLC window was controlled by changing the outdoor temperature. When the ambient temperature exceeded thresholds the state of PDLC window changed to opaque, and if not, it remained transparent. The selected temperatures for Riyadh and London are shown in Table 2-8.

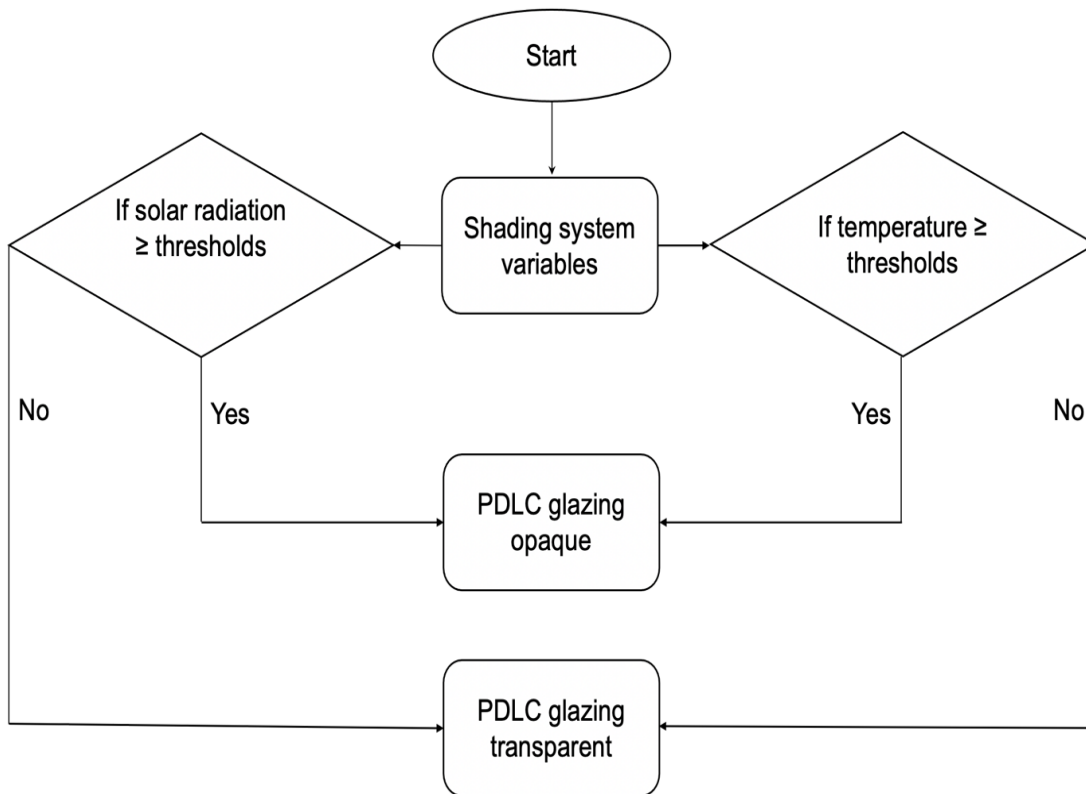


Figure 2-14. Workflow chart that illustrates the shading control strategy logic. The system simulates each variable independently for each control strategy.

### 2.8.3 Weather Data and Climate Zone

This simulation study utilised the weather data available on the EnergyPlus website [133]. Both cities (Riyadh, Saudi Arabia and London, United Kingdom) used in this study were a representative of the climate characteristics for each climate zone. Riyadh and London climate zones were classified according to Köppen-Geiger climate system [134]. Riyadh is located in Saudi Arabia (24°38N 46°43 E) and has an arid climate. The weather in Riyadh is hot and dry during the summer season where the maximum temperature reaches 46 °C, while in the winter the temperature drops to 4 °C. London is located in the United Kingdom (51°30 N 0°39 W) and has a temperate oceanic climate. In London, the annual

maximum temperature in summer is 31.3 °C, while in the winter is -5.9 °C. Table 2-8 reports the weather temperature in both cities. Figure 2-15 presents a comparative analysis of the monthly average temperature of Riyadh and London. The graph shows that Riyadh has higher monthly average temperatures in the summer months compared to London. This reflects the importance of air conditioning systems in Riyadh as more energy required to obtain thermal comfort in the summer. In contrary, London has lower monthly average temperature in the winter months indicating more heating load consumption compared to Riyadh.

The maximum and minimum temperature of Riyadh and London are utilised to develop a shading control strategy for each climate zone. The shading control strategy is used to control the transmittance of the PDLC glazing by utilising weather data variables. For Riyadh, the variables used for the shading control strategy are 46 °C as maximum temperature and 4 °C as minimum temperature. For London, the variables are 31.3 °C as maximum temperature and -5.9 °C as minimum temperature. For more details regarding the shading control strategy see section (2.8.2).

Table 2-8. Weather data for Riyadh and London climate zones.

		<b>Riyadh</b>	<b>London</b>
<b>Air Temperature (°C)</b>	Max	46	31.3
	Min	4	-5.9
	Average	26.2	10.2

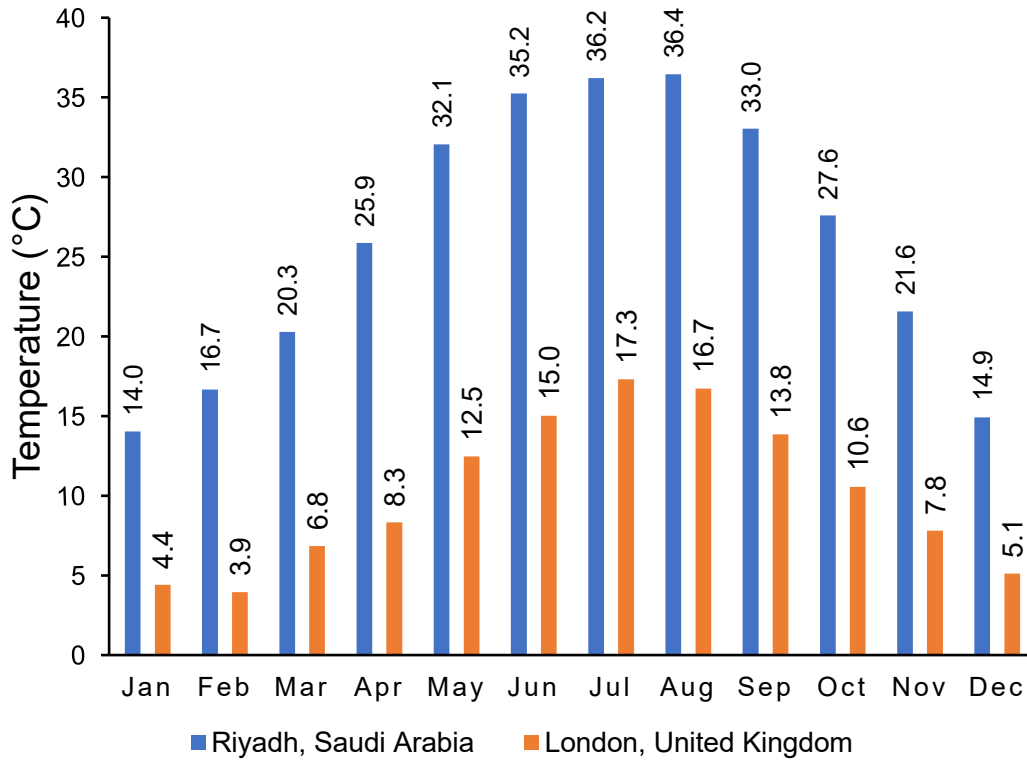
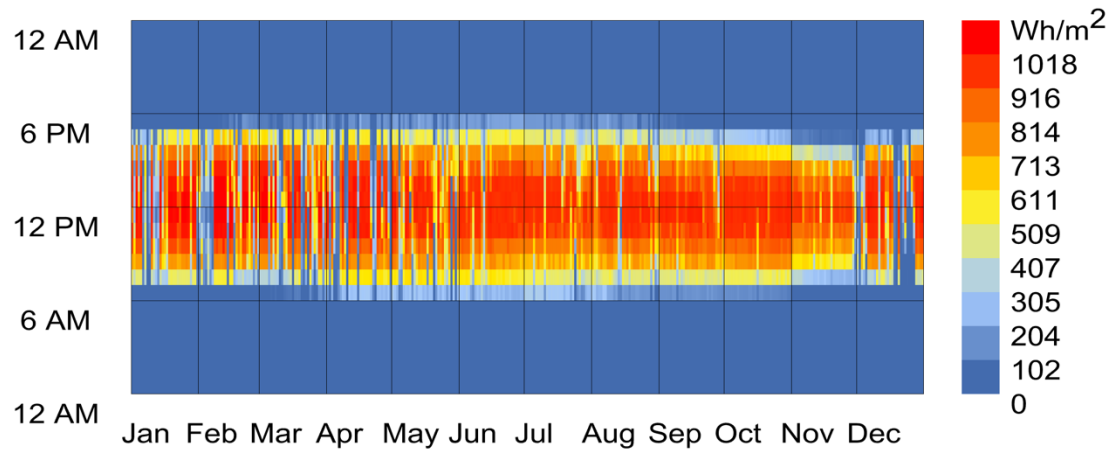


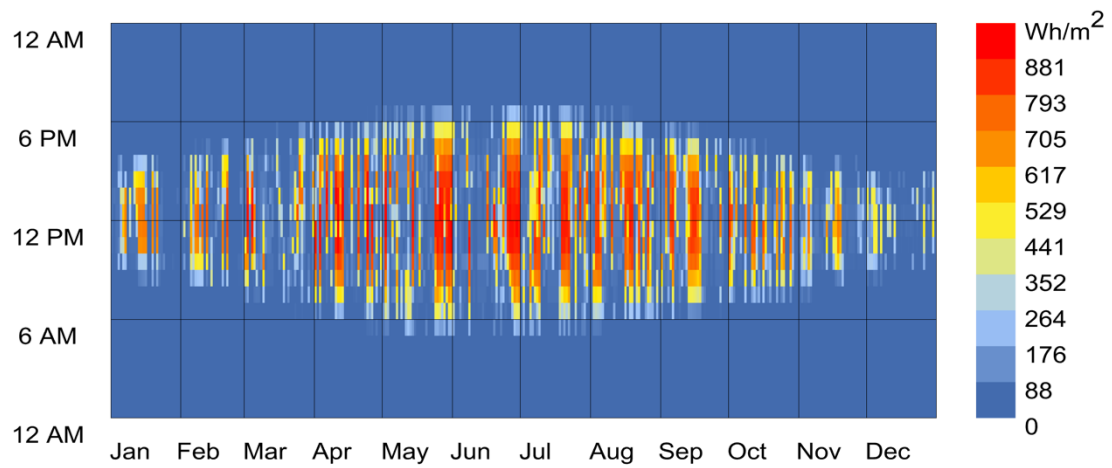
Figure 2-15. Comparative analysis of monthly average temperature for Riyadh and London climate zones.

Figure 2-16-a reports the hourly direct solar radiation in Riyadh, Saudi Arabia and London, United Kingdom. The annual direct solar radiation in Riyadh varies from a minimum of  $102 \text{ W/m}^2$  to a maximum of  $1018 \text{ W/m}^2$ . In general, Riyadh receives high amount of direct solar radiation throughout the year. However, in the summer months the amount of direct solar radiation is higher than the rest of the year. In London, the amount of direct solar radiation ranges from  $88$  to  $881 \text{ W/m}^2$  from January to December. Figure 2-16-b shows a comparison of the monthly average of the amount of direct solar radiation between Riyadh and London. The graph shows a clear difference in the monthly average amount of direct solar radiation between Riyadh and London. The highest average value for direct solar radiation in Riyadh can be seen in July ( $317 \text{ W/m}^2$ ), whilst in London it can be seen in May ( $143 \text{ W/m}^2$ ). The lowest average amount of direct solar radiation can be seen in December for Riyadh ( $119 \text{ W/m}^2$ ) and for London ( $22 \text{ W/m}^2$ ).

a)



Direct Normal Radiation (Wh/m<sup>2</sup>) - Hourly  
RIYADH\_SAU



Direct Normal Radiation (Wh/m<sup>2</sup>) - Hourly  
LONDON/GATWICK\_GBR

b)

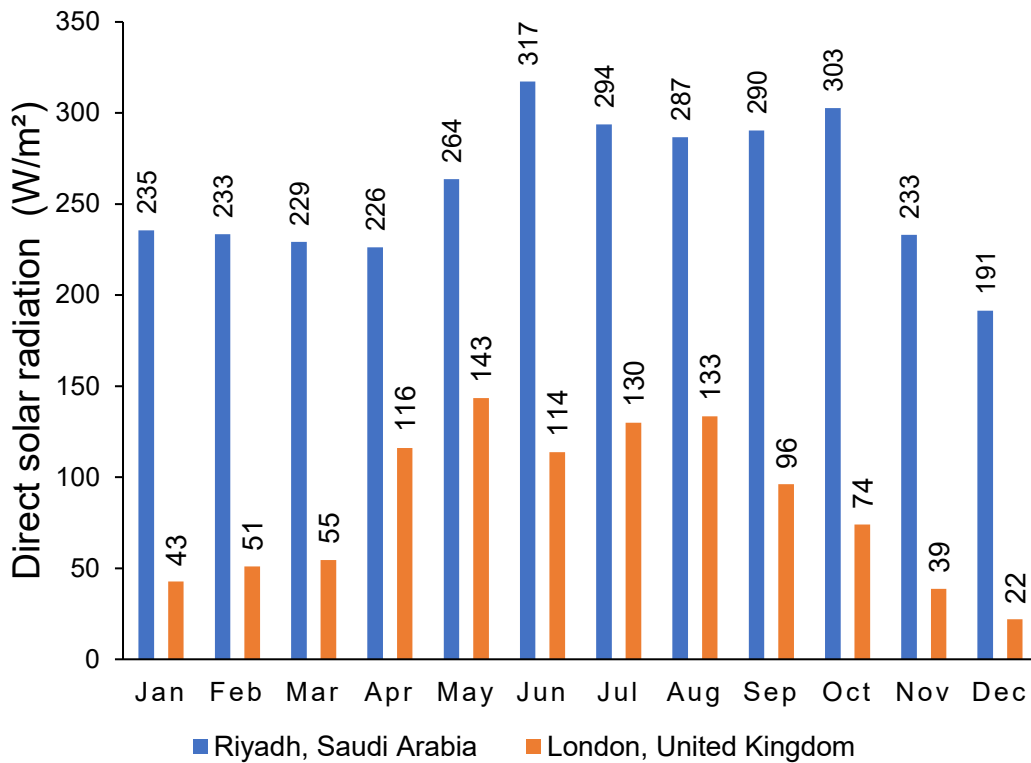
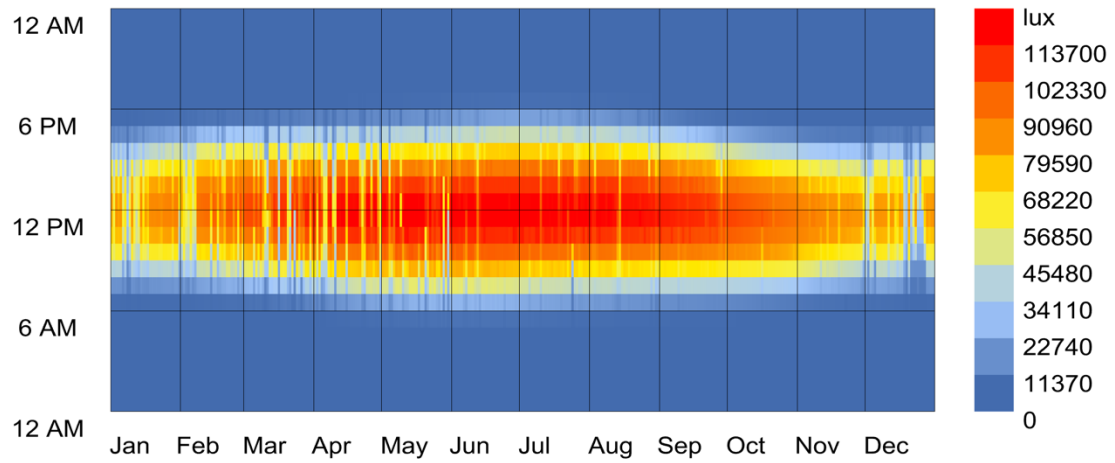


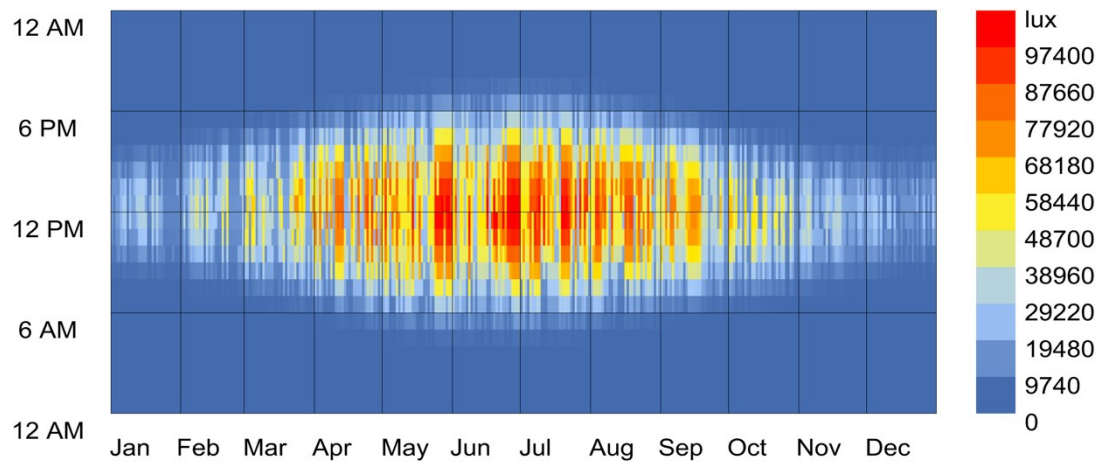
Figure 2-16. a) The graph reports the hourly direct solar radiation in Riyadh and London. b) shows the monthly average of direct solar radiation.

Figure 2-17-a presents the hourly global horizontal illuminance in Riyadh, Saudi Arabia and London, United Kingdom. In Riyadh, the amount of global horizontal illuminance is higher in the summer months than the winter months. The amount of global horizontal illuminance in Riyadh varies between 11,370 to 113,700 lux from January to December. In London, the global horizontal illuminance can reach to a maximum of 97,4000 lux and a minimum of 9,740 lux. Figure 2-17-b presents a comparative data of the monthly average of global horizontal illuminance between Riyadh and London. In Riyadh, the highest monthly average value of global horizontal illuminance is in June (35,646 lux), whilst in London the highest average value is in July (23,149 lux). Both cities have the lowest monthly average of global horizontal illuminance in December of 16,197 lux and 2,496 lux for Riyadh and London, respectively.

a)



Global Horizontal Illuminance (lux) - Hourly  
RIYADH\_SAU



Global Horizontal Illuminance (lux) - Hourly  
LONDON/GATWICK\_GBR



b)

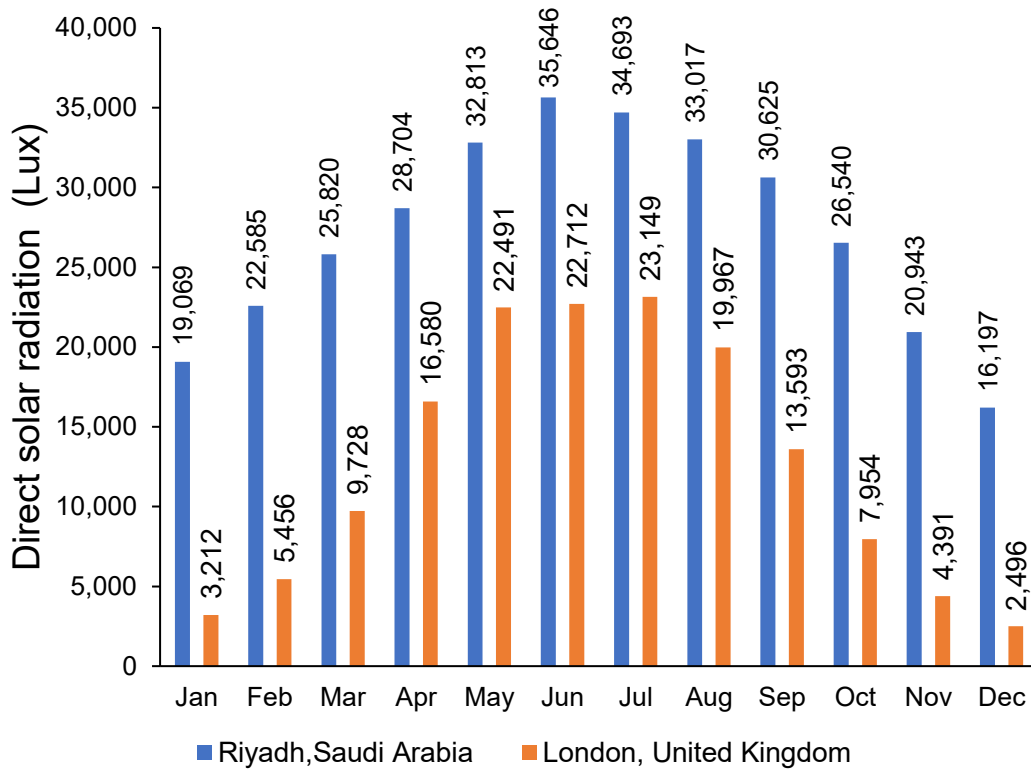


Figure 2-17 a) The graph presents the annual global horizontal illuminance in Riyadh and London. b) presents the monthly average values of global horizontal illuminance.

#### 2.8.4 Energy simulation parameters

To perform building energy simulation for the PDLC window EnergyPlus 8.9 component was utilised. Windows used in this simulation study were characterised by  $U$ -value, SHGC, and visible transmittance. These parameters for the PDLC window were obtained from the indoor results. The reference window was adopted from the EnergyPlus database library. The simulation was performed on hourly basis for 12 months and only daytime energy usage was considered.

#### 2.8.5 Daylight simulation parameters

To accomplish the balance between adequate daylighting level and energy usage, artificial lighting should be used when the amount of daylight in the room is insufficient. It was suggested by Velds and Christoffersen to divide a room into

three daylighting zones, considering on the distance of a daylight zone from the window [135]. The room was divided into three daylight zones (high daylight zone, intermediate daylight zone, and low daylight zone) to establish an appropriate evaluation of the discomfort glare and the interior illuminance. The effective window height was calculated by Eq 2-1. The daylighting zones were divided into three zones, as follow:

1. High daylight zone (where artificial lighting is not usually required) starts from the window and has a depth of 2 x EWH.
2. Intermediate daylight zone starts from the end of the high daylight zone to a depth of 1.5 x EWH.
3. Low daylight zone (where the artificial light is required) starts from the border of the intermediate daylight zone to the end of the room.

$$EWH = \frac{ab\tau}{c} \quad \text{Eq 2-1}$$

Where EWH is effective window height (m);  $ab\tau$  effective window area ( $m^2$ );  $ab$  the actual window area above 0.9 m from the façade ( $m^2$ );  $a$  the width of the window (m);  $\tau$  the transmission of the window plane;  $c$  the width of the façade. Figure 2-18 shows the reference points of the daylight glare index for all three daylight zones.

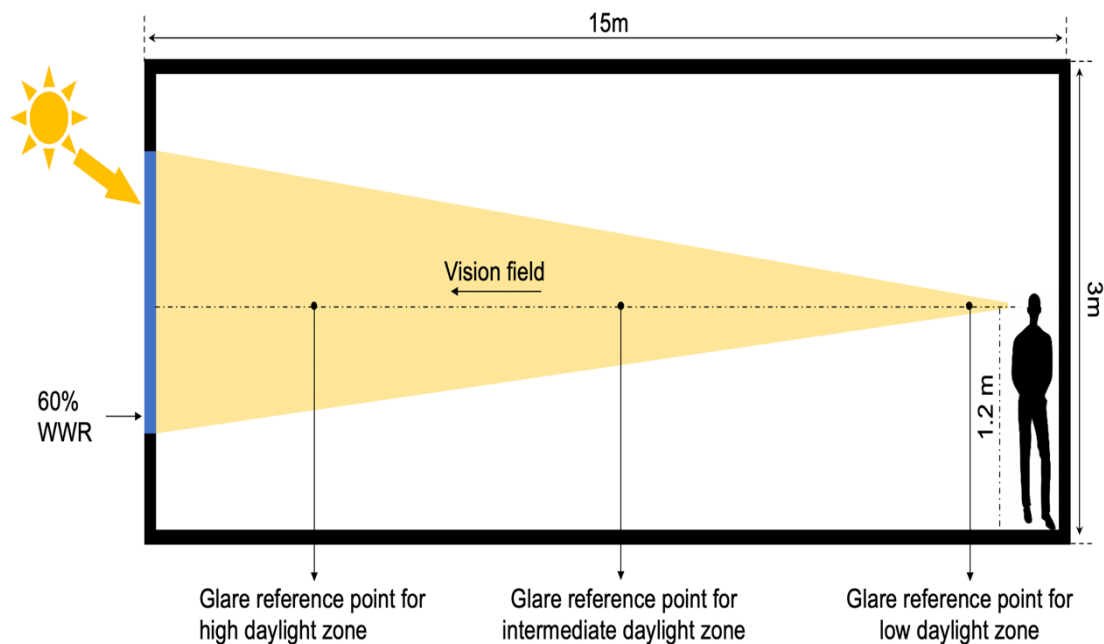


Figure 2-18. Illustration of DGI reference points and daylight zones.

### **2.8.6 Artificial lighting system**

This section discusses the parameters used to perform the simulation to explore the potential of artificial lighting energy savings employing PDLC glazing for an office building. The building model was equipped with two fluorescent lamps in each daylighting zone that require 100 W for each lamp. The fluorescent lights were programmed to be fully dimmable when the light sensors receive illuminance equal to the illuminance setpoint. The minimum fraction power for each fluorescent lamp was 0.15. The illuminance setpoint for office buildings was set to be 500 lux as recommended design for interior illuminance level. The lighting management system considered for the evaluation was a continuous dimming control. The artificial lighting control was simulated hourly, once the final daylight illuminance value was determined for each reference point considering the shading control strategy.

### **2.9 Conclusion**

PDLC switchable glazing was investigated to characterised thermal and daylight performance in indoor and outdoor conditions for transparent and opaque state. Two small-scale test cells were fabricated representing an unfurnished room. SHGC and  $U$ -value were determined by employing an indoor experimental setup. In addition, thermal and daylight performance were characterised for a PDLC glazing and combined PDLC with solar film using outdoor experimental setup. Instruments such as pyranometers, light sensors, thermocouples were utilised to measure solar radiation, illuminance, and temperatures, respectively.

EnergyPlus software was utilised to perform an evaluation of the annual saving for an office building equipped with a PLDC glazing. Solar radiation and outdoor temperature parameters were used to control the PDLC glazing transmission as shading control strategies. Furthermore, daylight glare discomfort analysis and artificial lighting reduction evaluation were performed. Two climate zones were utilised.

## **Chapter 3. Indoor investigation of thermal performance for an electrically switchable polymer dispersed liquid crystal (PDLC) glazing**

### **3.1 Introduction**

The aim of this chapter is to calculate the SHGC and  $U$ -value of a PDLC glazing system conducted in indoor conditions by utilising a small-scale test cell equipped with small area of PDLC glazing and temperature sensors to measure the solar energy entering the test cell through the PDLC glazing. In addition, the optical characteristics and protection factors were also evaluated. In this work, the investigation of the thermal performance of the PDLC glazing under various solar radiation was discussed in addition to the spectral transmittance.

### **3.2 Optical properties of PDLC glazing**

The solar radiation reaches the earth's surface, including visible light (VIS), ultraviolet (UV), and near-infrared (NIR) is approximately located between (300 nm and 3000 nm). The visible light is located between (380 nm and 780 nm) while the UV and NIR are located below and above the VIS spectrum. When the incident solar radiation falls onto glazing, it will be transmitted, reflected, and absorbed. The optical properties of the glazing, the incident angle, and the wavelength of the radiation determine the amount of solar radiation that is transmitted, reflected, and absorbed. Furthermore, the optical properties influence the transmitted solar radiation to produce distinct incident angle dependencies applied to the different relative intensity of the components of direct, diffuse, and ground reflected solar radiation. The diffuse light can determine the satisfaction of a room illumination whereas; the direct solar radiation influences the solar material protection factor and the skin solar protection factor [13]. The high energy of solar radiation like UV can have a negative impact on the glazing lifetime, the interior building materials, and human skin. Thus, such knowledge is important to determine what type of glazing should be used for low energy building.

In order to evaluate the optical characteristics of the PDLC glazing system, a spectrophotometer was employed to measure the solar transmission and reflection. The UV transmittance, visible transmittance and reflectance, solar transmittance and reflectance, and solar absorption, were determined using the following equations Eq 3-1 to Eq 3-6 [136]:

$$\text{UV transmittance } \tau_{uv} = \frac{\sum_{\lambda=300}^{380nm} T(\lambda)S_{\lambda}\Delta\lambda}{\sum_{\lambda=300}^{380nm} S_{\lambda}(\lambda)\Delta\lambda} \quad \text{Eq 3-1}$$

$$\text{Visible transmittance } \tau_{vis} = \frac{\sum_{\lambda=380nm}^{780nm} T(\lambda)D_{65}(\lambda)V(\lambda)\Delta\lambda}{\sum_{\lambda=380nm}^{780nm} D_{65}(\lambda)V(\lambda)\Delta\lambda} \quad \text{Eq 3-2}$$

$$\text{Visible reflectance } R_{vis} = \frac{\sum_{\lambda=380nm}^{780nm} D_{65}(\lambda)R(\lambda)V(\lambda)\Delta\lambda}{\sum_{\lambda=380nm}^{780nm} D_{65}(\lambda)V(\lambda)\Delta\lambda} \quad \text{Eq 3-3}$$

$$\text{Solar transmittance } \tau_{sol} = \frac{\sum_{\lambda=300nm}^{2500nm} T(\lambda)S(\lambda)\Delta\lambda}{\sum_{\lambda=300nm}^{2500nm} S(\lambda)\Delta\lambda} \quad \text{Eq 3-4}$$

$$\text{Solar reflectance } R_{sol} = \frac{\sum_{\lambda=300}^{2500nm} R(\lambda)S(\lambda)\Delta\lambda}{\sum_{\lambda=300nm}^{2500nm} S(\lambda)\Delta\lambda} \quad \text{Eq 3-5}$$

where,  $S_{uv}(\lambda)$  is the relative spectral distribution of ultraviolet solar radiation.  $D_{65}$  is the relative spectral distribution of illuminant [137],  $V(\lambda)$ , which is the spectral efficiency of a standard photopic observer,  $S(\lambda)$  relative spectral distribution of solar radiation, and  $\Delta\lambda$  is the wavelength interval.  $D_{65}V(\lambda)\Delta\lambda$  values at different wavelengths are given in Table 3-1.  $T(\lambda)$  and  $R(\lambda)$  are the spectral transmission and reflection of glazing. In addition, solar absorption is calculated using the written Eq 3-6:

$$\text{Solar absorption } \alpha_s = 1 - \tau_s - \rho_s \quad \text{Eq 3-6}$$

The selectivity index is the ratio of light transmissivity with the total transmitted energy from the glazing. The higher the value of the selectivity index, the better the solar control performance for glazing. Haze percentage was determined for the considered glazing using Eq 3-8, where  $T_d$  and  $T_{Total}$  illustrate the diffuse and total transmission.

$$\text{Selectivity} = \frac{\tau_v}{g} \quad \text{Eq 3-7}$$

$$\text{Haze} = \frac{T_d}{T_{Total}} 100\% \quad \text{Eq 3-8}$$

Table 3-1. Values of relative spectral distribution  $D_{65}V(\lambda)\Delta\lambda$  at different wavelengths, which were used for the calculation of the visible transmittance and visible reflectance [18].

Wavelength $\lambda$ (nm)	$D_{65}V(\lambda)\Delta\lambda$	Wavelength $\lambda$ (nm)	$D_{65}V(\lambda)\Delta\lambda$
380	0	590	0.063306
390	0.000005	600	0.053542
400	0.00003	610	0.042491
410	0.000103	620	0.031502
420	0.000352	630	0.020812
430	0.000948	640	0.01381
440	0.002274	650	0.00807
450	0.004192	660	0.004612
460	0.006663	670	0.002485
470	0.00985	680	0.001255
480	0.015189	690	0.000536
490	0.021336	700	0.000276
500	0.033491	710	0.000146
510	0.051393	720	0.000057
520	0.070523	730	0.000035
530	0.08799	740	0.000021
540	0.094427	750	0.000008
550	0.098077	760	0.000001
560	0.094306	770	0
570	0.086891	780	0
580	0.078994		

### 3.3 Evaluation of solar material protection and solar skin protection factor

Some part of the solar radiation such as the ultraviolet and visible spectrum can have a negative impact on human skin and materials inside a building. The impact on materials varies from discolouration to loss of functionality, while human skin may experience pale skin to severe sunburn. The level of damage depends on

the time and degree of exposure. The level of impact for human skin might be minimised by clothing and sun lotions, while the light stabiliser application may protect the materials. PDLC glazings can be of interest in this aspect as they have the potential to control the solar radiation. This section aims to evaluate how well the PDLC glazing system protects human skin and materials inside buildings from the solar radiation. In order to measure the protection level, the solar material protection factor (SMPF), and solar skin protection factor (SSPF) was calculated. The values of (SMPF) and (SSPF) range from 0 to 1, where a higher value indicates a high protection level [18]. To show that a larger part of the visible solar spectrum can degrade materials, the SMPF was calculated in the wavelength of today's value between 300 nm – 600 nm instead of the earlier value 300 nm – 500 nm [136]. The evaluation of (SMPF) and (SSPF) was achieved by mathematical calculations.

Solar material protection factor

$$\text{SMPF} = 1 - \frac{\sum_{\lambda=300nm}^{600nm} T(\lambda) C_{\lambda} S_{\lambda} \Delta\lambda}{\sum_{\lambda=300nm}^{600nm} C_{\lambda} S_{\lambda} \Delta\lambda} \quad \text{Eq 3-9}$$

Where  $C_{\lambda} = e^{-0.012\lambda}$

Solar skin protection factor

$$\text{SSPF} = 1 - \frac{\sum_{\lambda=300nm}^{400nm} T(\lambda) E_{\lambda} S_{\lambda} \Delta\lambda}{\sum_{\lambda=300nm}^{400nm} E_{\lambda} S_{\lambda} \Delta\lambda} \quad \text{Eq 3-10}$$

$E_{\lambda}$  CIE erythermal effectiveness

### 3.4 Calculation of Solar heat gain coefficient

Solar heat gain coefficient (SHGC) is the fraction of incident solar radiation that passes through a glazing system to a room in the form of transmitted radiation [138]. The solar gain passively causes the room temperature to rise, which is desirable during the winter season, although not during the summer months. SHGC is a primary factor to evaluate the glazing system and the energy consumption of a building [12]. SHGC can be influenced by several elements

such as the wind conditions, the spectrum of the incident radiation, and the internal and external temperature, however, the wind condition is neglected in this case [139]. Thus, the SHGC was calculated for the PDLC glass by the following equation.

The solar heat gain coefficient can be calculated by Eq 3-11 [136,140].

$$g = \tau_s + q_i = \tau_s + \alpha \frac{h_i}{h_i + h_e} \quad \text{Eq 3-11}$$

Where  $h_i$  and  $h_e$  stand for the internal and external heat transfer coefficient,  $\tau_s$  represents solar transmittance, and  $\alpha$  is the solar absorbance.

### 3.5 Calculation of Overall heat transfer coefficient

Thermal transmission through a glazing system is determined by the difference of temperature between external and internal surfaces with consideration of the thermal conduction, convection, and radiation [141]. Room temperature is usually maintained constant, whereas the external temperature varies based on environmental conditions, such as solar radiation and wind velocity. Overall heat transfer coefficient determines how well a glazing system can insulate heat loss from inside of a room to the outside environment. Therefore, the  $U$ -value of the PDLC glass was determined using mathematical models.

Overall, the heat transfer coefficient can be calculated by Eq 3-17 [57,142]. The parameters required to calculate  $U$ -value are presented in Table 3-2.

$$Q_{in} = Q_{PDLC} + Q_{testcell} + Q_{loss} \quad \text{Eq 3-12}$$

Where  $Q_{in}$  is the incident radiation.

$Q_{in}$  can be calculated using (Eq 3-12).

$$Q_{in} = I\alpha\tau A_{PDLC} \quad \text{Eq 3-13}$$

Total heat transfer through the glazing is expressed in Eq 3-10 [27].



$$Q_{PDLC} = U_{PDLC}A_{PDLC}\Delta T \quad \text{Eq 3-14}$$

Total heat transfer inside the test cell is provided by Eq 3-15 [59].

$$Q_{testcell} = m_{testcell}C_{air} \frac{dT}{dt} \quad \text{Eq 3-15}$$

The total heat losses through the test cell are given by Eq 3-16.

$$Q_{loss} = (UA)_{testcell}(\Delta T) \quad \text{Eq 3-16}$$

Overall heat transfer of the PDLC glazing is calculated using Eq 3-17.

$$U_{PDLC} = \frac{Q_{in} - Q_{testcell} - Q_{loss}}{A_{PDLC}\Delta T} \quad \text{Eq 3-17}$$

Table 3-2. Parameters required to calculate  $U$ -value

	Value	
<b>Fixed Parameters</b>	Aperture area of glazing ( $A_{PDLC}$ )	0.021 m <sup>2</sup>
	Interior wall surface ( $A_{wall}$ )	0.401 m <sup>2</sup>
	Internal volume of test cell ( $V_{air}$ )	0.0164 m <sup>3</sup>
	Thickness of Polystyrene ( $L_{pl}$ )	0.025 m
	Mass of air inside test cell ( $M_{tc} = V_{air} \times \rho_{air}$ )	0.02 kg
<b>Physical</b>	Density of air ( $\rho_{air}$ )	1.2250 kg/m <sup>3</sup>
	Heat capacity of air ( $C_{air}$ )	1.006 kJ/kg K
	Thermal conductivity of polystyrene ( $K_{pl}$ )	0.038 W/m·K
	Incident radiation from simulator ( $I$ )	1000 (W/m <sup>2</sup> )
<b>Variables</b>	Temperature inside the test cell ( $T_{in,tc}$ )	Measured by thermocouple (T)
	Temperature outside the test cell ( $T_{out,tc}$ )	Measured by thermocouple (T)

### 3.6 Experimental setup

Complete experimental setup is explained in section 2.7.1 with a photograph for the experiment Figure 2-9. The test cell description is provided in 2.6 in Chapter 2. Details of the PDLC glazing is available in section 2.5.1.

### 3.7 Results of the indoor investigation

#### 3.7.1 PDLC transmission measurements

Figure 3-1 shows the measured total transmission of the PDLC glazing by using a spectrophotometer, with results of 62% for the transparent state and 42% for the opaque state. The PDLC glazing offered UV transmission of 17% in the transparent state and 8% in the opaque state. It controlled the NIR radiation by 44% in the opaque state and 61% in the transparent state. Moreover, PDLC scatters light, starting from the edges or conductive electrode, and increases towards the centre. This process occurs because the refractive index does not match between the droplets and the polymer matrix during the opaque state. Comparatively, when PDLC is in the transparent state, the LC molecules align and enable light to pass through, which indicates that the refractive index between the polymer matrix and droplets are matched. The spectrophotometer measurements demonstrate that the diffused light was collected by the sphere from both states and scattered forward. Besides, the LC particles make the light scatter, resulting in higher transmission during the opaque state.

The same Figure 3-1 reports the measurements of the total reflectance of the PDLC glazing for the transparent and opaque states. The total solar reflectance was calculated for the PDLC glazing in the transparent and opaque states using Eq 3-5. A low value of solar reflectance indicates a low reflection of solar radiation, whereas a high value indicates high solar reflectance. In general, solar reflectance is represented in percentage values between 0 and 100%. It is worth noting that the solar spectrum covered in the calculations is between 2500 and 300 nm. The results showed the PDLC glazing had solar reflectance of 17% in the transparent state and 18% in the opaque state. In addition, the PDLC glazing offered a reflection of 14% and 18% of UV radiation in the transparent and opaque states. In terms of NIR radiation, the reflection values were 15% and 16% in the transparent and opaque states, respectively. The visible reflectance was calculated using Eq 3-3 and the results were 18% for the transparent state and 24% for the opaque state. The total solar reflectance was always lower than the total solar transmission for both states of the PDLC glazing. A nearly equal amount of solar reflection of both states of the PDLC glazing indicates that the

diffuse light was due to forward scattering. The transmission and reflectance curves clearly show that the PDLC glazing absorbed a considerable amount of solar radiation. The solar absorption was calculated for the PDLC glazing for both states using Eq 3-6. The solar absorption value is a number between 0 and 1, which is usually represented by a percentage value. The higher the percentage value the higher the absorption. The solar absorption of PDLC glazing for the transparent state was 21% and for the opaque state was 40%. It was observed that the opaque state possesses higher absorption value than the transparent state due to the random alignment of the particles, which indicates less amount of solar radiation passes through. The transmission measurements for PDLC glazing are presented in Table 3-3.

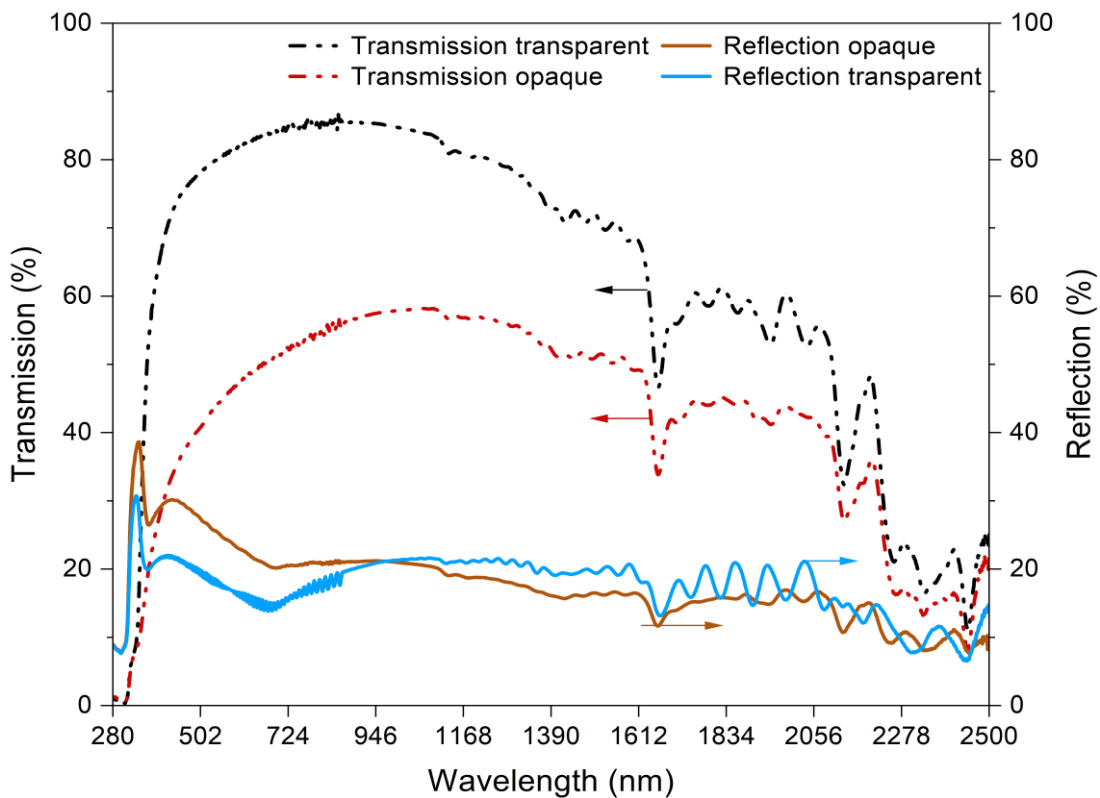


Figure 3-1. Total transmission (regular + diffuse) and reflection of PDLC glazing for the transparent and opaque states.

Table 3-3. Measurements of the spectrophotometer for PDLC glazing for the transparent and opaque states.

<b>transmittance</b>		<b>PDLC/ OFF</b>	<b>PDLC/ ON</b>
<b>Solar transmittance (300–2500)</b>	total	42%	62%
	regular	12%	59%
	diffuse	30%	4%
<b>Solar reflectance (300–2500)</b>	total	18%	17%
<b>Visible transmittance (380–780)</b>	total	44%	79%
	regular	2%	72%
	diffuse	42%	7%
<b>Visible Reflectance (380-780)</b>		24%	18%

Figure 3-2 reports the regular and diffuse transmissions of PDLC glazing. The regular transmission was 59% and 12% for the transparent and opaque state, respectively. Comparatively, the diffuse transmission was 4% in the transparent state and 30% in the opaque state. During the transparent state, the PDLC offers higher regular transmission and lower diffuse transmission. The higher regular transmission is a result of the alignment of the particles during the transparent (ON) state, which enables light to pass through the PDLC.

Light is scattered at a wider viewing angle in the transparent state, while the angular distribution of light can be affected by haze. From (Eq 3-8), haze coefficient was calculated for the transparent state and was determined to be (6.4%). In contrast, the opaque state offers lower regular transmission and higher diffuse transmission. The high diffuse transmission is a result of the dispersed particles in the liquid crystal. The haze coefficient in the switch-off state was 71.4%, which is considered high value and results in the PDLC becoming opaque. Selectivity index for the investigated glazing was found to be 1.16 and 0.7 for the transparent and opaque states, respectively.

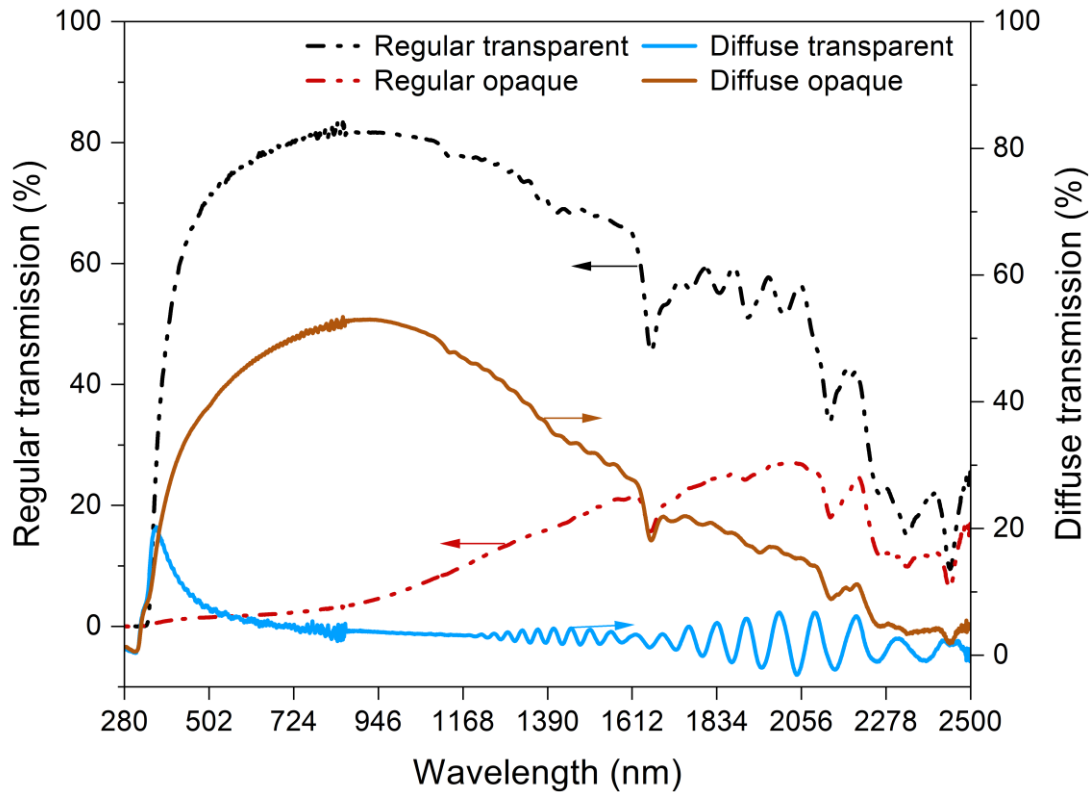


Figure 3-2. Regular and diffuse transmission of PDLC glazing for the transparent state and opaque state.

### 3.7.2 Solar material and solar skin protection factors

Solar material protection factor (SMPF) was calculated for the investigated PDLC glazing using Eq 3-9 for both the transparent and opaque state, and the value was 0.39 and 0.69, respectively. Solar skin protection factor (SSPF) was found to be 0.71 for the transparent-state and 0.87 for the opaque off-state of PDLC glazing. PDLC opaque state offers better protection levels for human skin and material of building interior compared to the transparent state. The SMPF and SSPF results are reported in Table 3-4.

Table 3-4. List of factor values for PDLC glazing for the transparent and opaque states.

	<b>PDLC/ OFF</b>	<b>PDLC/ ON</b>
<b>SMPF</b>	0.69	0.39
<b>SSPF</b>	0.87	0.71
<b>Selectivity index</b>	0.7	1.16
<b>Haze percentage</b>	71.4%	6.4%
<b>SHGC</b>	0.63	0.68
<b>U-value</b>	2.44 W/m <sup>2</sup>	2.79 W/m <sup>2</sup>

### 3.7.3 PDLC glazing thermal performance

The PDLC glazing system was exposed to a constant indoor solar simulator at different radiation intensities (1000, 800, 600, 400 W/m<sup>2</sup>) for 180 minutes for both the transparent and opaque states. It was observed that the PDLC system behaved similarly during all various radiation intensities.

Figure 3-3 illustrates the temperature variation of the system during the transparent state under the radiation of 1000 W/m<sup>2</sup>. The test cell temperature increased from 27.3 °C to 51.22 °C following 180 minutes of exposure, while the ambient temperature increased from 24.00 °C to 25.54 °C. During the first 55 minutes, the test cell temperature increased at a rate of 2.0 °C/min, while the ambient temperature increased at 0.09 °C/min. Comparatively, it was determined that the internal glass temperature was higher than the external glass temperature, which indicates higher energy transmission; therefore, greater heat flow.

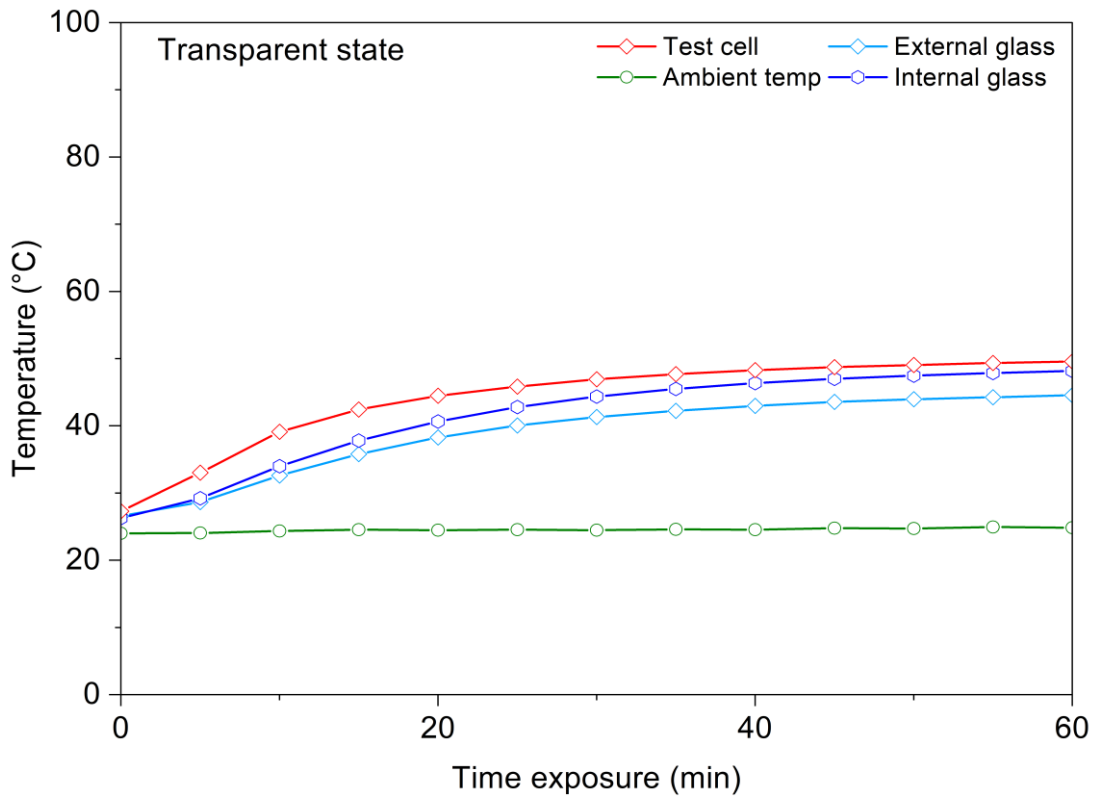


Figure 3-3. Measured temperature of external and internal glazing surface, test cell and ambient temperature in transparent state under 1000 W/m<sup>2</sup> solar radiation.

Figure 3-4 presents the temperature variation of the PDLC glazing system during the opaque state under 1000 W/m<sup>2</sup> radiation. In comparison, during the opaque state, the test cell temperature increased from 30.56 °C to 53.91 °C, while the ambient temperature increased from 25.07 °C to 26.78 for the same exposure time as the transparent state. During the first 55 minutes, the test cell temperature increased at a rate of 1.96 °C/min, while the ambient temperature increased at 0.084 °C/min.

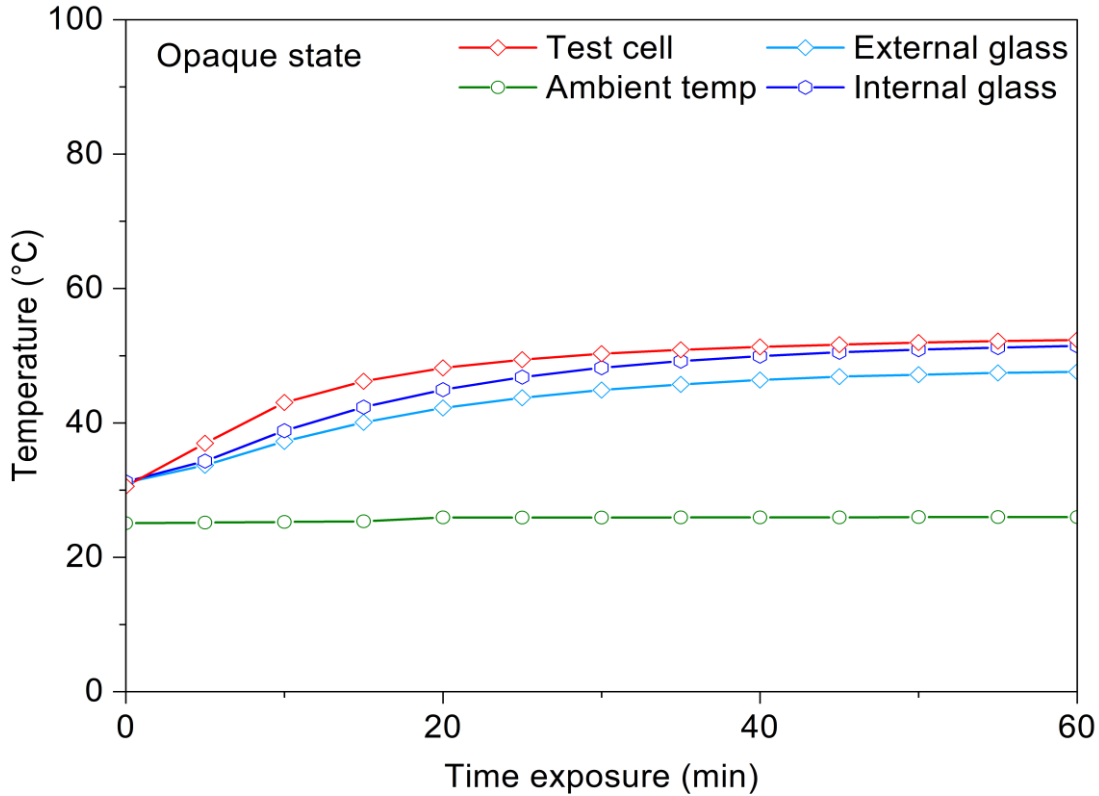


Figure 3-4. Measured temperature of external and internal glazing surface, test cell and ambient temperature in the opaque state under 1000 W/m<sup>2</sup>.

Figure 3-5 shows the temperature variation of the PDLC glazing system during the transparent state under various solar radiation intensities (800, 600, 400 W/m<sup>2</sup>). When the PDLC glazing system was exposed to solar radiation at 800 W/m<sup>2</sup> the test cell temperature reached the maximum temperature of 47.7 °C, while the ambient temperature was 25 °C after 180 min of exposure to solar radiation. The external PDLC glazing surface maximum temperature was 43.5 °C, while the internal surface was 46.5 °C. At 600 solar radiations, the maximum test cell temperature was 43.4 °C. The external and internal surfaces reached to the maximum temperature of 38 °C and 42.5 °C, respectively. At 400 solar radiation, the test cell reached the highest temperature of 41.8 °C. The external surface maximum temperature was 38.7 °C and the internal surface was 41.1 °C. It was observed that the internal glass temperature was always higher than the external glass in all different solar radiation intensities. In addition, the test cell temperature was always higher than the glazing surfaces in all solar radiation intensities. These measurements show agreement with the measurements taken at 1000 W/m<sup>2</sup>. The test cell maximum temperature decreased as the solar



radiation intensity was reduced, while the ambient temperature was always constant at 25 °C.

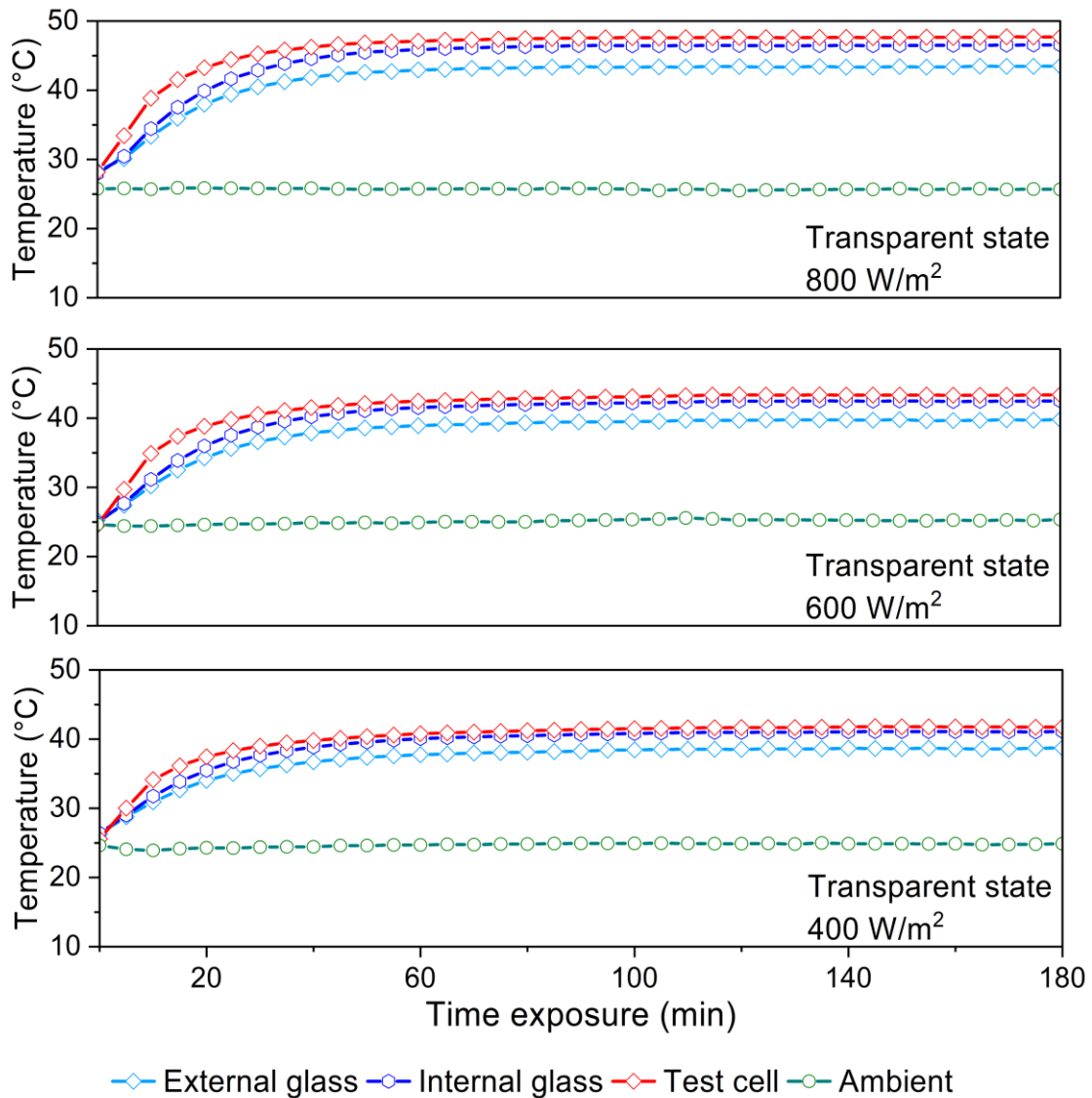


Figure 3-5. Measured temperature of external and internal glazing surface, test cell and ambient temperature in the transparent state under 800, 600, 400 W/m<sup>2</sup> solar radiation.

Figure 3-6 presents the temperature variation of the PDLC glazing system during the opaque state under various solar radiation intensities (800, 600, 400 W/m<sup>2</sup>). At 800 solar radiation, the test cell reached the maximum temperature of 50.4 °C and the ambient temperature was 26 °C. The highest temperature of the external glass was 46.4 °C, while the internal glass temperature was 49.8 °C. At 600 solar radiation, the maximum temperature of the test cell was 44.2 °C. The external

glass maximum temperature (40.4 °C) was lower than the internal glass (43.3 °C). At 400 solar radiation, the test cell maximum temperature decreased to 41.2 °C as solar radiation was reduced to 400 W/m<sup>2</sup>. The external and internal glass highest temperature were 38.1 °C and 40.4 °C, respectively. Data analysis showed that internal temperature of the test cell in the opaque state was higher than the internal temperature in the transparent state at 800 W/m<sup>2</sup> and 600 W/m<sup>2</sup>. At 400 solar radiation, the test cell temperature was nearly similar in both the opaque and transparent state. Table 3-5 shows the maximum temperature of the PDLC glazing system.

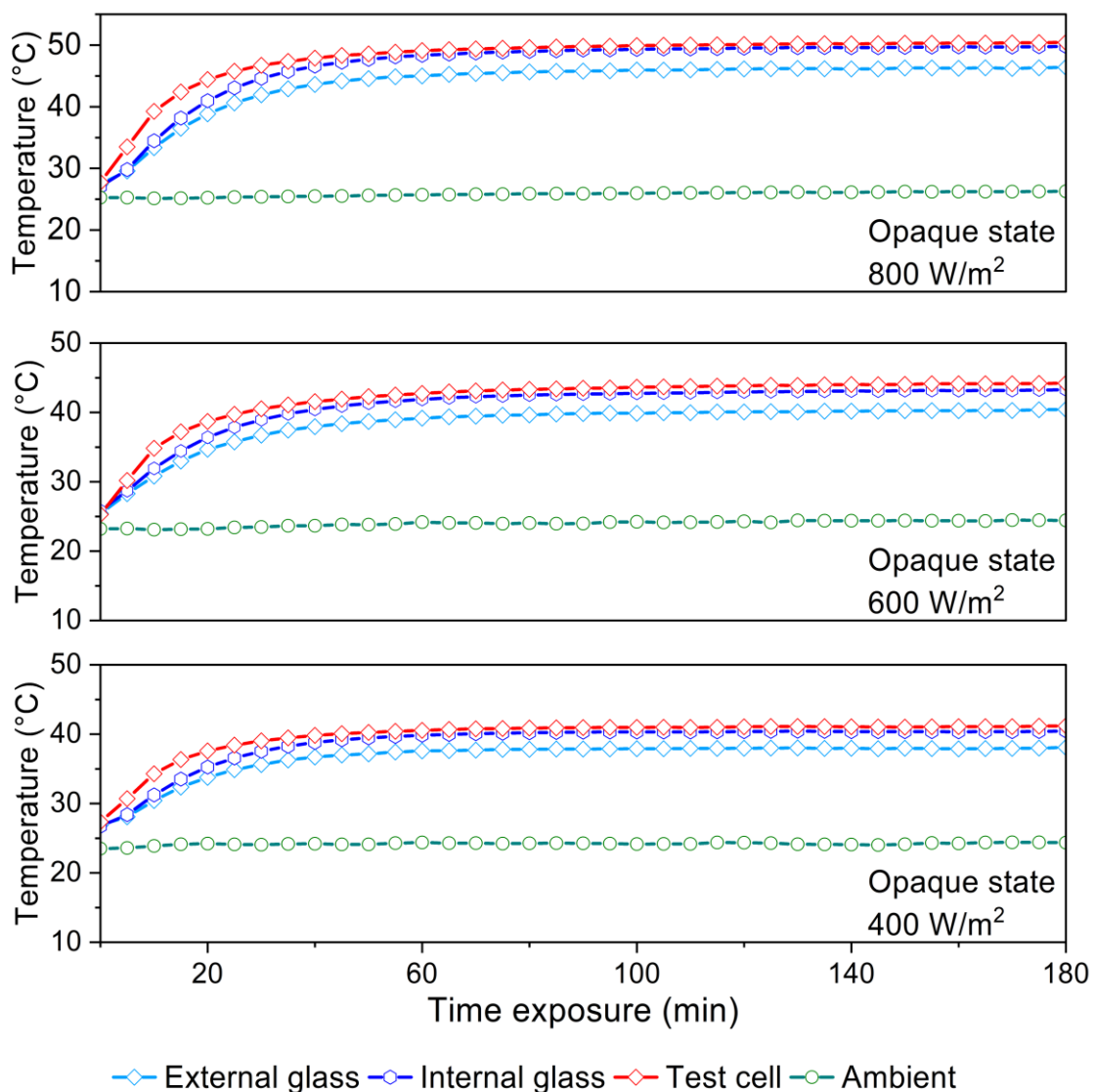


Figure 3-6. Measured temperature of external and internal glazing surface, test cell and ambient temperature in the opaque state under 800, 600, 400 W/m<sup>2</sup> solar radiation.

Table 3-5. The maximum temperature (°C) of the PDLC glazing system.

	Transparent state (ON)				Opaque state (OFF)			
<b>Solar radiation (W/m<sup>2</sup>)</b>	1000	800	600	400	1000	800	600	400
<b>External glazing (°C)</b>	46.3	43.5	39.8	38.7	49.1	46.4	40.4	38.1
<b>Internal glazing (°C)</b>	50	46.5	42.5	41.1	53	49.8	43.3	40.4
<b>Test cell (°C)</b>	51.2	47.7	43	41.8	53.9	50.4	44.2	42.2
<b>Ambient (°C)</b>	25.6	25.9	25.6	25	26.8	26.3	24.5	24.4

Figure 3-7 shows the time variation of the temperature difference ( $\Delta T_g$ ) between the internal and external PDLC glazing surfaces across all various radiation intensities. The temperature of the internal and external glass steadily increased for both the transparent and opaque states at a similar rate, which demonstrates that the PDLC system exhibits uniform behaviour under various radiation intensities. The average increase of temperature difference during the transparent state was 2.11 °C for all solar radiation intensities, while in the opaque state was 2.62 °C. It was also found that the opaque state has higher temperature differences than the transparent state. This indicates that the PDLC system exhibits higher absorption levels of radiation, rather than reflection.

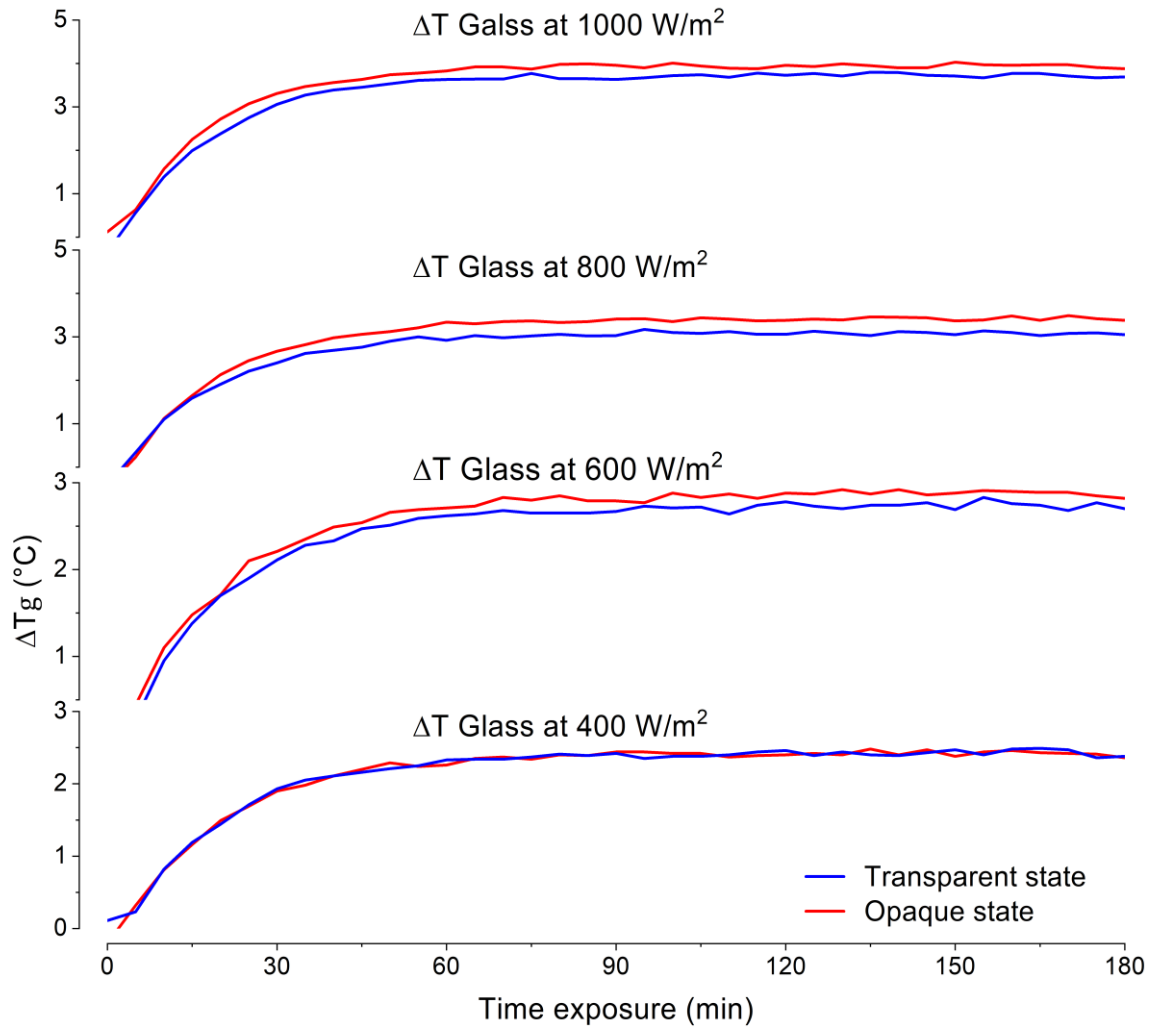


Figure 3-7. The time variation of the temperature difference ( $\Delta T_g$ ) between the internal and external PDLC glazing surfaces for both the transparent (blue line) and opaque (red line) states under various radiation intensities.

Figure 3-8 illustrates the time variation of the temperature difference ( $\Delta T_{cell}$ ) between the internal cell temperature and external ambient across all various radiation intensities. The graph highlights that the test cell has steady performance through the entire measurements. The average increase of temperature difference during the transparent state was 18.79 °C, while the opaque state was 20.12 °C under various radiation intensities. It was observed that the test cell temperature was always higher than the ambient temperature during the opaque state, due to the absorption property of PDLC glazing, which indicates that the convection heat transfer is higher. In addition, the overall heat flow to the test cell through the PDLC glazing in the opaque state is higher compared to the transparent state. Moreover, the thermal performance of the

PDLC glazing demonstrates the ability to reduce the heat loads during the cold months.

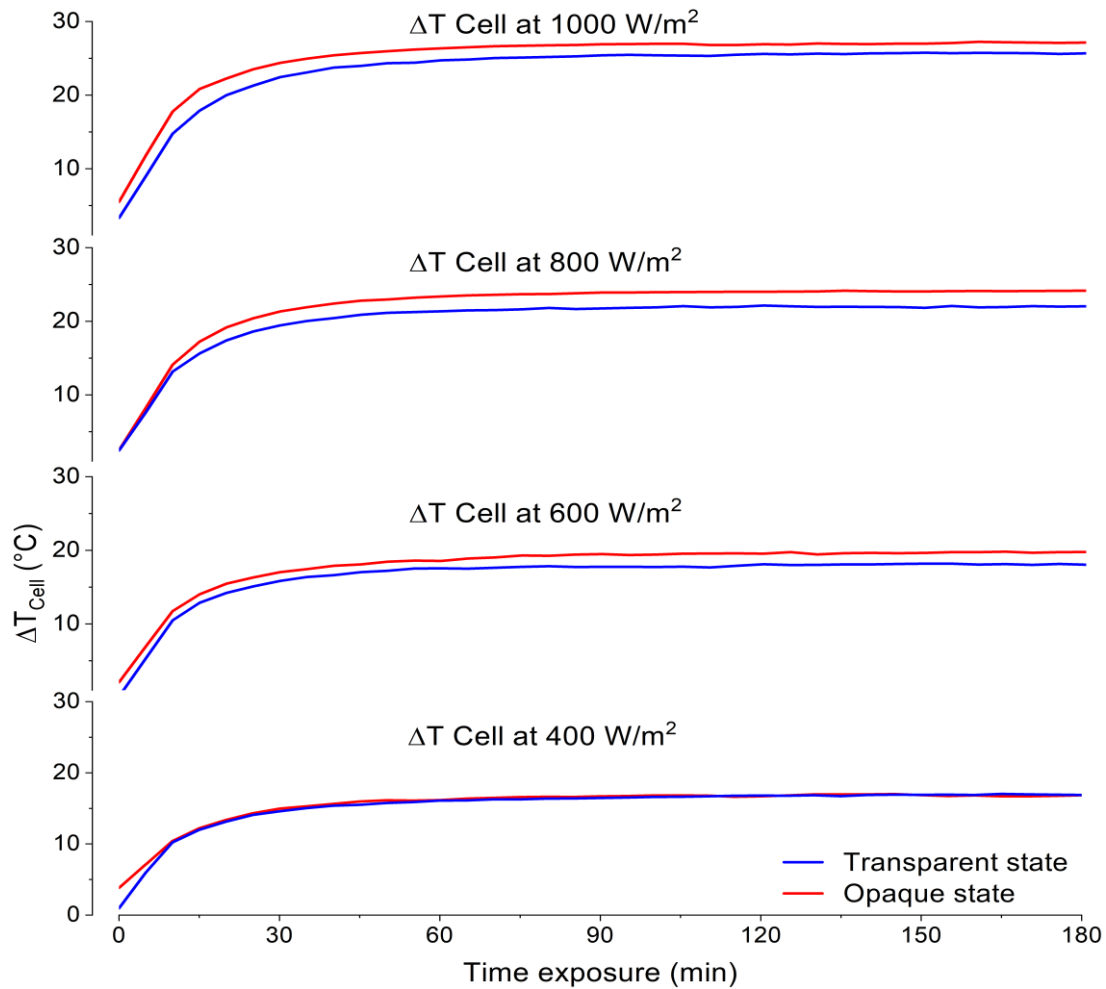


Figure 3-8. The time variation of the temperature difference ( $\Delta T_{\text{cell}}$ ) between the test cell and the ambient temperature for both the transparent (blue line) and opaque (red line) states under various radiation intensities.

### 3.7.4 Solar heat gain coefficient (SHGC)

The solar heat gain coefficient for the PDLC glazing was found to be 0.68 and 0.63 for the transparent and opaque states, respectively. It was observed that the value of SHGC was roughly similar in both the transparent state and opaque state, due to low solar reflection and transmission in both states. In particular, high SHGC values indicate that PDLC glazing is suitable for cold climates.

### 3.7.5 Overall heat transfer (*U*-value)

The value of overall heat transfer was calculated when the interior and exterior glazing surfaces temperatures achieved a steady state. Figure 3-9 and Figure 3-10 report the PDLC glazing's *U*-value of 2.79 W/m<sup>2</sup>·K for the transparent state and 2.44 W/m<sup>2</sup>·K for the opaque state. The difference in the *U*-value was due to the variation of transmission of both states. The PDLC glazing *U*-value was compared to typical contemporary static transparent double-glazing system. An outdoor experiment of a double glazing showed *U*-value of 2.98 W/m<sup>2</sup>·K [57]. Thus, PDLC glazing offered 6% lower thermal transmission while the optical transmission was 32% lower than that of transparent state.

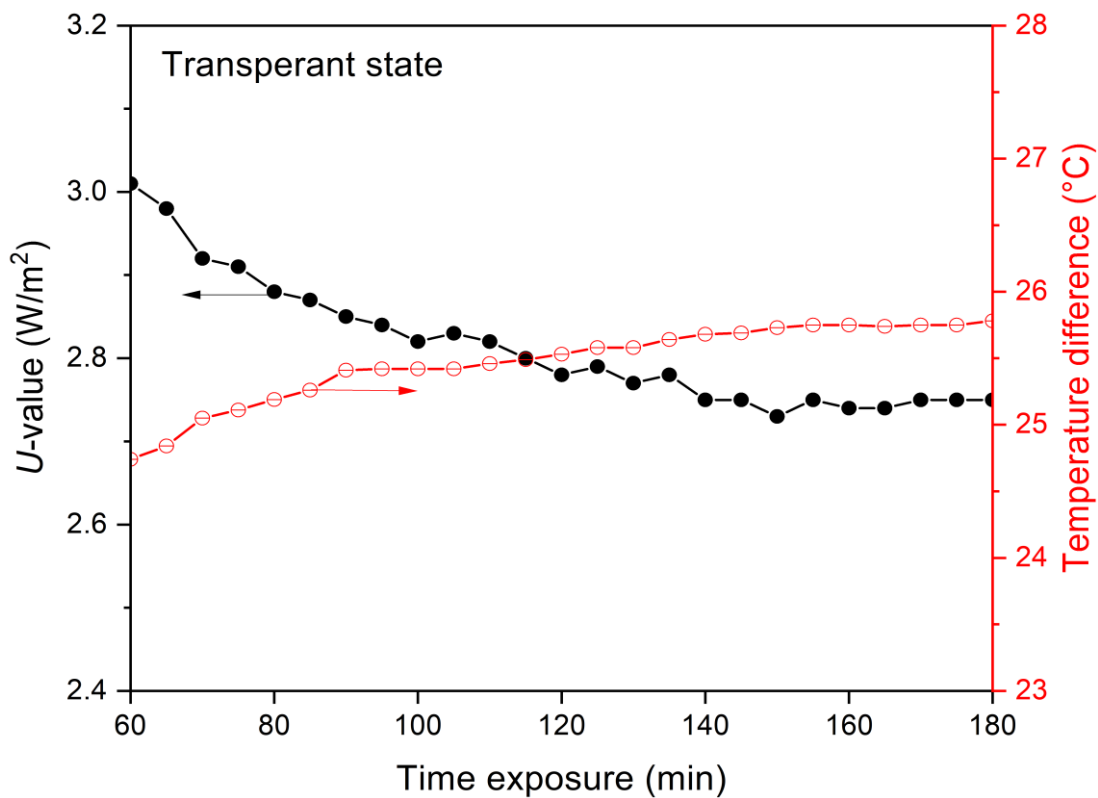


Figure 3-9. *U*-value and temperature difference between the ambient and test cell when PDLC glazing was in the transparent state.

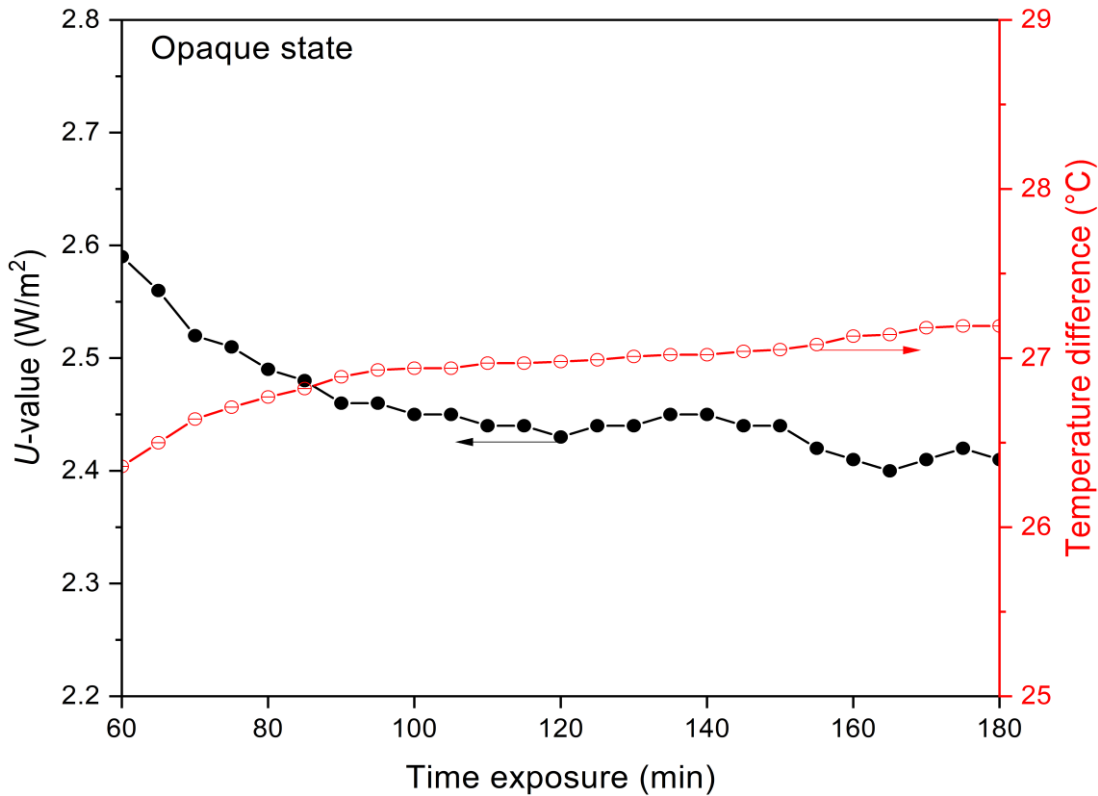


Figure 3-10.  $U$ -value and temperature difference between the ambient and test cell when the PDLC glazing was in the opaque state.

### 3.8 Conclusion

In this work, measurements of the optical characteristics were carried out using UV-vis-NIR (1050) spectrophotometer, and the SMPF and SSPF were calculated to evaluate a PDLC glazing system for future low energy buildings. Moreover, SHGC and  $U$ -value were investigated in indoor conditions. The PDLC glazing system was exposed to constant solar radiation with different radiation intensities (1000, 800, 600, 400 W/m<sup>2</sup>) for 180 minutes for both the transparent (ON) and opaque (OFF) states. The results of the investigation are summarised as follows.

1. The result of the optical properties showed that the PLDC system is a good candidate for variable transparency glazing with solar modulation between 62% and 42% for the transparent and opaque states, respectively.
2. The optical evaluation showed that the investigated PDLC glazing offered low transmissions for UV 14% and NIR 37% in the opaque state, respectively. In addition, the system has a high degree of protecting the human skin in both states which indicate that the investigated PDLC has

the potential to control the exposure to UV. The system could be significantly effective in replacing the conventional curtains as it could control the UV exposure and offer the view to the outside environment simultaneously.

3. The highest temperature for the PDLC glazing surface achieved was 52.97 °C and 49.95 °C for the opaque and transparent states, respectively, under 1000 W/m<sup>2</sup>. In terms of the test cell, the highest temperature achieved was 53.91 °C and 51.22 °C for the opaque and transparent states, respectively. The major finding was that the PDLC glazing system demonstrated effective thermal performance in reducing heat load in a cold dominated climate with SHGC 0.68 and 0.63 for the transparent and opaque states, respectively. However, it was observed that the internal glass had a higher surface temperature, which could generate secondary heat gain resulting in thermal discomfort for the occupants.



## **Chapter 4. Outdoor investigation of thermal and daylight performance of PDLC glazing and PDLC<sub>F</sub> combined with solar control film**

### **4.1 Introduction**

The objective of this chapter is to investigate the PDLC glazing under real weather conditions. The PDLC glazing prototype was characterised for different sky conditions (a sunny day, an intermittent day, and a cloudy day) to evaluate the thermal performance. In addition, the glare subjective rating was evaluated for the PDLC glazing prototype. The investigation was conducted in two different experiments.

### **4.2 First experiment**

A test cell was fabricated in the solar lab and was utilised to investigate the PDLC glazing prototype. The PDLC glazing was mounted on the test cell in addition to several sensors and equipment were equipped on the test cell. The aim of this work was to evaluate the temperature behaviour of the PDLC glazing's surfaces and the test cell temperature in addition to the daylight glare. Further details about the test cell and the equipment are provided in section 2.6.

### **4.3 Second experiment**

A solar control film was combined with the PDLC glazing, which was referred to as (PDLC<sub>F</sub>) and then was mounted on the test cell. The aim of this work was to assess the impact of the film on the thermal behaviour and visual comfort of the PDLC glazing. More details about the PDLC glazing and solar film can be found in sections 2.5.2 and 2.5.3.

### **4.4 Thermal performance of PDLC glazing and PDLC combined with solar film**

Indoor comfort in buildings is determined by several parameters such as lighting, humidity, and temperature. In most cases, thermal comfort inside buildings is

achieved by mechanical systems such as fans or HVAC systems. However, the use of mechanical systems could result in high energy consumption. Generally, windows are responsible for undesired heat gain and heat loss between buildings and the outdoor environment. Solar heat gain can significantly affect thermal comfort and could increase the cooling and heating loads. Windows technologies have advanced significantly to enhance the energy performance for buildings, such as solar control films, thin-film coatings, and low-emittance coatings. According to Lampert “solar control films are designed to reflect the incident solar radiation, in order to diminish solar heat gains through the glass” [143]. Many studies have investigated glazing with or without solar control films in the past. A study investigated the heat transfer in multiple glazing with or without solar control film, taking into account environmental parameters such as temperature and wind velocity [144]. The thermal conductance for a clear double glass without solar control film was  $3 \text{ W/m}^2\text{K}$  and with the solar control film, the value was reduced to  $2 \text{ W/m}^2\text{K}$ . A simulation study used eQUEST software to evaluate the energy-saving for a commercial building equipped with solar window films in Shanghai, China [145]. The simulation results showed that the shading coefficient and solar heat gain could be decreased by 44% and 22% by applying the solar control film on the outside and inside the existing windows, respectively. Another simulation study utilised the Energy-10 software to evaluate the energy consumption of two departments with two rooms. One room had a window with simple glass and the other room had a window with a solar control film. The annual energy consumption decreased by approximately 16% for the room equipped with a window with a solar control film.

In this work, PDLC switchable glazing was investigated to characterise thermal and daylight performance under different sky conditions. Then a solar film was attached to the exterior surface of the PDLC glazing to evaluate the film effect on solar heat gain and glare discomfort level in outdoor conditions. The parameter considered in this experiment is global solar irradiance, diffuse solar irradiance, ambient, glazing surfaces, and test cell internal temperature. The incident solar radiation falling onto a glazing would be transmitted, reflected, and absorbed in different amounts depending on the glazing optical properties. The solar radiation transmitted through the glazing would influence the thermal comfort inside a

room, whereas the diffuse radiation would determine the illuminance level. Applying a solar control film on a glazing would change the amount of transmitted, reflected, and absorbed solar radiation. In other words, solar control film would influence the thermal and visual comfort level inside a room.

Spectral transmittance measurements were carried out using a Perkin Elmer Lambda 1050 UV/vis/NIR spectrophotometer. Figure 4-1 shows the spectral transmittance of the PDLC glazing and combined PDLC<sub>F</sub> in the transparent and opaque states. The PDLC glazing offered 68% visible transmittance in the transparent (ON) state and 39% in the opaque (OFF) state. The combined PDLC<sub>F</sub> visible transmittance was 49% and 28% in the transparent and opaque states, respectively. The solar film reduced the PDLC glazing visible transmittance by 28% in the transparent and the opaque states. This indicates that the solar control film would have some effect on solar heat gain and glare level.

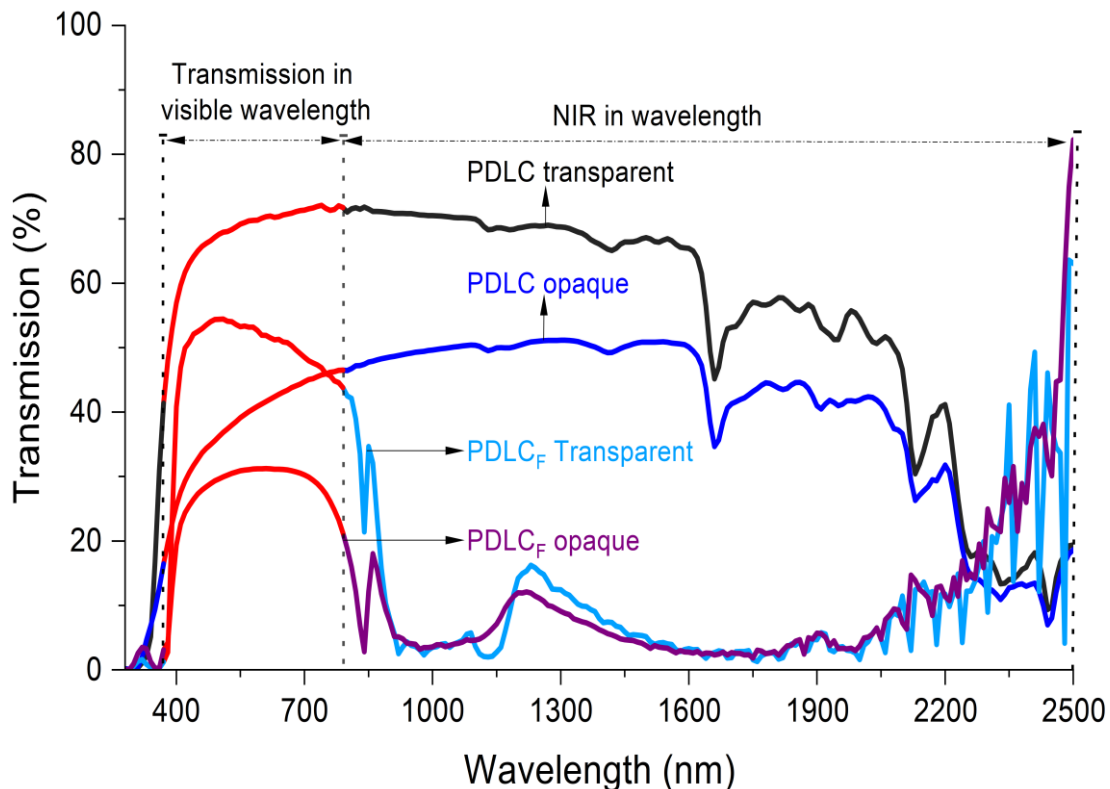


Figure 4-1. The solar transmittance of the PDLC glazing prototype and combined PDLC<sub>F</sub> for the transparent and opaque states.

## 4.5 Daylight glare discomfort

Glare is a sensation caused by direct sunlight that causes visual discomfort because the luminance from the source is greater than the eyes adaptation [44]. In the literature, there are several methods to evaluate glare; however, there is not a unique reliable method agreed upon researchers to evaluate glare worldwide. Glare Subjective Rating (SR) method is used in this study to evaluate glare discomfort. Pervious experiments suggested that glare level is strongly correlated to the direct vertical illuminance received by the observer's eyes [146,147]. Glare was calculated using the equation Eq 4-1 [120].

$$SR = 0.1909 E_v^{0.31} \quad \text{Eq 4-1}$$

Where  $E_v$  is the vertical illuminance from the light source. Table 4-1 presents the level of discomfort glare.

Table 4-1. Levels of discomfort glare indexes.

Glare Subjective Rating	SR indexes
Just intolerable	2.5
Just disturbing	1.5
Just noticeable	0.5
Just imperceptible	0

## 4.6 Experimental setup

A complete explanation of the experiment setup is available in Chapter 2. Details of the test cell are provided in section 2.6. For the PDLC glazing description see sections 2.5.2 and 2.5.3.

## 4.7 Results of the outdoor investigation

### 4.7.1 Thermal analysis of the PDLC glazing prototype

Figure 4-2 reports the temperature variation as a function of time for the PDLC glazing prototype in the transparent state for different sky conditions. On a sunny day, the maximum recorded temperature of the test cell was 46.8 °C, while the maximum internal PDLC surface temperature was 41.5 °C and the external surface temperature was 38.6 °C. The test cell increased at a rate of 2.5 °C/h

between 9:00 to 13:00, while the ambient temperature increased at 0.5 °C/h. The internal temperature of the test cell remained higher than the ambient temperature from 9:00 to 17:00. Between 14:00 to 17:00, the test cell temperature increased at a higher rate due to an increase in the global solar irradiance from 355 W/m<sup>2</sup> to 783 W/m<sup>2</sup>. For an intermittent day, the test cell reached the maximum temperature of 39.5 °C at a rate of 3.5 °C/h. The ambient temperature increased from 15 °C to the maximum of 21.6 °C at 0.6 °C/h. In addition, the internal surface of the PDLC glazing reached the maximum temperature of 35 °C at 2.5 °C/h. The test cell temperature decreased as the global irradiance decreased from 812 W/m<sup>2</sup> to 476 W/m<sup>2</sup> between 14:00 and 17:00. However, the test cell temperature remained higher than the ambient temperature. For a cloudy day, the maximum recorded temperature for the test cell was 37.8 °C and increased by 2.4 °C/h. The highest ambient temperature was 25 °C and increased by 0.7 °C/h. The internal surface of the PDLC glazing reached the maximum temperature of 35 °C when the ambient temperature was 24 °C. In general, the global irradiance readings were low and varied between 584 W/m<sup>2</sup> and 77 W/m<sup>2</sup>. It was found that the internal surface of the PDLC glazing temperature was always higher than the external surface in the transparent state. Table 4-2 presents the temperatures for the PDLC glazing prototype for different sky conditions. Table 4-3 shows the readings of the solar irradiance for different sky conditions.

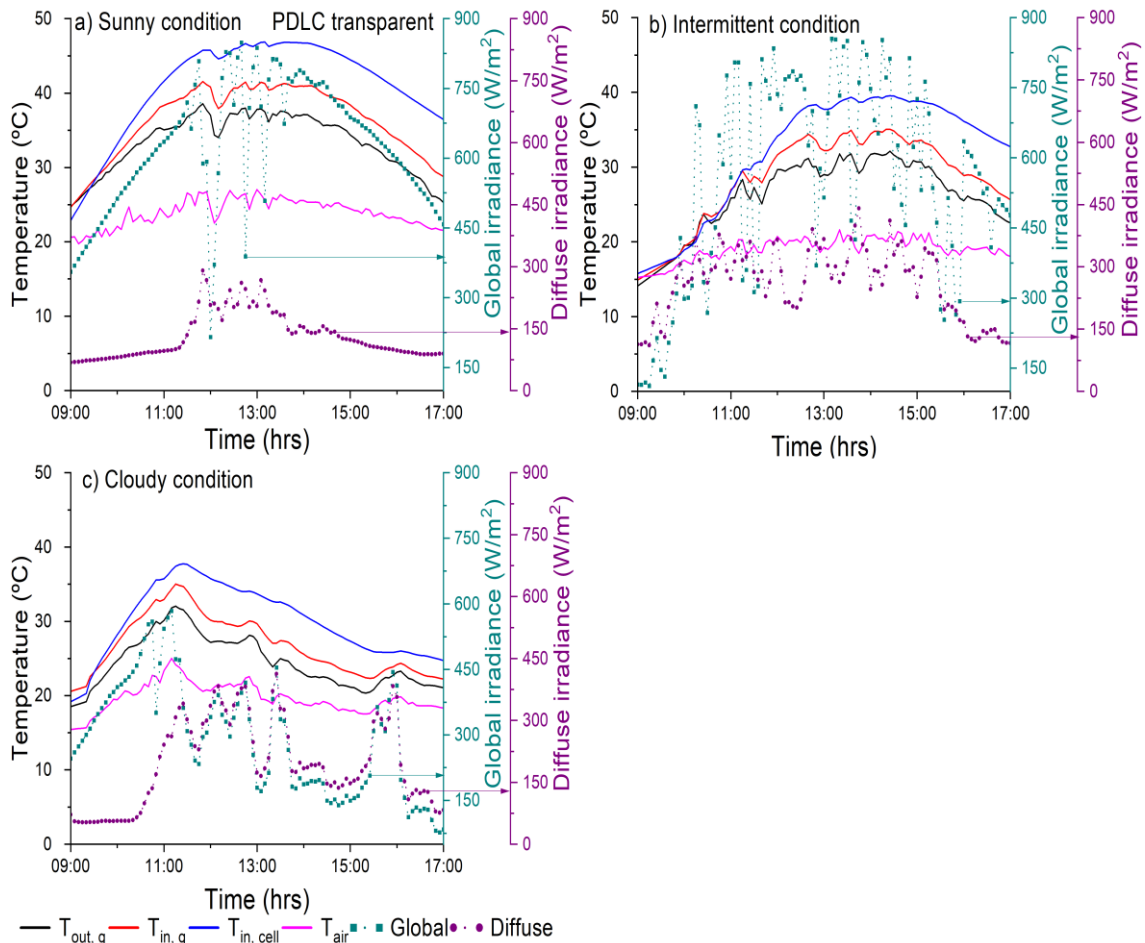


Figure 4-2. Temperature variation as a function of time for the PDLC glazing prototype in the transparent state for different sky conditions. a) Shows sunny sky condition. b) Shows intermittent sky condition. c) Shows cloudy sky condition.

Table 4-2. The temperature readings for the PDLC glazing prototype in the transparent state.

	Maximum temperature (°C)			Rate of increment (°C/h)		
	Sunny	Intermittent	Cloudy	Sunny	Intermittent	Cloudy
<b>Ambient</b>	27	21.6	25	0.5	0.6	0.7
<b>Test cell</b>	46.9	39.5	37.8	2.5	3.5	2.4
<b>External surface</b>	38.6	32.2	32	0.9	2	1
<b>Internal surface</b>	41.5	35.1	35	1.4	2.5	1.1

Table 4-3. The solar irradiance measurements for different sky conditions when the PDLC glazing prototype was in the transparent state.

Sky condition	Global solar irradiance (W/m <sup>2</sup> )			Diffuse solar irradiance (W/m <sup>2</sup> )		
	Max	Min	Average	Max	Min	Average
<b>Sunny</b>	848	215	625	290	68	132
<b>Intermittent</b>	885	112	548	441	111	261
<b>Cloudy</b>	584	77	293	413	53	196

Figure 4-3 shows the diurnal variation of the PDLC glazing prototype in the opaque state for different sky conditions. On a sunny day, the test cell steadily increased from 18.9 °C to the maximum temperature of 39.9 °C, while the internal surface of the PDLC glazing increased to the maximum temperature of 35.6 °C at a rate of 3.4 °C/h. The highest ambient temperature recorded was 21.3 °C between 9:00 and 14:00. The test cell and ambient temperatures increased at a rate 2.6 °C/h and 0.6 °C/h, respectively. The temperature difference between the test cell and the internal surface of the PDLC glazing was 7.3 °C at 17:00, indicating low heat loss from the cell due to the opaque property of the PDLC glazing. In comparison, the maximum temperature of the test cell was 46.9 °C when the PDLC was in the transparent (ON) state, while when the PDLC glazing was switched to the opaque state, the maximum temperature was 39.9 °C. It was observed that the PDLC glazing was able to reduce the solar energy entering the test cell in the opaque state. For an intermittent day, the highest temperature was recorded for the test cell and ambient temperature was 43.2 °C and 27.2 °C at a rate of 3.2 °C/h and 1.4 °C/h, respectively. Both the maximum temperature for the test cell and ambient was reached between 9:00 am and 15:00. The internal surface of the PDLC glazing prototype increased by 2.2 °C/h to reach the maximum temperature of 39.8 °C. It was observed that the global irradiance readings were high between 12:00 and 15:00, resulting in higher energy transfer entering the test cell. On a cloudy day, the test cell reached the highest temperature of 24.6 °C between 9:00 and 15:00 and increased 1 °C/h. The highest recorded ambient temperature was 21.8 °C and increased by 0.3 °C/h. The external surface temperature of the PDLC glazing increased 0.6 °C/h to

reach the maximum of 25.4 °C. Table 4-4 reports the PDLC glazing prototype temperature. The solar irradiance values are presented in Table 4-5.

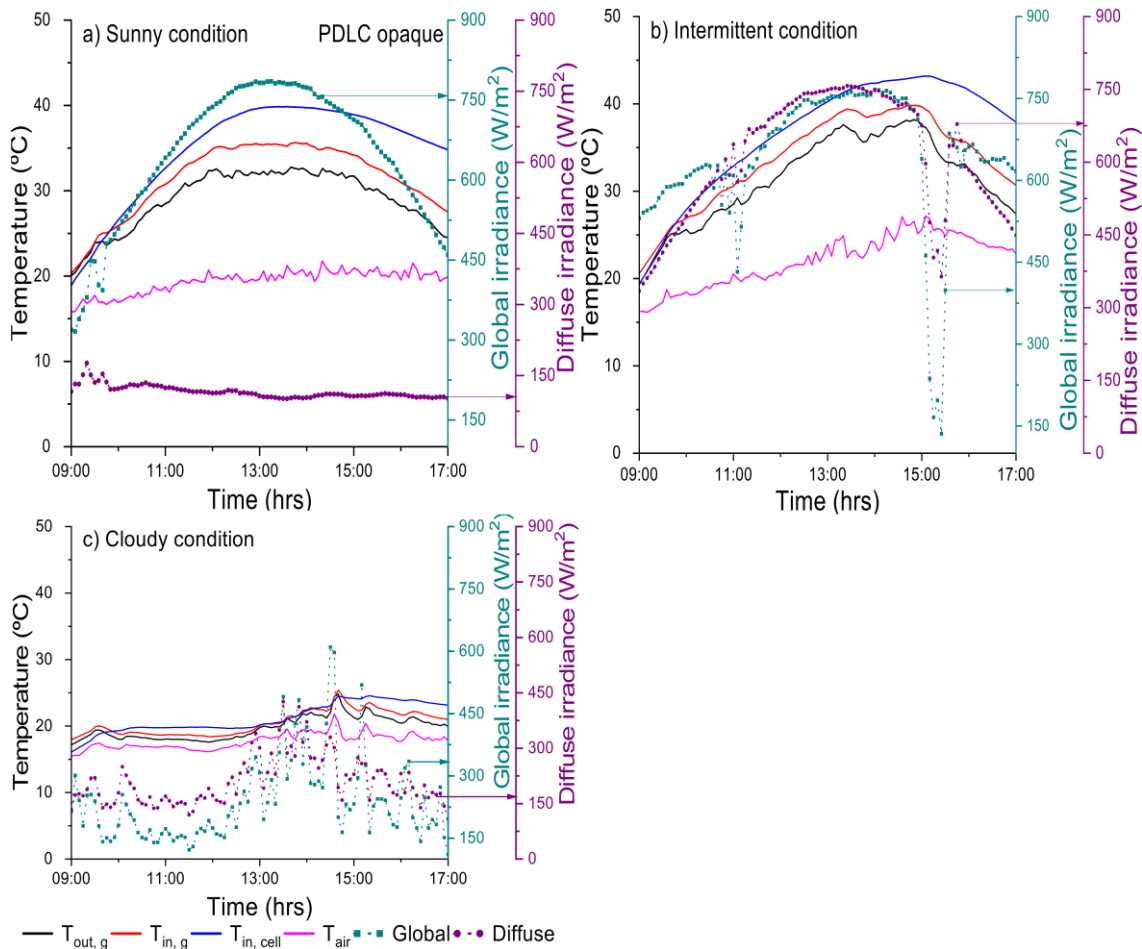


Figure 4-3. Temperature variation as a function of time for the PDLC glazing prototype in the opaque state for different sky conditions. a) shows sunny sky condition. b) shows intermittent sky condition. c) shows cloudy sky condition.

Table 4-4. The temperature readings for the PDLC glazing prototype in the opaque state.

	Maximum temperature (°C)			Rate of increment (°C/h)		
	Sunny	Intermittent	Cloudy	Sunny	Intermittent	Cloudy
<b>Ambient</b>	21.8	27.2	21.8	0.6	1.4	0.3
<b>Test cell</b>	39.9	43.2	24.6	2.6	3.2	1
<b>External surface</b>	32.8	38.2	24.8	1.2	1.9	0.5
<b>Internal surface</b>	35.6	29.8	25.4	1.6	2.2	0.6



Table 4-5. The solar irradiance measurements for different sky conditions when the PDLC glazing was in the opaque state.

Sky condition	Global solar irradiance (W/m <sup>2</sup> )			Diffuse solar irradiance (W/m <sup>2</sup> )		
	Max	Min	Average	Max	Min	Average
<b>Sunny</b>	785	316	644	176	101	116
<b>Intermittent</b>	766	136	641	757	335	609
<b>Cloudy</b>	610	112	236	426	109	210

Figure 4-4 reports the time variation of the temperature difference between the internal test cell temperature and the ambient temperature for the PDLC glazing in the transparent and opaque state. The PDLC glazing shows positive performance in all different sky conditions. In other words, the internal test cell temperature was always hotter than the ambient temperature. The graph shows that the temperature difference is lower for the PDLC glazing in the opaque state in almost the entire measurements in all different sky conditions. The highest temperature difference was found in a sunny sky condition in the amount of 22.5 °C in the case of the PDLC glazing in the transparent state and 20.4 °C in the opaque state. However, the highest temperature difference in cloudy sky conditions was 15.8 °C and 6.5 °C for the transparent and the opaque states, respectively. This indicates low energy transfer in the opaque state due to the random alignment of PDLC particles which decreases the amount of light passing through the glass. The mean value of the temperature differences of the test cell representing all sky conditions was 12.9 °C and 10 °C for the transparent and opaque state of the PDLC glazing, respectively.

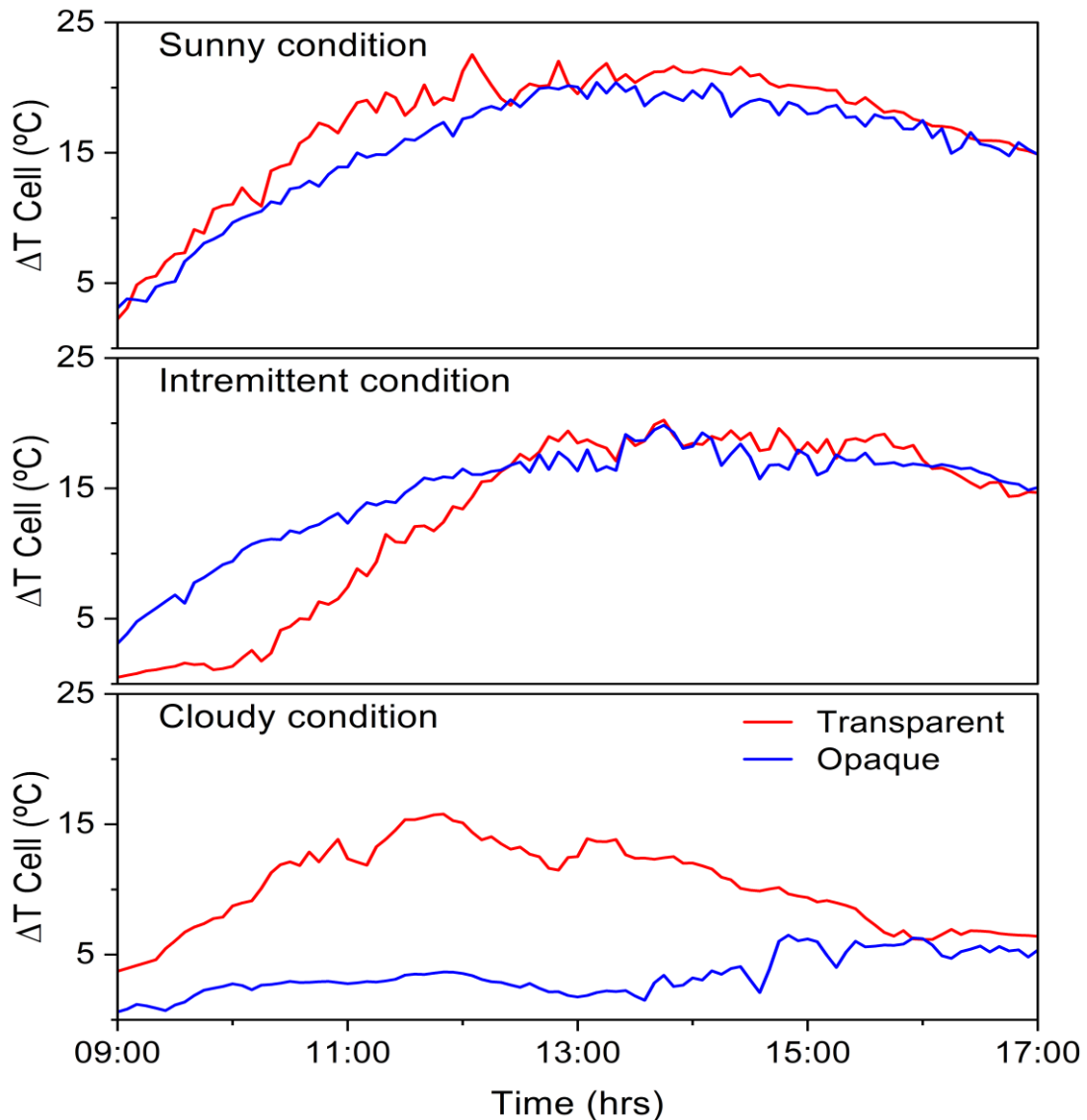


Figure 4-4. The time variation of the temperature difference between the internal test cell temperature and the ambient temperature for the PDLC glazing in the transparent and the opaque states for different sky conditions.

Figure 4-5 presents the time variation of the temperature difference between the external glass and the internal glass temperature of the PDLC glazing in transparent and opaque state. When the PDLC glazing was in the transparent state, the highest temperature difference was 4.6 °C and the internal test cell temperature was 45.1 °C in a sunny sky condition. In the opaque state, the highest temperature difference was 3.6 °C and the test cell temperature was 39.8 °C in sunny sky conditions. In the cloudy condition, the highest temperature difference in the PDLC transparent state was 3.4 °C, while the internal test cell temperature was 32.8 °C. In the opaque state, the highest temperature difference

was 1.5 °C and the internal test cell temperature was 24.6 °C. The mean value of the temperature difference between the surfaces representing all sky conditions is 2.5 °C and 1.8 for the transparent and opaque states, respectively.

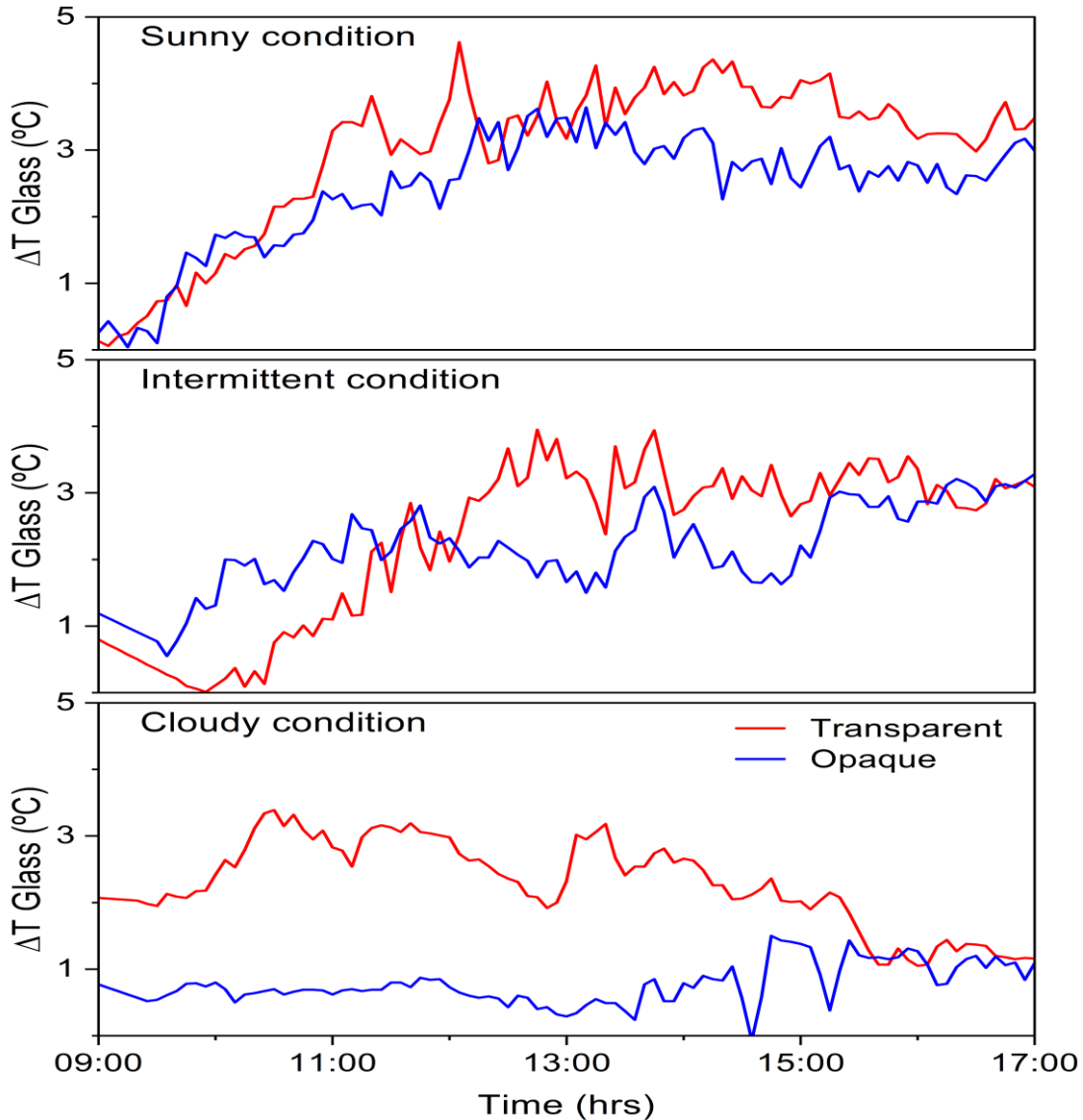


Figure 4-5. The time variation of the temperature difference between the external glass and the internal glass temperature of the PDLC glazing in the transparent and the opaque states for different sky conditions.

#### 4.7.2 Visual comfort analysis of the PDLC glazing prototype

Figure 4-6 reports the readings of glare level (SR) and internal illuminance for the PDLC glazing prototype in the transparent state for sunny, intermittent, and cloudy days. Most of the readings were below 2.5, which means glare level is “just intolerable” for all sky conditions except for the mid-day for intermittent sky

conditions. The PDLC glazing could not provide visual comfort for sunny and intermittent days as the glare level ranged between (2.5 and 1.5). On a cloudy day, the glare discomfort level decreased below 1.5, “just noticeable” as the sun position changed after the hour 16:00.

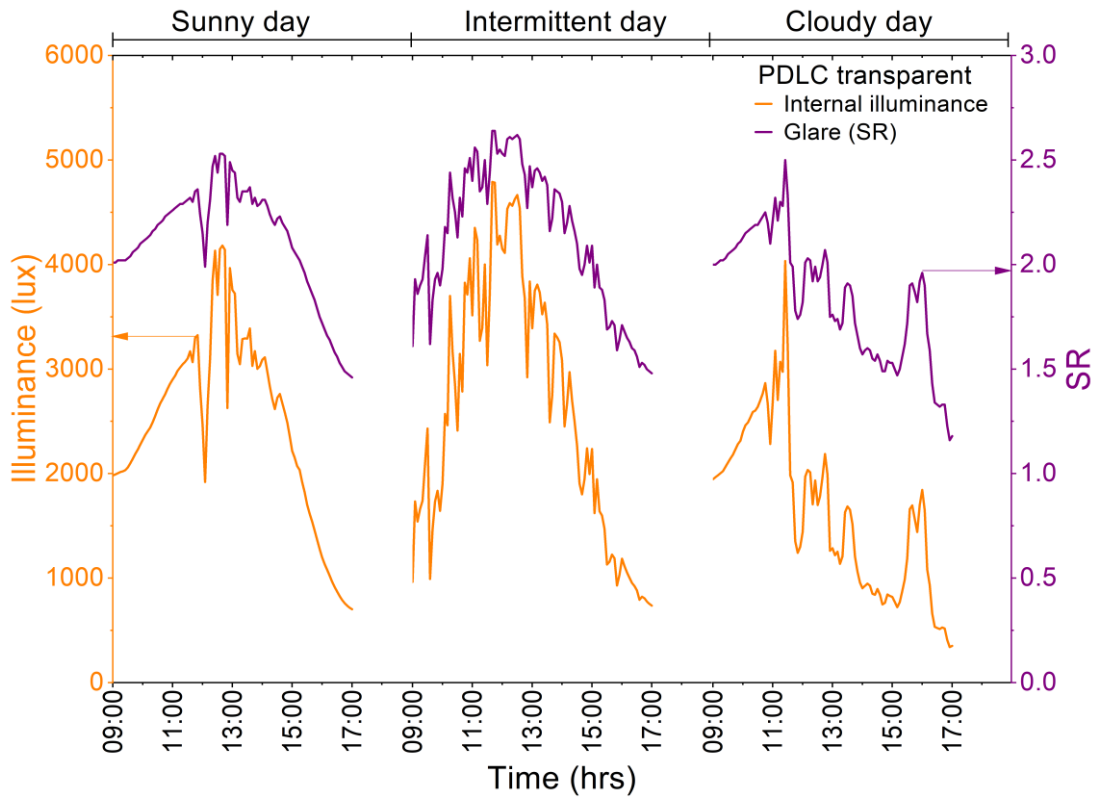


Figure 4-6. The time variation of the discomfort glare (SR) level for the PDLC glazing prototype in the transparent state for different sky conditions.

Figure 4-7 presents the glare (SR) level and indoor illuminance measurements for the PDLC glazing prototype in the opaque state for different sky conditions. For sunny and intermittent days, the glare level exceeded the “just intolerable” level between 10:00 and 14:00. It was observed that the glare level decreased from above “just intolerable” to “just disturbing” between 14:00 and 17:00. On a cloudy day, the PDLC glazing was able to reduce the glare level below the “just disturbing” level from 10:30 to 13:00 and from 15:00 to 16:00. PDLC films scatter incident light in the opaque state resulting in high diffuse transmission. PDLC films allow incident light to pass through in the transparent state as the haze coefficient is at its lowest. However, the PDLC films have significant scattering (opacity) for incident light in the opaque state because the haze factor is at its

highest. The haze coefficient for this PDLC film is 4 in the transparent (ON) state and 96 in the opaque (OFF) state.

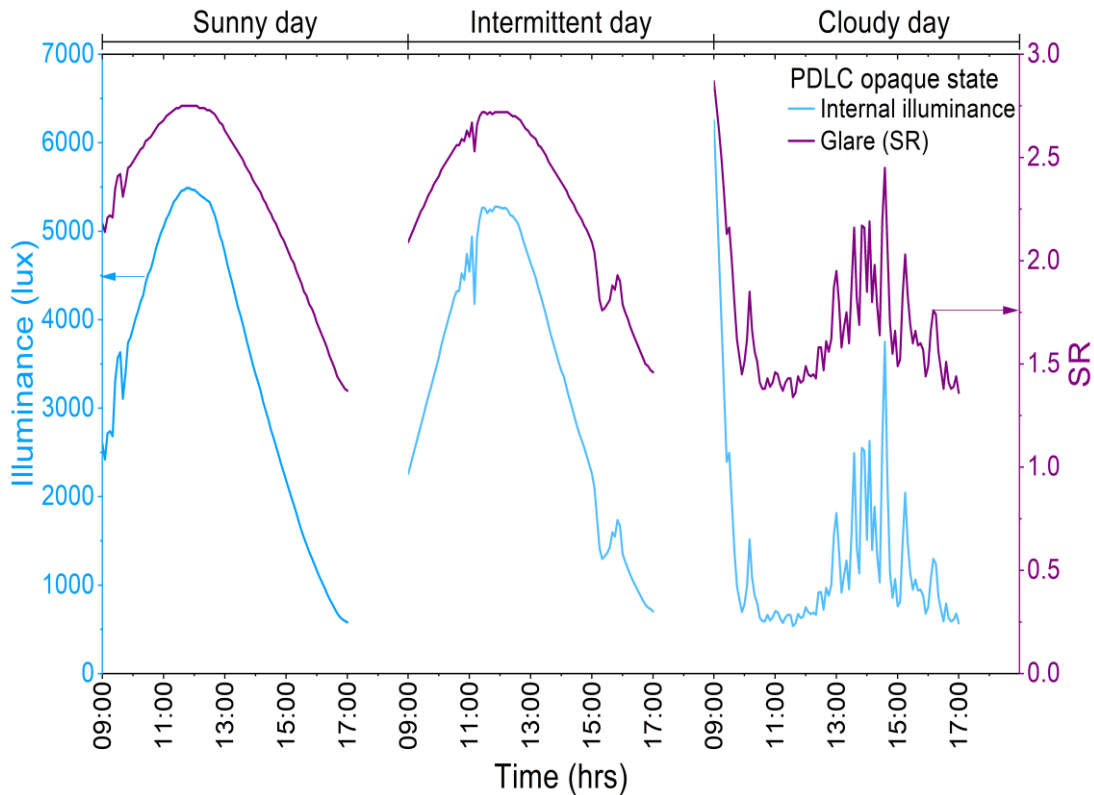


Figure 4-7. The time variation of the discomfort glare (SR) level for the PDLC glazing prototype in the opaque state for different sky conditions.

Figure 4-8 shows the external ( $E_V^{out}$ ), internal illuminance ( $E_V^{in}$ ) and working plane illuminance ( $E_H^{in}$ ) for the PDLC glazing prototype for the transparent and opaque states for different sky conditions. The results show that the mean value of the internal illuminance in the transparent state during mid-day was higher than the mean value of the internal illuminance in the opaque state. However, the glare level was higher in the opaque state, indicating higher diffuse transmission, particularly in the sunny and intermittent sky conditions. The working plane illuminance range between 2322 lux to 42 lux for transparent and opaque states for all sky condition. It was observed that between 16:00 to 17:00, the working plane illuminance decreased to approximately 290 to 42, which indicates that the illuminance was not suitable for office tasks.

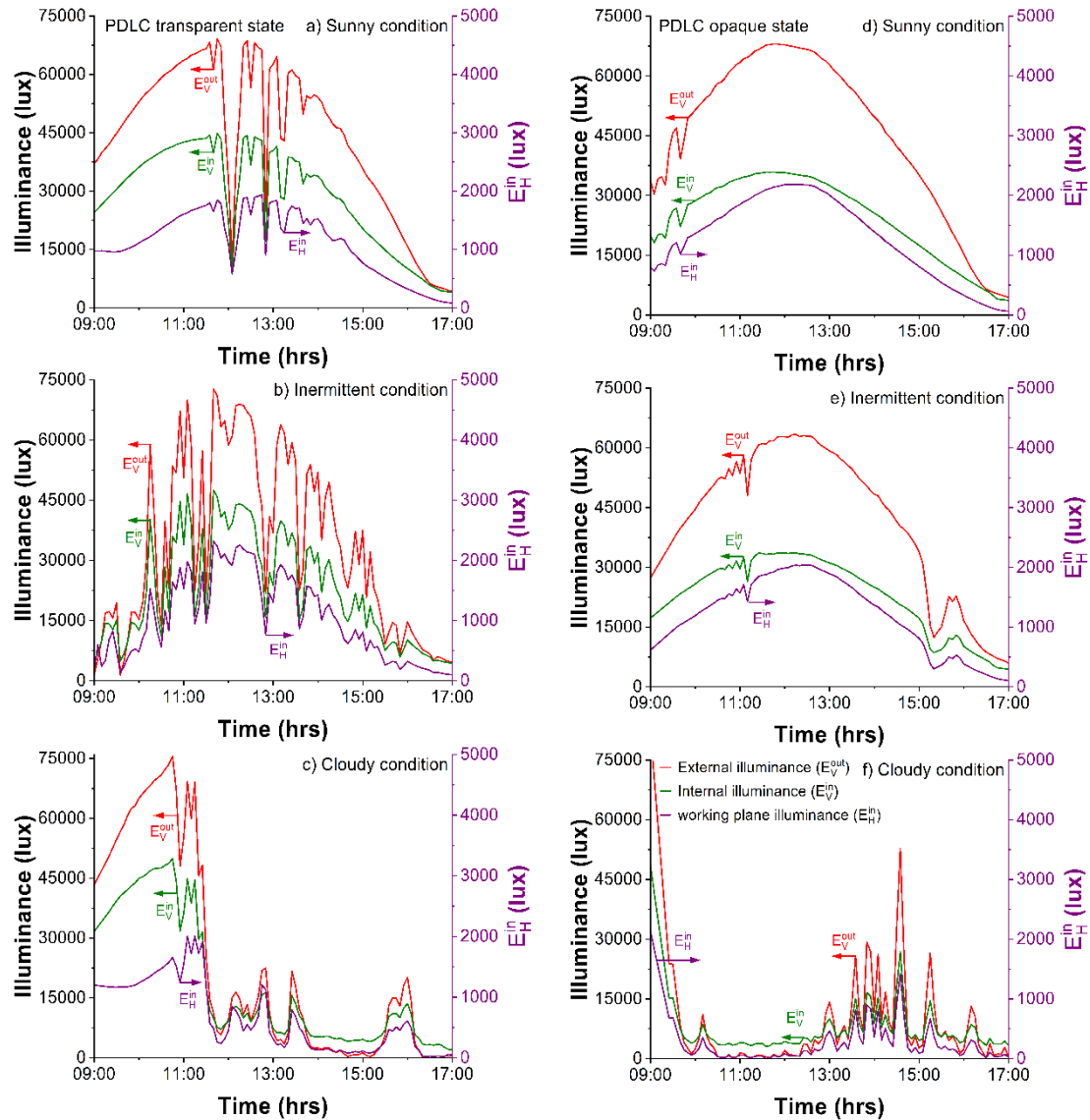


Figure 4-8. The time variation of the external (red lines), internal illuminance (green lines) and working plane illuminance (purple lines) of the PDLC glazing prototype in the transparent and opaque states for different sky conditions. Graphs from a to c show sunny, intermittent, and cloudy sky conditions when PDLC in transparent state. Graphs from e to f show sky condition when PDLC in opaque state.

#### 4.7.3 Thermal analysis of the PDLC<sub>F</sub> glazing prototype combined with the solar control film

Figure 4-9 presents the temperature variation as a function of time for the PDLC<sub>F</sub> glazing in the transparent state for sunny, intermittent, and cloudy sky conditions.

It is clear from the graph that the solar film contributed to rejecting solar heat and maintaining the test cell temperature lower than the internal surface of the glazing in all sky conditions. On a sunny day, the highest recorded temperature of the test cell was 39.9 °C and the ambient temperature was 25 °C. The test cell and ambient temperature increased by 2.7 °C/h and 0.8 °C/h, respectively. The test cell maximum temperature was recorded between 9:00 and 14:00. The external and internal surfaces of the PDLC<sub>F</sub> glazing reached the highest temperature of 42 °C. For an intermittent day, the test cell temperature increased 1.6 °C/h to reach the maximum temperature of 35.4 °C. The highest ambient temperature was 23 °C and increased by 0.6 °C/h. The external surface increased by 1.7 °C/h and the maximum temperature reached 38.5 °C. In addition, the maximum internal surface temperature was 38 °C and increased by 2.3°C/h. For a cloudy day, the maximum test cell recorded was 28 °C and the ambient temperature was 20°C. The test cell and ambient temperature increased by 2.4 °C/h and 0.6 °C/h between 9:00 and 13:00, respectively. Both the external and internal surface temperatures were 29.3 °C and increased by 1 °C/h. It was observed that the test cell temperature was lower than the internal and external surface of the PDLC<sub>F</sub> glazing before it reached the maximum temperature in all sky conditions. However, after the test cell reached the maximum temperature, it maintained a higher temperature than both surfaces. This indicates that the solar film was able to reject the solar heat and maintain a lower temperature than the glazing surfaces inside the test cell. On the contrary, the test cell temperature was always higher than the PDLC glazing surfaces without the solar film as shown in Figure 4-2. Table 4-6 presents the temperature of the PDLC<sub>F</sub> glazing prototype combined with the solar control film. Table 4-7 reports the solar irradiance readings for all sky conditions.

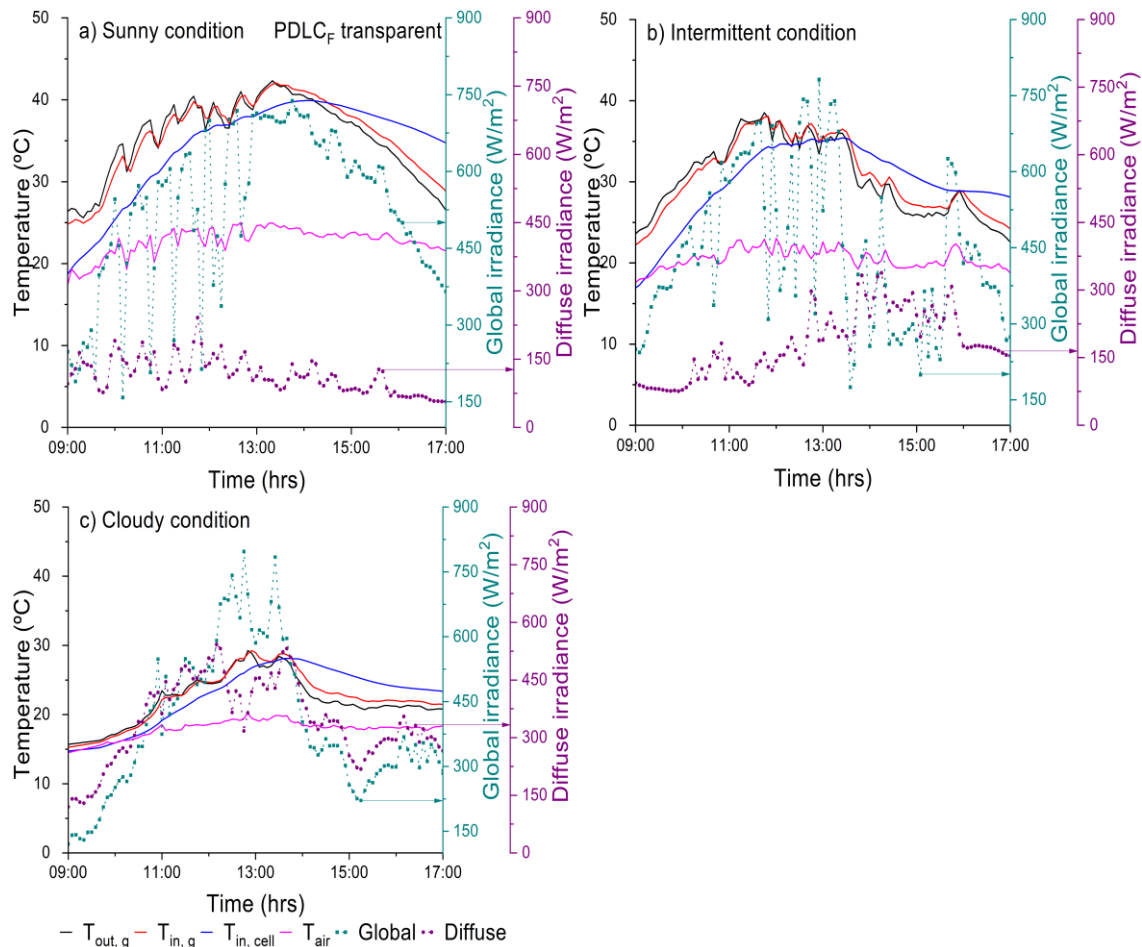


Figure 4-9. Temperature variation as a function of time for the PDLC<sub>F</sub> glazing prototype combined with the solar control film in the transparent state for different sky conditions. a) Shows sunny condition. b) Shows intermittent sky condition. c) Shows cloudy condition.

Table 4-6. The temperature readings for the PDLC<sub>F</sub> glazing prototype combined with the solar control film in the transparent state.

	Maximum temperature (°C)			Rate of increment (°C/h)		
	Sunny	Intermittent	Cloudy	Sunny	Intermittent	Cloudy
<b>Ambient</b>	25	23	20	0.8	0.6	0.6
<b>Test cell</b>	39.9	35.4	28	2.7	1.6	2.4
<b>External surface</b>	42	38.5	29.3	1.3	1.7	1.2
<b>Internal surface</b>	42	38	29.3	1.7	2.3	1



Table 4-7. The solar irradiance measurements for different sky conditions when the PDLC<sub>F</sub> glazing was in the transparent state.

Sky condition	Global solar irradiance (W/m <sup>2</sup> )			Diffuse solar irradiance (W/m <sup>2</sup> )		
	Max	Min	Average	Max	Min	Average
<b>Sunny</b>	738	158	530	241	57	115
<b>Intermittent</b>	782	175	442	338	76	179
<b>Cloudy</b>	797	121	399	542	120	345

Figure 4-10 shows the temperature variation as a function of time PDLC<sub>F</sub> glazing in the opaque state for different sky conditions. In general, between 9:00 and 15:25, the test cell temperature was lower than the internal surface of the PDLC<sub>F</sub> glazing in all sky conditions except for the intermittent day. On a sunny day, the test cell reached a maximum temperature of 33.3 °C, while the ambient was 22°C. The test cell increased 1.7 °C/h and the ambient increased 0.3 °C/h. The external and internal surfaces temperatures of the PDLC<sub>F</sub> glazing were higher than the test cell and the maximum temperatures were 35 °C and 34 °C, respectively. For an intermittent day, the maximum test cell temperature was 34.7°C and increased by 1.9 °C/h. The highest ambient temperature recorded was 24 and increased by 1 °C/h. Between 9:00 and 12:00, the external and internal surfaces of the glazing reached the maximum of 42.4 °C and 40.4 °C, respectively. The test cell temperature was lower than the internal surface between 9:00 and 12:30; however, the internal surface temperature increased between 15:00 and 16:00 due to an increase in the ambient temperature and solar irradiance. On a cloudy day, the test cell temperature reached a maximum of 28 °C and the ambient temperature was 19 °C. The external and internal surfaces temperature reached the maximum of 30 °C and 29 °C, respectively. It was found that the internal surface temperature was always higher than the test cell between the morning and afternoon in all different sky conditions. This indicates that the solar control film rejected a portion of the solar energy from entering the test cell. In addition, when the PDLC<sub>F</sub> glazing was switched to the transparent state, the test cell reached the maximum temperature faster than when the PDLC<sub>F</sub> glazing was switched to the opaque state. Therefore, the PDLC<sub>F</sub> glazing in the opaque state reduced the heat transfer into the test cell. Table 4-8

reports a list of the temperature of the PDLC<sub>F</sub> glazing prototype. Table 4-9 shows the solar irradiance measurements for all sky conditions.

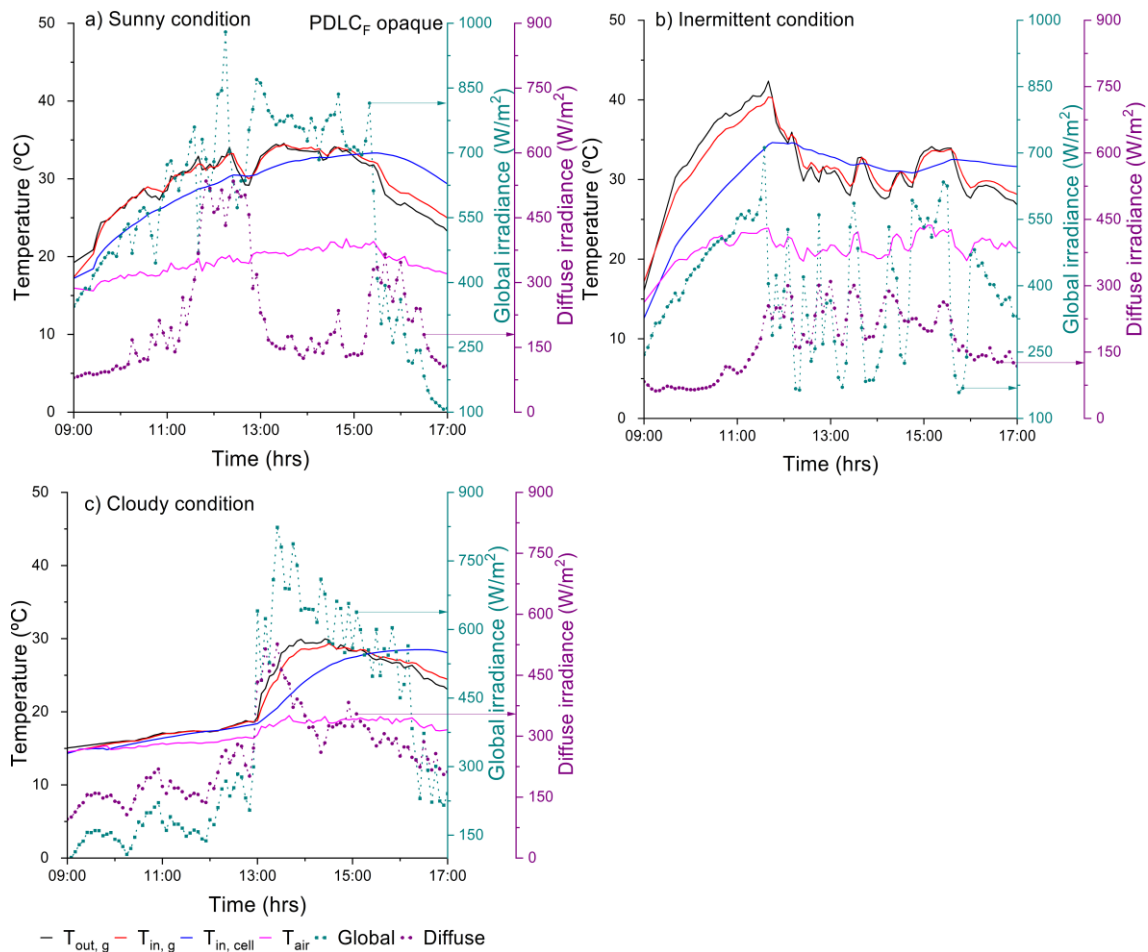


Figure 4-10. Temperature variation as a function of time for the PDLC<sub>F</sub> glazing prototype combined with the solar control film in the opaque state for different sky conditions. a) Shows sunny condition. b) Shows intermittent sky condition. c) Shows cloudy condition.

Table 4-8. The temperature readings for the PDLC<sub>F</sub> glazing prototype combined with the solar control film in the opaque state.

	Maximum temperature (°C)			Rate of increment (°C/h)		
	Sunny	Intermittent	Cloudy	Sunny	Intermittent	Cloudy
<b>Ambient</b>	22	24	19	0.3	1	0.7
<b>Test cell</b>	33.3	34.7	28	1.7	1.9	2.2
<b>External surface</b>	35	42.4	30	1.3	1.3	2
<b>Internal surface</b>	34	40.4	29	1.6	1.7	1.2

Table 4-9. The solar irradiance measurements for different sky conditions when the PDLC<sub>F</sub> glazing was in the opaque state.

Sky condition	Global solar irradiance (W/m <sup>2</sup> )			Diffuse solar irradiance (W/m <sup>2</sup> )		
	Max	Min	Average	Max	Min	Average
<b>Sunny</b>	980	107	572	535	80	219
<b>Intermittent</b>	712	159	396	309	62	172
<b>Cloudy</b>	823	96	363	527	96	251

Figure 4-11 reports the time variation of the temperature difference between the internal test cell temperature and the ambient temperature for the PDLC<sub>F</sub> glazing in the transparent and opaque state. The measurements illustrate a positive performance of the PDLC<sub>F</sub> glazing as about 7 hours of the measurements show that the temperature difference was lower in the case of the PDLC<sub>F</sub> glazing in the opaque state. The internal test temperature difference was always hotter than the ambient temperature difference. Data analysis showed that the maximum temperature difference was found in the transparent state 16.5 °C in a sunny sky condition and the internal test temperature was recorded as 39.8 °C. In the opaque state the temperature difference was lower by 3 °C and the internal temperature was recorded as 32.3 °C. In cloudy sky conditions, the maximum temperature difference in the transparent state was 9.5 °C and the registered test cell temperature was 27.9 °C. The mean value of the temperature difference for all sky conditions was 8.4 °C in the transparent state and 7.4 °C in the opaque state. The solar control film reduced the test cell temperature in all sky conditions compared to the PDLC glazing without the solar control film.

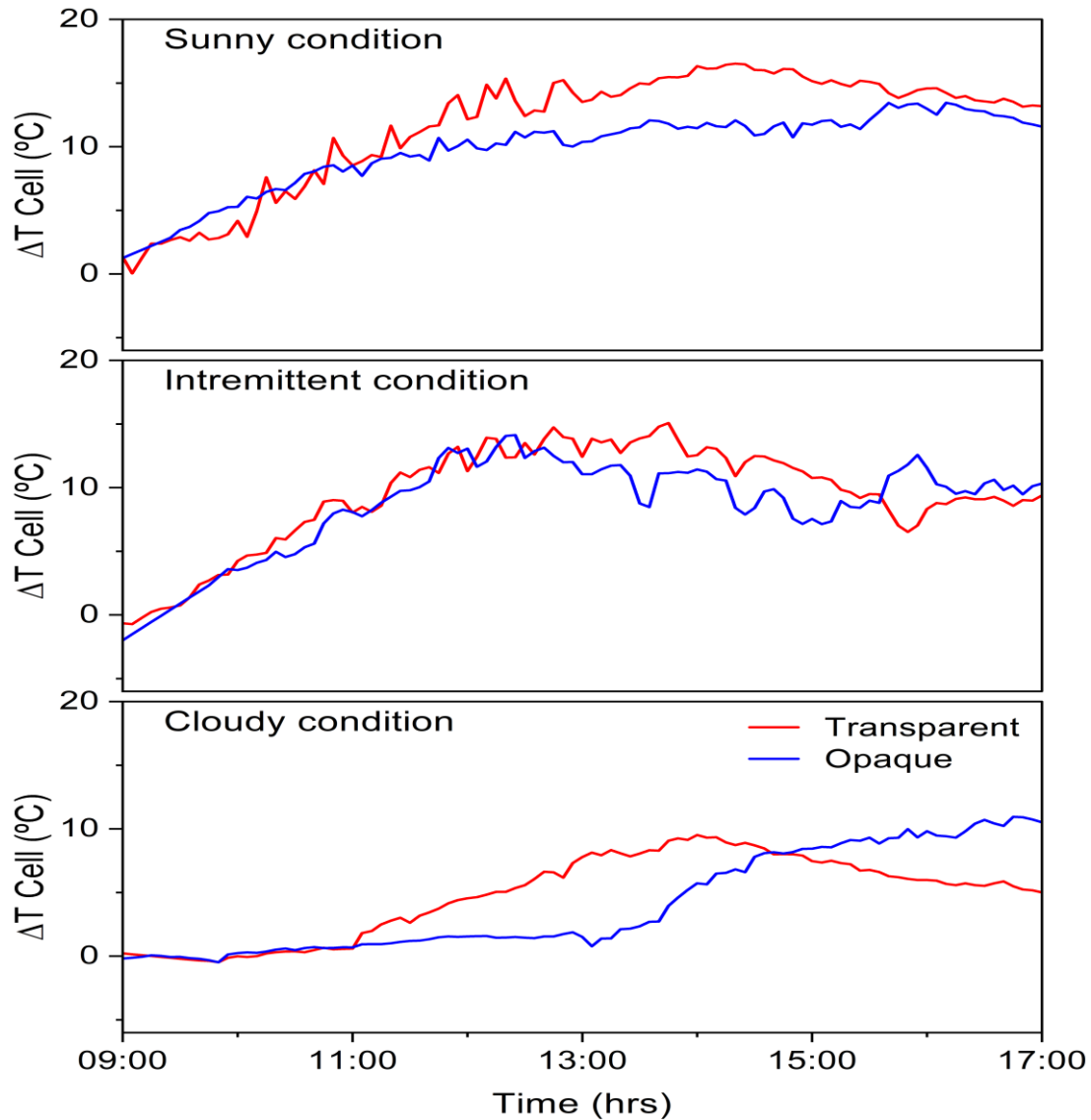


Figure 4-11. The time variation of the temperature difference between the internal test cell temperature and the ambient temperature for the PDLC<sub>F</sub> (with solar control film) glazing in transparent and opaque states for different sky conditions.

Figure 4-12 shows the time variation of the temperature difference between the external glass temperature and the internal glass temperature for the PDLC<sub>F</sub> glazing in the transparent and opaque state. It was found that the internal glass temperature was lower than the external glass in all sky conditions for the transparent and opaque states. The peak value of internal and external glass temperatures was 42 °C for both and the test cell temperature was 39.9 °C for the transparent state in a sunny sky condition. In the opaque state, the peak value was 35 °C for the external glass and 34 °C for the internal one, while the test cell

temperature was 33.3 °C. Data analysis showed that the temperature difference was lower for the PDLC<sub>F</sub> in the opaque state.

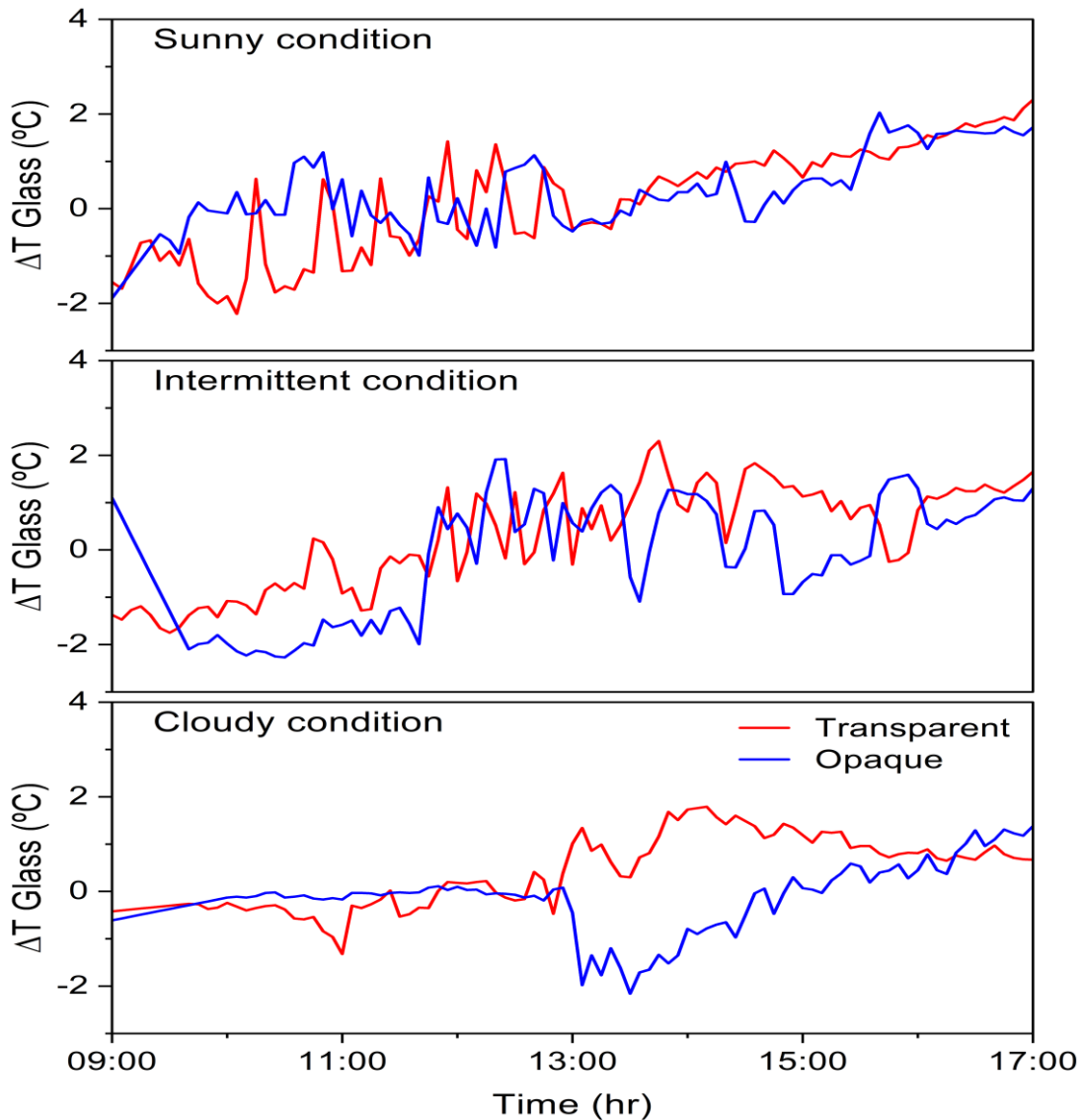


Figure 4-12. The time variation of the temperature difference between the external glass and the internal glass temperature of the PDLC<sub>F</sub> glazing in transparent and opaque states for different sky conditions.

#### 4.7.4 Visual comfort analysis of the PDLC<sub>F</sub> glazing prototype combined with the solar control film

Figure 4-13 presents the glare level (SR) measurements and internal illuminance for the PDLC<sub>F</sub> glazing in the transparent state for a sunny, intermittent, and cloudy day. The solar control film reduced the glare level below 2 for all sky conditions. On a sunny day, the glare level varied between 1.5 to 1.9 from 9:00 to 14:55.

Between 15:00 to 17:00, as the sun changed its position, the internal illuminance decreased inside the test cell and the glare level decreased below 1.5. The level of visual comfort the PDLC<sub>F</sub> glazing provided was between “just intolerable” and “just disturbing” from the morning until the late afternoon. However, between 15:00 to 17:00, the PDLC<sub>F</sub> glazing was able to offer visual comfort below “just disturbing”. For an intermittent day, the level of glare was below “just disturbing” between 13:45 to 17:00. For a cloudy day, the PDLC<sub>F</sub> glazing offered glare level below “Just disturbing” in the range of 1.13 to 1.5 from 9:00 to 10:30 and 14:00 to 17:00. Approximately, the PDLC<sub>F</sub> glazing provided 56% of the time glare level below “just disturbing”, while 44% of the time were above “just disturbing”. In general, the PDLC<sub>F</sub> glazing provided discomfort glare level above “just disturbing” during the mid-day, when the internal illuminance was at the maximum level for all sky conditions.

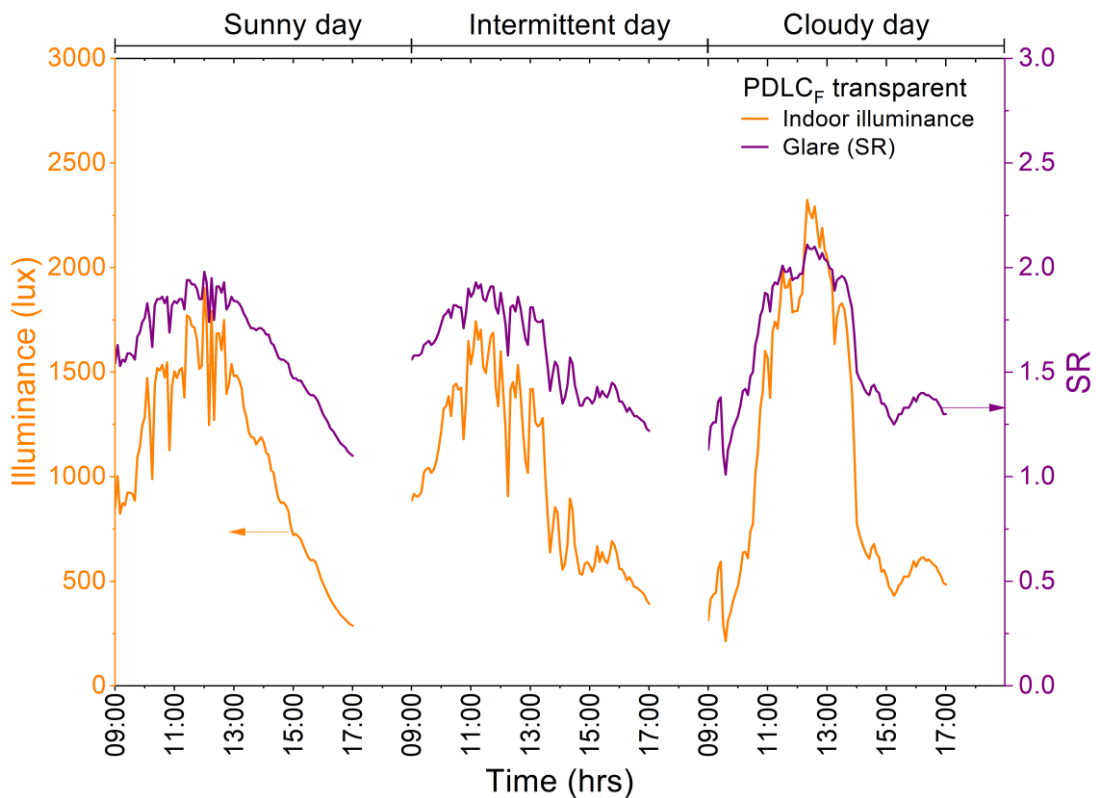


Figure 4-13. The time variation of the discomfort glare (SR) level for the PDLC<sub>F</sub> glazing prototype combined with solar control film in the transparent state for sunny, intermittent, and cloudy sky conditions.

Figure 4-14 shows the time variation of the glare level and internal illuminance for the PDLC<sub>F</sub> glazing in the opaque state for different sky conditions. The discomfort glare level exceeded 1.5, above “just disturbing” when the internal illuminance was at the highest level for all sky conditions. However, the glare level decreased to below 1.5 during the late afternoon hours. On a sunny day, the PDLC<sub>F</sub> glazing decreased the glare level to reach between 1.49 to 0.95 from 15:00 to 17:00. According to the glare rating index, the glare level was between “just noticeable” and “just disturbing”. On an intermittent day, the level of glare above “just noticeable” was reached after 13:30, which ranges between 1.13 to 1.46. On a cloudy day, the glare level decreased to the lowest level, ranging between 0.79 to 1.45 during 9:00 to 13:00 and 15:30 to 17:00. The PDLC<sub>F</sub> glazing was able to achieve a glare level above “just noticeable” in a cloudy sky condition. It was found that the solar control film improved the visual comfort compared to the PDLC glazing without the film in the opaque state. In comparison, the glare level of the PDLC glazing for sunny and intermittent sky conditions was between “just disturbing” and “just intolerable”, while the glare level for the PDLC<sub>F</sub> was between “just noticeable” and “just disturbing” for all sky conditions. The solar control film achieved to reduce discomfort glare level by 29% for the opaque state.

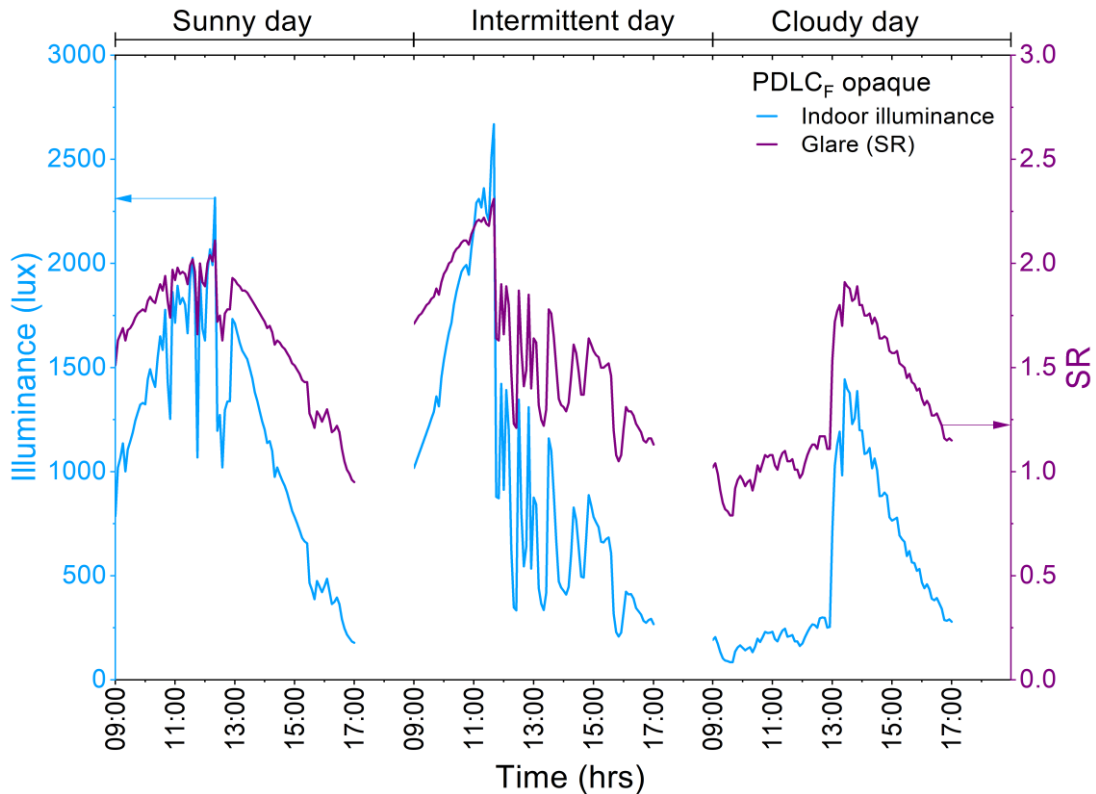


Figure 4-14. The time variation of the discomfort glare (SR) level for the PDLC<sub>F</sub> glazing prototype combined with solar control film in the opaque state for sunny, intermittent, and cloudy sky conditions.

Figure 4-15 shows the external ( $E_V^{out}$ ), internal illuminance ( $E_V^{in}$ ) and working plane illuminance ( $E_H^{in}$ ) for the PDLC<sub>F</sub> glazing prototype for the transparent and opaque states for different sky conditions. The internal illuminance of the PDLC<sub>F</sub> glazing range between 19705 lux to 1146 lux, while without the solar control film the range was from 49858 lux to 2086 lux. The result showed that there was a reduction in the internal illuminance; however, the working plane illuminance mean value was approximately 609 lux for the transparent state and 483 lux for the opaque state, which are suitable for office tasks. It was found that after 15:00, the working plane illuminance decreased below 300 lux, which is not compatible with office tasks.



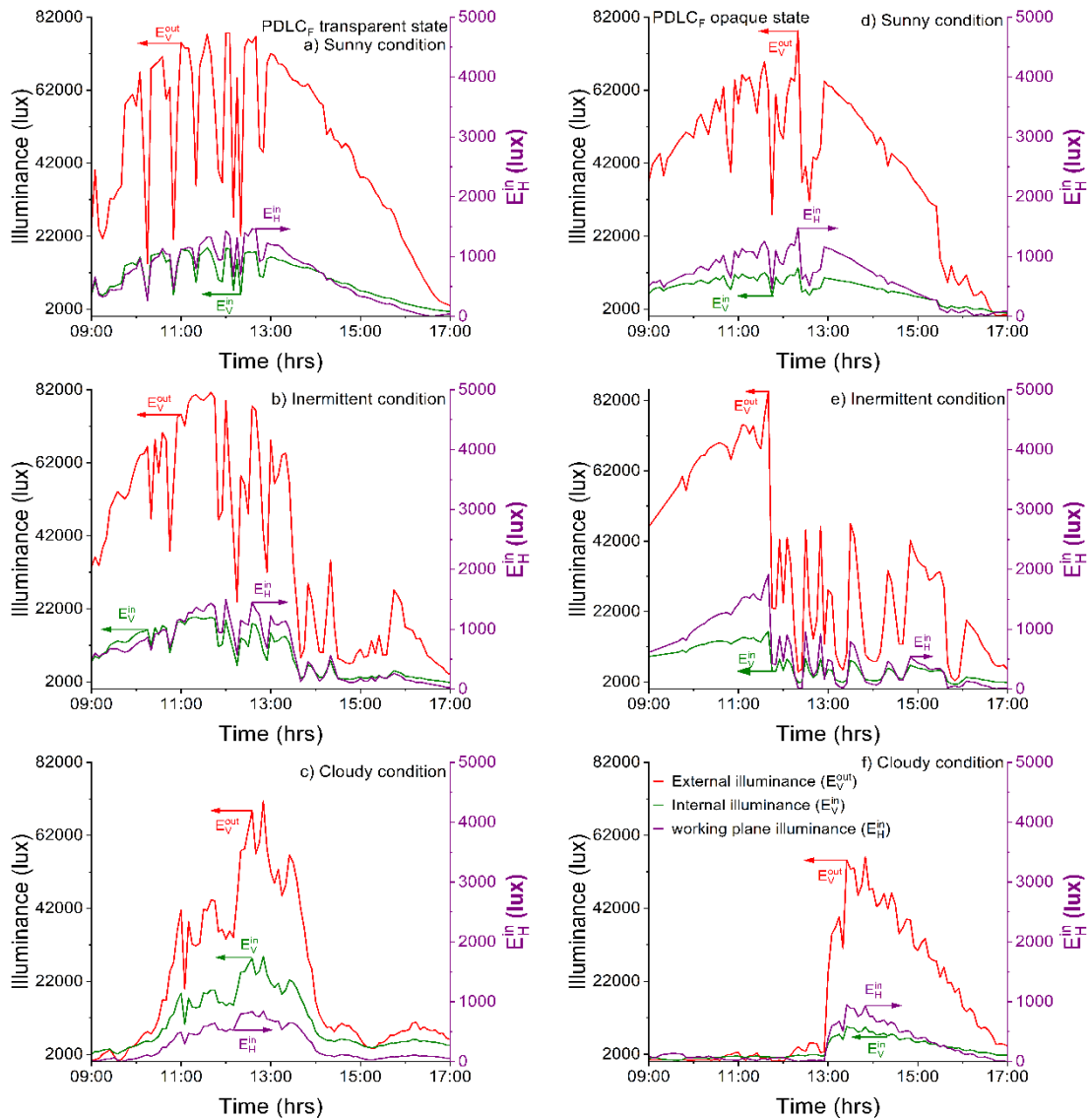


Figure 4-15. The time variation of the external (red lines), internal (green lines) and working plane illuminance (purple lines) of the PDLC<sub>F</sub> glazing with solar control film in the transparent and opaque states for different sky conditions. Graphs from a to c show sunny, intermittent, and cloudy sky conditions when combined PDLC<sub>F</sub> in transparent state. Graphs from e to f show sky condition when combined PDLC<sub>F</sub> in opaque state.

#### 4.8 Conclusion

A PDLC glazing prototype and a combined PDLC<sub>F</sub> with a solar control film were characterised under real weather conditions to assess the thermal performance and evaluate glare. A small test cell was utilised to characterise the PDLC glazing

prototype for different sky conditions. The results of the investigation can be summarised as follow:

1. The results of the study showed that the internal temperature of the test cell remained higher than the ambient temperature for the transparent and opaque state for all sky conditions. The PDLC glazing internal surface temperature was always higher than the external surface temperature for all sky conditions. The test cell temperature of the PDLC in the opaque state was lower than the test cell temperature when the glazing was switched to the transparent state for a sunny sky condition. The PDLC glazing could positively impact reducing the heat load in the winter due to low heat loss.
2. The data analysis showed that the PDLC glazing prototype was not able to reduce the glare discomfort in the transparent state for all sky conditions. However, visual comfort was achieved between 10:00 to 12:40 and 15:00 to 17:00 when the PDLC glazing was switched to the opaque state for a cloudy sky condition.
3. The solar control film because of its NIR limiting ability, achieved to reduce the solar heat gain as the PDLC<sub>F</sub> glazing's surfaces temperature was higher than the test cell temperature in the transparent and opaque states for all sky conditions. When the test cell reached the maximum temperature, it remained higher than the glazing's surfaces in both states for all-sky conditions.
4. Visual comfort was improved when the solar film was added to the PDLC glazing for both states in all sky conditions. The PDLC<sub>F</sub> glazing was able to reduce the glare level during the late afternoon hours to below 1.5 "just disturbing" in the transparent and opaque states for all sky conditions.

## **Chapter 5. Simulation energy modelling study for a smart switchable adaptive polymer dispersed liquid crystal for two climate zones**

### **5.1 Introduction**

In this chapter, the PDLC switchable window was investigated to evaluate the energy and daylight performance for an office building in two contrasting climatic zones (Riyadh, Saudi Arabia and London, United Kingdom) using an energy modelling tool. A building model was developed in order to assess the impact of the PDLC switchable window on cooling, heating, and lighting loads. Moreover, the daylight performance was evaluated for three daylight zones (a low daylight zone, an intermediate daylight zoned, and high daylight zone).

### **5.2 Simulation modelling**

The PDLC switchable window was investigated for an office building to evaluate the cooling, heating, and lighting loads and glare discomfort for two climate zones; and the results were compared against a double pane reference window. Rhinoceros© modelling tool was used to construct a two-story office building according to the American Society of Heating, Refrigerating and Air-conditioning Engineers ASHRAE standards. Further details of the building envelope properties are available in section 2.8.1. The PDLC switchable glazing was controlled using two shading control strategies. Firstly, various solar radiation thresholds (100 W/m<sup>2</sup>, 250 W/m<sup>2</sup>, 500 W/m<sup>2</sup>, 750 W/m<sup>2</sup>, and 1000 W/m<sup>2</sup>) were employed to control the transmittance of the PDLC glazing. The PDLC glazing will only change to opaque state when the vertical solar radiation on the PDLC glazing's surface exceeds the thresholds. Secondly, outdoor temperature control was employed to change the PDLC glazing transmittance form transparent to opaque. The PDLC glazing transmittance will change to opaque when the outdoor temperature becomes higher than the thresholds. The outdoor temperatures for Riyadh, Saudi Arabia were 4 °C, 20 °C, and 46 °C and for London, United Kingdom were -5.9 °C, 20 °C, and 31.3 °C. The shading control strategies and weather data are explained in detail in section 2.8.2.

### 5.3 Building energy simulation

Windows are an important building component that can help to achieve energy balance and provide visual comfort. To evaluate windows performance for buildings, the required windows parameters are  $U$ -value, SHGC, and visible transmittance. In the summer months heat passes through windows into the building and in the winter months heat escapes. The new technology of windows for example, multilayer glazing, low emissivity (low-e) glazing, and vacuum glazing could provide energy balance as they have competitive  $U$ -value. However, these window technologies do not have variable  $U$ -value and SHGC. Double glazing windows are commonly used in existing buildings due to low cost but they cannot control daylight and glare. However, switchable windows can have variable  $U$ -value and SHGC and have the potential to offer visual comfort. Therefore, in the current research the reference window was chosen to represent the standard double-glazing window that commonly used in the old existing buildings. EnergyPlus 8.9 component was utilised to assess the energy saving for an office building for arid climate zone; Riyadh, Saudi Arabia, and temperate oceanic climate zone; London, United Kingdom. EnergyPlus was developed by the Department of Energy of the US government and has been made available for the public to perform annual building energy simulation. The software combines the best feature of BLAST and DOE-2 programs [148] and utilises the heat balance energy method, recommended by ASHRAE as the proper method for building energy modelling [149]. The capability of EnergyPlus has been extensively tested and validated for performing building energy analysis [150]. EnergyPlus is an excellent tool that allows users to investigate the switchable window and provides comprehensive data for annual analysis of heating, cooling, and lighting loads on an hourly basis [151,152]. The construction of the model used in this study is characterised by building geometry, envelop properties, mechanical system properties, lighting system properties, occupancy schedule, and HVAC system setpoint. More details of the building model and envelop properties are provided in Table 2-6.

The PDLC switchable window and reference window were defined in the simulation algorithm by three parameters: solar heat gain coefficient (SHGC),

thermal transmittance ( $U$ -value), and visible transmittance ( $\tau_{vis}$ ). Data analysis was carried out to evaluate the heating, cooling, and lighting loads for the office building on an annual basis. Two control shading strategies were utilised to control the PDLC window in two different climate zones.

#### **5.4 Daylight simulation**

OpenStudio 2.9 component was utilised to evaluate the interior illuminance performance and daylight glare index (DGI) of the investigated PDLC window. OpenStudio is an open-source tool that allows advanced thermal and daylight analysis for building modelling. It is a strong tool used to perform energy performance analysis for both residential and commercial buildings [153]. To investigate the potential of the PDLC switchable window, which could improve indoor visual comfort, an analysis of glare metrics should be considered.

Grasshopper© was used to evaluate glare discomfort for an office building. The software allows to evaluate glare discomfort using Daylight Glare Index (DGI) or Daylight Glare Probability (DGP) methods. The objective of this work is to evaluate glare discomfort on an annual basis for every hour of the operation schedule. DGP is an image-based metric and would not be appropriate for annual based analysis. Therefore, DGI was more suitable to evaluate the visual discomfort for this study.

The OpenStudio component was used to evaluate the DGI and interior illuminance for the south orientation of the first floor, and natural daylight only was considered for the analysis. The evaluation of DGI was based on the percentage of time in which the DGI value was 22 or below for the total annual operation schedule hours. The maximum recommended value for office buildings is 22 which defines the borderline between comfortable and uncomfortable glare level (see Table 5-1) [88]. The discomfort glare at a reference point results from luminance difference between a window and an interior surface surrounding the window.

Table 5-1. Levels of discomfort glare indexes.

DGI level	DGI index
Just perceptible	16
Perceptible	18
Just acceptable	20
Acceptable	22
Just uncomfortable	24
Uncomfortable	26
Just intolerable	28

The interior illuminance was calculated as percentage of time for the total annual schedule hours and the illuminance setpoint was set to 300 lx. The analysis of the interior illuminance considered natural daylight only. Artificial lighting was controlled to dim when there was enough natural daylight. All sensors were facing the window view and the data of DGI and interior illuminance were calculated as a percentage of the total annual time according to the operation schedule. The DGI was calculated by Eq 5-1:

$$G = \frac{L_{\omega}^{1.6} \Omega^{0.8}}{L_b + 0.07 \omega^{0.5} L_{\omega}} \quad \text{Eq 5-1}$$

Where

$G$  = discomfort glare constant.

$L_{\omega}$  = average luminance of the window as seen from the reference point.

$\Omega$  = solid angle subtended by window, modified to take into account the direction of occupant view.

$L_b$  = luminance of window into  $N_x$  by  $N_y$  rectangular elements, as is done for calculating the direct component of interior illuminance.

## 5.5 Simulation results

### 5.5.1 Evaluation of heating, cooling, and lighting energies in relation to solar radiation in Riyadh

Figure 5-1 reports the total annual cooling, heating, and lighting energy consumption in Riyadh compared to the reference window. The figure clearly shows that the PDLC window reduced the total annual cooling, heating, and lighting loads compared to the reference window for all the control variables. The highest total annual cooling, heating, and lighting reduction in Riyadh climate were achieved at 100 W/m<sup>2</sup> with a primary energy reduction of 8.1%. However, in Riyadh energy reduction amount decreased as the setpoint of solar radiation variables increased, which indicated more energy required for cooling during the summer months. Additionally, the PDLC was able to control the solar radiation transmission and reduce the annual energy consumption at the highest solar radiation setpoint 1000 W/m<sup>2</sup> by 5.2%. Table 5-2 presents the results of the annual energy usage in Riyadh. The results show the cooling load increased over all solar radiation thresholds reflecting the importance of air conditioning in the summer months when electricity usage is double of that in the winter months [14]. The heating load increased when the solar radiation was set to 100 W/m<sup>2</sup> and 250 W/m<sup>2</sup> due to low solar radiation level in Riyadh. However, when PDLC window was controlled at 500 W/m<sup>2</sup> and higher solar radiation level the heating demand decreased, which indicated less need for heating system.

Figure 5-2 shows the total monthly cooling, heating, and lighting energy consumption in Riyadh. The PDLC window was able to control the solar radiation at various thresholds and had an excellent impact on reducing the cooling load during the summer months. When the PDLC was controlled to change its transparency from transparent to translucent at 100 W/m<sup>2</sup>, it achieved 12.7% of cooling load reduction during the summer. However, there was no heating load reduction due to Riyadh's weather pattern, which is cooling dominated. Table 5-3 reports the monthly energy consumption in Riyadh in relation to solar radiation against the reference window.

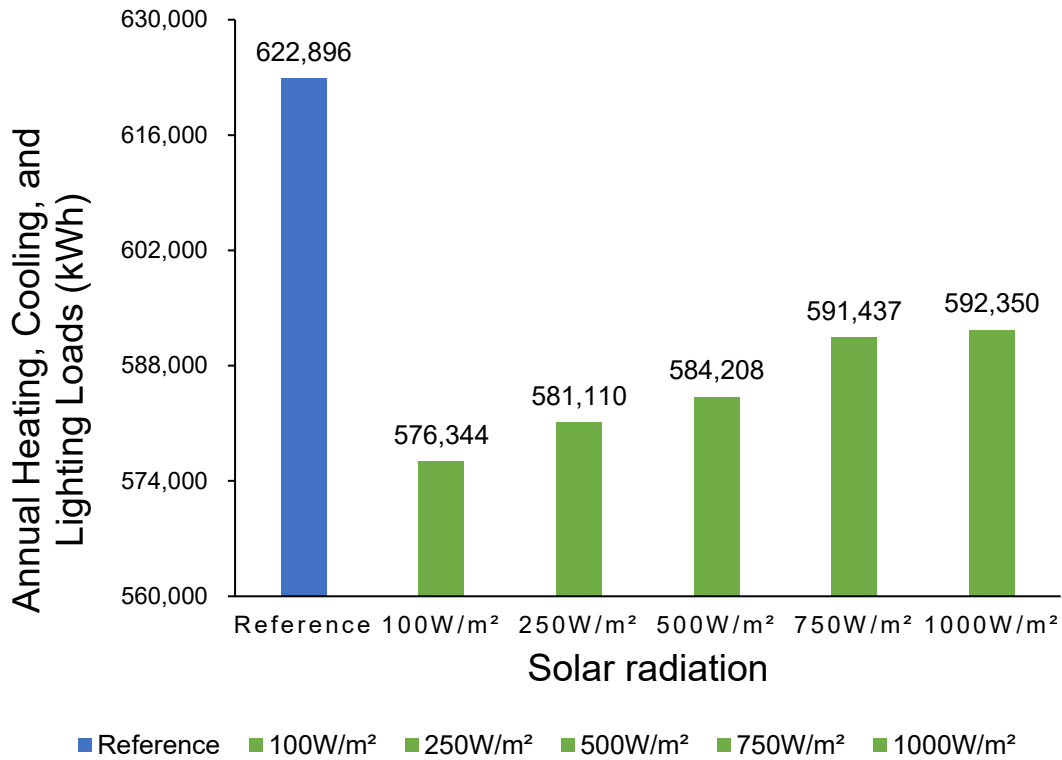


Figure 5-1 Total annual cooling, heating, and lighting energy consumption in relation to solar radiation in Riyadh. The graph illustrates the performance of PDLC glazing at various solar radiation intensities (green bars) compared to the reference window (blue bar).

Table 5-2. The total annual energy consumption in Riyadh in relation to solar radiation.

Energy (kWh)	100 W/m²	250 W/m²	500 W/m²	750 W/m²	1000 W/m²	Reference
<b>Cooling</b>	368222	372854	376198	383293	384216	415019
<b>Heating</b>	4374	4508	4261	4396	4385	4128
<b>Total Energy</b>	576344	949456	584208	591437	592350	622896



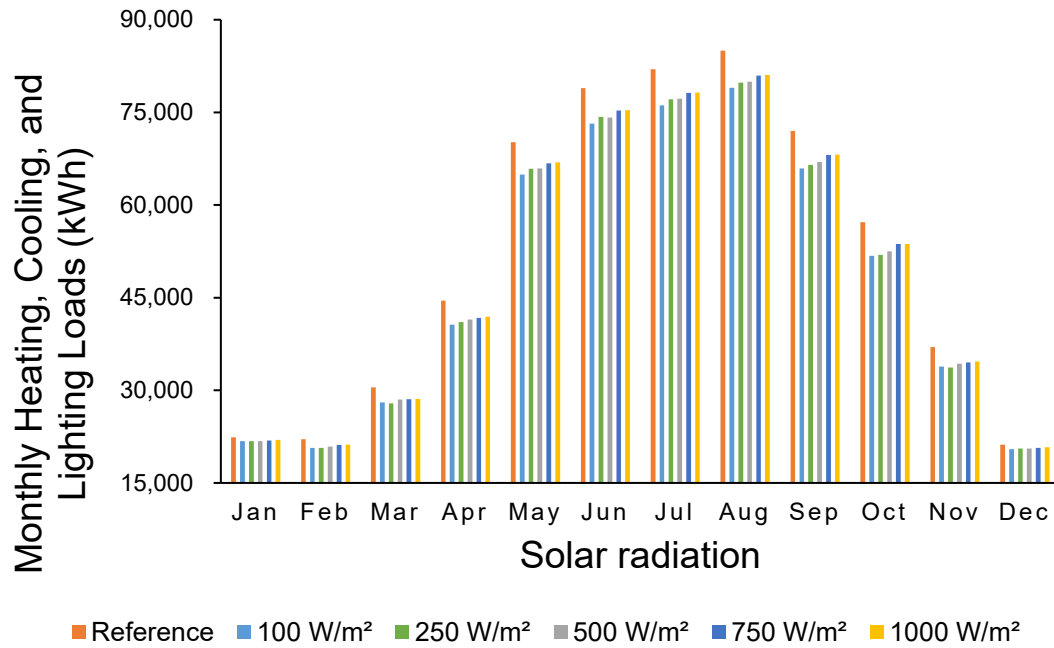


Figure 5-2. Total monthly cooling, heating, and lighting energy consumption in relation to solar radiation in Riyadh. The graph shows the performance of the PDLC window at various solar radiation intensities (light blue, green, grey, dark blue, and yellow bars) compared to the reference window (orange bar).

Table 5-3. Total monthly cooling, heating, and lighting loads in relation to solar radiation in Riyadh

Month	100 W/m <sup>2</sup>	250 W/m <sup>2</sup>	500 W/m <sup>2</sup>	750 W/m <sup>2</sup>	1000 W/m <sup>2</sup>	Reference
Jan	21,756	21,742	21,745	21,872	21,970	22,375
Feb	20,690	20,700	20,880	21,125	21,176	22,081
Mar	28,044	27,899	28,492	28,543	28,613	30,461
Apr	40,609	41,039	41,441	41,741	41,913	44,528
May	64,933	65,879	65,913	66,767	66,880	70,178
Jun	73,195	74,243	74,181	75,303	75,339	78,903
Jul	76,131	77,103	77,235	78,172	78,177	81,983
Aug	78,972	79,818	79,980	80,956	81,032	84,975
Sep	65,904	66,510	66,979	68,116	68,141	72,005
Oct	51,790	51,947	52,510	53,665	53,670	57,210
Nov	33,836	33,685	34,297	34,498	34,663	36,991
Dec	20,485	20,546	20,555	20,678	20,775	21,205

### 5.5.2 Evaluation of heating, cooling, and lighting energies in relation to solar radiation in London

Figure 5-3 presents the data analysis of the PDLC window against the reference window for the total annual cooling, heating, and lighting loads in London. From the total annual energy consumption results, the PDLC window performed better in saving energy than the reference window through all the solar radiation variables. It was found that in London the highest annual energy saving was 1.2% at 500 W/m<sup>2</sup>. The annual energy amount decreased at 100 W/m<sup>2</sup>, and 250 W/m<sup>2</sup>, was lower than 500 W/m<sup>2</sup> due to more heating required at lower solar radiation level. Figure 5-4 shows the monthly energy consumption in London in relation to solar radiation as well as the monthly energy saving compared to the reference window. As cold is a dominant weather condition in London, the PDLC window decreased the monthly heating loads during the winter months under all solar radiation thresholds. When the solar radiation variables were set to 500 W/m<sup>2</sup> and 1000 W/m<sup>2</sup>, the PDLC window decreased the heating loads by 4.9% and 4.2%, respectively. Table 5-4 reports the results of the annual energy consumption in London. Table 5-5 reports the monthly energy consumption in London in relation to solar radiation for the PDLC window and reference window.

Analysis showed that the PDLC window controlled by various solar radiation variables, was found that the highest energy saving was at 100 W/m<sup>2</sup> and 500 W/m<sup>2</sup> in Riyadh and London, respectively. In comparison, Riyadh had a reduction in the annual cooling load by 12.7% at 100 W/m<sup>2</sup>, which was the most significant effect, unlike London had a 4.9 % heating load decrease at 500 W/m<sup>2</sup>. Therefore, the PDLC window demonstrated better performance in cooling-based weather condition than heating-based weather condition. The results suggest that controlling the PDLC window at 100 W/m<sup>2</sup> for Riyadh (arid climate zone) would improve energy efficiency.

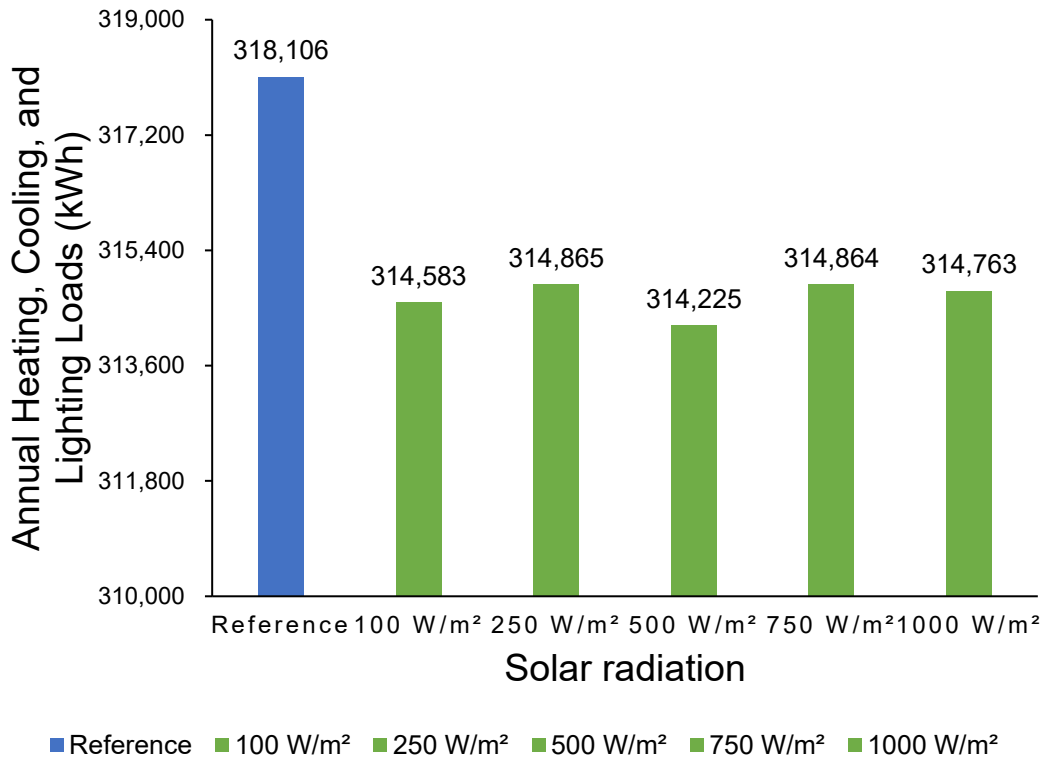


Figure 5-3. Total annual cooling, heating, and lighting energy consumption in relation to solar radiation in London. The graph illustrates the performance of the PDLC glazing at various solar radiation intensities (green bars) compared to the reference window (blue bar).

Table 5-4. The total annual energy consumption in London in relation to solar radiation.

Energy (kWh)	100 W/m²	250 W/m²	500 W/m²	750 W/m²	1000 W/m²	Reference
Cooling	10962	10999	11768	11710	11656	10830
Heating	99872	100117	98709	99406	99360	103528
<b>Total Energy</b>	314583	314865	314225	314864	314763	318106

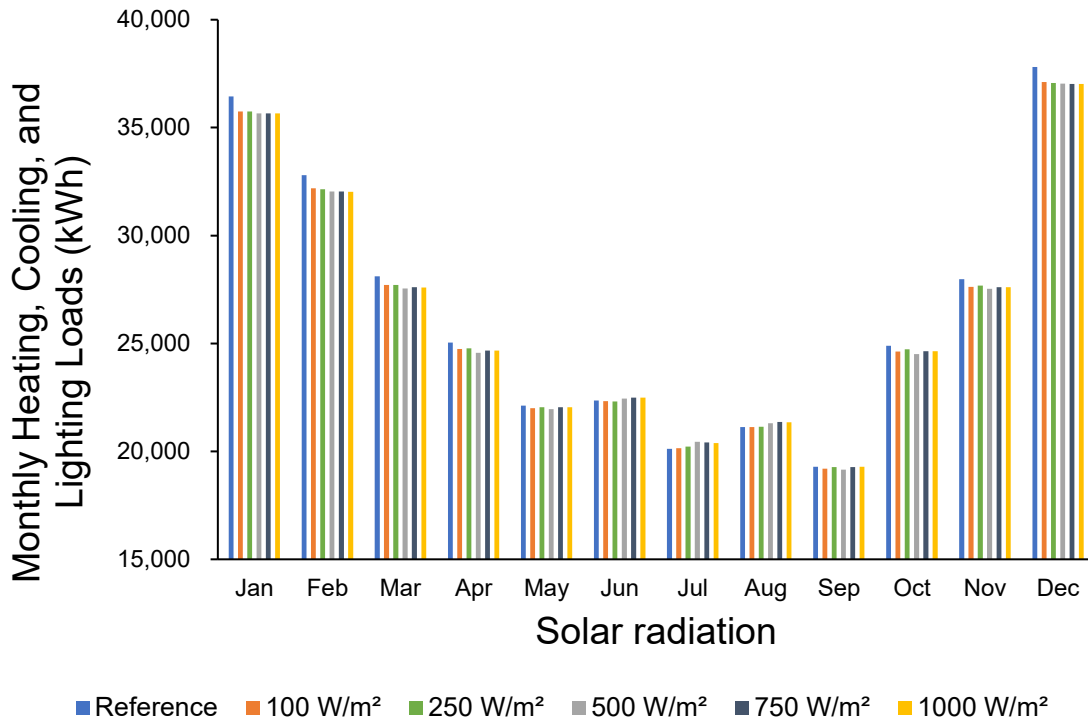


Figure 5-4. Total monthly cooling, heating, and lighting energy consumption in relation to solar radiation in London. The graph shows the performance of the PDLC window at various solar radiation intensities (light blue, green, grey, dark blue, and yellow bars) compared to the reference window (orange bar).

Table 5-5. Total monthly cooling, heating, and lighting energies in relation to solar radiation in London

Month	100 W/m <sup>2</sup>	250 W/m <sup>2</sup>	500 W/m <sup>2</sup>	750 W/m <sup>2</sup>	1000 W/m <sup>2</sup>	Reference
Jan	35,745	35,748	35,654	35,667	35,654	36,453
Feb	32,183	32,150	32,047	32,040	32,029	32,796
Mar	27,717	27,704	27,553	27,605	27,598	28,111
Apr	24,751	24,768	24,563	24,673	24,671	25,046
May	21,997	22,050	21,962	22,052	22,039	22,124
Jun	22,334	22,308	22,454	22,496	22,485	22,357
Jul	20,146	20,222	20,448	20,409	20,382	20,125
Aug	21,134	21,149	21,302	21,370	21,353	21,131
Sep	19,204	19,277	19,160	19,277	19,286	19,285
Oct	24,630	24,727	24,514	24,638	24,635	24,896
Nov	27,626	27,688	27,529	27,610	27,604	27,972
Dec	37,115	37,073	37,038	37,027	37,027	37,810

### 5.5.3 Evaluation of heating, cooling, and lighting energies in relation to outdoor temperature in Riyadh

Figure 5-5 shows that the total annual energy saving for the PLDC window compared to the reference window. The energy decrease was the highest at the minimum temperature 4 °C with an 8.1% energy reduction in the total annual cooling, heating, and lighting loads. As Riyadh reached the maximum air temperature 46 °C, the total annual energy reduction dropped to 5.2%, indicating that outdoor temperature influences the indoor climate and more cooling energy is required. Even though the energy saving at maximum temperature 46 °C decreased, the PDLC window reduced the cooling load compared to the reference window as shown in Table 5-6.

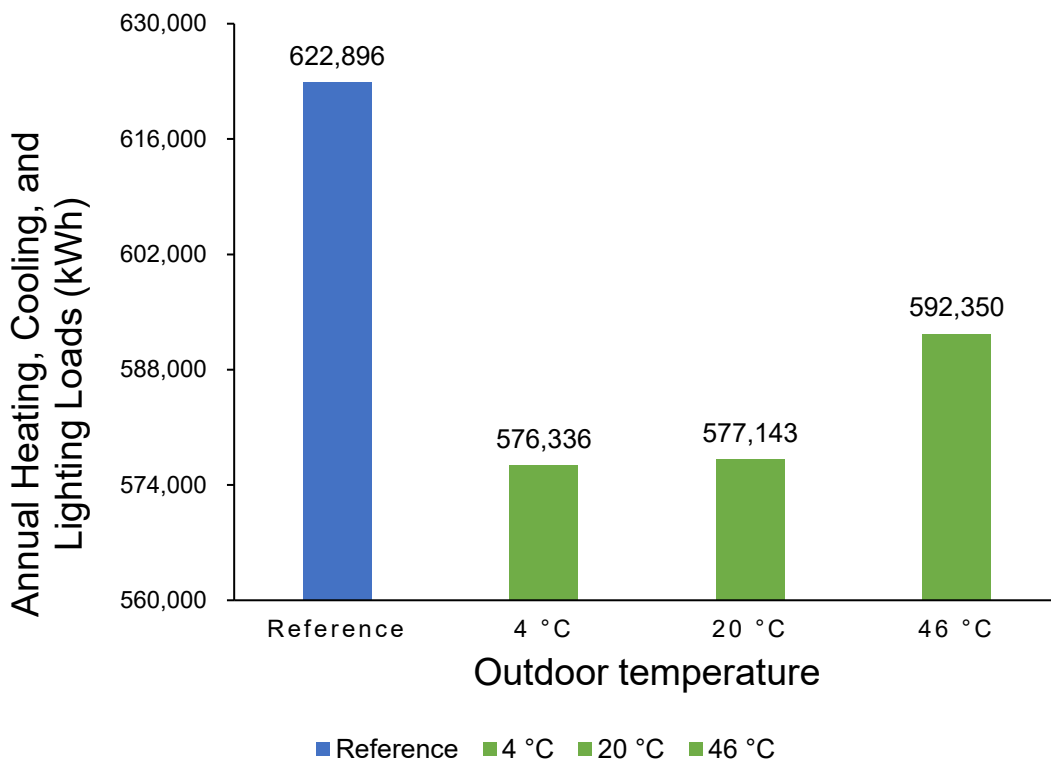


Figure 5-5. Total annual cooling, heating, and lighting energy consumption in relation to outdoor temperature in Riyadh. The graph illustrates the performance of the PDLC glazing at various outdoor temperatures (green bars) compared to the reference window (blue bar).

Table 5-6. The total annual energy consumption in Riyadh in relation to outdoor temperature.

Energy (kWh)	4 °C	20 °C	46 °C	Reference
<b>Cooling</b>	367979	368991	384216	415019
<b>Heating</b>	4609	4404	4385	4128
<b>Total Energy</b>	576336	577143	592350	622896

Figure 5-6 shows that the amount of monthly energy saving during the summer months for the PDLC window is higher than the reference window. From the graph, during the summer months, the PDLC window reduced the cooling loads due to the switching behaviour of the PDLC. The most significant annual cooling loads reduction for the PDLC window was achieved at the minimum temperature 4 °C, and the cooling reduction was 12.8%. In comparison, the PDLC window had a slightly better performance using the outdoor temperature control variables than the solar radiation. Table 5-7 shows the values of the monthly energy consumption in Riyadh in relation to outdoor temperature.

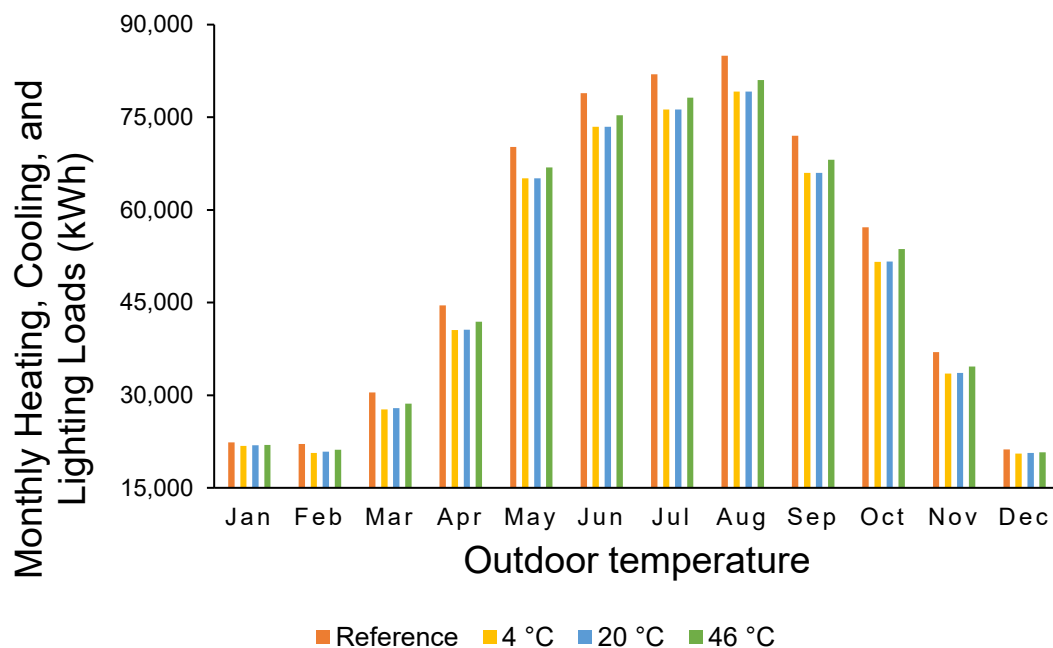


Figure 5-6. Total monthly cooling, heating, and lighting energy consumption in relation to outdoor temperature in Riyadh. The graph shows the performance of the PDLC window at various outdoor temperatures (yellow, light blue, and green bars) compared to the reference window (orange bar).

Table 5-7. Total monthly cooling, heating, and lighting energy consumption in relation to outdoor temperature in Riyadh

Month	4 °C	20 °C	46 °C	Reference
Jan	21,790	21,911	21,970	22,375
Feb	20,657	20,838	21,176	22,081
Mar	27,714	27,887	28,613	30,461
Apr	40,558	40,614	41,913	44,528
May	65,124	65,124	66,880	70,178
Jun	73,446	73,446	75,339	78,903
Jul	76,275	76,275	78,177	81,983
Aug	79,155	79,155	81,032	84,975
Sep	66,011	66,011	68,141	72,005
Oct	51,587	51,625	53,670	57,210
Nov	33,482	33,625	34,663	36,991
Dec	20,538	20,632	20,775	21,205

#### 5.5.4 Evaluation of heating, cooling, and lighting energies in relation to outdoor temperature in London

Figure 5-7 shows an annual energy decrease for the PDLC window in comparison to the reference window under all control condition variables. Unlike Riyadh, the PDLC window best performance in London was not at the minimum temperature, but rather at 20 °C. The results show that the PDLC window achieved a 1.3% reduction in the total annual cooling, heating, and lighting loads at 20 °C. This performance was attributed to the decreased in heating loads at 20 °C, and contrastingly higher demand for heating energy was required at the minimum temperature can be seen in Table 5-8.

Figure 5-8 shows that the reduction of the heating loads of the PDLC window from January to April was higher compared to the reference window. Controlling the PDLC window with outdoor temperature yielded 4.2% of heating loads reduction at 20 °C. During the summer months, the PDLC window had slightly better performance than the reference window, particularly when the PDLC window was controlled to switch to translucent state at 20 °C. The cooling and

heating loads during the summer months are minimal due to the moderate weather conditions in London. Table 5-9 shows the values of the monthly energy consumption in London in relation to outdoor temperature.

The results demonstrate that Riyadh and London had the lowest annual energy reduction at 4 °C and 20 °C, respectively. Specifically, Riyadh’s best performance was seen with a reduction of 12.8% in its annual cooling loads, whilst London decreased the annual heating loads by 4.2%. The highest energy reduction was achieved in Riyadh when the PDLC window was controlled by outdoor temperature. On the contrary, the highest energy decrease in London was when solar radiation was used as a control condition variable. Therefore, it can be deduced that outdoor temperature control for the PDLC window is more effective in Riyadh (arid climate) in regard to the cooling, heating, and lighting energy, than in London (temperate climate).

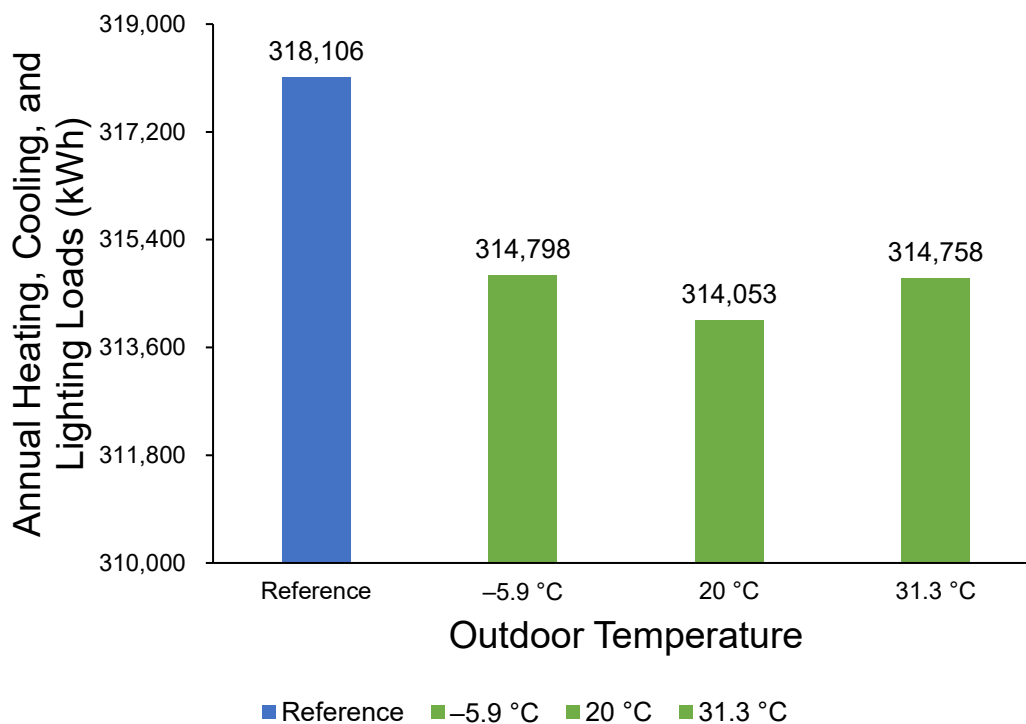


Figure 5-7. Total annual cooling, heating, and lighting energy consumption in relation to outdoor temperature in London. The graph illustrates the performance of the PDLC glazing at various outdoor temperatures (green bars) compared to the reference window (blue bar).



Table 5-8. The total annual energy consumption in London in relation to outdoor temperature.

Energy (kWh)	-5.9 °C	20 °C	31.3 °C	Reference
Cooling	10927	10920	11650	10830
Heating	100123	99385	99360	103528
<b>Total Energy</b>	<b>314798</b>	<b>314053</b>	<b>314758</b>	<b>318106</b>

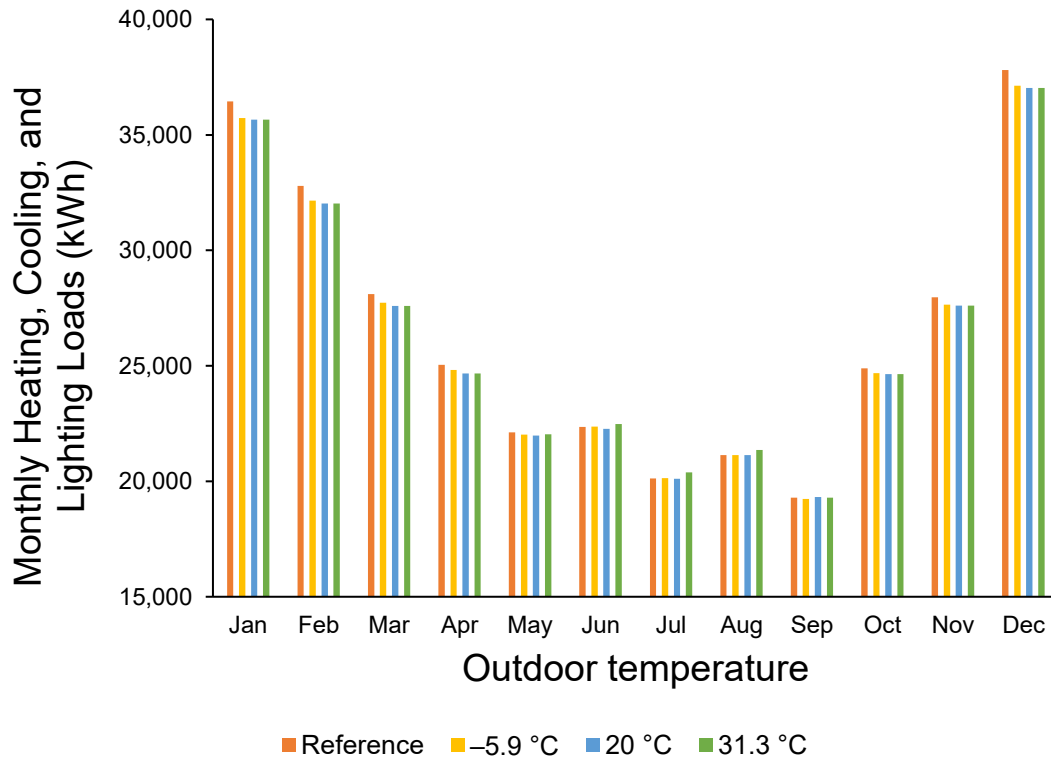


Figure 5-8. Total monthly cooling, heating, and lighting energy consumption in relation to outdoor temperature in London. The graph shows the performance of the PDLC window at various outdoor temperatures (yellow, light blue, and green bars) compared to the reference window (orange bar).

Table 5-9. Total monthly cooling, heating, and lighting energies in relation to outdoor temperature in London

Month	-5.9 °C	20 °C	31.3 °C	Reference
Jan	35,726	35,654	35,654	36,453
Feb	32,155	32,029	32,029	32,796
Mar	27,730	27,598	27,598	28,111
Apr	24,825	24,671	24,671	25,046
May	22,026	21,976	22,039	22,124
Jun	22,374	22,275	22,480	22,357
Jul	20,141	20,112	20,382	20,125
Aug	21,128	21,140	21,353	21,131
Sep	19,235	19,323	19,286	19,285
Oct	24,686	24,644	24,635	24,896
Nov	27,648	27,604	27,604	27,972
Dec	37,123	37,027	37,027	37,810

### 5.5.5 Daylight performance of PDLC window in Riyadh in relation to solar radiation

One of the objectives of the smart windows is to control solar radiation in order to provide visual comfort. Therefore, OpenStudio component was utilised to evaluate the daylight performance using the same shading control strategy used for energy evaluation. The daylight glare index value (DGI) for an office building is suggested as 22 for acceptable DGI [154]. The DGI values were recorded hourly for an entire year, and the interior illuminance was set to dim to 300 lux when there is enough daylight. The interior illuminance and DGI were evaluated for three daylight zones, high, intermediate, and low daylight zone.

Figure 5-9 reports the results of the percentage of annual DGI of the PDLC window in Riyadh. In general, The PDLC window performance in all three daylight zones and solar radiation thresholds was higher than the reference window. In the low daylight zone, the PDLC window was able to control the glare at 100 W/m<sup>2</sup> only by 24.2% during the year, while 75.8% of the DGI value was above 22. However, in the case of the reference window, the DGI value above 22 was 89.28% during the year for the low daylight zone. It is clear from the graph that

the higher the solar radiation, the higher the DGI value was in the low daylight zones. For the intermediate and high daylight zones, the DGI value above 22 was 90.14% and 90.67%, respectively for the PDLC window in all solar radiation thresholds. For the reference window, the DGI value above 22 was 90.39% and 90.80% during the year for the intermediate and high daylight zones, respectively. Table 5-10 shows the results of the percentage of annual DGI above 22 in Riyadh.

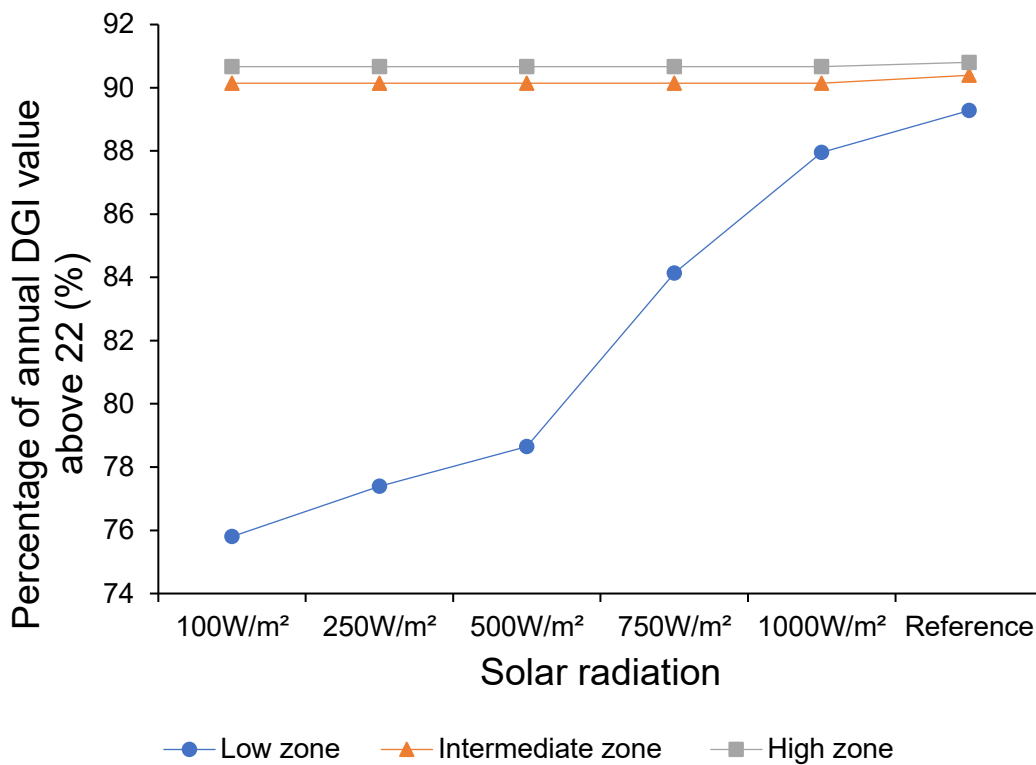


Figure 5-9. Percentage of annual daylight glare index above 22 in relation to solar radiation in Riyadh.

Table 5-10. Percentage of annual daylight glare index (DGI) in Riyadh in relation to solar radiation.

Daylight Zone	The percentage of annual DGI above 22 (%)					
	100 W/m <sup>2</sup>	250 W/m <sup>2</sup>	500 W/m <sup>2</sup>	750 W/m <sup>2</sup>	1000 W/m <sup>2</sup>	Reference
<b>Low</b>	75.80	77.40	78.65	84.13	87.96	89.28
<b>Intermediate</b>	90.14	90.14	90.14	90.14	90.14	90.39
<b>High</b>	90.67	90.67	90.67	90.67	90.67	90.80

Figure 5-10 shows the results of the interior illuminance comfort in Riyadh in relation to solar radiation. The PDLC window offered the best interior illuminance in the low daylight zone at 750 W/m<sup>2</sup> compared to the reference window, while the lowest performance was in the high daylight zone at 1000 W/m<sup>2</sup>. When solar radiation was set to 100 to 500 W/m<sup>2</sup>, the PDLC window performed better in the intermediate daylight zone than in the low daylight zone. In contrast, the performance of the PDLC window was higher in the low daylight zone when the solar radiation was between 750 to 1000 W/m<sup>2</sup> indicating that the PDLC window offers high diffuse transmission at high solar radiation. The PDLC window provided low interior illuminance comfort in the high daylight zone in all solar radiation thresholds; however, the performance was better than the reference window with the exception at 1000 W/m<sup>2</sup>. Table 5-11 presents the percentage of annual illuminance at setpoint 300 lx.

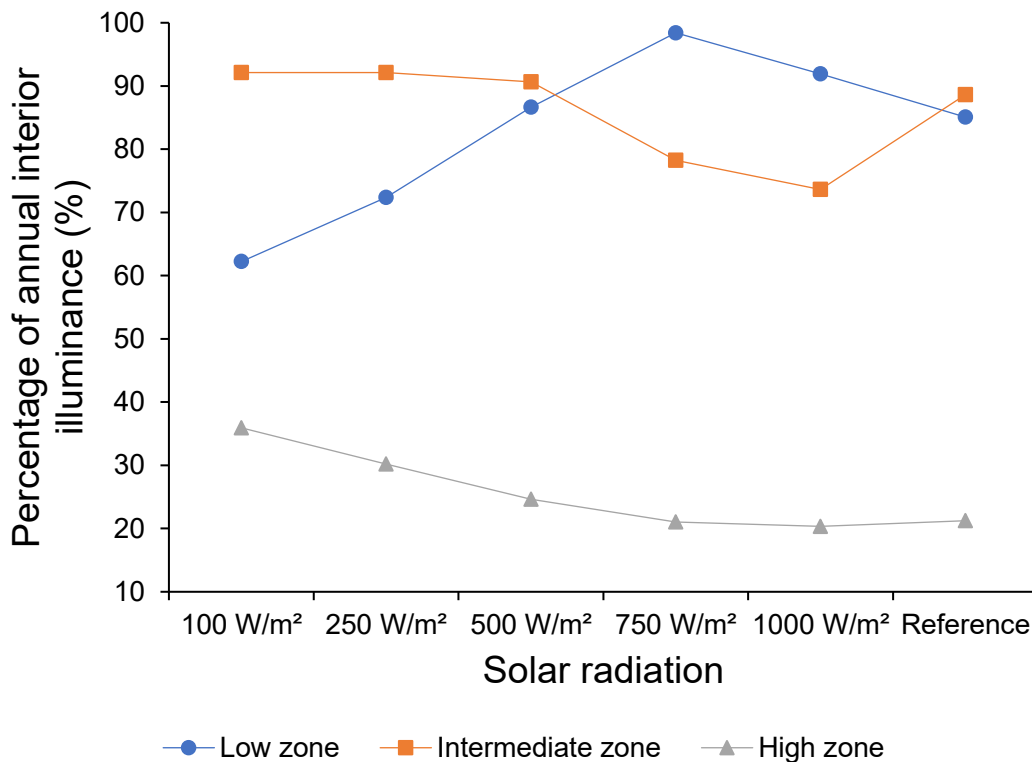


Figure 5-10. Percentage of annual daylight illuminance comfort in Riyadh in relation to solar radiation.

Table 5-11. Interior daylight illuminance in Riyadh in relation to solar radiation.

Daylight Zone	Percentage (%) of annual illuminance at setpoint 300 lx					
	100 W/m <sup>2</sup>	250 W/m <sup>2</sup>	500 W/m <sup>2</sup>	750 W/m <sup>2</sup>	1000 W/m <sup>2</sup>	Reference
Low	62.22	72.36	86.64	98.41	91.89	85.10
Intermediate	92.12	92.12	90.66	78.23	73.63	88.61
High	35.93	30.21	24.62	21.02	20.35	21.26

### 5.5.6 Daylight performance of PDLC window in London relation to solar radiation

Figure 5-11 illustrates the results of the percentage of annual DGI of the PDLC window in London in relation to solar radiation. The best performance of the PDLC window for controlling the glare during the year was in the low daylight zone at 100 W/m<sup>2</sup>. In addition, glare was reduced by the PDLC window by 36.94% compared to the reference window which controlled the glare by 34.45% during the year in the low daylight zone. The performance of the PDLC window to control the glare was reducing as the solar radiation was increasing. The annual percentage of the DGI for the PDLC window was almost similar in the intermediate and high daylight zone and was higher than the reference window. The results of the annual percentage of DGI were the same in the intermediate and high daylight zone regardless of the amount of solar radiation. Daylight illuminance is a variable parameter and generally diminishes as the distance from the window increases. Thus, the data analysis showed that all high daylight zones exhibited high daylight illuminance due to the close distance between the window and the daylight reference point (see Table 5-12).

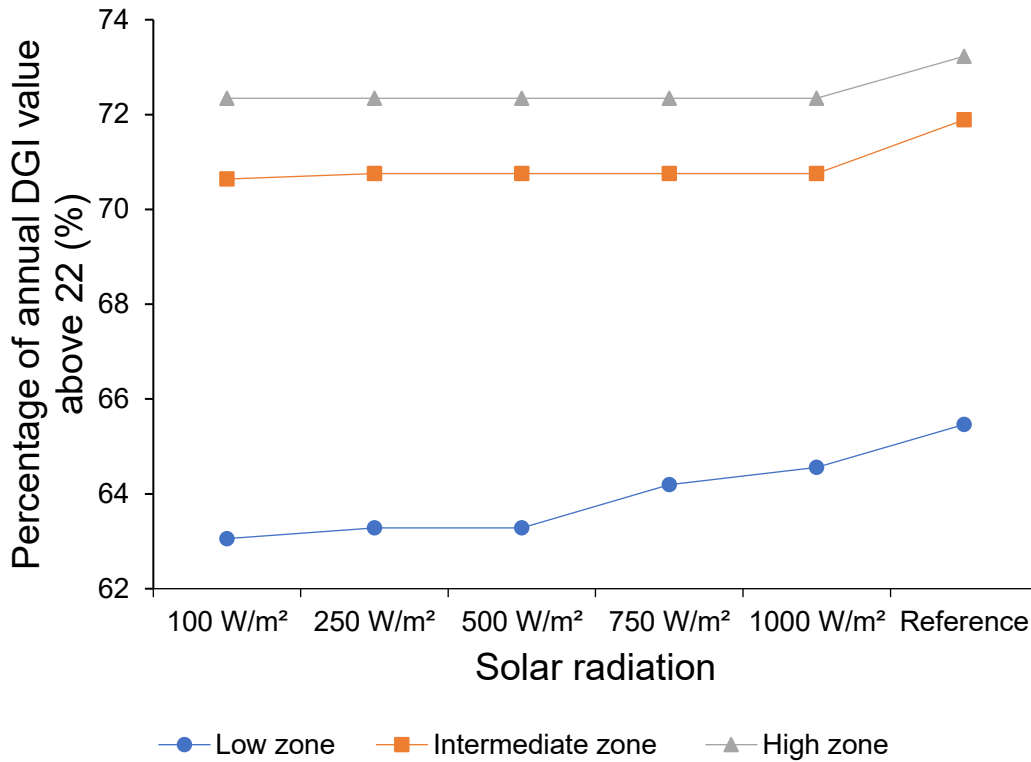


Figure 5-11. Percentage of annual daylight glare index in London in relation to solar radiation.

Table 5-12. Exceeded hours of DGI above 22 in London in relation to solar radiation.

Daylight Zone	The percentage of annual DGI above 22 (%)					
	100 W/m <sup>2</sup>	250 W/m <sup>2</sup>	500 W/m <sup>2</sup>	750 W/m <sup>2</sup>	1000 W/m <sup>2</sup>	Reference
Low	63.06	63.28	63.28	64.19	64.55	65.46
Intermediate	70.64	70.75	70.75	70.75	70.75	71.89
High	72.34	72.34	72.34	72.34	72.34	73.23

Figure 5-12 shows the results for the interior illuminance for the PDLC window in London. The PDLC window delivered an excellent performance for providing adequate interior illuminance in the intermediate daylight zone by 96.44 at 750 W/m<sup>2</sup>. In general, the daylight performance of the PDLC window was acceptable in all daylight zones, except for the high daylight zone. The data analysis of the interior illuminance showed that the performance of the PDLC window was improving as the amount of solar radiation was getting higher. The daylight performance of the PDLC window was higher compared to the reference window

in both the intermediate and low daylight zones at 500 W/m<sup>2</sup>, 750 W/m<sup>2</sup>, and 1000 W/m<sup>2</sup>. The lowest daylight performance of the PDLC window was in the high daylight zone due to the small distance between the daylight zone and the window. However, the PDLC window provided better interior illuminance in comparison to the reference window, particularly at 100 W/m<sup>2</sup> as can be seen in Table 5-13.

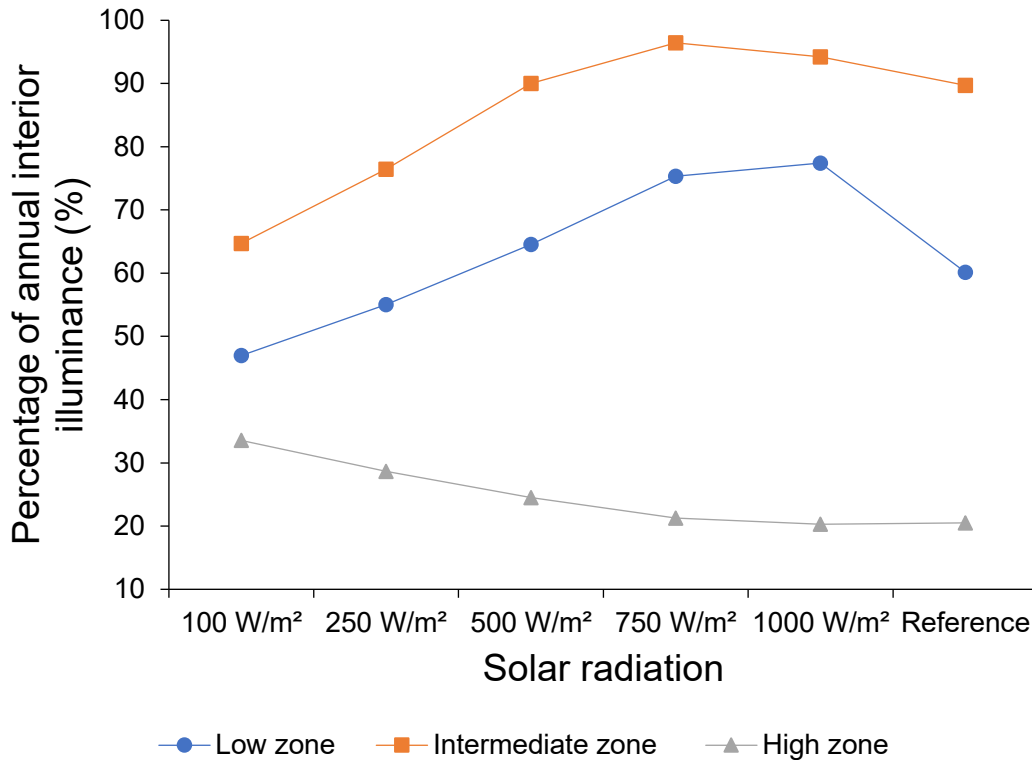


Figure 5-12. Percentage of annual daylight illuminance comfort in London in relation to solar radiation.

Table 5-13. Percentage of annual daylight illuminance comfort in London in relation to solar radiation.

Daylight Zone	Percentage (%) of annual illuminance at setpoint 300 lx					
	100 W/m <sup>2</sup>	250 W/m <sup>2</sup>	500 W/m <sup>2</sup>	750 W/m <sup>2</sup>	1000 W/m <sup>2</sup>	Reference
<b>Low</b>	46.98	55.03	64.57	75.33	77.42	60.18
<b>Intermediate</b>	64.73	76.46	90.02	96.44	94.20	89.71
<b>High</b>	33.55	28.64	24.50	21.26	20.29	20.53

### 5.5.7 Daylight performance of PDLC window in Riyadh in relation to outdoor temperature

Figure 5-13 reports the results of the annual DGI in Riyadh with respect to outdoor temperature. The graph shows that the performance of the PDLC window in controlling the annual DGI exceeded the reference window performance in all daylight zones. The percentage of annual DGI above 22 increased as the outdoor temperature was going higher when the PDLC window was employed due to the increase in the amount of solar radiation. The PDLC window achieved the best performance in the low daylight zone with 68.53% of the annual DGI above 22 at 4 °C. Table 5-14 shows that the PDLC window performance reduced in the intermediate and high daylight zones due to the short distance to the window, indicating higher solar radiation transmission. In addition, the PDLC window demonstrated a higher performance compared to the reference window in the intermediate and high daylight zones, particularly at 4 °C.

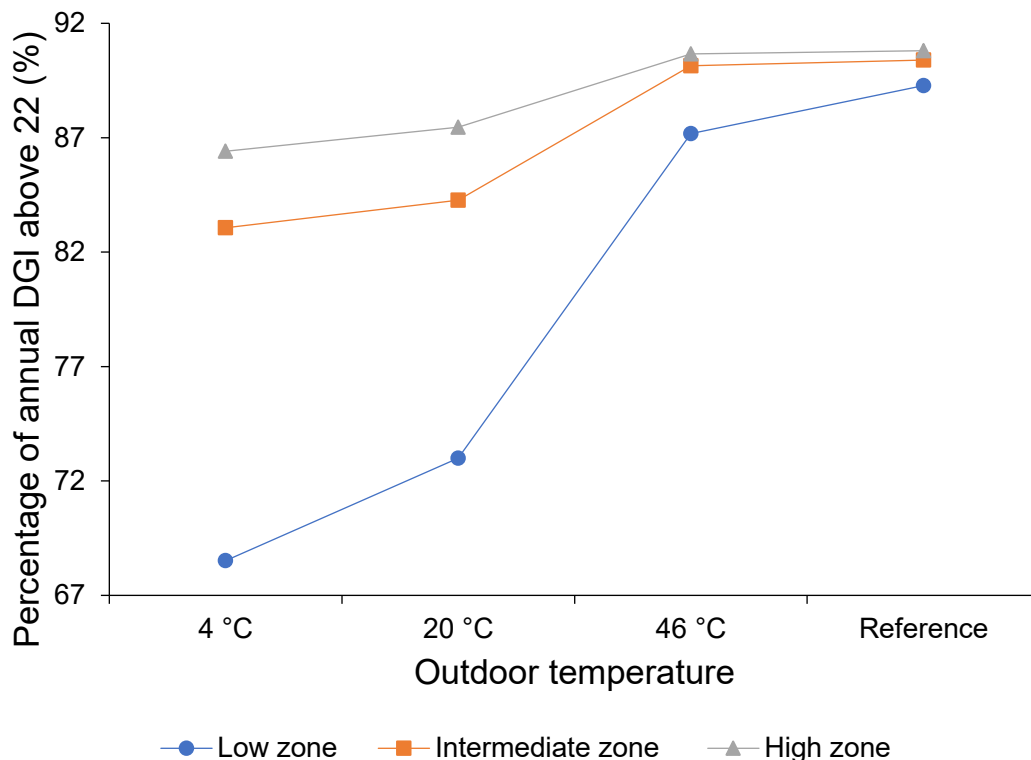


Figure 5-13. Percentage of annual daylight glare index in Riyadh in relation to outdoor temperature.



Table 5-14. Percentage of annual daylight glare index in Riyadh in relation to outdoor temperature.

Daylight Zone	The percentage of annual DGI above 22 (%)			
	4 °C	20 °C	46 °C	Reference
<b>Low</b>	68.52	73.00	87.18	89.28
<b>Intermediate</b>	83.06	84.27	90.14	90.39
<b>High</b>	86.41	87.46	90.67	90.80

Figure 5-14 illustrates the results of the interior illuminance of the PDLC window in Riyadh. The PDLC window achieved the best performance in the intermediate and low daylight zones by 93.09% at 20 °C and 91.89% at 46 °C by, respectively. When the PDLC window was utilised in the low light zone, the interior illuminance improved as the outdoor temperature increased. The quality of the interior illuminance of the PDLC window reduced in the intermediate daylight zone at 46 °C, indicating that a high amount of solar radiation was transmitted. It is clear from the graph that the interior illuminance of the PDLC window in the high daylight zone decreased as the outdoor temperature increased. Table 5-15 reports the results of the percentage of annual daylight illuminance comfort in Riyadh.

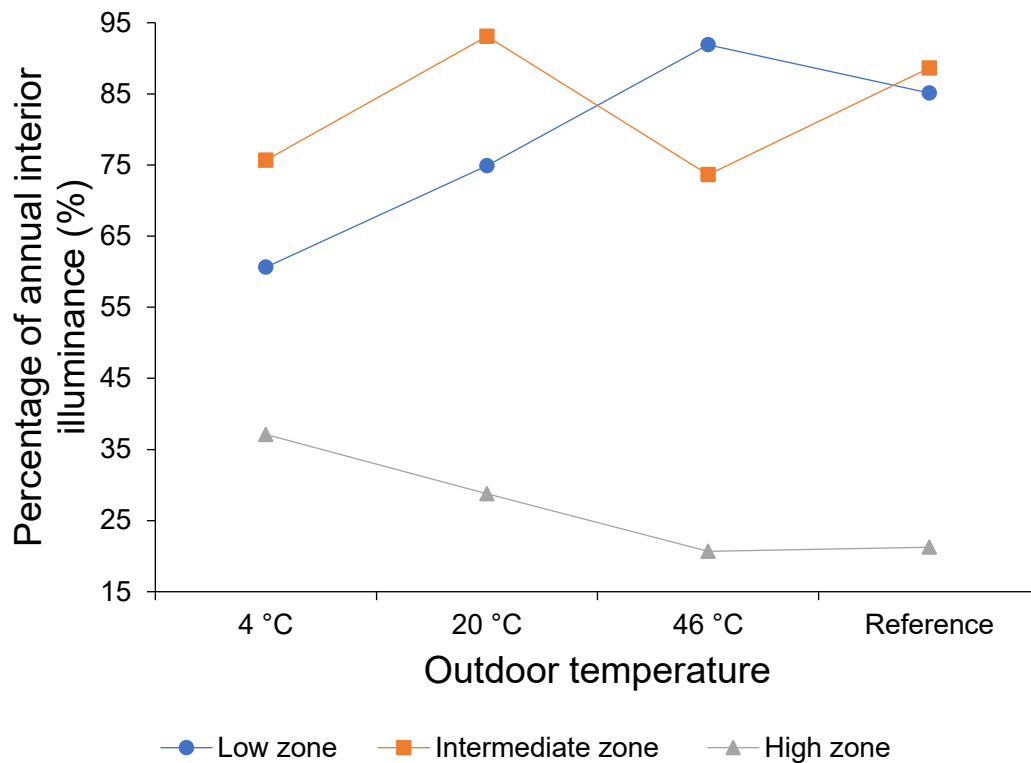


Figure 5-14. Percentage of annual daylight illuminance comfort in Riyadh in relation to outdoor temperature.

Table 5-15. Percentage of annual daylight illuminance comfort in Riyadh in relation to outdoor temperature.

Daylight Zone	Percentage (%) of annual illuminance at 300 lx			
	4 °C	20 °C	46 °C	Reference
Low	60.62	74.92	91.89	85.10
Intermediate	75.66	93.09	73.63	88.61
High	37.11	28.78	20.68	21.26

### 5.5.8 Daylight performance of PDLC window in London in relation to outdoor temperature

Figure 5-15 reports the results of the annual DGI in London. The performance of the PDLC window exceeded the reference window's performance in all daylight zones and all outdoor temperature thresholds. The best performance achieved by the PDLC window was in the low daylight zone by 55.09% at -5.9 °C. The percentage of annual DGI decreased as the outdoor temperature increased when the PDLC window was employed in all daylight zones (see Table 5-16). The PDLC showed similar behaviour in Riyadh and London when the solar radiation

control was used. In the intermediate daylight zone, the PDLC window showed similar performance with the low daylight zone at -5.9 °C by 57.36%. The percentage of annual DGI decreased in the PDLC window after -5.9 °C for both intermediate and high daylight zones due to the high amount of solar radiation and close distance to the window.

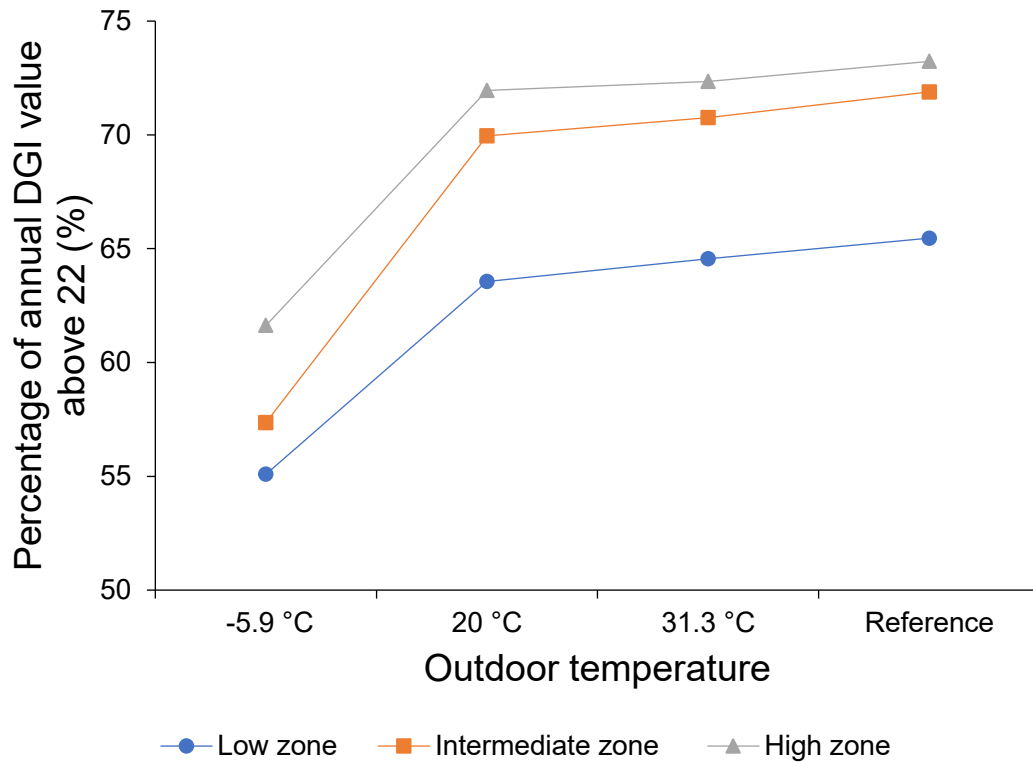


Figure 5-15. Percentage of annual daylight glare index in London in relation to outdoor temperature.

Table 5-16. Percentage of annual daylight glare index in London in relation to outdoor temperature.

Daylight Zone	The percentage of annual DGI above 22 (%)			
	-5.9 °C	20 °C	31.3 °C	Reference
<b>Low</b>	55.09	63.56	64.55	65.46
<b>Intermediate</b>	57.36	69.96	70.75	71.89
<b>High</b>	61.63	71.96	72.34	73.23

Figure 5-16 shows the results of the annual interior illuminance in London. The PDLC window performance was higher than the reference window in all daylight

zones except at -5.9 °C in the low and intermediate daylight zones. The PDLC window achieved excellent performance by 97.77% and 94.2% in the intermediate daylight zone at 20 °C and 31.3 °C, respectively. The small distance between the window and the high daylight zone greatly affected the performance of the PDLC window. Table 5-17 illustrates that the low daylight zone had acceptable interior illuminance, precisely at 20 °C and 31.3 °C, indicating that the PDLC window exhibit high diffuse transmission.

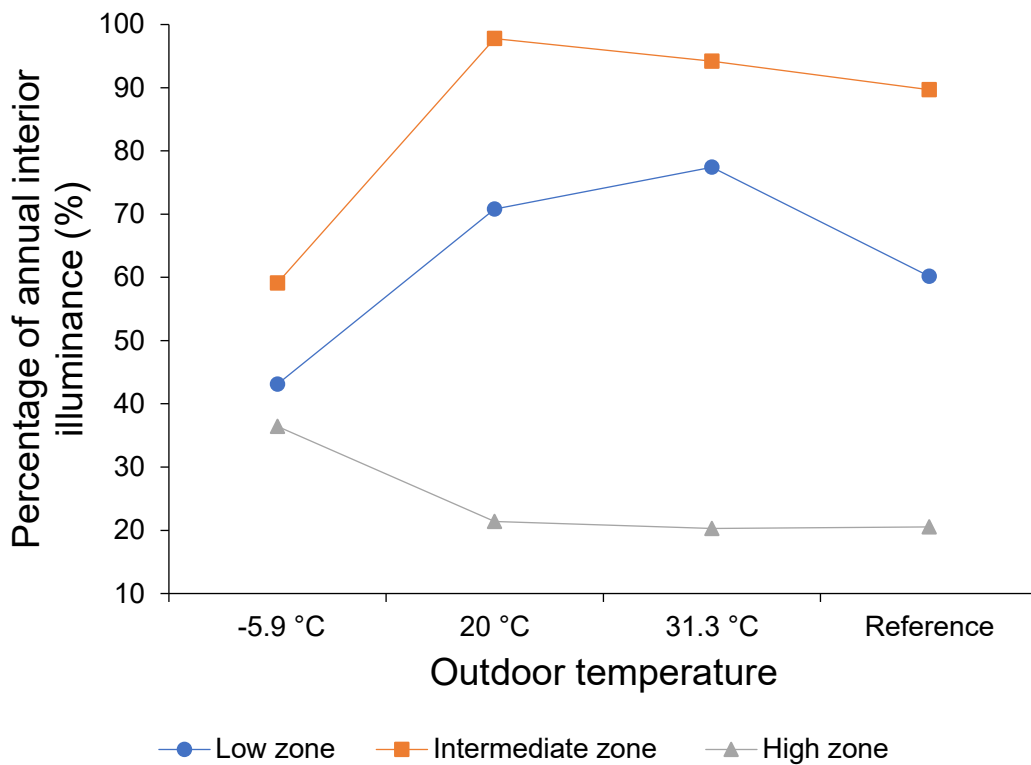


Figure 5-16. Percentage of annual daylight illuminance comfort in London in relation to outdoor temperature.

Table 5-17. Percentage of annual daylight illuminance comfort in London in relation to outdoor temperature.

Daylight Zone	Percentage (%) of annual illuminance at setpoint 300 lx			
	-5.9 °C	20 °C	31.3 °C	Reference
Low	43.12	70.79	77.42	60.18
Intermediate	59.12	97.77	94.20	89.71
High	36.43	21.40	20.29	20.53

## 5.6 Conclusion

EnergyPlus simulation tool was employed to evaluate the impact of the PDLC window performance of an office building in regards to cooling, heating, and lighting loads in Riyadh, Saudi Arabia (arid climate), and London, United Kingdom (temperate oceanic climate). In addition, the annual glare percentage and interior daylight were evaluated. The control shading strategy variables used for the simulation study were solar radiation and outdoor temperature. The following conclusion can be drawn from the present study:

1. The results of this study showed that the PDLC window was able to control the solar radiation and decrease the annual cooling and heating loads under all solar radiation control variables. The current findings enhance our understanding of the PDLC window performance as it can be utilised for smart façade for buildings envelope. The PDLC window has the potential to replace shading devices such as curtains and blinds which require extensive maintenance. The results showed that the investigated PDLC window had the best performance to decrease the annual energy consumption in relation to solar radiation at  $100 \text{ W/m}^2$  and  $500 \text{ W/m}^2$  in Riyadh and London, respectively. The highest cooling load reduction was 12.7% in Riyadh, while the greatest heating load decrease was in London by 4.9%. Data analysis showed that the PDLC window is more effective in Riyadh (arid climate) than London (temperate climate).
2. The results of controlling the PLDC window by outdoor temperature variables showed that the PDLC window reduced the annual cooling load by 12.8% at the minimum temperature of  $4 \text{ }^\circ\text{C}$  in Riyadh. In London, the annual heating load reduction was 4.2% when the PDLC window was controlled at  $20 \text{ }^\circ\text{C}$ . The results indicate that the outdoor temperature control strategy was more influential in Riyadh than in London.
3. The daylight performance of the PDLC window was evaluated and compared against a reference window using solar radiation control. The results showed that the PDLC window performed best in Riyadh's low daylight zone, while the intermediate daylight zone was the best performance for the PDLC window in London. The PDLC window achieved

75.8% and 63.06% of annual DGI during the year at 100 W/m<sup>2</sup> in both cities when solar radiation control was used. In addition, the PDLC window offered the best interior illuminance performance in the low daylight zone at 750 W/m<sup>2</sup> in Riyadh. In London, the best interior illuminance achieved in the intermediate daylight zone at 750 W/m<sup>2</sup>.

4. Outdoor temperature was utilised to control the PDLC window and evaluate the daylight performance. The PDLC window achieved 68.52% of annual DGI above 22 during the year at 4 °C in the low daylight zone in Riyadh. While in London, the PDLC window achieved 55.09% of annual DGI in the same daylight zone. In terms of interior illuminance, the PDLC window showed the highest performance in two different daylight zones. In Riyadh, the highest interior illuminance achieved was in the low daylight zone at 46 °C while, in London was in the intermediate daylight zone at 20 °C.

This investigation was undertaken to assess the energy and daylight performance of the PDLC window in only two contrasting climate zones of Riyadh, Saudi Arabia, and London, United Kingdom. It developed an analysis model and limited its utilisation exclusively to office buildings. However, the optimal control results from the analysis are not to be standardised, as the investigated climate zones were limited only to arid and temperate oceanic weather conditions. In addition, the results do not indicate whether the optimal control conditions, as the research shows, can be applied to all type of buildings. Therefore, an investigation of PDLC window control would benefit from analysis in more diverse climate zones.

## **Chapter 6. Evaluation of artificial lighting saving for a smart switchable adaptive polymer dispersed liquid crystal glazing PDLC for two climate zones**

### **6.1 Introduction**

Artificial lighting load evaluation was carried out to assess the effect of the PDLC glazing on lighting energy savings for an office building and compared the results against a reference double window. Building energy modelling tool was utilised to conduct the assessments in two climate zones, Riyadh (arid climate) and London (temperate climate). In the following sections, a discussion of artificial lighting load reduction is provided for three daylighting zones (a high daylighting zone, an intermediate daylighting zone, and a low daylighting zone).

### **6.2 Artificial lighting energy savings**

Enhancing energy efficiency in buildings will potentially lead to energy reduction and, therefore, CO<sub>2</sub> emissions into the environment [155]. According to Lancashir et al., one kWh of reduced energy, decreases carbon dioxide emissions by 680.39 g, sulfur dioxide by 5.67 g, and nitrogen dioxide by 2.27 g [156]. Artificial lighting energy accounts for 20% to 45% of the total energy consumption in office buildings [157]. Natural daylight is an excellent light source because it has good colour rendering and matches human visual response. The significance of natural daylight in buildings was extensively investigated. Natural daylight has a positive influence on energy in buildings and human physical activities, which provides comfort and health benefits for occupants [158–161]. It is essential to control natural daylight in order to use it as a source of indoor lighting. Otherwise, it would have a negative impact. Excessive natural daylight could lead to high solar gains and a high cooling load. Moreover, natural daylight decreases as one moves away from the window.

Despite the positive benefits of natural daylight, electrical lighting is an excellent alternative for engineers as it can control interior illuminance levels. However, electrical lighting could increase the total annual primary energy. Adequate

integration of natural daylight with artificial lighting could improve indoor visual and thermal comfort for occupants in buildings. Exploiting natural daylight may not only reduce the artificial lighting load but would have an impact on cooling energy as well [41]. Many studies have investigated the impact of natural daylight on artificial lighting load reduction.

A study investigated the impact of artificial lighting load on global energy savings in office buildings by utilising natural daylight [162]. The results showed that natural daylight could reduce artificial lighting load from 50% to 80%. In addition, the global primary energy savings could reach 40% for glazing that is commonly used in office buildings in Belgium. Another study suggested a methodology to evaluate the artificial lighting load reduction by integrating natural daylight with the artificial lighting system [163]. The study utilised the Visual DOE software for the climate zone of Leeds, in the United Kingdom and Florianopolis, in Brazil. It was found that the potential of the artificial lighting load reduction was between 10.8% to 44% in Leeds and 20.6% to 86.2% in Florianopolis. In the US, a researcher studied the impact of natural daylight on electrical energy savings taking into account the building geometry, window size, and glazing type [164]. The potential of electrical energy savings was found to be about 70%. Field measurements of indoor illuminance levels and daylighting availability for a fully air-conditioned plan office were performed to evaluate artificial lighting savings [165]. The study suggested that the artificial lighting reduction was over 30%. Therefore, smart windows such as PDLC glazing, which could control solar radiation due to changing its optical properties, could potentially reduce the artificial lighting load. A recent study was performed in Egypt amid to evaluate the energy performance for an office building [166]. Six different types of glazing were utilised including (electrochromic, gas-chromic, thermochromic, tinted blue, tinted green, and tinted brown glazing) with a window to floor ratio of 8%, 16%, 24%, and 32%. The results showed that the electrochromic glazing achieved the best performance as it was able to reduce artificial lighting for the south orientation by 43% at 8% WFR and 61% at 32% WFR. Therefore, this work presents the results of the analysis of the PDLC glazing performance in an office building in Riyadh and London climate zones taking into account solar radiation and outdoor temperature.



### **6.3 Simulation modelling**

This work was performed using a building energy modelling simulation software, described in detail in section 2.8. The simulation parameters and building properties in addition to the climate zone data are provided in sections 2.8.1 and 2.8.3. The detail of the lighting control system used for evaluating the artificial lighting load is discussed in section 2.8.6.

### **6.4 Simulation results**

#### **6.4.1 Evaluation of artificial lighting load in relation to solar radiation in Riyadh**

The analysis is focused solely on artificial lighting load; therefore, the heating and cooling loads were not considered. Artificial lighting load reduction is primarily dependent on the office area, the window area, and the window transmittance. As the window area is larger, the more sunlight is allowed in a room, which potentially leads to artificial lighting energy reduction. However, windows transmittance has a crucial impact on reducing the artificial lighting load. The office room was divided into three daylighting zones, where each zone had one light sensor. The light sensors were controlled by the illuminance level of a setpoint. When the illuminance level decreases below 500 lux, the artificial lighting will switch on to compensate for the required illuminance.

Figure 6-1 reports the total annual artificial lighting energy consumption in relation to solar radiation compared to a reference window in Riyadh. In high daylighting zone, the PDLC glazing performed similarly to the reference window for all solar radiation thresholds. This means that the light sensor received more daylight illuminance than the illuminance setpoint of 500 lux for all solar radiation thresholds. The high amount of daylight illuminance was due to the small distance between the window and the light sensor. In intermediate daylighting zone, the artificial lighting load decreased as the solar radiation thresholds increased to 500  $W/m^2$ , 750  $W/m^2$  and 1000  $W/m^2$ . When the solar radiation thresholds were set to 100  $W/m^2$  and 250  $W/m^2$  there was no artificial lighting energy reduction. However, the PDLC glazing achieved to reduce the artificial lighting energy in the intermediate daylighting zone by 2%, 25%, and 27% when the solar radiation

thresholds were set to 500 W/m<sup>2</sup>, 750 W/m<sup>2</sup>, and 1000 W/m<sup>2</sup>, respectively. In low daylighting zone, the PDLC glazing could not reduce the artificial daylighting load when the solar radiations thresholds were set to 100 W/m<sup>2</sup>, 250 W/m<sup>2</sup>, and 500 W/m<sup>2</sup>. This is due to the large distance between the window and the low daylighting zone, which means the light sensor received less daylight illuminance. However, when the solar radiation threshold was set to 750 W/m<sup>2</sup> and 1000 W/m<sup>2</sup>, the PDLC glazing was able to achieve artificial lighting savings by 4% for both solar radiation thresholds. The PDLC glazing performed well in Riyadh's intermediate and low daylighting zones (arid climate). In addition, the total annual artificial lighting load reduction was found when the solar radiation threshold was set to 500 W/m<sup>2</sup>, 750 W/m<sup>2</sup>, and 1000 W/m<sup>2</sup> by 1%, 9%, and 10%, respectively. Table 6-1 presents the annual artificial lighting loads in relation to solar radiation for the PDLC and reference window in all daylighting zones.

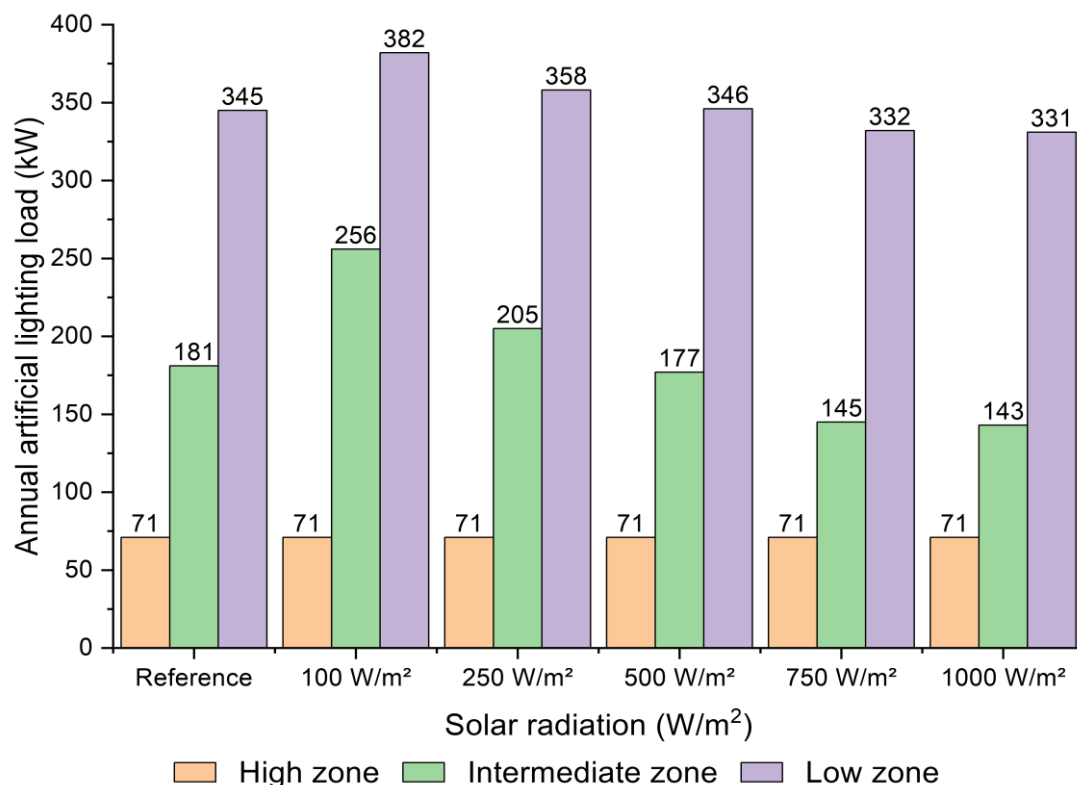


Figure 6-1. Total annual artificial lighting load in relation to solar radiation for the PDLC compared to a reference window for high, intermediate, and low daylighting zones in Riyadh.

Table 6-1. Total annual artificial lighting loads (kW) for the PDLC and reference window in Riyadh.

Energy (kW)	High zone (Unit)	Intermediate zone	Low zone
<b>Reference</b>	71	181	345
<b>100 W/m<sup>2</sup></b>	71	256	382
<b>250 W/m<sup>2</sup></b>	71	205	358
<b>500 W/m<sup>2</sup></b>	71	177	346
<b>750 W/m<sup>2</sup></b>	71	145	332
<b>1000 W/m<sup>2</sup></b>	71	143	331

Figure 6-2 presents the monthly artificial lighting energy consumption for the PDLC and reference window for all daylighting zones in Riyadh. The PDLC glazing was able to reduce the artificial lighting load compared to the reference window for all months when the solar radiation thresholds were set to 750 W/m<sup>2</sup> and 1000 W/m<sup>2</sup>. The PDLC glazing achieved the lowest monthly artificial lighting load reduction in November. The artificial lighting load for the PDLC glazing was 39 kW and the reference window was 47 kW. Data analysis showed that the light sensors received a high amount of daylight illuminance in November. Consequently, the PDLC was able to reduce the monthly artificial lighting in both intermediate and low daylighting zones compared to the reference window. When the solar radiation thresholds were set to 100 W/m<sup>2</sup> and 250 W/m<sup>2</sup>, the PDLC glazing could not reduce the artificial lighting load in all daylighting zones due to low solar radiation. On the contrary, at 750 W/m<sup>2</sup> and 1000 W/m<sup>2</sup> thresholds, the PDLC glazing switched to the opaque state and reduced the artificial lighting load, particularly in the intermediate daylighting zone. This shows that the PDLC glazing was able to offer illuminance that was either above or approximately near the illuminance setpoint for the whole year. The highest and lowest monthly illuminance values for the PDLC were 540 lux and 313 lux when the solar radiation threshold 1000 W/m<sup>2</sup> in the intermediate zone. The highest monthly illuminance value for the reference window in the intermediate zone was 495 lux and the lowest was 291 lux. Table 6-2 provides the monthly artificial lighting energy consumption in relation to solar radiation for the PDLC and reference window in Riyadh.

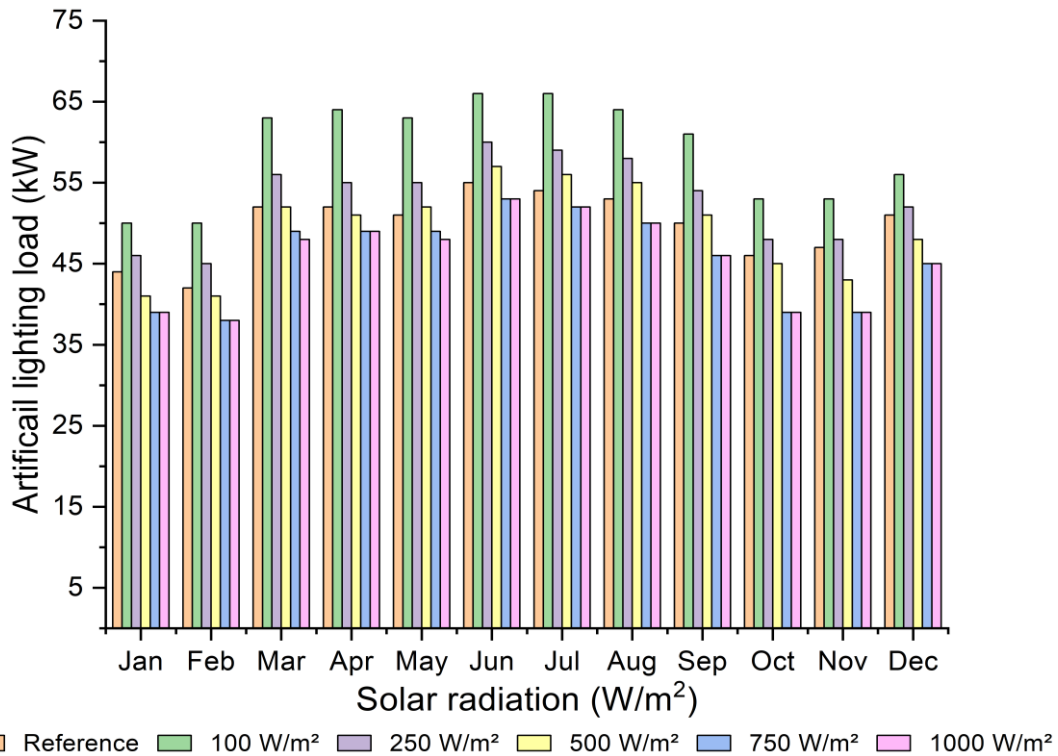


Figure 6-2. Monthly artificial lighting energy consumption in relation to solar radiation for the PDLC glazing compared to a reference window in Riyadh.

Table 6-2. Monthly artificial lighting load (kW) for the PDLC glazing and reference window in Riyadh.

Energy (kW)	Solar radiation thresholds for the PDLC glazing					
	100 W/m²	250 W/m²	500 W/m²	750 W/m²	1000 W/m²	Reference
Jan	50	46	41	39	39	44
Feb	50	45	41	38	38	42
Mar	63	56	52	49	48	52
Apr	64	55	51	49	49	52
May	63	55	52	49	48	51
Jun	66	60	57	53	53	55
Jul	66	59	56	52	52	54
Aug	64	58	55	50	50	53
Sep	61	54	51	46	46	50
Oct	53	48	45	39	39	46
Nov	53	48	43	39	39	47
Dec	56	52	48	45	45	51

Figure 6-3 shows the average annual interior illuminance readings of the PDLC glazing compared to the reference window for all daylighting zones in Riyadh. The interior illuminance results strongly agree with the artificial lighting load results. The average interior illuminance in the high daylighting zone was high for both the reference window and the PDLC glazing across all solar radiation thresholds. In the high daylighting zone, the light sensor received an average high daylight illuminance above the setpoint. Therefore, the artificial lighting load was similar for both the PDLC glazing and the reference window. The interior illuminance diminished rapidly as the distance increased from the window. However, the PDLC glazing offered higher interior illuminance in the intermediate and low daylighting zones compared to the reference windows. Consequently, the PDLC glazing required less energy to compensate for the needed illuminance in the intermediate and low daylighting zones, particularly in 750 W/m<sup>2</sup> and 1000 W/m<sup>2</sup> thresholds. In addition, the PDLC glazing was able to offer an average illuminance value that was approximately near to the needed illuminance of 500 lux in the intermediate zone. Table 6-3 presents the average annual interior illuminance values for the PDLC glazing and reference window. In the intermediate zone, the highest average annual interior illuminance offered by the PDLC glazing was 412 lux and the reference window was 371 lux.

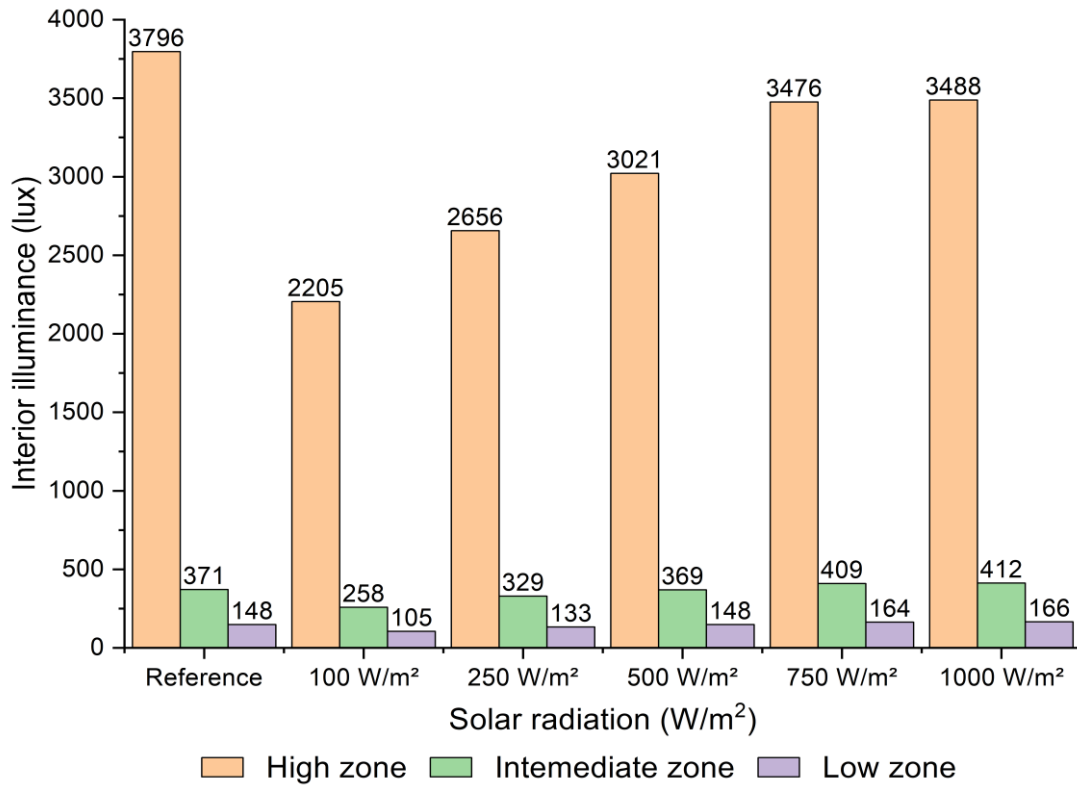


Figure 6-3. The average annual interior illuminance reading in relation to solar radiation for the PDLC glazing compared to a reference window for all daylighting zones in Riyadh.

Table 6-3. Average annual interior illuminance in (lux) for the PDLC and reference window in Riyadh.

	Interior illuminance (lux) for all daylighting zones		
	High zone	Intermediate zone	Low zone
<b>Reference</b>	3,796	371	148
<b>100 W/m²</b>	2,205	258	105
<b>250 W/m²</b>	2,656	329	133
<b>500 W/m²</b>	3,021	369	148
<b>750 W/m²</b>	3,476	409	164
<b>1000 W/m²</b>	3,488	412	166

#### 6.4.2 Evaluation of artificial lighting load in relation to solar radiation in London

Figure 6-4 shows the total annual artificial lighting energy consumption in relation to solar radiation compared to a reference window in London. When the solar radiation thresholds were set to 100 W/m<sup>2</sup> and 250 W/m<sup>2</sup>, the PDLC glazing performed similarly to the reference window in the high daylighting zone. In addition, the PDLC glazing could not reduce artificial lighting load in the intermediate and low daylighting zones due to the increased distance from the window and low solar radiation. When the control strategy was activated, the PDLC glazing changed to the opaque state and the particles randomly aligned resulting in higher diffuse transmittance. Therefore, as the solar radiation thresholds increased, the PDLC glazing reduced the artificial lighting load compared to the reference window. The PDLC achieved to reduce artificial lighting load in the intermediate daylighting zone when the solar radiation thresholds were 500 W/m<sup>2</sup>, 750 W/m<sup>2</sup>, and 1000 W/m<sup>2</sup> by 2%, 5% and 5%, respectively. In the low daylighting zone, the performance of the PDLC glazing was approximately similar to the reference window. The total annual artificial lighting load reduction for the PDLC glazing was achieved at solar radiation thresholds 750 W/m<sup>2</sup> and 1000 W/m<sup>2</sup> by 2% for both. In comparison, the PDLC glazing performance in London (temperate climate) was lower than the performance in Riyadh (arid climate). This is attributed to lower global illuminance in London compared to Riyadh. Table 6-4 presents the annual artificial lighting load results in relation to solar radiation for the PDLC glazing and the reference window in London climate.

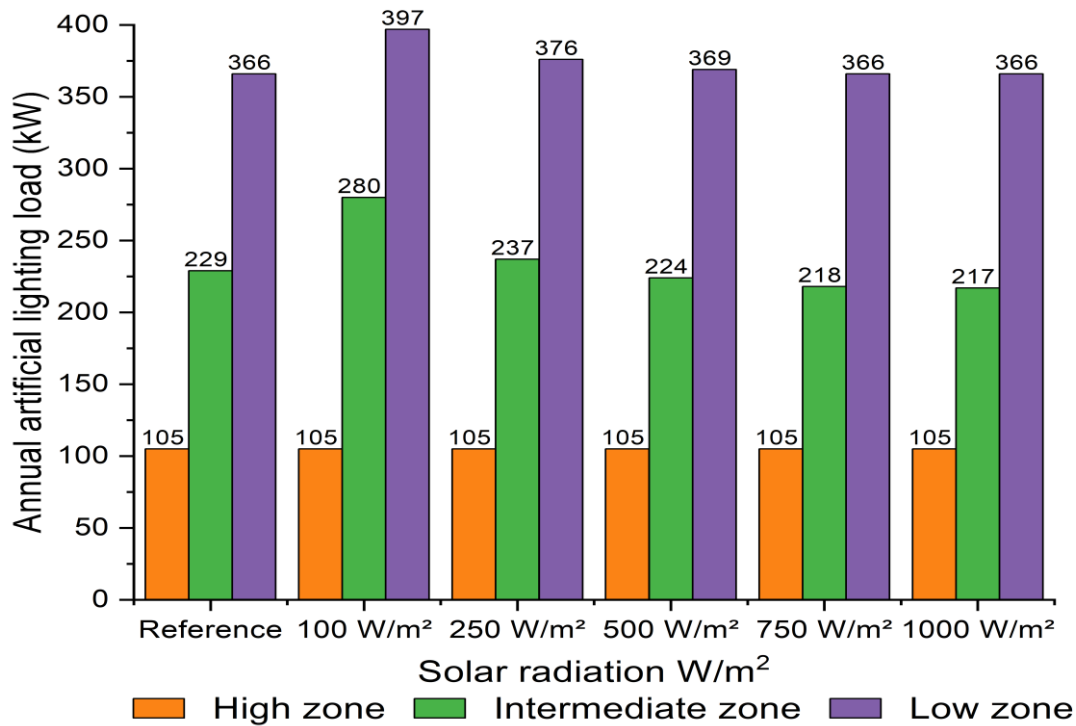


Figure 6-4. Total annual artificial lighting energy consumption in relation to solar radiation for the PDLC glazing compared to a reference window in London.

Table 6-4. Total annual artificial lighting loads (kW) for the PDLC and reference window in London.

Energy (kW)	High zone	Intermediate zone	Low zone
<b>Reference</b>	105	229	366
<b>100 W/m<sup>2</sup></b>	105	280	397
<b>250 W/m<sup>2</sup></b>	105	237	376
<b>500 W/m<sup>2</sup></b>	105	224	369
<b>750 W/m<sup>2</sup></b>	105	218	366
<b>1000 W/m<sup>2</sup></b>	105	217	366

Figure 6-5 presents the monthly artificial lighting energy consumption for the PDLC and reference window for all daylighting zones in London. During the year 75% of the measurements, the PDLC glazing was able to reduce the annual artificial lighting load in the case of 750 W/m<sup>2</sup> and 1000 W/m<sup>2</sup> thresholds compared to the reference window. The highest monthly artificial lighting load reduction was achieved in October. When the solar radiation threshold was set to 750 W/m<sup>2</sup>, and 1000 W/m<sup>2</sup>, the PDLC glazing artificial lighting loads were 54



kW for both. For the same period, the artificial lighting load for the reference window was 57 kW. The results showed that the illuminance was high in the case of the PDLC glazing in 750 W/m<sup>2</sup> and 1000 W/m<sup>2</sup> solar radiation thresholds resulting in artificial lighting load reduction. The PDLC glazing could not reduce artificial lighting load in all solar radiation thresholds in the low daylighting zone for all months due to the increased distance from the window. In addition, the global illuminance in London (temperate climate) is generally low. In October, the monthly daylight illuminance in the intermediate zone for the PDLC glazing was 399 lux, while the reference window was 379 lux. In comparison, the PDLC glazing performed better in Riyadh (arid climate) than in London (temperate climate). In Riyadh, the PDLC glazing was able to reduce the artificial lighting load during the whole year when the solar radiation thresholds were set to 750 W/m<sup>2</sup> and 1000 W/m<sup>2</sup>. On the contrary, the PDLC glazing reduced the annual artificial lighting load 75% of the time during the year in London. This indicates that the PDLC glazing performs better in a country where the global illuminance is usually high. Table 6-5 provides the monthly artificial lighting energy consumption in relation to solar radiation for the PDLC and reference window in London.

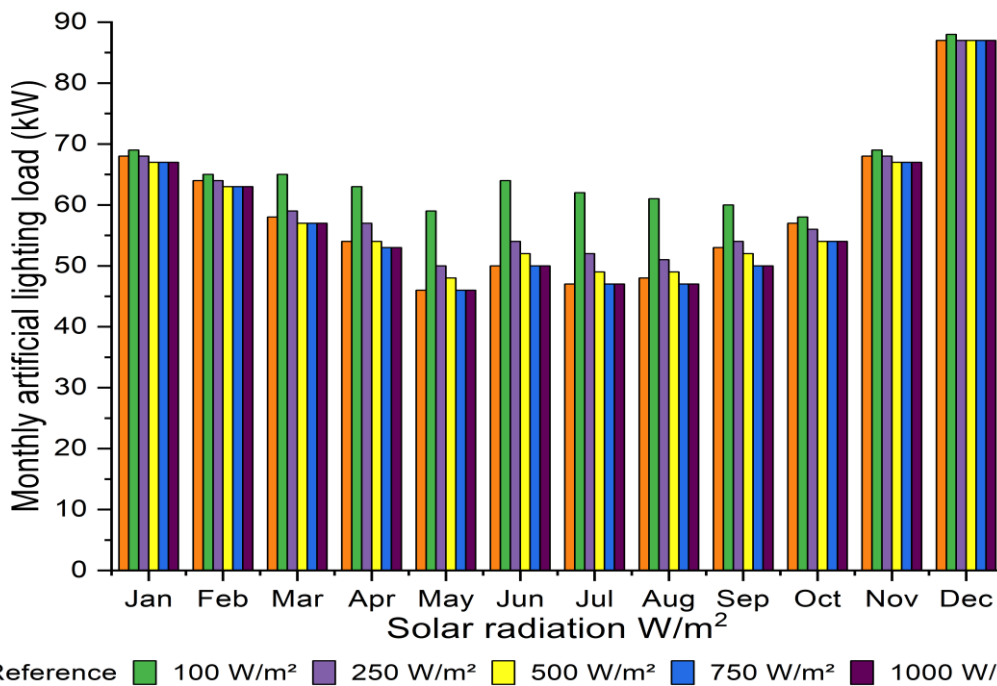


Figure 6-5. Monthly artificial lighting energy consumption in relation to solar radiation for the PDLC glazing compared to a reference window in London.

Table 6-5. Monthly artificial lighting load (kW) for the PDLC glazing and reference window in London.

Energy (kW)	Solar radiation thresholds for the PDLC glazing					Reference
	100 W/m <sup>2</sup>	250 W/m <sup>2</sup>	500 W/m <sup>2</sup>	750 W/m <sup>2</sup>	1000 W/m <sup>2</sup>	
<b>Jan</b>	69	68	67	67	67	68
<b>Feb</b>	65	64	63	63	63	64
<b>Mar</b>	65	59	57	57	57	58
<b>Apr</b>	63	57	54	53	53	54
<b>May</b>	59	50	48	46	46	46
<b>Jun</b>	64	54	52	50	50	50
<b>Jul</b>	62	52	49	47	47	47
<b>Aug</b>	61	51	49	47	47	48
<b>Sep</b>	60	54	52	50	50	53
<b>Oct</b>	58	56	54	54	54	57
<b>Nov</b>	69	68	67	67	67	68
<b>Dec</b>	88	87	87	87	87	87

Figure 6-6 shows the average annual interior illuminance readings of the PDLC glazing compared to the reference window for all daylighting zones in London. The interior illuminance results reflect the artificial lighting energy needed for the PDLC glazing and the reference window in all daylighting zones. As the interior illuminance decreased, more artificial lighting energy was required. In the high daylighting zone, the average annual interior illuminance was higher than the illuminance setpoint, which did not result in artificial lighting energy reduction. The PDLC glazing offered higher interior illuminance in the intermediate and low daylighting zones when the thresholds were 750 W/m<sup>2</sup> and 1000 W/m<sup>2</sup> compared to the reference window. Therefore, the artificial lighting energy needed to reach the illuminance setpoint was less. The highest average annual interior illuminance for the PDLC glazing was 385 lux and for the reference window was 382 lux in the intermediate daylighting zone. Table 6-6 shows the average annual interior illuminance values for the PDLC glazing and reference window in London.

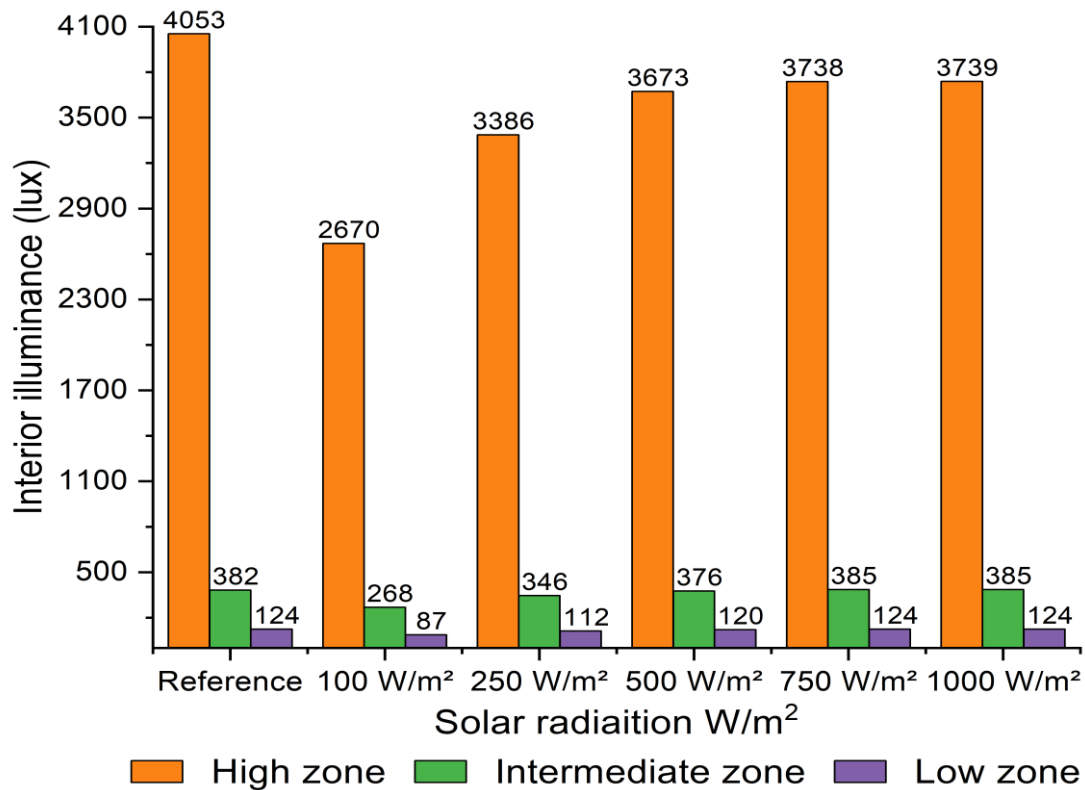


Figure 6-6. The average annual interior illuminance readings in relation to solar radiation of the PDLC glazing compared to a reference window for all daylighting zones in London.

Table 6-6. Average annual interior illuminance in (lux) for the PDLC and reference window in London.

	Interior illuminance (lux) for all daylighting zones		
	High zone	Intermediate zone	Low zone
<b>Reference</b>	4,053	382	124
<b>100 W/m²</b>	2,670	268	87
<b>250 W/m²</b>	3,386	346	112
<b>500 W/m²</b>	3,673	376	120
<b>750 W/m²</b>	3,738	385	124
<b>1000 W/m²</b>	3,739	385	124

### 6.4.3 Evaluation of artificial lighting load in relation to outdoor temperature in Riyadh

Figure 6-7 reports the total annual artificial lighting energy consumption in relation to outdoor temperature compared to a reference window in Riyadh. In high

daylighting zone, the PDLC glazing performed similarly in all outdoor temperature thresholds as to when the solar radiation control strategy was utilised. In intermediate daylighting zone, there was no artificial lighting reduction as the interior illuminance was generally low when the outdoor temperature thresholds were 4 °C and 20 °C. However, when the outdoor temperature threshold was set to a maximum temperature 46 °C, the PDLC glazing achieved to reduce the artificial lighting load by 26% compared to the reference window. Additionally, at the maximum temperature 46 °C, the artificial lighting energy reduction was 4% in the low daylighting zone. Moreover, the PDLC glazing was able to achieve 9% of annual artificial lighting savings compared to the reference window. The PDLC performed approximately similarly in both solar radiation and outdoor temperature control strategies in Riyadh (arid climate). Table 6-7 presents the annual artificial lighting load results in relation to outdoor temperature for the PDLC glazing and reference window in Riyadh climate.

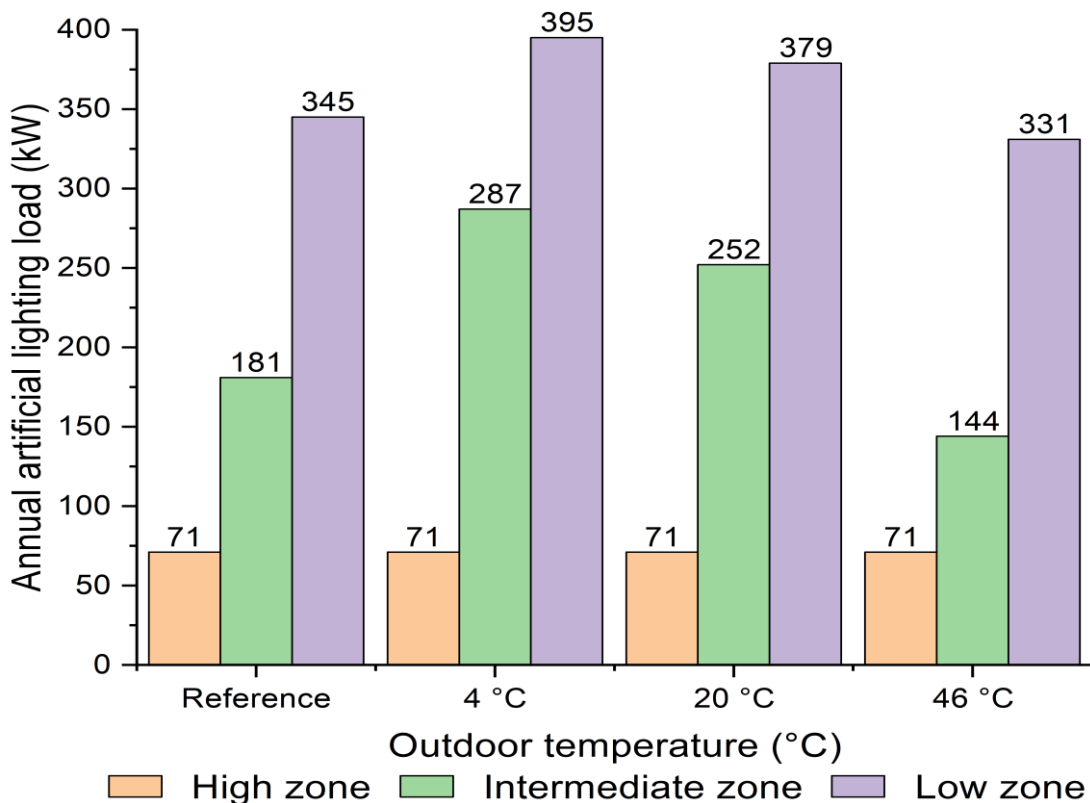


Figure 6-7. The total annual artificial lighting energy consumption in relation to outdoor temperature compared to a reference window in Riyadh.

Table 6-7. Total annual artificial lighting loads (kW) for the PDLC and reference window in Riyadh.

<b>Energy (kW)</b>	<b>High zone</b>	<b>Intermediate zone</b>	<b>Low zone</b>
<b>Reference</b>	71	181	345
<b>4 °C</b>	71	287	395
<b>20 °C</b>	71	252	379
<b>46 °C</b>	71	144	331

Figure 6-8 presents the monthly artificial lighting energy consumption for the PDLC and reference window for all daylighting zones in Riyadh. The artificial lighting load was higher during the whole year in the case of the PDLC glazing when the threshold was 4 °C compared to the reference window. When the threshold was set to 20 °C, there was artificial lighting load reduction only in January and December. In this case, the artificial lighting load was high due to the low monthly daylight illuminance received by the light sensors compared to the reference window. Consequently, more energy was required to achieve the illuminance setpoint. When the threshold was set to the maximum temperature 46 °C, the PDLC glazing was able to reduce the artificial lighting load for the whole year compared to the reference window. The highest artificial lighting load reduction was achieved in November. The artificial lighting consumption in the case of the PDLC glazing was 39 kW and in the case of the reference window was 47 kW. This indicates that the PDLC glazing offered higher interior illuminance compared to the reference window. The average monthly interior illuminance in the case of the PDLC glazing in the intermediate daylighting zone was 541 lux and in the case of the reference window was 455 lux. This means that the PDLC glazing required less energy to achieve the illuminance setpoint compared to the reference window. Table 6-8 provides the monthly artificial lighting energy consumption in relation to outdoor temperature for the PDLC and reference window in Riyadh.

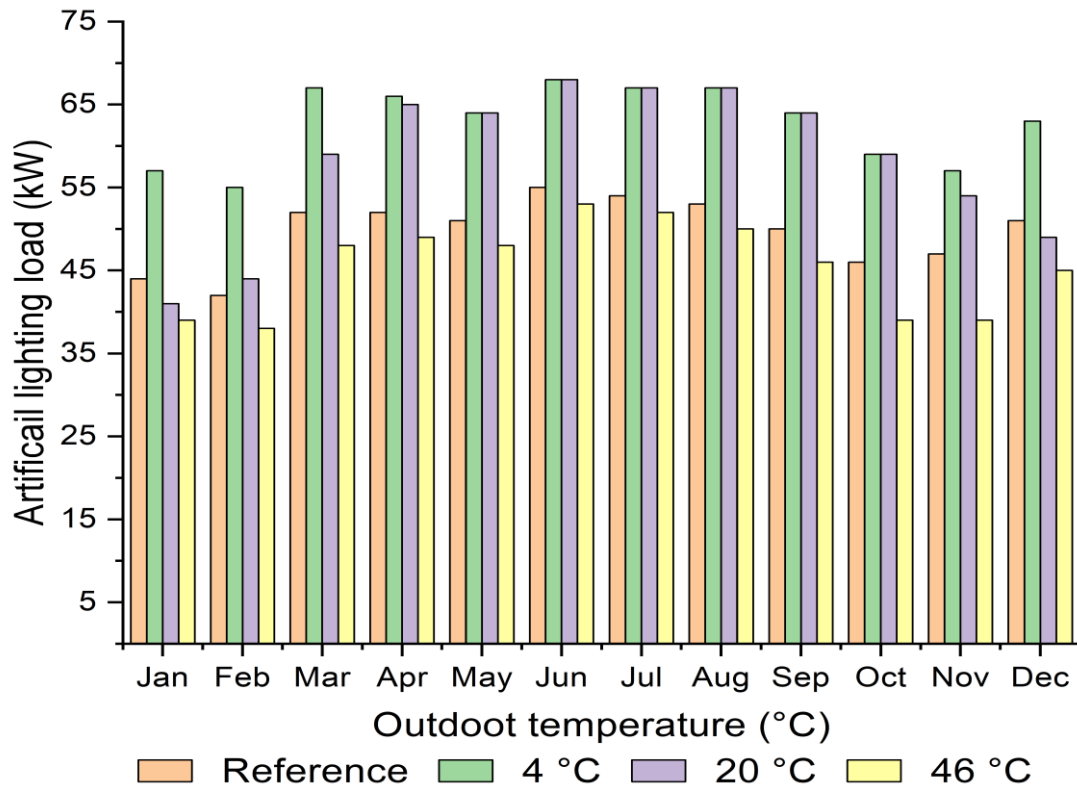
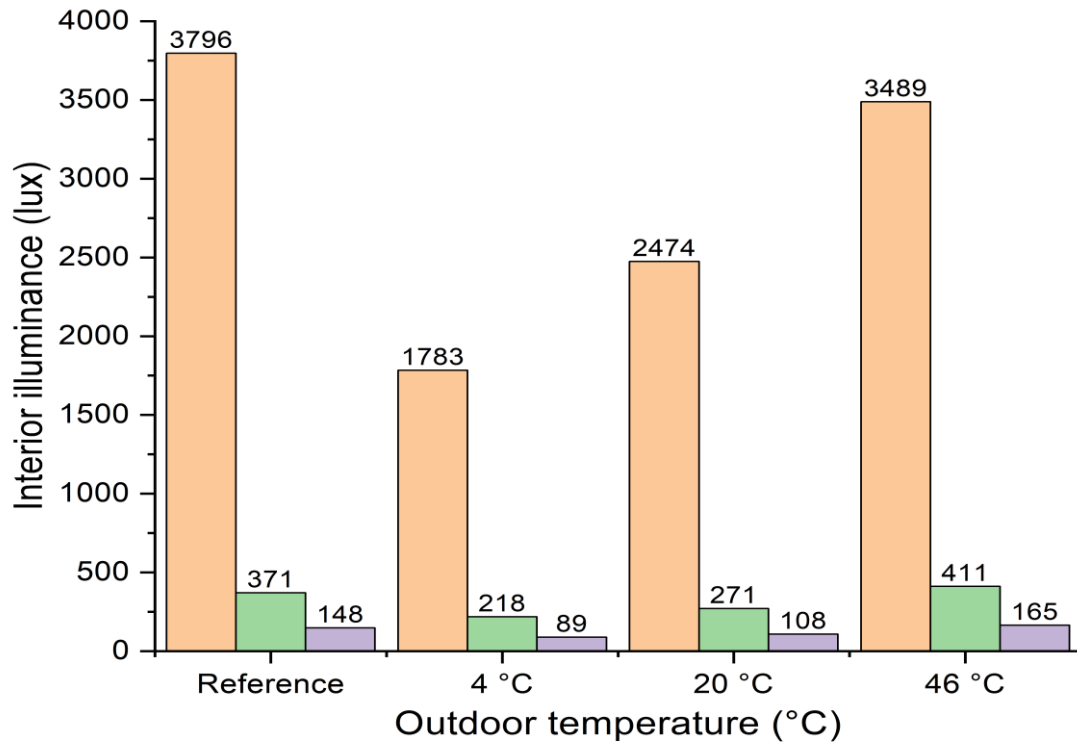


Figure 6-8. Monthly artificial lighting energy consumption in relation to outdoor temperature for the PDLC glazing compared to a reference window in Riyadh.

Table 6-8. Monthly artificial lighting load (kW) for the PDLC glazing and reference window in Riyadh.

Energy (kW)	Outdoor temperature thresholds for the PDLC glazing			
	4 °C	20 °C	46 °C	Reference
<b>Jan</b>	57	41	39	44
<b>Feb</b>	55	44	38	42
<b>Mar</b>	67	59	48	52
<b>Apr</b>	66	65	49	52
<b>May</b>	64	64	48	51
<b>Jun</b>	68	68	53	55
<b>Jul</b>	67	67	52	54
<b>Aug</b>	67	67	50	53
<b>Sep</b>	64	64	46	50
<b>Oct</b>	59	59	39	46
<b>Nov</b>	57	54	39	47
<b>Dec</b>	63	49	45	51

Figure 6-9 shows the average annual interior illuminance readings of the PDLC glazing compared to the reference window for all daylighting zones in Riyadh. The interior illuminance readings show an agreement with the artificial lighting load results. In high daylighting zone, the interior illuminance readings were extremely higher than the illuminance setpoint for the reference window and the PDLC glazing in all outdoor temperature thresholds. Thus, the artificial lighting load was expected to be lower than the intermediate and low daylighting zones due to the artificial lighting would be switched off most of the time. In intermediate daylighting zone, when the thresholds were set to 4 °C and 20 °C, the interior illuminance readings for the PDLC were relatively low. In the case of the reference window, the interior illuminance was higher than the PDLC glazing. Therefore, the energy consumption when the PDLC glazing was utilised was higher compared to the reference window. However, When the threshold was set to the maximum temperature 46 °C, the interior illuminance for the PDLC glazing was higher than the reference window. As a result, in the case of the PDLC glazing, the artificial lighting load was lower compared to the reference window. In low daylighting zone, the PDLC glazing had higher interior illuminance reading than the reference window. Therefore, the PDLC glazing required less energy to compensate for the needed illuminance compared to the reference window. The highest interior illuminance reading for the PDLC was 411 lux when the threshold was set to 46 °C in the immediate zone. In the case of the reference window, the highest interior illuminance window was 371 lux in the intermediate zone. Table 6-9 shows the average annual interior illuminance values for the PDLC glazing and reference window in Riyadh.



High zone Intermediate zone Low zone

Figure 6-9. The average annual interior illuminance readings in relation to outdoor temperature for the PDLC glazing compared to the reference window for all daylighting zones in Riyadh.

Table 6-9. Average annual interior illuminance in (lux) for the PDLC and reference window in Riyadh.

	Interior illuminance (lux) for all daylighting zones		
	High zone	Intermediate zone	Low zone
<b>Reference</b>	3,796	371	148
<b>4 °C</b>	1,783	218	89
<b>20 °C</b>	2,474	271	108
<b>46 °C</b>	3,489	411	165



#### **6.4.4 Evaluation of artificial lighting load in relation to outdoor temperature in London**

Figure 6-10 shows the total annual artificial lighting energy consumption in relation to outdoor temperature compared to a reference window in London. In high daylighting zone, the artificial lighting load was approximately equal for the PDLC glazing and reference window with the exception of when the threshold was set to the minimum temperature  $-5.9\text{ }^{\circ}\text{C}$ . Due to the low temperature below zero degrees, the sunlight is expected to be low, resulting in low interior illuminance transmitted through the PDLC glazing. In this case, the energy required for artificial lighting to compensate for the needed illuminance was higher compared to the reference window. In intermediate daylighting zone, the PDLC glazing was able to reduce the artificial lighting load when the shading control was set to the maximum outdoor temperature  $31.3\text{ }^{\circ}\text{C}$ . The artificial lighting load reduction for the PDLC glazing was 5% compared to the reference window. As the light sensor was further away from the window in the low daylighting zone, the interior illuminance extremely diminished, resulting in a high artificial lighting load for all outdoor temperature thresholds. The primary annual savings of the artificial lighting load was 2% for the PDLC glazing when the outdoor temperature was  $31.3\text{ }^{\circ}\text{C}$ . It was observed that the PDLC glazing performance was approximately similar to solar radiation and outdoor temperature control strategies. In addition, the annual artificial lighting load savings were higher in Riyadh (arid climate) than in London (temperate climate) when the outdoor temperature control strategy control was used. Table 6-10 presents the annual artificial lighting load results in relation to outdoor temperature for the PDLC glazing and reference window in London climate.

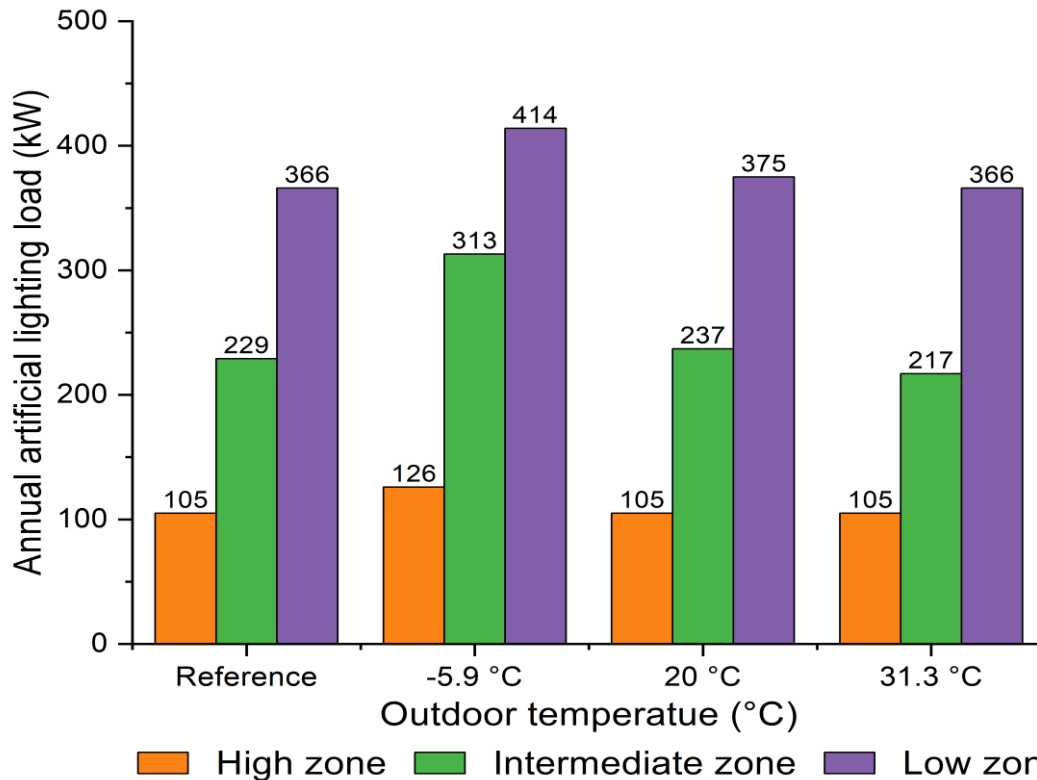


Figure 6-10. Total annual artificial lighting energy consumption in relation to outdoor temperature for the PDLC glazing compared to a reference window in London.

Table 6-10. Total annual artificial lighting loads (kW) for the PDLC and reference window in London.

Energy (kW)	High zone	Intermediate zone	Low zone
<b>Reference</b>	105	229	366
<b>- 5.9 °C</b>	126	313	414
<b>20 °C</b>	105	237	375
<b>31.3 °C</b>	105	217	366

Figure 6-11 presents the monthly artificial lighting energy consumption for the PDLC and reference window for all daylighting zones in London. The graph shows that the PDLC glazing was able to reduce the monthly artificial lighting load when the outdoor temperature thresholds were 20 °C and 31.3 °C. When the outdoor temperature was set to 20 °C, the artificial lighting reduction occurred from January to April and September to November. However, the artificial lighting load was significantly higher from May to August and December. Thus, the artificial lighting reduction did not reflect on the annual energy consumption.

When the outdoor temperature was set to 31.1 °C, the PDLC glazing reduced the artificial lighting load except in June, July, and December. The highest artificial lighting load reduction occurred in October and was 54 kW, while the reference window was 57 kW. In October, the average monthly interior illuminance for the PDLC glazing was 398 lux in the intermediate daylighting zone. In the case of the reference window, the interior illuminance was 379 lux in the same zone. Table 6-11 provides the monthly artificial lighting energy consumption in relation to outdoor temperature for the PDLC and reference window in London.

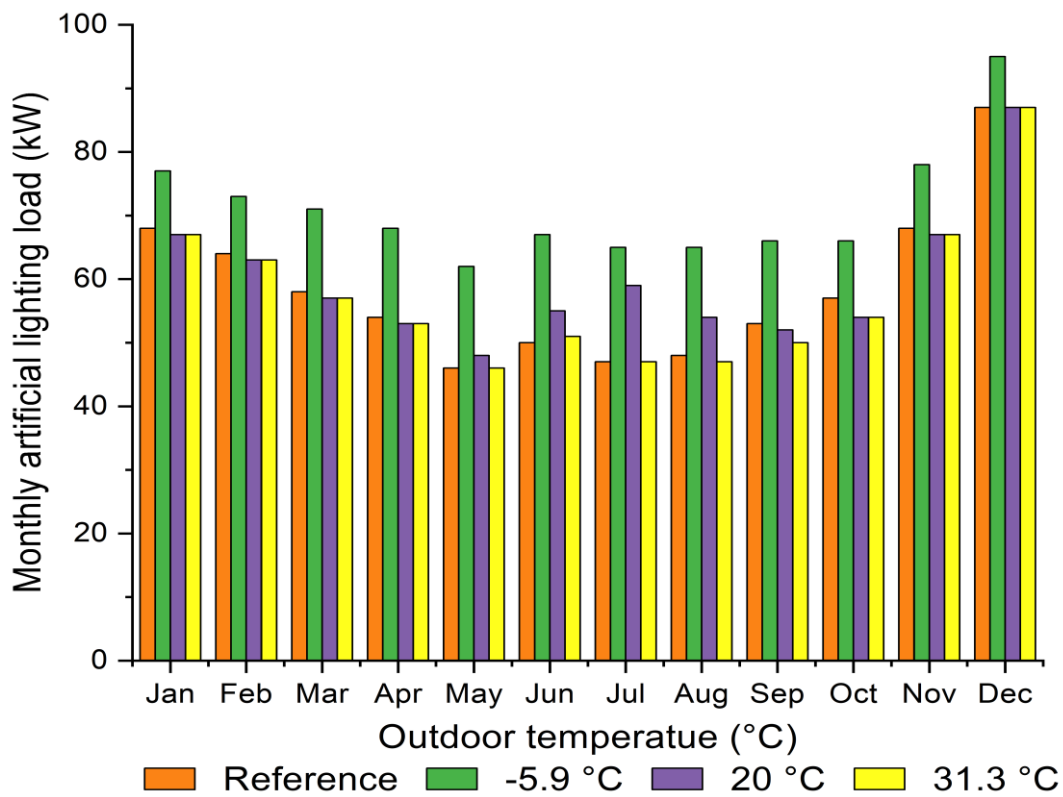


Figure 6-11. Monthly artificial lighting energy consumption in relation to outdoor temperature for the PDLC and reference window for all daylighting zones in London.

Table 6-11. Monthly artificial lighting load (kW) for the PDLC glazing and reference window in London.

Energy (kW)	Outdoor temperature thresholds for the PDLC glazing			
	-5.9 °C	20 °C	31.3 °C	Reference
<b>Jan</b>	77	67	67	68
<b>Feb</b>	73	63	63	64
<b>Mar</b>	71	57	57	58
<b>Apr</b>	68	53	53	54
<b>May</b>	62	48	46	46
<b>Jun</b>	67	55	51	50
<b>Jul</b>	65	59	47	47
<b>Aug</b>	65	54	47	48
<b>Sep</b>	66	52	50	53
<b>Oct</b>	66	54	54	57
<b>Nov</b>	78	67	67	68
<b>Dec</b>	95	87	87	87

Figure 6-12 shows the average annual interior illuminance readings of the PDLC glazing compared to the reference window for all daylighting zones in London. In high daylighting zone, when the outdoor temperature threshold was set to the minimum -5.9 °C, the interior illuminance was significantly low compared to the reference window. Therefore, the artificial lighting load was the highest in this case. In intermediate daylighting zone, the highest illuminance was when the PDLC was controlled at the maximum outdoor temperature 31.3 °C. Thus, the artificial lighting load was the lowest of all the cases. On the contrary, when the PDLC was controlled at outdoor temperature -5.9 °C and 20 °C, the interior illuminance readings were lower than the reference window. In this case, the artificial lighting load was higher compared to the reference window. In low daylighting zone, when the outdoor temperature was set to the maximum temperature 31.3 °C, the PDLC glazing and reference window had the same interior illuminance readings. Therefore, the artificial lighting load was the same for the PDLC glazing and reference window. The highest interior illuminance in the intermediate daylighting zone for the PDLC glazing was 585 lux and for the

reference window was 582 lux. Table 6-12 shows the average annual interior illuminance values for the PDLC glazing and reference window in London.

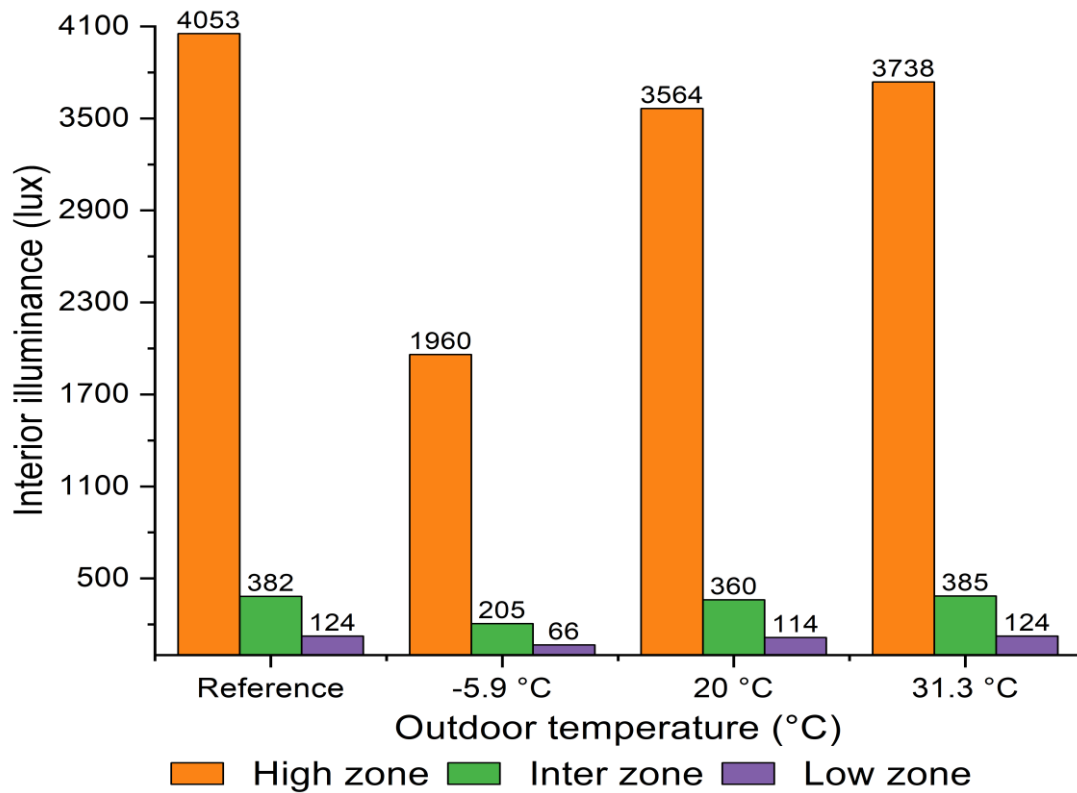


Figure 6-12. The average annual interior illuminance readings in relation to outdoor temperature for the PDLC glazing compared to the reference window for all daylighting zones in London.

Table 6-12. Average annual interior illuminance in (lux) for the PDLC and reference window in London.

	Interior illuminance (lux) for all daylighting zones		
	High zone	Intermediate zone	Low zone
<b>Reference</b>	4,053	382	124
<b>-5.9 °C</b>	19,60	205	66
<b>20 °C</b>	3,564	360	114
<b>31.3 °C</b>	3,738	385	124

## 6.5 Conclusion

EnergyPlus simulation work was carried out to evaluate the PDLC glazing effect on artificial lighting load for an office building in two contrasting climate zones, Riyadh (arid climate) and London (temperate climate). Solar radiation and outdoor temperature were utilised as shading control strategies. The results can be summarised as follow:

- 1- The PDLC glazing was able to control solar radiation and reduce the annual artificial lighting load. The results suggest that the PDLC glazing has the potential to be utilised as smart façade for building envelopes. In addition, The PDLC glazing is an excellent candidate to replace shading devices, which eliminates regular maintenance. The best performance of the PDLC glazing was when the solar radiation threshold was set to 1000 W/m<sup>2</sup> and reduced 10% of the annual artificial lighting energy in Riyadh (arid climate). In London, the PDLC glazing achieved a 2% annual artificial lighting energy reduction when solar radiation thresholds were set to 1000 W/m<sup>2</sup> and 750 W/m<sup>2</sup>. Moreover, it was found that the PDLC glazing performed better in Riyadh weather (arid climate) than in London weather (temperate climate).
- 2- Outdoor temperature was utilised to evaluate the effect of the PDLC glazing on the annual artificial lighting load. The PDLC glazing achieved to reduce the annual artificial lighting load when the outdoor temperature was set to the maximum temperature 46 °C by 9% in Riyadh. The artificial lighting load savings in London was 2% when the PDLC glazing was controlled on the maximum outdoor temperature 31.3 °C. It was found that the results of the PDLC glazing performance in Riyadh and London were approximately the same when the solar radiation and outdoor temperature control strategies were utilised. In addition, the PDLC glazing performed significantly better in a hot arid climate (Riyadh), where the global illuminance was higher.

## Chapter 7. Conclusions and recommendations

### 7.1 Conclusions

The energy demand for the building sector has significantly increased in the last few years in Saudi Arabia and the United Kingdom due to rapid economic and population growth. Stringent environmental regulations have been put in place to reduce carbon emissions and energy demand for the building sector in both countries. Electrically actuated switchable PDLC glazing modulates solar radiation by changing transparency from opaque to transparent using electrical power, which may potentially reduce energy demand. Therefore, this research aims to investigate the thermal and daylight performance of electrically switchable PDLC glazing for Net-Zero buildings in Saudi Arabia and the United Kingdom. This study provides a comprehensive analysis of the thermal, daylight, and energy performance of the PDLC glazing through an outdoor investigation and simulation study, which has not been conducted before this research. The findings from this research are summarised as follows:

- 1- The results of the indoor investigation showed that the PDLC glazing modulates solar radiation by 62% and 42% in the transparent and opaque state, respectively when a potential of 20 V AC is applied. In the opaque state, the PDLC glazing provides privacy due to the random alignment of the particles. The results suggest that the switchable PDLC glazing can be considered for building applications as it provides privacy, which is a key factor in building design in Saudi Arabia. The calculation of SHGC for this PDLC glazing was 0.63 and 0.68 for the transparent and opaque states, respectively. This indicates that the PDLC glazing could effectively reduce the heating load in a cold climate.
- 2- In the outdoor investigation, the aim was to evaluate the thermal behaviour and daylight characteristics of the PDLC glazing with and without a solar control film. One of the more significant findings to emerge from the investigation is that the PDLC glazing was able to reduce the temperature inside the test cell when it was switched to the opaque state. The results showed that the PDLC glazing reduced the test cell temperature from 46.9 °C in the transparent state to 39.9 °C in the opaque state. In terms of

daylight analysis, the PDLC glazing successfully controlled glare in the opaque state in a cloudy sky condition. It offered acceptable visual comfort below “just noticeable” in the morning and late afternoon hours. Furthermore, the solar control film had a positive effect on the thermal and daylight performance of the PDLC<sub>F</sub> glazing. The PDLC<sub>F</sub> glazing with the solar control film achieved to reduce solar heat gain inside the test in both states due to its NIR limiting ability. Thus, the temperature inside the test cell was lower than the temperature of the test cell when the PDLC glazing had no solar control film attached. The daylight investigation result suggests that the PDLC<sub>F</sub> with the solar control film achieved to improve the visual comfort level. The PDLC<sub>F</sub> glazing offered acceptable visual comfort below “just disturbing” in the late afternoon hours in transparent and opaque states in all sky conditions.

- 3- The outcome of the building energy modelling analysis showed that the PDLC glazing was a promising candidate for autonomous electrically switchable glazing. The most significant heating and cooling load reduction were achieved when the PDLC glazing was controlled by solar radiation control strategy. The PDLC glazing achieved to decrease the annual cooling load by 12.7% in Riyadh (arid climate) and the annual heating load by 4.9% in London (temperate climate) compared to the conventional reference window. Furthermore, the PDLC glazing reduced the annual artificial lighting load by 10% and 2% for Riyadh and London, respectively. The daylight analysis revealed that the PDLC glazing offered 68.52% of discomfort glare (DGI) above 22 in Riyadh and 55.05% of DGI in London when the temperature control strategy was used.

In summary, the PDLC glazing was investigated to characterise its thermal and daylight performance by theoretical and experimental methods. The outcome of this research suggests that the PDLC glazing has a promising performance and the technology could be a potential candidate for building applications. The current findings add substantially to our understanding of switchable PDLC glazing technology to assess its utilisation for Net-Zero buildings. In addition, a comprehensive analysis of building energy savings of the PDLC glazing can be useful for architect engineers to design green buildings.



## 7.2 Recommendations and future research

Based on the outcomes and the findings from literature review conducted in this research, the following future works are suggested:

- Long term outdoor study and comprehensive switching characterisation are required to evaluate PDLC device structure and assess the mechanical and electrical stresses in different climate conditions.
- Further experimental investigation is required to evaluate the effect of applying low-e coatings on PDLC glazing surface. In particular, the effect of temperature and soiling need to be characterised for longer term effect on its glazing performance to determine dynamic  $U$ -value and solar gain from the samples and durability of the devices.
- Life cycle carbon and cost analysis of energy efficiency simulation study for commercial buildings.
- Evaluating PDLC switchable glazing performance using renewable sources of power.
- A comprehensive simulation study for commercial buildings to evaluate PDLC glazing performance including energy efficiency, thermal and visual comfort for occupants in different climate conditions such as cold and Mediterranean climates.

## Bibliography

- [1] J.M. Dussault, L. Gosselin, T. Galstian, Integration of smart windows into building design for reduction of yearly overall energy consumption and peak loads, *Sol. Energy*. 86 (2012) 3405–3416. doi:10.1016/j.solener.2012.07.016.
- [2] A. Alardhi, A. S Alaboodi, R. Almasri, Impact of the new Saudi energy conservation code on Saudi Arabia residential buildings, *Aust. J. Mech. Eng.* 00 (2020) 1–15. doi:10.1080/14484846.2020.1802919.
- [3] T.D. Searchinger, T. Beringer, B. Holtsmark, D.M. Kammen, E.F. Lambin, W. Lucht, P. Raven, J.-P. van Ypersele, Europe’s renewable energy directive poised to harm global forests, *Nat. Commun.* 9 (2018) 1–4.
- [4] M. Shin, J.-C. Baltazar, J.S. Haberl, E. Frazier, B. Lynn, Evaluation of the energy performance of a net zero energy building in a hot and humid climate, *Energy Build.* 204 (2019) 109531. doi:https://doi.org/10.1016/j.enbuild.2019.109531.
- [5] R. Salem, A. Bahadori-Jahromi, A. Mylona, P. Godfrey, D. Cook, Investigating the potential impact of energy-efficient measures for retrofitting existing UK hotels to reach the nearly zero energy building (nZEB) standard, *Energy Effic.* (2019) 1–18.
- [6] European Commission, Energy performance of buildings, 2019.
- [7] EIA, Monthly Energy Review, 2019. <https://www.eia.gov/tools/faqs/faq.php?id=86&t=1> (accessed February 1, 2019).
- [8] SEC., SEC, Electrical data 2000-2013, KSA Saudi Electr. Co. (2015). <https://www.se.com.sa/ar-sa/Pages/home.aspx> (accessed September 9, 2019).
- [9] M. Asif, Growth and sustainability trends in the buildings sector in the GCC region with particular reference to the KSA and UAE, *Renew. Sustain.*

Energy Rev. 55 (2016) 1267–1273. doi:10.1016/j.rser.2015.05.042.

- [10] EIA, EIA Country Analysis Brief – United Kingdom, 2018. [http://www.eia.gov/EMEU/cabs/United\\_Kingdom/pdf.pdf](http://www.eia.gov/EMEU/cabs/United_Kingdom/pdf.pdf).
- [11] S.D. Rezaei, S. Shannigrahi, S. Ramakrishna, A review of conventional, advanced, and smart glazing technologies and materials for improving indoor environment, *Sol. Energy Mater. Sol. Cells.* 159 (2017) 26–51. doi:10.1016/j.solmat.2016.08.026.
- [12] T.E. Kuhn, Calorimetric determination of the solar heat gain coefficient  $g$  with steady-state laboratory measurements, *Energy Build.* 84 (2014) 388–402. doi:10.1016/j.enbuild.2014.08.021.
- [13] B.P. Jelle, A. Gustavsen, T.N. Nilsen, T. Jacobsen, Solar material protection factor (SMPF) and solar skin protection factor (SSPF) for window panes and other glass structures in buildings, *Sol. Energy Mater. Sol. Cells.* 91 (2007) 342–354. doi:10.1016/j.solmat.2006.10.017.
- [14] K. Dubey, N. Howarth, M. Krarti, Evaluating Building Energy Efficiency Investment Options for Saudi Arabia, *Kapsarc.* (2016) 1–64. [https://www.kapsarc.org/wp-content/uploads/2016/10/KS-1655-DP049A-Evaluating-Building-Energy-Efficiency-Investment-Options-for-SA\\_web.pdf](https://www.kapsarc.org/wp-content/uploads/2016/10/KS-1655-DP049A-Evaluating-Building-Energy-Efficiency-Investment-Options-for-SA_web.pdf).
- [15] H.M. Government, The Climate Change Act 2008 (2050 Target Amendment) Order 2019, 2019. doi:9780111187654.
- [16] BEIS, Annex: 2018 UK Greenhouse Gas Emissions, final figures by end user and fuel type, (n.d.). <https://cutt.ly/5o3keV0> (accessed March 23, 2022).
- [17] H.M. Government, Industrial strategy: construction sector deal, Department of business, energy and industrial strategy, (2018). <https://www.gov.uk/government/publications/construction-sector-deal> (accessed March 23, 2022).

- [18] B.P. Jelle, Solar radiation glazing factors for window panes, glass structures and electrochromic windows in buildings - Measurement and calculation, *Sol. Energy Mater. Sol. Cells.* 116 (2013) 291–323. doi:10.1016/j.solmat.2013.04.032.
- [19] S. Lu, Z. Li, Q. Zhao, F. Jiang, Modified calculation of solar heat gain coefficient in glazing façade buildings, *Energy Procedia.* 122 (2017) 151–156. doi:10.1016/j.egypro.2017.07.335.
- [20] IOS 9050, Glass in Building-Determination of Light Transmittance, Solar Direct Transmittance, Total Solar Energy Transmittance, Ultraviolet Transmittance and Related Glazing Factors, *Int. Organ. Stand. Geneva.* (2003).
- [21] F. Gloriant, P. Tittlein, A. Joulin, S. Lassue, Modeling a triple-glazed supply-air window, *Build. Environ.* 84 (2015) 1–9. doi:10.1016/j.buildenv.2014.10.017.
- [22] J.S. Carlos, H. Corvacho, Evaluation of the performance indices of a ventilated double window through experimental and analytical procedures: SHGC-values, *Energy Build.* 86 (2015) 886–897. doi:10.1016/j.enbuild.2014.11.002.
- [23] J.H. Klems, J.L. Warner, Solar heat gain coefficient of complex fenestrations with a venetian blind for differing slat tilt angles, *ASHRAE Trans.* 103 (1997) 1026–1034.
- [24] M.S. Bhandari, N.K. Bansal, Solar heat gain factors and heat loss coefficients for passive heating concepts, *Sol. Energy.* 53 (1994) 199–208. doi:10.1016/0038-092X(94)90482-0.
- [25] C.A. Gueymard, W.C. duPont, Spectral effects on the transmittance, solar heat gain, and performance rating of glazing systems, *Sol. Energy.* 83 (2009) 940–953. doi:10.1016/j.solener.2008.12.012.
- [26] G. Oliveti, N. Arcuri, R. Bruno, M. De Simone, An accurate calculation

- model of solar heat gain through glazed surfaces, *Energy Build.* 43 (2011) 269–274. doi:10.1016/j.enbuild.2010.11.009.
- [27] A. Ghosh, B. Norton, A. Duffy, Measured thermal performance of a combined suspended particle switchable device evacuated glazing, *Appl. Energy.* 169 (2016) 469–480. doi:10.1016/j.apenergy.2016.02.031.
- [28] F. Aleo, A. Pennisi, S. Scalia, F. Simone, Optical and energetic performances of an electrochromic window tested in a “PASSYS” cell, *Electrochim. Acta.* 46 (2001) 2243–2249. doi:10.1016/S0013-4686(01)00367-X.
- [29] E. Cuce, S.B. Riffat, A smart building material for low/zero carbon applications: Heat insulation solar glass-characteristic results from laboratory and in situ tests, *Int. J. Low-Carbon Technol.* 12 (2017) 126–135. doi:10.1093/ijlct/ctw009.
- [30] J.L. Wright, Effective U-values and Shading Coefficients of Preheat/Supply Air Glazing Systems, in: *UWSpace*, 1986. <http://hdl.handle.net/10012/11624>.
- [31] J.S. Carlos, H. Corvacho, Evaluation of the thermal performance indices of a ventilated double window through experimental and analytical procedures: Uw-values, *Renew. Energy.* 63 (2014) 747–754. doi:10.1016/j.renene.2013.10.031.
- [32] P.H. Baker, M. McEvoy, Test cell analysis of the use of a supply air window as a passive solar component, *Sol. Energy.* 69 (2000) 113–130. doi:10.1016/S0038-092X(00)00048-7.
- [33] S. Hoffmann, E.S. Lee, C. Clavero, Examination of the technical potential of near-infrared switching thermochromic windows for commercial building applications, *Sol. Energy Mater. Sol. Cells.* 123 (2014) 65–80. doi:10.1016/j.solmat.2013.12.017.
- [34] W. Zhang, L. Lu, X. Chen, Performance Evaluation of Vacuum Photovoltaic

- Insulated Glass Unit, *Energy Procedia*. 105 (2017) 322–326. doi:10.1016/j.egypro.2017.03.321.
- [35] A. Ghosh, B. Norton, A. Duffy, Measured thermal & daylight performance of an evacuated glazing using an outdoor test cell, *Appl. Energy*. 177 (2016) 196–203. doi:10.1016/j.apenergy.2016.05.118.
- [36] S. Chirarattananon, P. Chaiwiwatworakul, S. Pattanasethanon, Daylight availability and models for global and diffuse horizontal illuminance and irradiance for Bangkok, *Renew. Energy*. 26 (2002) 69–89.
- [37] M. Krarti, P.M. Erickson, T.C. Hillman, A simplified method to estimate energy savings of artificial lighting use from daylighting, *Build. Environ*. 40 (2005) 747–754.
- [38] L.D. Öztürk, Determination of energy losses in lighting in terms of good vision efficiency, *Archit. Sci. Rev*. 51 (2008) 39–47.
- [39] A. Chel, G.N. Tiwari, A. Chandra, A model for estimation of daylight factor for skylight: an experimental validation using pyramid shape skylight over vault roof mud-house in New Delhi (India), *Appl. Energy*. 86 (2009) 2507–2519.
- [40] C.P. Kurian, R.S. Aithal, J. Bhat, V.I. George, Robust control and optimisation of energy consumption in daylight—artificial light integrated schemes, *Light. Res. Technol*. 40 (2008) 7–24.
- [41] D.H.W. Li, J.C. Lam, Evaluation of lighting performance in office buildings with daylighting controls, *Energy Build*. 33 (2001) 793–803.
- [42] D.H.W. Li, T.N.T. Lam, S.L. Wong, Lighting and energy performance for an office using high frequency dimming controls, *Energy Convers. Manag*. 47 (2006) 1133–1145.
- [43] D.H.W. Li, T.N.T. Lam, W.W.H. Chan, A.H.L. Mak, Energy and cost analysis of semi-transparent photovoltaic in office buildings, *Appl. Energy*.

86 (2009) 722–729.

- [44] I.E.S. Iesna, *Lighting handbook*, Illum. Eng. Soc. North Am. New York, USA. (2000).
- [45] J.E. Kaufman, *IES lighting handbook*, 1984.
- [46] H.D. Einhorn, A new method for the assessment of discomfort glare, *Light. Res. Technol.* 1 (1969) 235–247.
- [47] C.I. de l'Eclairage, Discomfort glare in interior lighting, in: CIE, 1995.
- [48] P. Chauvel, J.B. Collins, R. Dogniaux, J. Longmore, Glare from windows: current views of the problem, *Light. Res. Technol.* 14 (1982) 31–46.
- [49] P. Petherbridge, R.G. Hopkinson, Discomfort glare and the lighting of buildings, *Trans. Illum. Eng. Soc.* 15 (1950) 39–79.
- [50] W.K.E. Osterhaus, Discomfort glare assessment and prevention for daylight applications in office environments, *Sol. Energy.* 79 (2005) 140–158.
- [51] A.A. Nazzal, New daylight glare evaluation method. Introduction of the monitoring protocol and calculation method, *Energy Build.* 33 (2001) 257–265. doi:10.1016/S0378-7788(00)00090-6.
- [52] J. Wienold, *Dynamic daylight glare evaluation: Proceedings of Building Simulation*, (2009).
- [53] C.E. Waters, R.G. Mistrick, C.A. Bernecker, Discomfort glare from sources of nonuniform luminance, *J. Illum. Eng. Soc.* 24 (1995) 73–85.
- [54] A. Ghosh, B. Norton, Durability of switching behaviour after outdoor exposure for a suspended particle device switchable glazing, *Sol. Energy Mater. Sol. Cells.* 163 (2017) 178–184. doi:10.1016/j.solmat.2017.01.036.
- [55] A. Ghosh, B. Norton, A. Duffy, Effect of sky conditions on light transmission

- through a suspended particle device switchable glazing, *Sol. Energy Mater. Sol. Cells.* 160 (2017) 134–140. doi:10.1016/j.solmat.2016.09.049.
- [56] A. Ghosh, Daylighting and Thermo-Electrical performance of an Autonomous Suspended Particle Device Evacuated Glazing, (2016). doi:10.21427/D7P31T.
- [57] A. Ghosh, B. Norton, A. Duffy, Measured overall heat transfer coefficient of a suspended particle device switchable glazing, *Appl. Energy.* 159 (2015) 362–369. doi:10.1016/j.apenergy.2015.09.019.
- [58] A. Ghosh, B. Norton, A. Duffy, Daylighting performance and glare calculation of a suspended particle device switchable glazing, *Sol. Energy Mater. Sol. Cells.* 157 (2016) 114–128. doi:10.1016/j.solmat.2016.05.013.
- [59] A. Ghosh, B. Norton, A. Duffy, Behaviour of a SPD switchable glazing in an outdoor test cell with heat removal under varying weather conditions, *Appl. Energy.* 180 (2016) 695–706. doi:10.1016/j.apenergy.2016.08.029.
- [60] A. Ghosh, B. Norton, Interior colour rendering of daylight transmitted through a suspended particle device switchable glazing, *Sol. Energy Mater. Sol. Cells.* 163 (2017) 218–223. doi:10.1016/j.solmat.2017.01.041.
- [61] R. Vergaz, J.M. Sánchez-Pena, D. Barrios, C. Vázquez, P. Contreras-Lallana, Modelling and electro-optical testing of suspended particle devices, *Sol. Energy Mater. Sol. Cells.* 92 (2008) 1483–1487. doi:10.1016/j.solmat.2008.06.018.
- [62] D. Barrios, R. Vergaz, J.M. Sanchez-Pena, C.G. Granqvist, G.A. Niklasson, Toward a quantitative model for suspended particle devices: Optical scattering and absorption coefficients, *Sol. Energy Mater. Sol. Cells.* 111 (2013) 115–122. doi:10.1016/j.solmat.2012.12.012.
- [63] C.G. Granqvist, M.A. Arvizu, I. Bayrak Pehlivan, H.Y. Qu, R.T. Wen, G.A. Niklasson, Electrochromic materials and devices for energy efficiency and human comfort in buildings: A critical review, *Electrochim. Acta.* 259 (2017)



1170–1182. doi:10.1016/j.electacta.2017.11.169.

- [64] S.K. Deb, Optical and photoelectric properties and colour centres in thin films of tungsten oxide, *Philos. Mag.* 27 (1973) 801–822.
- [65] L. Beverina, G.A. Pagani, M. Sassi, Multichromophoric electrochromic polymers: colour tuning of conjugated polymers through the side chain functionalization approach, *Chem. Commun.* 50 (2014) 5413–5430.
- [66] C.G. Granqvist, A. Azens, A. Hjelm, L. Kullman, G.A. Niklasson, D. Rönnow, M. Strømme Mattsson, M. Veszeli, G. Vaivars, Recent advances in electrochromics for smart windows applications, *Sol. Energy.* 63 (1998) 199–216. doi:10.1016/S0038-092X(98)00074-7.
- [67] S.K. Deb, Opportunities and challenges in science and technology of WO<sub>3</sub> for electrochromic and related applications, *Sol. Energy Mater. Sol. Cells.* 92 (2008) 245–258. doi:10.1016/j.solmat.2007.01.026.
- [68] I. Sorar, E. Pehlivan, G.A. Niklasson, C.G. Granqvist, Electrochromism of DC magnetron sputtered TiO<sub>2</sub> thin films: Role of deposition parameters, *Sol. Energy Mater. Sol. Cells.* 115 (2013) 172–180.
- [69] J.Z. Ou, S. Balendhran, M.R. Field, D.G. McCulloch, A.S. Zoofakar, R.A. Rani, S. Zhuiykov, A.P. O'Mullane, K. Kalantar-Zadeh, The anodized crystalline WO<sub>3</sub> nanoporous network with enhanced electrochromic properties, *Nanoscale.* 4 (2012) 5980–5988.
- [70] D. Di Yao, J.Z. Ou, K. Latham, S. Zhuiykov, A.P. O'Mullane, K. Kalantar-zadeh, Electrodeposited  $\alpha$ - and  $\beta$ -phase MoO<sub>3</sub> films and investigation of their gasochromic properties, *Cryst. Growth Des.* 12 (2012) 1865–1870.
- [71] D.D. Yao, R.A. Rani, A.P. O'Mullane, K. Kalantar-zadeh, J.Z. Ou, High performance electrochromic devices based on anodized nanoporous Nb<sub>2</sub>O<sub>5</sub>, *J. Phys. Chem. C.* 118 (2013) 476–481.
- [72] Ö.D. Coşkun, S. Demirel, G. Atak, The effects of heat treatment on optical,

- structural, electrochromic and bonding properties of Nb<sub>2</sub>O<sub>5</sub> thin films, *J. Alloys Compd.* 648 (2015) 994–1004.
- [73] S. Ulrich, C. Szyszko, S. Jung, M. Verg<sup>hl</sup>, Electrochromic properties of mixed oxides based on titanium and niobium for smart window applications, *Surf. Coatings Technol.* 314 (2017) 41–44. doi:10.1016/j.surfcoat.2016.11.078.
- [74] M. Laurenti, S. Bianco, M. Castellino, N. Garino, A. Virga, C.F. Pirri, P. Mandracci, Toward plastic smart windows: optimization of indium tin oxide electrodes for the synthesis of electrochromic devices on polycarbonate substrates, *ACS Appl. Mater. Interfaces.* 8 (2016) 8032–8042.
- [75] D.R. Rosseinsky, R.J. Mortimer, Electrochromic systems and the prospects for devices, *Adv. Mater.* 13 (2001) 783–793.
- [76] M. Grätzel, Materials science: ultrafast colour displays, *Nature.* 409 (2001) 575.
- [77] R. Baetens, B.P. Jelle, A. Gustavsen, Properties, requirements and possibilities of smart windows for dynamic daylight and solar energy control in buildings: A state-of-the-art review, *Sol. Energy Mater. Sol. Cells.* 94 (2010) 87–105. doi:10.1016/j.solmat.2009.08.021.
- [78] X. Lou, X. Zhao, J. Feng, X. Zhou, Electrochromic properties of Al doped B-substituted NiO films prepared by sol-gel, *Prog. Org. Coatings.* 64 (2009) 300–303. doi:10.1016/j.porgcoat.2008.09.006.
- [79] F. Carpi, D. De Rossi, Colours from electroactive polymers: Electrochromic, electroluminescent and laser devices based on organic materials, *Opt. Laser Technol.* 38 (2006) 292–305.
- [80] Y. Ji, C. Qin, H. Niu, L. Sun, Z. Jin, X. Bai, Electrochemical and electrochromic behaviors of polyaniline-graphene oxide composites on the glass substrate/Ag nano-film electrodes prepared by vertical target pulsed laser deposition, *Dye. Pigment.* 117 (2015) 72–82.

- [81] V. Stockhausen, P. Martin, J. Ghilane, Y. Leroux, H. Randriamahazaka, J. Grand, N. Felidj, J.C. Lacroix, Giant plasmon resonance shift using poly (3, 4-ethylenedioxythiophene) electrochemical switching, *J. Am. Chem. Soc.* 132 (2010) 10224–10226.
- [82] J. Fei, K.G. Lim, G.T.R. Palmore, Polymer composite with three electrochromic states, *Chem. Mater.* 20 (2008) 3832–3839.
- [83] X. Fu, C. Jia, Z. Wan, X. Weng, J. Xie, L. Deng, Hybrid electrochromic film based on polyaniline and TiO<sub>2</sub> nanorods array, *Org. Electron.* 15 (2014) 2702–2709.
- [84] M. Casini, Active dynamic windows for buildings: A review, *Renew. Energy.* 119 (2018) 923–934. doi:10.1016/j.renene.2017.12.049.
- [85] N.L. Sbar, L. Podbelski, H.M. Yang, B. Pease, Electrochromic dynamic windows for office buildings, *Int. J. Sustain. Built Environ.* 1 (2012) 125–139. doi:10.1016/j.ijbsbe.2012.09.001.
- [86] A. Piccolo, F. Simone, Performance requirements for electrochromic smart window, *J. Build. Eng.* 3 (2015) 94–103. doi:10.1016/j.jobbe.2015.07.002.
- [87] P. Tavares, H. Bernardo, A. Gaspar, A. Martins, Control criteria of electrochromic glasses for energy savings in mediterranean buildings refurbishment, *Sol. Energy.* 134 (2016) 236–250. doi:10.1016/j.solener.2016.04.022.
- [88] A. Piccolo, F. Simone, Effect of switchable glazing on discomfort glare from windows, *Build. Environ.* 44 (2009) 1171–1180. doi:10.1016/j.buildenv.2008.08.013.
- [89] Z. Li, J. Ju, W. Xu, Daylighting Control Performance and Subject Responses to Electrochromic Windows in a Meeting Room, in: *Procedia Eng.*, Elsevier B.V., 2015: pp. 27–32. doi:10.1016/j.proeng.2015.08.1014.
- [90] A. Piccolo, Thermal performance of an electrochromic smart window tested

- in an environmental test cell, *Energy Build.* 42 (2010) 1409–1417. doi:10.1016/j.enbuild.2010.03.010.
- [91] Sageglass, Proven Reliability, (2015). <http://sageglass.dreamhosters.com/wp-content/uploads/2015/05/MKT-049.1-Reliability-Sheet.pdf> (accessed April 25, 2018).
- [92] G. Macrelli, Optical characterization of commercial large area liquid crystal devices, *Sol. Energy Mater. Sol. Cells.* 39 (1995) 123–131. doi:10.1016/0927-0248(95)00044-5.
- [93] K. Li, M. Pivnenko, D. Chu, A. Cockburn, W. O'Neill, Uniform and fast switching of window-size smectic A liquid crystal panels utilising the field gradient generated at the fringes of patterned electrodes, *Liq. Cryst.* 43 (2016) 735–749. doi:10.1080/02678292.2016.1142012.
- [94] D.J. Gardiner, S.M. Morris, H.J. Coles, High-efficiency multistable switchable glazing using smectic A liquid crystals, *Sol. Energy Mater. Sol. Cells.* 93 (2009) 301–306. doi:10.1016/j.solmat.2008.10.023.
- [95] Y. Anjaneyulu, D.W. Yoon, A PCGH liquid crystal window to control solar energy, *Sol. Energy Mater.* 14 (1986) 223–232. doi:10.1016/0165-1633(86)90049-3.
- [96] J.C. Torres, R. Vergaz, D. Barrios, J.M. Sánchez-Pena, A. Viñuales, H.J. Grande, G. Cabañero, Frequency and temperature dependence of fabrication parameters in polymer dispersed liquid crystal devices, *Materials (Basel).* 7 (2014) 3512–3521. doi:10.3390/ma7053512.
- [97] A. Hadj Sahraoui, S. Delenclos, S. Longuemart, D. Dadarlat, Heat transport in polymer-dispersed liquid crystals under electric field, *J. Appl. Phys.* 110 (2011) 33510. doi:10.1063/1.3610445.
- [98] S. Park, J.W. Hong, Polymer dispersed liquid crystal film for variable-transparency glazing, *Thin Solid Films.* 517 (2009) 3183–3186. doi:10.1016/j.tsf.2008.11.115.

- [99] W. Zhang, J. Lin, T. Yu, S. Lin, D. Yang, Effect of electric field on phase separation of polymer dispersed liquid crystal, *Eur. Polym. J.* 39 (2003) 1635–1640. doi:10.1016/S0014-3057(03)00074-0.
- [100] L. Petti, P. Mormile, W.J. Blau, Fast electro-optical switching and high contrast ratio in epoxy-based polymer dispersed liquid crystals, *Opt. Lasers Eng.* 39 (2003) 369–377. doi:10.1016/S0143-8166(01)00119-1.
- [101] D. Cupelli, G. De Filpo, G. Chidichimo, F.P. Nicoletta, The electro-optical and electrochromic properties of electrolyte-liquid crystal dispersions, *J. Appl. Phys.* 100 (2006). doi:10.1063/1.2219696.
- [102] D. Cupelli, F.P. Nicoletta, S. Manfredi, G. De Filpo, G. Chidichimo, Electrically switchable chromogenic materials for external glazing, *Sol. Energy Mater. Sol. Cells.* 93 (2009) 329–333. doi:10.1016/j.solmat.2008.11.010.
- [103] D. Cupelli, F.P. Nicoletta, S. Manfredi, M. Vivacqua, P. Formoso, G. De Filpo, G. Chidichimo, Self-adjusting smart windows based on polymer-dispersed liquid crystals, *Sol. Energy Mater. Sol. Cells.* 93 (2009) 2008–2012. doi:10.1016/j.solmat.2009.08.002.
- [104] A. Ghosh, B. Norton, T.K. Mallick, Daylight characteristics of a polymer dispersed liquid crystal switchable glazing, *Sol. Energy Mater. Sol. Cells.* 174 (2018) 572–576. doi:10.1016/j.solmat.2017.09.047.
- [105] A. Ghosh, T.K. Mallick, Evaluation of optical properties and protection factors of a PDLC switchable glazing for low energy building integration, *Sol. Energy Mater. Sol. Cells.* 176 (2018) 391–396. doi:10.1016/j.solmat.2017.10.026.
- [106] A. Ghosh, T.K. Mallick, Evaluation of colour properties due to switching behaviour of a PDLC glazing for adaptive building integration, *Renew. Energy.* 120 (2018) 126–133. doi:10.1016/j.renene.2017.12.094.
- [107] D. Jung, W. Choi, J.Y. Park, K.B. Kim, N. Lee, Y. Seo, H.S. Kim, N.K. Kong,

- Inorganic gel and liquid crystal based smart window using silica sol-gel process, *Sol. Energy Mater. Sol. Cells.* 159 (2017) 488–495. doi:10.1016/j.solmat.2016.10.001.
- [108] A.H. Hisham, A. and Amawgani, Smart and Efficient Energy Saving System, *Smart City Symp. Prague.* (2019) 1–5.
- [109] S. Saboor, S. Nundy, M. Venkata Ramana, A. Ghosh, A. Afzal, Polymer dispersed liquid crystal retrofitted smart switchable glazing: Energy saving, diurnal illumination, and CO<sub>2</sub> mitigation prospective, *J. Clean. Prod.* (2022) 131444. doi:10.1016/j.jclepro.2022.131444.
- [110] P.A. Strachan, L. Vandaele, Case studies of outdoor testing and analysis of building components, *Build. Environ.* 43 (2008) 129–142. doi:https://doi.org/10.1016/j.buildenv.2006.10.043.
- [111] T. Lopez, C. Gimenez-Molina, Influence of double glazing with circulating water chamber on a thermal energy saving in buildings, *Energy Build.* 56 (2012) 56–65.
- [112] L. Olivieri, E. Caamaño-Martin, F. Olivieri, J. Neila, Integral energy performance characterization of semi-transparent photovoltaic elements for building integration under real operation conditions, *Energy Build.* 68 (2014) 280–291. doi:https://doi.org/10.1016/j.enbuild.2013.09.035.
- [113] J. Han, L. Lu, J. Peng, H. Yang, Performance of ventilated double-sided PV façade compared with conventional clear glass façade, *Energy Build.* 56 (2013) 204–209. doi:https://doi.org/10.1016/j.enbuild.2012.08.017.
- [114] C. Lodi, P. Bacher, J. Cipriano, H. Madsen, Modelling the heat dynamics of a monitored Test Reference Environment for Building Integrated Photovoltaic systems using stochastic differential equations, *Energy Build.* 50 (2012) 273–281. doi:https://doi.org/10.1016/j.enbuild.2012.03.046.
- [115] M. Ahmad, A. Bontemps, H. Sallée, D. Quenard, Thermal testing and numerical simulation of a prototype cell using light wallboards coupling

- vacuum isolation panels and phase change material, *Energy Build.* 38 (2006) 673–681. doi:<https://doi.org/10.1016/j.enbuild.2005.11.002>.
- [116] S. Roels, M.J. Jiménez, Reliability of characterization models and methods: a round robin experiment on a test box, in: *Proc. Dynastee Work. on'Real Build. Energy Perform. Assessment'*, Ghent, Belgium, 2014.
- [117] G. Macrelli, Electrochromic windows, *Renew. Energy.* 15 (1998) 306–311. doi:[https://doi.org/10.1016/S0960-1481\(98\)00178-5](https://doi.org/10.1016/S0960-1481(98)00178-5).
- [118] E.S. Lee, D.L. DiBartolomeo, Application issues for large-area electrochromic windows in commercial buildings, *Sol. Energy Mater. Sol. Cells.* 71 (2002) 465–491. doi:[https://doi.org/10.1016/S0927-0248\(01\)00101-5](https://doi.org/10.1016/S0927-0248(01)00101-5).
- [119] A.W. Czanderna, D.K. Benson, G.J. Jorgensen, J.-G. Zhang, C.E. Tracy, S.K. Deb, Durability issues and service lifetime prediction of electrochromic windows for buildings applications, *Sol. Energy Mater. Sol. Cells.* 56 (1999) 419–436. doi:[https://doi.org/10.1016/S0927-0248\(98\)00183-4](https://doi.org/10.1016/S0927-0248(98)00183-4).
- [120] E.S. Lee, D.L. DiBartolomeo, Application issues for large-area electrochromic windows in commercial buildings, *Sol. Energy Mater. Sol. Cells.* 71 (2002) 465–491. doi:[10.1016/S0927-0248\(01\)00101-5](https://doi.org/10.1016/S0927-0248(01)00101-5).
- [121] H.R. Wilson, Chromogenic Glazing: Performance and Durability Issues as addressed in IEA Task 27, *Proc. IEA Sol. Heat. Cool. Program. Task. 27* (2002).
- [122] S. Grynning, A. Gustavsen, B. Time, B.P. Jelle, Windows in the buildings of tomorrow: Energy losers or energy gainers?, *Energy Build.* 61 (2013) 185–192. doi:<https://doi.org/10.1016/j.enbuild.2013.02.029>.
- [123] P.G. Loutzenhiser, H. Manz, S. Carl, H. Simmler, G.M. Maxwell, Empirical validations of solar gain models for a glazing unit with exterior and interior blind assemblies, *Energy Build.* 40 (2008) 330–340.

- [124] E.L. Krüger, M. Adriazola, A. Matoski, S. Iwakiri, Thermal analysis of wood–cement panels: Heat flux and indoor temperature measurements in test cells, *Constr. Build. Mater.* 23 (2009) 2299–2305.
- [125] P.H. Baker, M. McEvoy, Test cell analysis of the use of a supply air window as a passive solar component, *Sol. Energy.* 69 (2000) 113–130.
- [126] P. Wouters, L. Vandaele, P. Voit, N. Fisch, The use of outdoor test cells for thermal and solar building research within the PASSYS project, *Build. Environ.* 28 (1993) 107–113.
- [127] F.C. Winkelmann, Modeling Windows in EnergyPlus, *Proc. Build. Simul. 2001.* (2001) 1–11. [http://www.google.ca/url?sa=t&rct=j&q=ibpsa\\_2001\\_modeling\\_windows\\_in\\_energypus&source=web&cd=2&cad=rja&ved=0CDUQFjAB&url=http://simulationresearch.lbl.gov/dirpubs/47972.pdf&ei=N53HUPTiEqK-yQGx3ICQCg&usg=AFQjCNGNYnN6\\_QXVsTGKDE5pRcW2ISysAQ](http://www.google.ca/url?sa=t&rct=j&q=ibpsa_2001_modeling_windows_in_energypus&source=web&cd=2&cad=rja&ved=0CDUQFjAB&url=http://simulationresearch.lbl.gov/dirpubs/47972.pdf&ei=N53HUPTiEqK-yQGx3ICQCg&usg=AFQjCNGNYnN6_QXVsTGKDE5pRcW2ISysAQ).
- [128] J. González, F. Fiorito, Daylight design of office buildings: Optimisation of external solar shadings by using combined simulation methods, *Buildings.* 5 (2015) 560–580.
- [129] Ladybug Tools, Publications, (2021). <https://www.ladybug.tools/publication.html#intro>.
- [130] D. Erbe, T. Culp, J. Boldt, E. Conrad, C. Cottrell, S. Hanson, R. Heinisch, S. Hintz, J. Hogan, J. Humble, B. Ross, D. Brundage, J. Dunlap, A. Engineers, Energy standard for buildings except low-rise residential buildings, *ASHRAE Stand. 4723* (2016) 404–636.
- [131] U.S.D. of Energy, Getting Started, U.S. Dep. Energy. (2019) 4–6.
- [132] A.F. Handbook, American society of heating, refrigerating and air-conditioning engineers, Inc. Atlanta, GA, USA. (2009).
- [133] U.S. Department of Energy, EnergyPlus Weather Data, (n.d.).



<https://energyplus.net/weather> (accessed July 15, 2020).

- [134] M.C. Peel, B.L. Finlayson, T.A. McMahon, Updated world map of the Köppen-Geiger climate classification, *Hydrol. Earth Syst. Sci.* 11 (2007) 1633–1644.
- [135] M. Velds, J. Christoffersen, Monitoring procedures for the assessment of daylighting performance of buildings, *Daylighting Build. a Source B. Daylighting Syst. Components.* (2001).
- [136] I.S.O 9050, Glass in building—Determination of light transmittance, solar direct transmittance, total solar energy transmittance, ultraviolet transmittance and related glazing factors, (2003).
- [137] G. ISO, Determination of light transmittance, solar direct transmittance, total solar 376 energy transmittance, ultraviolet transmittance and related glazing factors, ISO9050. (2003).
- [138] F. Goia, V. Serra, Analysis of a non-calorimetric method for assessment of in-situ thermal transmittance and solar factor of glazed systems, *Sol. Energy.* 166 (2018) 458–471. doi:10.1016/j.solener.2018.03.058.
- [139] T.E. Kuhn, State of the art of advanced solar control devices for buildings, *Sol. Energy.* 154 (2017) 112–133. doi:10.1016/j.solener.2016.12.044.
- [140] B.S. Institution, Glass in Building: Determination of luminous and solar characteristics of glazing, British Standards Institution, 1998.
- [141] Y.T. Chae, J. Kim, H. Park, B. Shin, Building energy performance evaluation of building integrated photovoltaic (BIPV) window with semi-transparent solar cells, *Appl. Energy.* 129 (2014) 217–227. doi:10.1016/j.apenergy.2014.04.106.
- [142] A. Ghosh, S. Sundaram, T.K. Mallick, Investigation of thermal and electrical performances of a combined semi-transparent PV-vacuum glazing, *Appl. Energy.* 228 (2018) 1591–1600. doi:10.1016/j.apenergy.2018.07.040.

- [143] C.M. Lampert, Heat mirror coatings for energy conserving windows, *Sol. Energy Mater.* 6 (1981) 1–41.
- [144] M. Rubin, Calculating heat transfer through windows, *Int. J. Energy Res.* 6 (1982) 341–349.
- [145] R. Yin, P. Xu, P. Shen, Case study: Energy savings from solar window film in two commercial buildings in Shanghai, *Energy Build.* 45 (2012) 132–140.
- [146] W. Osterhaus, Discomfort glare from large area glare sources at computer workstations. *Building with daylight: Energy efficient design*, in: *Proc. Int. Daylight Work. Univ. West. Aust. Perth*, 1996, 1996.
- [147] M. Velds, Assessment of lighting quality in office rooms with daylighting systems [PhD dissertation]. [Delft, The Netherlands]: Technische Universiteit Delft (TUD). 231p, (2000).
- [148] D.B. Crawley, L.K. Lawrie, F.C. Winkelmann, C.O. Pedersen, EnergyPlus: New Capabilities in a Whole-Building Energy Simulation Program, *Build. Simul.* 2001. (2001) 51–58.  
[http://www.ibpsa.org/proceedings/BS2001/BS01\\_0051\\_58.pdf](http://www.ibpsa.org/proceedings/BS2001/BS01_0051_58.pdf)  
[http://www.ibpsa.org/?page\\_id=122](http://www.ibpsa.org/?page_id=122).
- [149] E.E. ASHRAE, *Modeling Methods*, ASHRAE Fundam. (2001).
- [150] U.S. Department of Energy, *Commercial Reference Buildings*, (n.d.).  
<http://energy.gov/eere/buildings/commercial-reference-buildings>  
(accessed June 13, 2021).
- [151] N. Deforest, A. Shehabi, S. Selkowitz, D.J. Milliron, A comparative energy analysis of three electrochromic glazing technologies in commercial and residential buildings, *Appl. Energy.* 192 (2017) 95–109.  
doi:10.1016/j.apenergy.2017.02.007.
- [152] A. Al Touma, D. Ouahrani, Shading and day-lighting controls energy savings in offices with fully-Glazed façades in hot climates, *Energy Build.*

151 (2017) 263–274. doi:10.1016/j.enbuild.2017.06.058.

- [153] E. Weaver, N. Long, K. Fleming, M. Schott, K. Benne, E. Hale, Rapid application development with Openstudio, National Renewable Energy Lab.(NREL), Golden, CO (United States), 2012.
- [154] R.G. Hopkinson, Glare from daylighting in buildings, *Appl. Ergon.* 3 (1972) 206–215. doi:10.1016/0003-6870(72)90102-0.
- [155] M.S. Alrubaih, M.F.M. Zain, M.A. Alghoul, N.L.N. Ibrahim, M.A. Shameri, O. Elayeb, Research and development on aspects of daylighting fundamentals, *Renew. Sustain. Energy Rev.* 21 (2013) 494–505. doi:https://doi.org/10.1016/j.rser.2012.12.057.
- [156] E.J. Gago, T. Muneer, M. Knez, H. Köster, Natural light controls and guides in buildings. Energy saving for electrical lighting, reduction of cooling load, *Renew. Sustain. Energy Rev.* 41 (2015) 1–13. doi:https://doi.org/10.1016/j.rser.2014.08.002.
- [157] L.T. Doulos, A. Kontadakis, E.N. Madias, M. Sinou, A. Tsangrassoulis, Minimizing energy consumption for artificial lighting in a typical classroom of a Hellenic public school aiming for near Zero Energy Building using LED DC luminaires and daylight harvesting systems, *Energy Build.* 194 (2019) 201–217. doi:https://doi.org/10.1016/j.enbuild.2019.04.033.
- [158] M.B.C. Aries, G.R. Newsham, Effect of daylight saving time on lighting energy use: A literature review, *Energy Policy.* 36 (2008) 1858–1866. doi:10.1016/j.enpol.2007.05.021.
- [159] P. Boyce, C. Hunter, O. Howlett, *The benefits of daylight through windows*, Troy, New York Rensselaer Polytech. Inst. (2003).
- [160] L. Heschong, Daylighting and human performance, *ASHRAE J.* 44 (2002) 65–67.
- [161] J.-H. Choi, L.O. Beltran, H.-S. Kim, Impacts of indoor daylight environments

on patient average length of stay (ALOS) in a healthcare facility, *Build. Environ.* 50 (2012) 65–75. doi:<https://doi.org/10.1016/j.buildenv.2011.10.010>.

[162] M. Bodart, A. De Herde, Global energy savings in offices buildings by the use of daylighting, *Energy Build.* 34 (2002) 421–429. doi:[https://doi.org/10.1016/S0378-7788\(01\)00117-7](https://doi.org/10.1016/S0378-7788(01)00117-7).

[163] E. Ghisi, J.A. Tinker, An ideal window area concept for energy efficient integration of daylight and artificial light in buildings, *Build. Environ.* 40 (2005) 51–61.

[164] M. Krarti, P.M. Erickson, T.C. Hillman, A simplified method to estimate energy savings of artificial lighting use from daylighting, *Build. Environ.* 40 (2005) 747–754. doi:[10.1016/j.buildenv.2004.08.007](https://doi.org/10.1016/j.buildenv.2004.08.007).

[165] D.H.W. Li, T.N.T. Lam, S.L. Wong, Lighting and energy performance for an office using high frequency dimming controls, *Energy Convers. Manag.* 47 (2006) 1133–1145. doi:[10.1016/j.enconman.2005.06.016](https://doi.org/10.1016/j.enconman.2005.06.016).

[166] A. Nageib, A.M. Elzafarany, M.H. Elhefnawy, F.O. Mohamed, Using smart glazing for reducing energy consumption on existing office building in hot dry climate, *HBRC J.* 16 (2020) 157–177. doi:[10.1080/16874048.2020.1794226](https://doi.org/10.1080/16874048.2020.1794226).